UNIVERSITÄT BAYREUTH

# Poly(limonene carbonate): Composites and Copolymers

## Dissertation

zur Erlangung des akademischen Grades eines

Doktors der Naturwissenschaften (Dr. rer. nat.)

in der Bayreuther Graduiertenschule für Mathematik und Naturwissenschaften (BayNAT)

der Universität Bayreuth

vorgelegt von

Simon Neumann

aus

Forchheim

Bayreuth 2021

Die vorliegende Arbeit wurde in der Zeit von Dezember 2016 bis Juni 2021 in Bayreuth am Lehrstuhl Makromolekulare Chemie II unter Betreuung von Herrn Professor Dr. Andreas Greiner angefertigt.

Vollständiger Abdruck der von der Bayreuther Graduiertenschule für Mathematik und Naturwissenschaften (BayNAT) der Universität Bayreuth genehmigten Dissertation zur Erlangung des akademischen Grades eines Doktors der Naturwissenschaften (Dr. rer. nat.).

Dissertation eingereicht am: 28.06.2021

Zulassung durch das Leitungsgremium: 14.07.2021

Wissenschaftliches Kolloquium: 29.11.2021

Amtierender Direktor: Prof. Dr. Hans Keppler

Prüfungsausschuss:

Prof. Dr. Andreas Greiner (Gutachter)

Prof. Dr. Matthias Breuning (Gutachter)

Prof. Dr. Hans-Werner Schmidt (Vorsitz)

Prof. Dr. Birgit Weber

# 1 Table of contents

# 2 List of symbols and abbreviations

| | |
|---|---|
| acetyl CoA | acetyl coenzyme A |
| AIBN | azobisisobutyronitrile |
| bdi | diiminate |
| BPO | benzoyl peroxide |
| bio-PET | bio-poly(ethylene terephthalate) |
| BD | butanediol |
| BR | polybutadiene rubber |
| BPA | bisphenol A |
| BPA-PC | bisphenol A polycarbonate |
| CHO | cyclohexene oxide |
| CoA | coenzyme A |
| $CO_2$ | carbon dioxide |
| COPE | segmented polyether ester (Arnitel EM400®) |
| DCM | dichloromethane |
| DEHP | bis(2-ethylhexyl) phthalate |
| diHLA | dihexyl-substitued lactide |
| DIOP | diisooctyl phthalate |
| DLLA | *D,L*-lactide |
| DOP | di-*n*-octylphthalat |
| DPC | diphenyl carbonate |
| DSC | differential scanning calorimetry |
| $\varepsilon_{br}$ | elongation at break |
| $E$ | *E*-modulus/Young's modulus |
| EG | ethylene glycol |
| ERBO | epoxidized rice bran oil |
| ESO | epoxidized soybean oil |
| EtOL | ethyl oleate |
| FDA | U.S. Food and Drug Administration |
| FDCA | 2,5-furandicarboxylic acid |
| GPC | gel permeation chromatography |
| HDPE | high-density poly(ethylene) |
| HIPS | high-impact poly(styrene) |
| HMF | hydroxymethyl furfural |
| LA | lactide |
| LCST | lower critical solution temperature |
| LLA | *L*-lactide |
| LO | limonene oxide |
| MeI | iodomethane |
| MeOH | methanol |
| mCL-PHA | medium chain length poly(hydroxyalkanoates) |
| $M_n$ | number average molar mass |
| $M_w$ | weight average molar mass |
| mol% | mole percent |
| $\eta_0$ | zero shear viscosity |
| OAc | acetate |
| P(3HB-3HV) | poly(3-hydroxybutyrate-co-3-hydroxyvalerate) |
| PA | polyamide |
| PA6 | polyamide 6 |
| PA12 | polyamide 12 |
| PBAT | poly(butylene adipate-co-terephthalate) (EcoFlex®) |
| PBD | polybutadiene rubber |
| PC | polycarbonate |
| PCHC | poly(cyclohexene carbonate) |
| PCL | poly(ϵ-caprolactone) |
| PdiHLA | poly(dihexyl substituted lactide) |
| PDLLA | poly((*D/L*))-lactic acid) |
| PE | polyethylene |

| | |
|---|---|
| PEC | poly(ethylene carbonate) |
| PEF | poly(ethylene furanoate) |
| PEG | poly(ethylene glycol) |
| PEI | poly(ether imide) |
| PES | poly(ethylene succinate) |
| PH3B | poly(3-hydroxybutyrate) |
| PHA | poly(hydroxyalkanoates) |
| PHC | poly(1-hexene carbonate) |
| PLA | poly(lactic acid) |
| PLimC | poly(limonene carbonate) |
| PLLA | poly((*L*))-lactic acid) |
| PMen2C | poly(menth-2-ene carbonate) |
| PMMA | poly(methyl methacrylate) |
| PO | propylene oxide |
| PP | polypropylene |
| PPC | poly(propylene carbonate) |
| ppm | parts per million |
| PPO | poly(phenylene oxide) |
| PS | polystyrene |
| PU | polyurethanes |
| PVA | poly(vinyl acetate) |
| PVOH | poly(vinyl alcohol) |
| PVC | polyvinyl chloride |
| ROP | ring-opening polymerization |
| ROCOP | ring-opening copolymerization |
| $\sigma_{max}$ | tensile strength |
| SA | succinic acid |
| SAN | poly(styrene-*co*-acrylonitrile) |
| SBS | polystyrene-*b*-polybutadiene-*b*-polystyrene |
| sc-PLA | stereocomplexed PLA |
| sCL-PHAs | short length poly(hydroxyalkanoates) |
| SEM | scanning electron microscopy |
| SSP | solid-state polycondensation |
| TEM | transmission electron microscopy |
| TPE | thermoplastic elastomer |
| $T$ | temperature |
| $T_c$ | crystallization temperature |
| $T_{cc}$ | cold crystallization temperature |
| TGA | thermogravimetric analysis |
| $T_g$ | glass transition temperature |
| $T_m$ | melting temperature |
| $T_{5\%}$ | temperature at 5% weight loss |
| vol% | volume percent |
| wt% | weight percent |

# 3 List of Publications

1. Unlocking the processability and recyclability of the biobased poly(limonene carbonate)

*Simon Neumann, Lisa-Cathrin Leitner, Holger Schmalz, Seema Agarwal and Andreas Greiner*

**ACS Sustainable Chem. Eng. 2020, 8, 6442−6448**

Received: February 3, 2020
Revised: March 22, 2020
Published: April 7, 2020

https://dx.doi.org/10.1021/acssuschemeng.0c00895

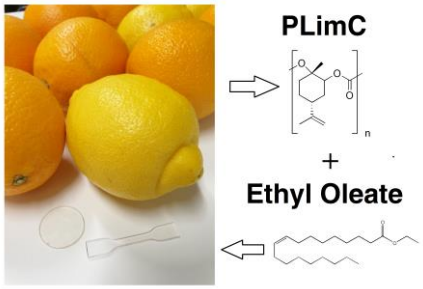


2. Blends of bio-based poly(limonene carbonate) with commodity polymers

*Simon Neumann, Pin Hu, Felix Bretschneider, Holger Schmalz and Andreas Greiner*

**Macromol. Mater. Eng. 2021, 2100090**

Received: February 7, 2021
Revised: April 11, 2021
Published: June 12, 2021

https://doi.org/10.1002/mame.202100090

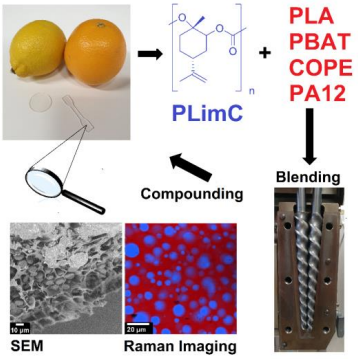


3. Sustainable block copolymers of poly(limonene carbonate)

*Simon Neumann, Sophia Barbara Däbritz, Sophie Edith Fritze, Lisa-Cathrin Leitner, Aneesha Anand, Andreas Greiner and Seema Agarwal*

**RSC Polym. Chem., 2021,12, 903-910**

Received: December 09, 2020
Accepted: January 09, 2021
Published: January 22, 2021

https://doi.org/10.1039/D0PY01685C

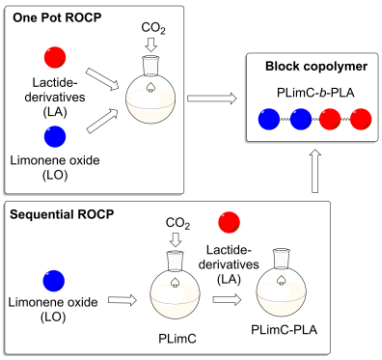

# 4 Summary

Sustainability and climate protection are keywords for upcoming decades. Bio-based polymers can contribute to these ambitious goals and so research is focusing more on these types of polymers (**Chapter 6**).[1–4] This thesis shall contribute to the further development and understanding of bio-based polymers. The main focus of this thesis is the terpene-based polymer poly(limonene carbonate) (PLimC) with its high glass transition temperature ($T_g$ = 130 °C). PLimC was first discovered by COATES et al.[5], who investigated the alternating copolymerization of limonene oxide (LO) and $CO_2$. Both monomers are non-food-based and non-crop-based, so competition for resources with the food industry is not present with these monomers. This makes PLimC an excellent candidate as an alternative to bisphenol-A polycarbonate (PC). By masking impurities within the monomer LO, the molecular weight of PLimC could be increased drastically (<100.000 Da).[6] PLimC has excellent properties and tuning possibilities for practical applications, so the interest in further development of PLimC is given.[6–8] Key factor for practical applications is processing via injection molding or hot-pressing, but neat PLimC is hard to process due to its high viscosity in the melt ($\eta_0$ = 0.89 MPa·s), the high onset of the viscous flow (~ $T$ = 167 °C) and its low degradation temperature (~ $T$ = 180 °C).

The main objective of this thesis is to show ways to process PLimC despite the aforementioned processing obstacles for PLimC. Additives, blending, or copolymerization can be used as effective tools to achieve the processability of PLimC.

**Additives**

The first investigated way involves a bio-based plasticizer, which allows the processing of PLimC without the loss of optically and mechanical properties (**Publication 1, Chapter 9.1**). Ethyl oleate (EtOL) was chosen as a bio-based plasticizer for PLimC due to its nontoxicity. EtOL is a fatty acid ester, which displays good plasticizing properties due to its long alkyl chains. A loading of 7.5 wt% EtOL reduces the viscosity of PlimC in the melt ($\eta_0$ = 0.12 MPa·s) and decreases the onset of the viscous flow ($T$ = 136 °C). At the same time, the glass transition temperature of PLimC is reduced to 90 °C. By applying EtOL, the narrow process window of PLimC can be extended and it can be processed at lower temperatures (~ $T$ = 160 °C). This enables PLimC processing without decomposition and with improved mechanical properties. The $E$-modulus ($E$ = 2.1 ± 0.19 GPa) and the elongation at break ($\varepsilon_{br}$ = 28 ± 9.3%) are increased significantly by the addition of 7.5 wt% EtOL. Higher amounts of EtOL (> 7.5 wt%) do not

result in improved mechanical properties. The optical properties of PLimC/EtOL compounds are comparable to the neat PLimC. The recyclability of PLimC/EtOL compounds was also investigated. It is shown that PLimC/EtOL compounds can at least be recycled once by melt reprocessing.

**Blending**

To explore the processing of PLimC even further, blends of PLimC as minority component and commodity polymers (e.g., polyamide (PA), polystyrene (PS), or poly(methyl methacrylate) (PMMA)) were produced. Blending should showcase the potential of bio-based polymers for sustainable applications (**Publication 2, Chapter 9.2**). The blend morphology was investigated by scanning electron microscopy (SEM) and Raman imaging. The difference in viscosity and incompatibility are usually leading to phase-separated blends with a bimodal PLimC domain distribution. Phase-separation also influences the thermal properties of the blends. Using differential scanning calorimetry (DSC), an increased crystallization temperature for PLimC could be observed. That is due to the nucleation effects of PLimC domains. Thermogravimetric analysis (TGA) of the different blends reveals higher thermal stability for matrix embedded PLimC. In terms of mechanical properties, blends of PLimC with polylactide (PLA), poly(butylene adipate-*co*-terephthalate) (PBAT), or copoly(ether ester) (COPE) show the most promising properties for applications. The most pronounced effect of PLimC in blends (e.g., PBAT or COPE blends) is, that it leads to a strong increased *E*-modulus, which can be interesting for applications.

**Copolymerization**

To improve the performances of phase-separated PLimC/PLA blends, block copolymers of PLimC and PLA were synthesized (**Publication 3, Chapter 9.3**). The produced block copolymers can be used as compatibilizers in blends to influence the morphology and mechanical properties. In this chapter, the copolymerization of LO, $CO_2$, and lactide (LA) is discussed in detail. One-pot ring-opening copolymerization (ROCOP) of (*D, L*)-lactide and LO is performed to investigate the actual polymer architecture in one-pot reactions. Based on TEM measurements and $^{1}$H-$^{1}$H-NOESY NMR experiments, a block copolymer structure could be identified. To show an active PLimC chain ending, sequential ring-opening copolymerization of (*L*)-lactide was performed to synthesize PLimC/PLLA block copolymers. Additionally, ROCOP was used as an efficient tool for tailoring the mechanical properties of PLimC. In a sequential approach, dihexyl-substituted lactides (diHLA) were used as monomers for ROCOP

with LO and $CO_2$. These block copolymers of PLimC and Poly(diHLA) (PdiHLA) showed an interesting elasticity and transparency for potential applications.

# 5 Zusammenfassung

Nachhaltigkeit und Klimaschutz sind die Schlüsselwörter für zukünftige Jahrzehnte. Bio-basierte Kunststoffe können zu diesen ambitionierten Zielen beitragen. Auch deshalb fokussiert sich die Forschung mehr und mehr auf diese Art von Kunstoffen (**Kapitel 6**).[1–4] Diese Arbeit soll zur weiteren Entwicklung und zum weiteren Verständnis über bio-basierte Kunststoffe beitragen. Der Hauptfokus dieser Arbeit ist der Kunststoff Poly(limonen carbonat) (PLimC) mit seiner hohen Glasübergangstemperatur ($T_g$ = 130 °C). PLimC wurde als erstes von COATES et al. entdeckt, der die alternierende Copolymerisierung von Limonenoxid (LO) und $CO_2$ untersuchte.[5] Beide Monomere basieren nicht auf Nahrungsmitteln, sodass es keinen Konkurrenzkampf um Ressourcen gibt. Das macht PLimC zu einem exzellenten Kandidaten als Alternative zu Bisphenol-A-Polycarbonat (BPA-PC). Indem Hydroxyl-Verunreinigungen im Monomer LO maskiert worden sind, konnte das Molekulargewicht drastisch erhöht werden (<100.000 Da).[6] PLimC besitzt exzellente Eigenschaften und Veränderungsmöglichkeiten für praktische Anwendungen, sodass das Interesse an weiteren Entwicklungen zu PLimC gegeben ist.[6–8] Schlüsselfaktor für praktische Anwendungen ist die Verarbeitbarkeit mittels Spritzgusses oder Heißpressens. Reines PLimC ist aufgrund seiner hohen Schmelzviskosität ($\eta_0$ = 0.89 MPa·s), seinem hohen Beginn des viskosen Fließens (~ $T$ = 167 °C) und seiner geringen Zersetzungstemperatur (~ $T$ = 180 °C) schwer zu verarbeiten.

Das Hauptziel dieser Arbeit ist es, trotz der obengenannten Verarbeitungshindernisse mehrere Wege aufzuzeigen, um PLimC zu verarbeiten. Additive, Blending oder Copolymerisierung können als effektives Werkzeug benutzt werden die Verarbeitbarkeit von PLimC zu erreichen.

**Additive**

Der als erste untersuchte Weg beinhaltet ein bio-basierten Weichmacher, welcher die Verarbeitung von PLimC ohne den Verlust von optischen und mechanischen Eigenschaften erlaubt (**Publikation 1, Kapitel 9.1**). Ethyl Oleat (EtOL) wurde aufgrund seiner Ungiftigkeit als bio-basierter Weichmacher ausgewählt. EtOL ist ein Fettsäureester, der aufgrund seiner langen Alkylketten gute weichmachende Eigenschaften zeigt. Eine Beladung mit 7.5 wt% EtOL reduziert die Viskosität von PLimC in der Schmelze ($\eta_0$ = 0.12 MPa·s) und verringert den Beginn des viskosen Fließens ($T$ = 136 °C). Gleichzeitig wird die Glasübergangstemperatur auf 90 °C reduziert. Indem man einen bio-basierten Weichmacher verwendet, kann man das enge Verarbeitungsfenster von PLimC erweitern und es kann bei niedrigeren Temperaturen verarbeitet werden (~ $T$ = 160 °C). Das ermöglicht die Verarbeitung von PLimC ohne

Zersetzung und mit verbesserten Eigenschaften. Nachdem man 7.5 wt% EtOL hinzugegeben hat, sind das Elastizitätsmodul ($E$ = 2.1 ± 0.19 GPa) und die Bruchdehnung ($\varepsilon_{br}$ = 28 ± 9.3%) sind signifikant angestiegen,. Größere Anteile von EtOL (> 7.5 wt%) resultieren nicht in verbesserten mechanischen Eigenschaften. Die optischen Eigenschaften der PLimC/EtOL-Komposite sind vergleichbar mit reinem PLimC. Die Recyclbarkeit von PLimC/EtOL-Kompositen wurde auch untersucht. Es konnte gezeigt werden, dass PLimC/EtOL-Komposite durch erneutes Wiederverarbeiten mindestens einmal wieder verwendet werden können.

**Blending**

Um die Verarbeitung von PLimC weiter zu untersuchen, wurden Blends aus technischen Polymeren (z.B. Polyamid (PA), Polystyrol (PS) oder Polymethylmethacrylat (PMMA)) mit PLimC als Minderheitskomponente hergestellt (**Publikation 2, Kapitel 9.2**). Das Blenden soll das Potenzial von bio-basierten Polymeren für nachhaltige Anwendungen zeigen. Die Blend Morphologie wurde mit dem Rasterelektronenmikroskop (SEM) und Raman Imaging untersucht. Der Unterschied in der Viskosität und die Unverträglichkeit führt gewöhnlicherweise zu phasenseparierten Blends mit einer bimodalen PLimC Domänen Verteilung. Die Phasenseparierung beeinflusst auch die thermischen Eigenschaften der Blends. Eine erhöhte Kristallisierungstemperatur von PLimC konnte mittels dynamischer Differenzkalorimetrie (DSC) beobachtet werden. Dies liegt an den Nukleierungseffekte der PLimC Domänen. Die thermogravimetrische Analyse (TGA) der verschiedenen Blends zeigt eine höhere Stabilität für PLimC, welches in eine Matrix eingebettet ist. In Bezug auf mechanische Eigenschaften zeigten Blends von PLimC mit Polylactid (PLA), Polybutylenadipat-terephthalat (PBAT) oder Copolyetherestern (COPE) die vielversprechendsten Eigenschaften für Anwendungen. Der stärkste Effekt von PLimC in Blends (z.B. COPE oder PBAT Blends) ist es, dass es zu einem erhöhten Elastizitätsmodul, welches für Anwendungen interessant sein könnte, führt.

**Copolymerisierung**

Um die Perfomance von phasenseparierten PLimC/PLA Blends zu verbessern, wurde Blockcopolymere von PLimC und PLA synthetisiert (**Publikation 3, Kapitel 9.3**). Die produzierten Blockcopolymere können als Phasenvermittler in Blends verwendet werden, um die Morphologie und die mechanischen Eigenschaften zu beeinflussen. In diesem Kapitel wird die Copolymerisierung von LO, $CO_2$ und (*D,L*)-Lactid (LA) im Detail diskutiert. Die ring-öffnende Eintopf-Copolymerisierung (ROCOP) von LA, $CO_2$ und LO wurde durchgeführt, um

die eigentliche Polymerarchitektur tatsächliche Polymerarchitektur von Eintopf-Reaktionen zu untersuchen. Basierend auf TEM-Messungen und $^{1}$H-$^{1}$H-NOESY-NMR-Experimenten konnte eine Blockcopolymer-Struktur identifiziert werden. Um das aktive PlimC Kettenende zu zeigen, wurde eine sequenzielle ROCOP mit *L*-Lactid durchgeführt, um PLimC/PLLA Blockcopolymere zu synthetisieren. Zusätzlich wurde in einem sequentiellen Ansatz dihexyl-substituierte Lactide (diHLA) für eine ROCOP mit LO und $CO_2$ als Monomere verwendet. Diese Blockcopolymere von PlimC und Poly(diHLA) (PdiHLA) zeigten eine interessante Elastizität und Transparenz für potenzielle Anwendungen.

# 6 Introduction

## 6.1 Bio-based polymers in general

Polymers are a part of our everyday life due to the need for clothing, transportation, packaging, buildings medical applications, and electronic devices.[4] Most of them are petroleum-based, which means, that they are relying on finite resources.[9,10] The way to achieve sustainability concerning plastics and polymers is to replace petroleum-based polymers with inexpensive, natural, renewable, biodegradable, and non-toxic materials. There are four renewable raw materials: carbon dioxide, terpenes, vegetable oils, and carbohydrates, which feature the possibility to create sustainable polymers (**Figure 1**).[4] In an economic view, polymer production should be not only sustainable but also highly efficient and inexpensive. This can be achieved by using combinations of raw materials or recycling of waste resources from agriculture or industry. Additional characteristics for the produced sustainable polymers should complementary or enhanced properties compared with currently available commodity plastics. The new "green" polymers should be usable in markets, in which high tonnages are produced like for example in the packaging industry.[11] Applications as thermoplastic elastomer or rigid plastic should be also possible. In terms of sustainability, the life-cycle assessment of polymers should be considered.[12] Recyclability of bio-based materials[13] and biodegradation[14] are also important aspects for a sustainable green polymer. Sustainable polymers can be divided into three different categories.[15] The first class deals with naturally derived biomass polymers. Here, the direct use of biomass as a polymeric material like for example cellulose, cellulose acetate, starches, chitin, modified starch is in the focus. The second category is about bio-engineered polymers: Microorganisms and plants are producing monomer materials via bio-synthesis like for example (hydroxy alkanoates (PHAs) or poly(glutamic acid). The third category are synthetic polymers like for example polylactide (PLA), poly(butylene succinate) (PBS), bio-polyolefins, bio-poly(ethylene terephthalic acid) (bio-PET).[16,17]

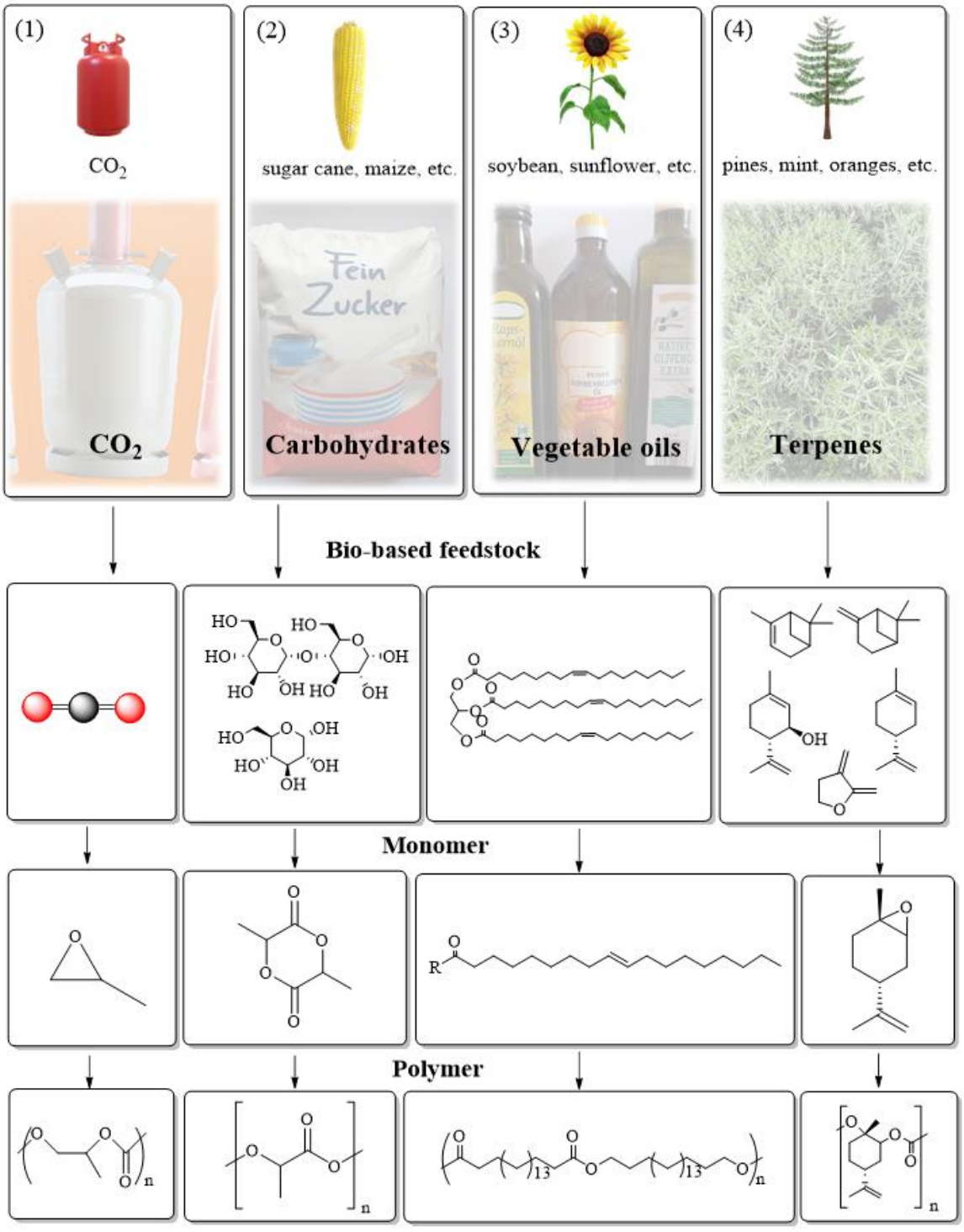


**Figure 1.** Overview of different bio-based polymers and the corresponding bio-based feedstock: (1) $CO_2$ is a renewable carbon resource, which can be copolymerized with propylene oxide to produce for example poly(propylene carbonate), (2) carbohydrates from sugar cane or maize can be converted to lactide and eventually is polymerized to PLA, (3) unsaturated fatty esters from vegetable oils (e.g., soybeans, castor oil or palm tree oil) can be converted into long-chain aliphatic polyesters, (4) terpenes, which can be extracted from plants such as pine, mint or orange peels. Limonene oxide is copolymerized with carbon dioxide to give PLimC (adapted from ZHU et al.[3] with permission of Springer © 2016).

## 6.2 Petro-based polycarbonates and bio-based polymers based on carbon dioxide ($CO_2$)

Polycarbonates (PC), whether they are bio-based or not, are a group of thermoplastic polymers containing carbonate groups in their chemical structures. Usually, when the term polycarbonate is used, it refers to polycarbonates on bisphenol A (BPA) basis. BPA–PC are possessing excellent features for commercial use like for example high durability, respectable mechanical properties, high transparency, and good processability. Due to these characteristics, it is applied in the automotive, electronics, and construction sector.[18] There are two main methods for the synthesis of petroleum-based polycarbonates: Interfacial (solvent-based) and melt condensation polymerizations.[19] Phosgene, aqueous sodium hydroxide, catalytic amine (e.g., triethylamine or pyridine), and BPA are used for the interfacial-based method (**Figure 2**). As solvent usually dichloromethane (DCM) is used.[20] Phenols (e.g., p-t-butylphenol or p-cumylphenol) are also applied to adjust the molecular weight. Melt polymerization of BPA-PC usually involves diphenyl carbonate (DPC). In this process, BPA reacts with DPC in the presence of a minimal amount of basic catalyst (e.g., NaOH/LiOH) at a high temperature.[20] The problematic factor in the reaction is not only toxic phosgene but also BPA. It is assumed to promote cancer in humans like for example breast cancer as shown by SOTO et al.[21] Safety concerns were also declared by MAIA et al., who investigated the release of BPA from PC baby bottles.[22] But not only the health aspects of BPA-PC are to mention, but also the environmental aspect like for example increased plastic pollution or fossil fuel depletion are important factors to consider. So, it is unavoidable to use natural feedstocks to prepare bio-based PC that possesses similar properties to petro-based polycarbonates. One of these naturally occurring materials for the synthesis of bio-based polycarbonates is the greenhouse gas carbon dioxide ($CO_2$). A lot of research has been conducted to make use of this source as a C1 building block.[23–25] For example, LEE et al. are using carbon dioxide as a monomer to form poly(propylene carbonate)-diols, which gives access to polyurethanes (PU).[26] Mechanistic aspects of the copolymerization of $CO_2$ and epoxides were investigated by REN et al., who showed the effective use of thermally stable cobalt(III) complexes, which show high activity and selectivity for polymer formation during $CO_2$/propylene oxide polymerization (PO).[27] Highly isotactic polycarbonates, which were produced by enantioselective β-diiminate catalysts using $CO_2$ and meso-epoxides were investigated by ELLIS et al. [28]

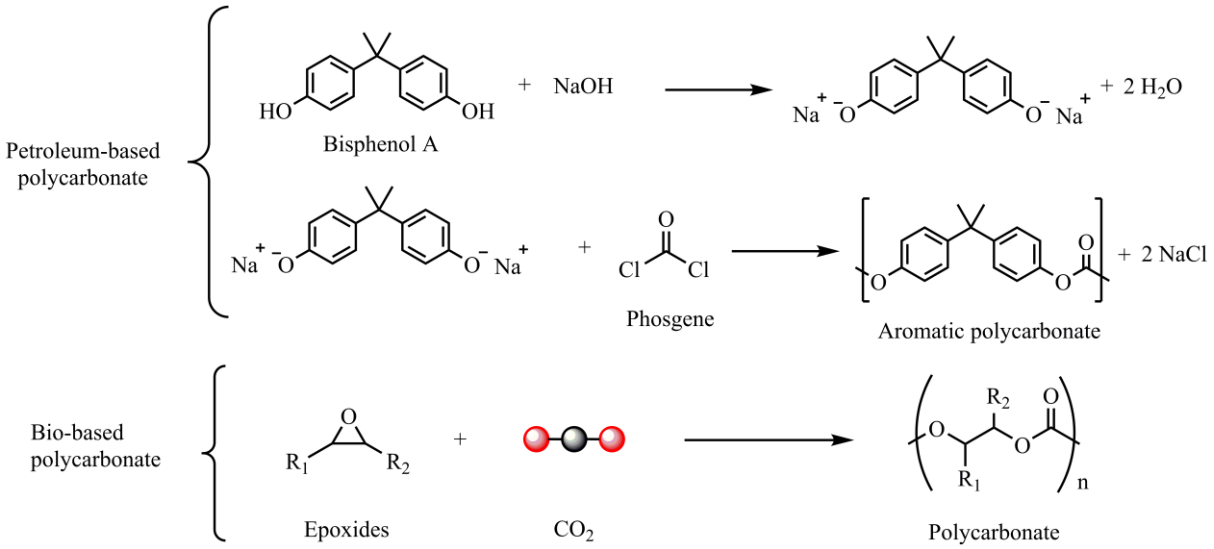


**Figure 2.** Synthesis of petro-based and bio-based polycarbonates. Petroleum-based polycarbonates are made from bisphenol A (BPA) and phosgene. Bio-based polycarbonates are based on carbon dioxide and epoxides (adapted from CUI et al.[18] and ZHU et al.[3] with permission of Springer © 2016 and Elsevier © 2019).

## 6.3 Bio-based polymers analogous to conventional petro-based polymers

### 6.3.1 Bio-based poly(ethylene) (bio-PE)

Bio-poly(ethylene) (bio-PE) can be synthesized using ethylene, which is obtained by the catalytic dehydration of ethanol.[29] The major advantage of using bio-PE is the fact that its optical and mechanical characteristics are similar to conventional petro-based poly(ethylene) (PE). Additionally, all types of PE are also available for bio-based PE like for example bio-HDPE with a low degree of short-chain branching or bio-LLDPE with a high degree of short-chain branching.[30] Another advantage is that the complete infrastructure for processing and recycling of PE is already available for bio-PE. The disadvantages are on the one side the competition on the market with conventional PE due to the low cost of shale gas. The disadvantage of PE despite the potential bio-based synthesis is the long-term stability of PE, which persists in the environment and is not practical to recycle.[4]

### 6.3.2 Bio-based poly(ethylene terephthalate) (bio-PET)

Another important source for bio-based monomers is cellulose, sugar, or starch, which comes from plants like sugar cane (Saccharum officinarum), wheat (Triticum spp.), or sugar beet (Beta vulgaris).[3,31] These monomers are the basis of many commercially available polymers: For example, ethylene glycol from starch is used as a monomer substitute in bio-poly(ethylene terephthalate) (bio-PET). There is also the possibility to produce PET that is fully derived from biomass as shown by PANG et al. It is based on ethylene glycol and terephthalic acid.[32] ZHANG et al. showed in a review the literature, which is available for the dehydration process of ethanol. This process can be effectively used for the synthesis of poly(ethylene) (PE).[33] In comparison to PE, PET is more sustainable due to the existing bottle recycling.[34] For PET not only mechanical recycling is possible, but also chemical recycling due to organic depolymerization as shown by FUKUSHIMA et al.[35] Not only ethylene glycol from starch is a source for bio-based polymers, but also sugar from polysaccharides is another option to produce monomers for polymerization reactions.

### 6.3.3 Bio-based poly(ethylene furanoate) (PEF)

Polyethylene furanoate (PEF) is an interesting candidate for future applications. It shows a melting temperature of $T_m$ = 210 °C and a glass transition temperature of $T_g$ = 80 °C.[36,37] The decomposition of PEF starts at around 300 °C.[38] PEF is brittle and rigid with an elongation at break of 4%.[39] The synthesis on a laboratory scale is done in three major steps: 1. Fructose is produced from corn starch 2. The conversion of fructose into Furanics is performed 3. The oxidation to the monomer 2,5-furandicarboxylic acid (FDCA) and polymerization with ethylene glycol (EG) into PEF is carried out.[40] During the process side reactions (e.g., levulinic acid) can happen, which hinders an efficient process. BURGESS et al. found a way to overcome this limitation to gain access to more stable hydroxymethyl furfural (HMF) ethers, which can be oxidized to FDCA.[41] PEF is then synthesized by polycondensation of ethylene glycol and FDCA. Both processes PET and PEF synthesis are quite similar to each other, so an easier switch to a more sustainable PEF manufacturing can be achieved.[41]

## 6.4 Bio-based polymers from polysaccharide

### 6.4.1 Polylactide (PLA)

Polylactide (PLA) is a bio-based polymer, which is already commercially available (e.g., from NatureWorks®) and it is produced from fermented plant starch such as from corn or sugar beet pulp.[42] To produced PLA for demanding markets, the production of the monomer source lactic acid must be improved. Nowadays usually bioprocess techniques facilitated by wild-type and/or engineered microbes are used to produce lactic acid in a microbial fermentation process.[43] There are also alternative production approaches based on a direct zeolite-based catalytic process, which converts lactic acid into lactide, which is shown by DUSSELIER et al.[44] Glycerol, agricultural waste, and algae-produced carbohydrates can also be used as a source of lactide.[43] Homogeneous and heterogeneous catalysis as part of chemocatalytic approaches show also a potential to produce lactic acid and other α-hydroxy acids.[45] After obtaining lactide polymerization reactions can be carried out. The so produced PLA is a growing alternative as a packaging material, according to a review of AURAS et al.[46] It can also be used as fiber material as shown by INKINEN et al.[47] Using selective polymerization techniques to enable sterecomplex formation between enantiomeric PLA. This can help to increase the thermal stability of PLA and also widen the application area.[48] A broader application area for PLA is also possible because the bio-based polymer shows recycling properties and compostability.[3] The resulting lactic acid from composting can be degraded by microbes. A life cycle assessment of the manufacture of lactide and PLA biopolymers from sugarcane in Thailand shows a decrease of < 40% in greenhouse-gas emissions and < 25% in non-renewable-energy use for PLA compared with petrochemical-derived polymers such as polyethylene or PET.[49,50] The life cycle assessment of PLA was also described by several groups.[12,51,52] One drawback of PLA production is the extended use of water and fertilizer for the cultivation of plants, which would influence the environment. Problematic is also the replacement of natural plants with lignocellulosic or leftover biomass.[3] PLA is based on lactic acid (LA), which is a 2-hydroxycarboxylic acid with a chiral carbon atom and exists in two optically active stereoisomers: *L*-lactic acid and *D*-lactic acid, which are enantiomers.[53] These variants are usually produced via bacteria fermentation (e.g., with *Lactobacillus*, *Streptococcus*, *Pediococcus*, *Aerococcus*, *Leuconostoc*, and *Coryne* species). Racemic *DL*-lactide acid is another important lactic acid variant, but rather with bacteria fermentation this variant is synthesized chemically.[53] The dimer of two lactic acid molecules is called lactide (LA) and

consists of different stereoisomeric lactic acid units. *L*-lactide is based on two *L*-lactic acid molecules, whereas *D*-lactide is made of two *D*-lactic acid molecules. The other variant *meso*-lactide consists of one *L*-lactic acid molecule and one *D*-lactic acid molecule. Racemic lactide (*rac*-lactide) is an equimolar mixture of *L*-lactides and *D*-lactides (**Figure 3**). *L*-lactides and *D*-lactides are showing a melting temperature of 95-98 °C, whereas *meso*-Lactide is displaying a melt temperature of 53-54 °C. *rac*-lactide is displaying a higher melting temperature with 122–126 °C.[53] For the polymerization of PLA high monomer purity is necessary because impurities interfere with the course of reaction and reduce the quality of polymer. As impurities water or hydroxyl and carboxylic functionalities are regarded. Initiator formation, chain transfer, and transesterification are induced by hydroxyl impurities. This could lead to a change in polymerization rate or to a lower molecular weight alongside a broader molecular weight distribution. Carboxylic impurities are affecting the polymerization differently. They lead to a deactivation reaction by making a complex with the catalyst and reduce the rate of polymerization.[54] PLA is accessible by using different polymerization routes like for example polycondensation or ring-opening polymerization (ROP) (**Figure 3**).[55–57] Usually these techniques are based on four different routes, especially in industrial synthetic procedures (**Figure 4**). By using ring-opening polymerization (ROP) high molecular weight PLA can be produced (**Figure 4A**), whereas direct polycondensation gives PLA with a tendency to lower molecular weight (**Figure 4B**).[42,58] For ROP of lactide different polymerization methods and mechanisms are available. The three main techniques are anionic, cationic, or coordination polymerization. Anionic and cationic polymerization are usually showing some disadvantages in comparison to coordination polymerization. By using anionic polymerization undesirable reactions like for example racemization, back-biting reaction or other side reactions can occur. The highly active anionic reactants can interfere with chain propagation. Cationic polymerization also favors undesirable side reactions and racemization, because of nucleophilic attacks on the activated monomers and the propagating species. Coordination polymerization with metal catalysts (mostly alkoxides) can overcome these limitations and produce high molecular weight polymers with high optical purity. For the tin-catalyzed polymerization of lactide DUDA and PENZEK proposed a comprehensive polymerization scheme based on the insertion-coordination mechanism (**Figure 3**).[59]

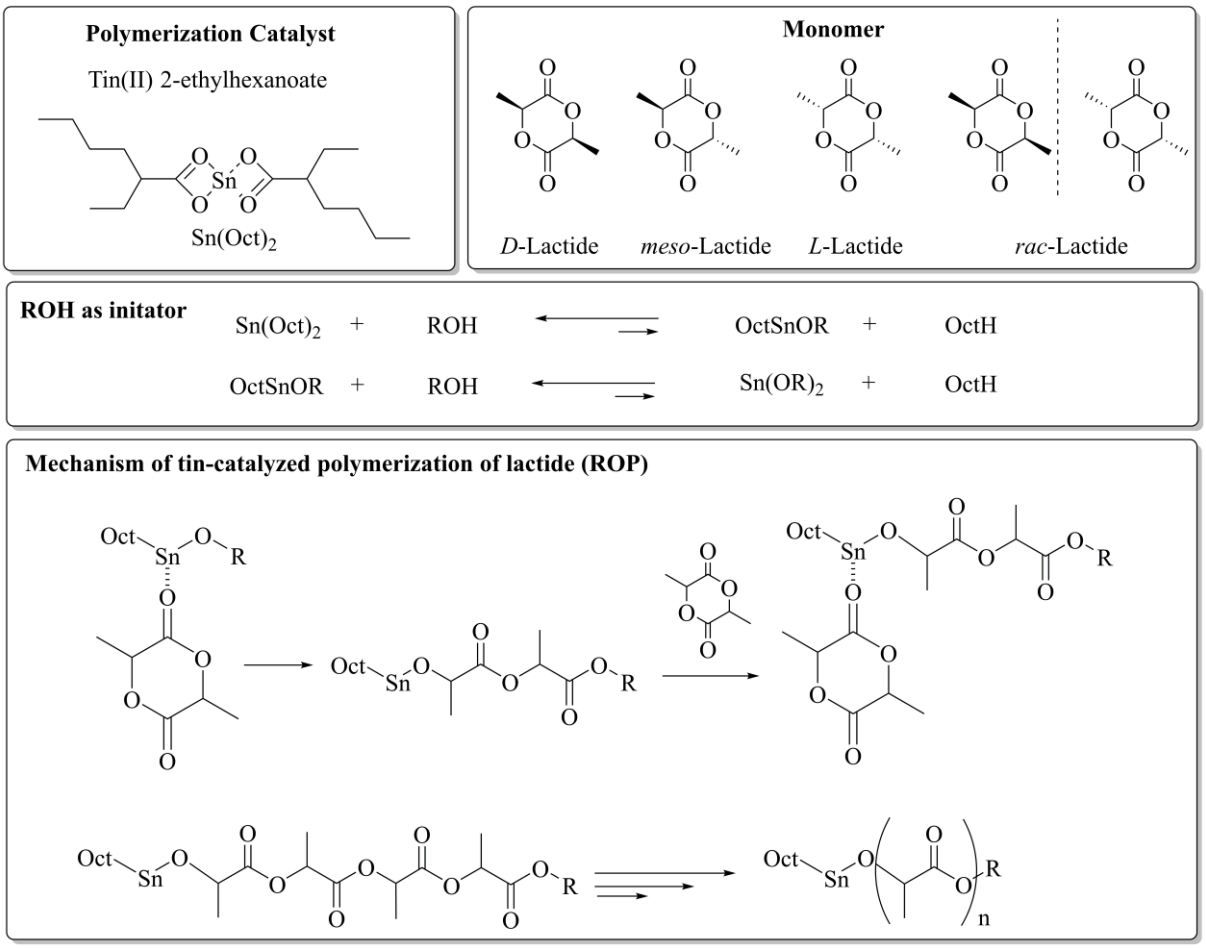


**Figure 3.** Ring-opening polymerization (ROP) of lactide by using $Sn(Oct)_2$ as catalyst according to KIMURA et al.[53] The polymerization scheme is based on the insertion-coordination mechanism of DUDA and PENZEK et al.[59]

To manage the drawbacks of low molecular weight PLA by polycondensation, solvent-assisted polycondensation and melt polycondensation followed by solid-state polycondensation (SSP) can be applied (**Figure 4C**).[42] This process consists of two steps: First, a prepolymer with a molecular weight of 20.000 Da is prepared by melt-polycondensation and then crystallized by heat-treatment at around 105 °C. Subsequently, it is heated at 140-150 °C for 10–30 h for polycondensation reaction**.** PLA with molecular weights over >500.000 Da can be obtained with this method.[60] Azeotropic condensation polymerization can also be used for the direct synthesis of high molecular weight PLA starting from lactic acid **(Figure 4D**). AJIOKA et al. demonstrated this way by overcoming the problem of water removal during polymerization by manipulating the equilibrium between monomer and polymer in organic solvents, so lactic acid is directly polycondensed into a high molar mass polymer.[61] Regarding the physical and mechanical properties of PLA, a strong impact of stereochemistry can be observed. There are two major forms of the homopolymer PLA with different stereochemistry, namely PLLA and PDLA. PLLA and PDLA are synthesized from mixtures of pure *L*- or *D*-lactic acid. The

copolymer PDLLA is obtained from the racemic mixture. These different types of PLA displaying different thermal and mechanical properties due to their stereochemistry. PLLA or PDLA are semi-crystalline polymers, which are showing a melting peak ($T_m$= 170 - 200 °C), whereas PDLLA shows amorphous behavior and no melting. The crystallinity of PLA is also significantly influenced by the thermal and mechanical history. The glass transition temperature of PLA shows values in the range of 45 - 60 °C for all types of PLA. Mechanical properties of PLA are strongly influenced by molecular weight, crystallinity, processing, or the testing procedure, so mechanical values are displayed in ranges.[62] Typical mechanical values for PLA are for example: σ = 21–60 MPa, *E*-modulus = 0.35 – 0.5 GPa, ϵ = 2.5 – 6 %.[63] The crystallinity of PLA strongly determines physical and mechanical properties (e.g., hardness, modulus, tensile strength, stiffness, and melting points). If the content of PLLA is high (>90 %) the polymer displays semicrystalline features, whereas lower content leads to amorphous behavior. Also, the density is influenced by crystallinity. Crystallinity also influences the solubility of PLA. Crystalline PLLA cannot be dissolved in acetone, ethyl acetate, or tetrahydrofuran. Amorphous PLA is soluble in dioxane, acetonitrile, chloroform, methylene chloride, 1,1,2-trichloroethane, and dichloroacetic acid. Thermal and mechanical treatment can alter properties as shown by CARRASCO et al. in the case of PLA degradation.[64] The mechanical and thermal properties of PLA can also be tuned by the addition of plasticizer[65,66] Blending is another possibility for improving the mechanical properties of PLA.[67] For blending two options are possible for PLA: On the one side, PLA can be blended with a biodegradable polymer or on the other side with a non-biodegradable polymer like polyethylene, polypropylene, polystyrene, poly(ethylene terephthalate), or polycarbonates.[68] PLA composites are another option for influencing the mechanical properties of PLA (e.g., addition of reinforcing fibers, micro- and/or nanofillers, and selected additives).[69] Blending of PLLA with PDLA leads to the formation of stereocomplexes, which exhibit higher melting temperature (or heat resistance), mechanical performance, and hydrolysis resistance compared to those of pure PLLA and PDLA.[70] Stereocomplexed PLA (sc-PLA) not only improves mechanical properties but also thermal properties like the thermal stability of PLA. A sc-PLA film can also be obtained from a compression-induced sterecomplexation at air−water interface according to YAN et al.[71] One remarkable property of sc-PLA is its high melting temperature ($T_m$ = 230 °C), which 50 °C high than the melting temperature of pure PLLA. Complex molecular architectures can also be made by using different PLA topologies like for example star-branched or long-chain branched.[72] Block copolymers of PLA are also well known like polyethylene glycol-*co*-polylactic acid

(PEG-PLA) block copolymer for hydrophilicity tuning or polylactic-*co*-caprolactone (PLCL) block copolmers.[73–77]

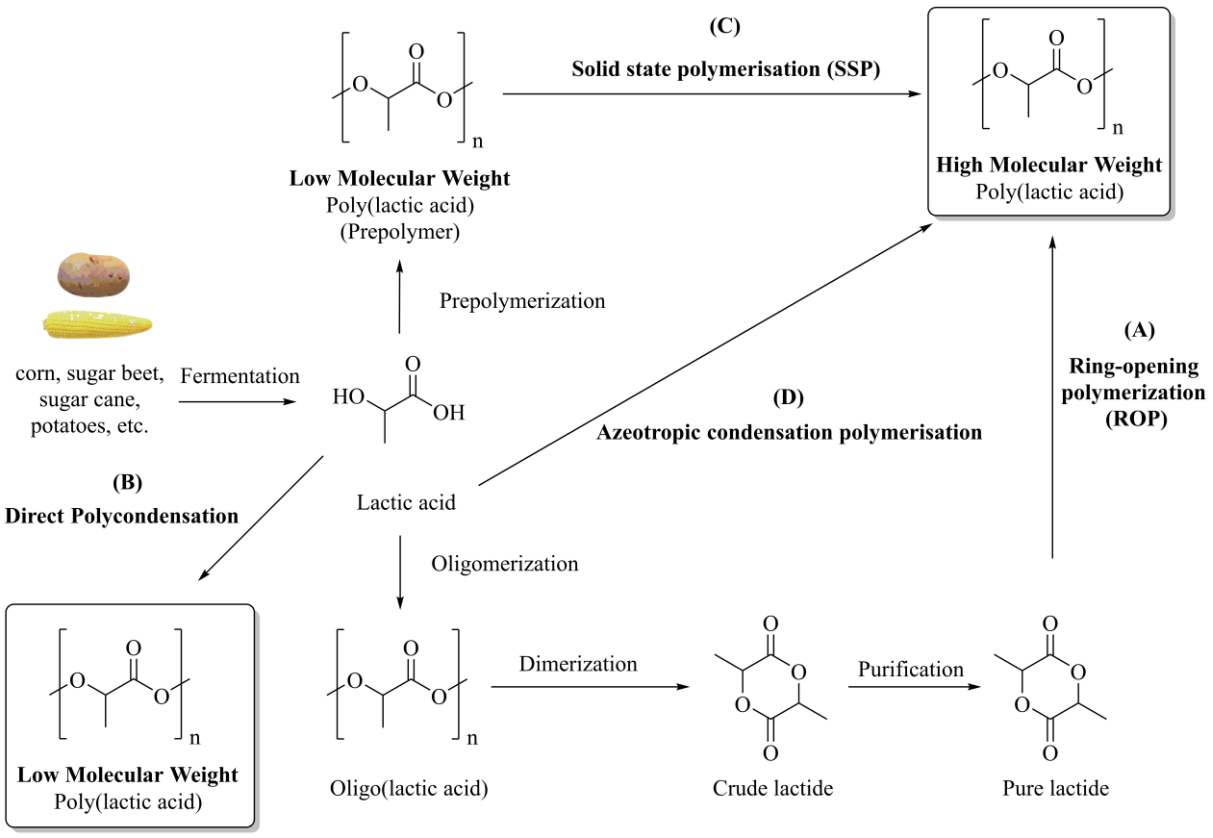


**Figure 4.** Different synthesis methods of poly(lactide acid) (PLA) according to KUMAR et al.[54] and LIN et al.[78]: (A) Ring-opening polymerization (ROP) by using cyclic dimmers; (B) direct polycondensation polymerization starting from lactic acid; (C) Solid state polymerization (SSP) by using a prepolymer and controlling process conditions; (D) azeotropic condensation polymerization by manipulating the equilibrium between monomer and polymer.

### 6.4.2 Poly(hydroxyalkanoates) (PHAs)

Polyhydroxyalkanoates (PHAs) are another bio-based polymer group, which is accessible through the fermentation of sugar as described by MÜLLER and SEEBACH.[79] PHAs are bio-based polyesters, which are build up from hyroxylalkonates monomers. PHAs also occur naturally as homopolymer (poly(3-hydroxybutyrate) [P(3HB)]) and also as copolymers poly(3-hydroxybutyrate-co-3-hydroxyvalerate (P(3HB-3HV)). [80] In bacteria, PHAs are used as an energy storage medium. In bacteria cells, P(3HB) is in the amorphous state and is present as a fluid, whereas after extraction from the cells with organic solvents, P(3HB) shows a highly crystalline and brittle behavior.[81] There are also efforts to produce P(3HB) not only from

bacteria but also from waste organic matter.[82] Genetic modification of bacteria and plants allows increased sustainable production of PHAs for future bulk applications.[83,84] Chemically, PHAs can be synthesized via ring-opening polymerization (ROP) of the corresponding lactone via metal catalysis or enzymatic routes.[85] For bacterial synthesized PHAs, REN et al. revealed that all monomeric units of PHA are enantiomerically pure and in R-configuration.[86] In comparison to that HAYWOOD et al. showed that if pure (S)-methyl 3-hydroxybutyrate is used as feedstock for the production of PHAs, the corresponding (S)-configuration polymer is generated.[87] In **Figure 5**, the biological synthesis of PHA is depicted. The synthesis involves sugars, which are converted into acetates, which are subsequently complexed to coenzyme A (CoA) and to form acetyl coenzyme A (acetyl CoA). Afterward, this compound is dimerized to acetoacetyl CoA, which is followed by a reduction to hydroxyl butyryl CoA and subsequent polymerization to PH3B.[15] There are different types of PHAs like for example short-length PHAs (sCL-PHAs), which consist of 4–14 carbon atoms in the monomer unit. Another well-known PHA is for example medium chain length PHA (mCL-PHA).[88] The chain length influences the thermal properties of PHAs. A longer polymer chain leads to a decreased melting temperature. PH3B shows a melting temperature of $T_m$ = 160 °C and a glass transition temperature of $T_g$ = 4 °C.[15] The glass transition temperature is decreasing with an increased PHA chain length. In terms of processing, PHAs show a problematic behavior due to the low degradation temperature of 180 °C and the optimum processing temperature in the same region. High shear forces during processing cause a high internal heat, which leads to degradation, a decrease of molecular weight, and discoloration. Therefore, high precision and good monitoring are necessary to ensure an unbroken polymer. Low durability and insufficient crystallinity are also challenging factors during processing.[15] Some PHAs show degradability and physical properties comparable to polyalkenes, which is advantageous for commercial use. The biosynthesis with bacteria is also quite cheap and might be up scalable in the future.[89]

### 6.4.3 Succinate Polymers

Succinate polymers are based on succinic acid (SA), which can be derived from the fermentation of agricultural carbohydrates or can be obtained from bacteria like Escherichia coli.[90,91] Poly(butylene succinate) (PBS) and its copolymers are a group of biodegradable polymers, which are showing biodegradability, thermoplastic processability, and balanced mechanical properties. It can be directly synthesized by direct polycondensation of succinic acid and butanediol (BD) (**Figure 5**).[92] Another interesting polymer from the succinate family is poly(ethylene succinate) (PES), which displays biodegradability and could be obtained from

a bio-based feedstock.[93] It shows promising film applications due to its good oxygen permeability and its high elongation at break. Several copolymers of succinic acid and other dicarboxylic acids have been synthesized like for example poly(butylene succinate-*co*-butylene adipate)[94], poly(butylene succinate-*co*-butylene terephthalate)[95], or poly(butylene succinate-*co*-butylene furandicarboxylate).[96] In terms of thermal and mechanical properties succinate polymers show soft properties due to the long alky chains they possess. This makes them excellent candidates for a bio-based alternative in the packing industry.[15]

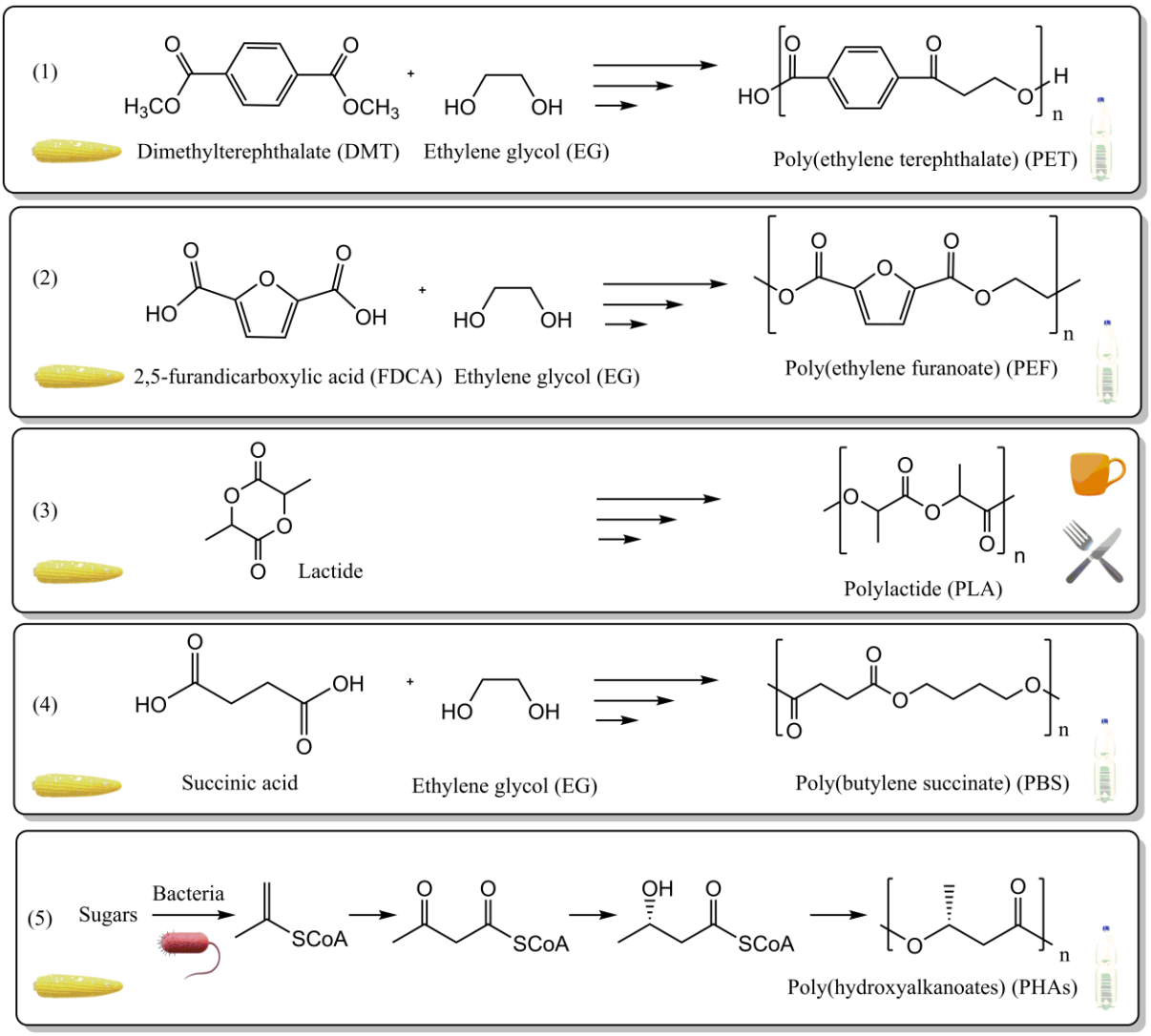


**Figure 5.** Synthesis of bio-based polymers based on polysaccharides: (1) Poly(ethylene terephthalate) (PET) (2) Polyethylene furanoate (PEF) (3) Polylactide (4) Polybutylene succinate (PBS) (5) Polyhxdroxyalkanoates (PHAs) (adapted from NAKAJIMA et al.[97] and WILLIAMS et al.[3] with permission of Springer © 2016).

## 6.5 Bio-based polymers based on terpenes and terpenoids

Terpenes and terpenoids are also a class of pre-monomers, which can be useful for the synthesis of bio-based polymers. These substances are based on the structure of isoprene and are obtainable from essential oils.[98] In nature plants are utilizing terpenes for defense and frightening herbivores. These terpenes can also be chemical modified and functionalized, which results in terpenoids. Terpenoids mainly originate from oxidation, hydrogenation, or rearrangement of the carbon skeleton.[15] Natural rubber is one of the most used polyterpenes. It is largely produced with over 10 megatons per year.[3] Other terpenes are investigated less for polymer production in comparison to natural rubber, but still, there is potential to find. For example, turpentine, which is extracted from pine trees (Pinus spp.) and it consists mainly of α-pinene (45–97%) and β-pinene (0.5–28%). Also, limonene, which is extracted from the peel of citrus fruits shows huge potential as a pre-monomer.[99] These terpenes are produced in moderate quantities and are available for polymer synthesis. In 2013, about 0.3 kilotons of turpentine[100] and about 0.7 kilotons of limone[101] were produced.[3] The produced terpenes and terpenoids are mostly used in essential oils and fragrances for perfumes, cosmetics, and pharmaceuticals. The possibility for terpene polymerization is extensively studied during the last decade due to the need for polymers from a natural feedstock (**Figure 6**).[102] A major disadvantage of terpene-based polymers is their low molecular weight, but this can be overcome by using for example cationic polymerization of β-pinene followed by hydrogenation as shown by SATOH et al.[103] Polymers, which based on β-pinene or α-phellandrene, show a high glass transition temperature of > 130 °C, high transparency, and amorphous character. This makes them ideal candidates for potential applications.[103–105] In comparison to this cationic polymerization methods, radical polymerization can also be applied to the more predominant α-pinene, as also shown by SATOH et al.[106] In comparison β-pinene, the more predominant α-pinene is difficult to polymerize into high molecular weight polymers, because of the large steric hindrance around the trisubstituted C=C bond. Due to that reason, the α-pinene is polymerized via pinocarvone to a bio-based polyketone.[106] This polymer shows a relatively high glass transition temperature ($T_g$ > 160 °C). Another terpene, which is produced in higher quantities (57.000 t $a^{-1}$)[107], is limonene. Limonene is a cyclic terpene, which exhibits the typical smell of citrus fruits. Not only commercial applications in the food or pharmaceutical industry are possible for limonene, but also the use as a monomer might be possible. SINGH et al. polymerized limonene radically with benzoyl peroxide (BPO) as a starter to produce poly(limonene) with a high glass transition temperature ($T_g$ = 116 °C).[108] Copolymers of limonene and N-vinyl pyrrolidone with azobisisobutyronitrile

(AIBN) as a starter were synthesized by SHARMA et al.[109] It is also possible to generate partial bio-based polymers like for example copolymers of terpenes and petrochemical-derived vinyl monomers, which was also investigated by SHARMA et al.[110,111] Copolymerization of limonene and $CO_2$ is also possible as shown by KLEIJ et al.[112] Stereocomplexity of poly(limonene carbonate) (PLimC) was investigated by COATES et al. in several publications.[5,113,114] GREINER et. al improved the synthesis method of PLimC by masking hydroxyl impurities in the monomer mixture to produce a high molecular weight polymer with high transparency and good mechanical properties.[6] Another bio-based terpene monomer, which was investigated by GREINER et al. for polymerization reactions is menthol. Copolymerization of menth-2-ene oxide derived from menthol and $CO_2$ was carried out to give in high molecular weight poly(menth-2-ene carbonate) (PMen2C) with high thermal stability (~$T_{5\%}$ = 300 °C).[115] The monoterpene myrcene is also interesting as a bio-based monomer. It can be readily obtained from plants[116] or from the pyrolysis of pinene.[117] HILLMAYR et al. investigated the synthesis of diene 3-methylenecyclopentene from the naturally occurring monoterpene myrcene by ring-closing metathesis using Grubbs second generation catalyst. Radical, anionic, and cationic polymerizations of this cyclic diene monomer were carried out to produce amorphous polymers with low glass transition temperatures ($T_g$ = -4 - 11 °C).[118] Rubbery copolymers from β-myrcene and dibutyl itaconate were investigated by BHOWMICK et al. for biobased elastomer applications.[119] A problem, which restricts the commercial use of terpene-based polymers is their high cost in comparison to petro-based polymers. A common use for polymers is their application as thermoplastic elastomers, which should be focused in future for terpene-based polymers as well. Petro-based polymers are produced in large quantities (> 3.5 mega tons per year) and show good mechanical properties for their use car suspension systems, window seals, coatings of household goods or electronics, shoe soles, or medical devices.[120] It is also possible to produce renewable ABA triblock copolymers by sequential polymerization of the plant-based monomers menthide or myrcene to gain access to terpene-based thermoplastic elastomers.[121,122] These thermoplastic elastomers can have moderate mechanical properties like for example a high *E*-modulus (6 MPa). This is comparable to commercial polystyrene-butadiene-styrene (SBS). The drawback of these terpene-based polymers is the relatively high glass transition temperature ($T_g$ = 170 -190 °C) or lower elongation at break values (< 1000%) in comparison to commercially available polymers. In terms of mechanical properties, terpene-based polymers are still improvable compared to petro-based polymers.[3]

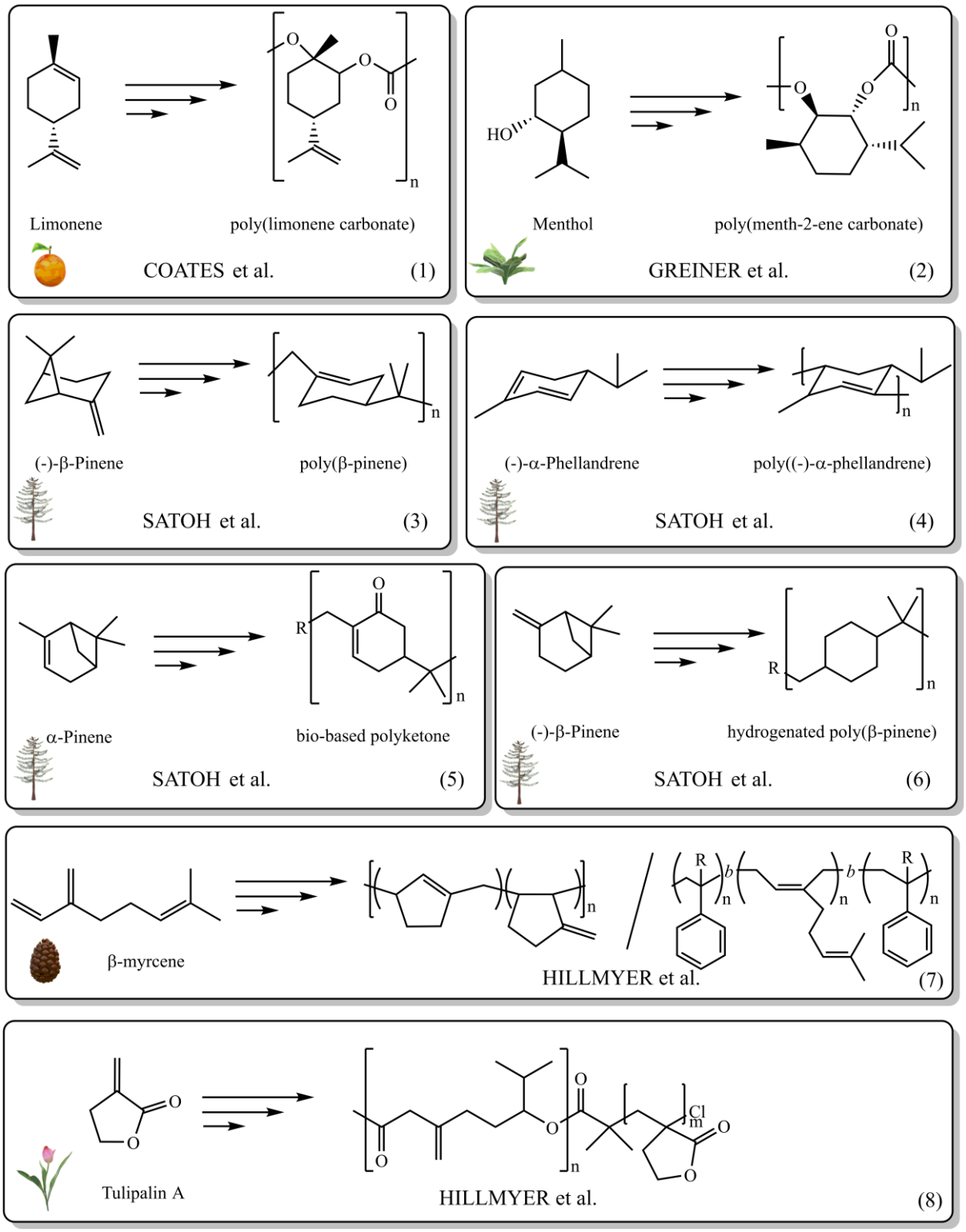


**Figure 6.** Synthesis of bio-based polymers based on terpenes and terpenoids: (1) poly(limonene carbonate)[5], (2) poly(menth-2-ene carbonate)[115], (3) poly(β-pinene)[103], (4) poly((-)-α -phellandrene)[104], (5) bio-based polyketone[106], (6) hydrogenated poly(β-pinene)[103], (7) (bio-based) polymers based on β-myrcene[118,119], (8) bio-based polymers based on Tulpipalin A[121].

## 6.6 Bio-based polymers based on vegetable oils

Vegetable oils can also be used as a source for monomers.[123] Triglycerides for example can be obtained from soybean (Glycine max), oil palm (Elaeis), oilseed rape (Brassica napus), and sunflower (Helianthus) and they are produced on a bigger scale due to the demand of the food industry. Parts of the produced vegetable oils are not only used in the food industry, but also as biofuels or as chemical feedstocks.[3,124] Resins, coatings, and paints are the main applications for epoxidized oils like for example linoleum, which is obtained from linseed oil. Castor oil is also an important vegetable oil because it can be used to produce PA 11, PA 6.10, or PA 4.10 (commercial name: Nylon®). It is harvested from the seeds of the castor oil plant (Ricinus communis). These bio-based polyamides (**Figure 7**) can have interesting properties for commercial applications like for example low water absorption, high chemical resistance, high-temperature stability, and a lack of long-term aging as shown by STEMPFLE et al.[124] The drawback of these polymers is the used castor oil, which contains impurities like for example hydroxyl groups that promote depolymerization reactions. Also, the cost factor of castor oil is to consider for the use of these castor oil-based polymers. The price of palm oil or rapeseed oil is twice as cheap as the price of castor oil.[3] The use of triglycerides is also limited due low amount in soybeans or other plants. Usually, only 20 wt% of triglycerides can be harvested from these plants.[3] The chemical composition of the obtained triglycerides within the plant is also problematic. It has a huge variety of different fatty-acid groups that are linked together through ester bonds to a glycerol unit, which has to be split by transesterification reactions to produce fatty esters and glycerol. The side product glycerol can be applied in resin production, epichlorohydrin synthesis, or in conversion to lactic acid.[125,126] Fatty acid-based thermoplastics, which are based on long alkyl chains (C12–C22), show the highest potential for applications because their properties and characteristics are lying in-between polyalkenes, such as polyethylene and more polar short-chain polyesters. Several polymerization techniques are using fatty acids to produce polymers. Despite the nonuniform content of unsaturated fatty esters (about 20–60 wt%) in plants oils, there are approaches to increase the number of fatty esters ( e.g., oleic acid) within soybean lines by targeted mutagenesis as shown by HAUN et al.[127] This would be quite useful for the production of bio-based polymers. There is a variety of methods and techniques (i.e, thiol-ene reaction, acyclic diene metathesis, epoxidation, and radical or thermal crosslinking reactions), which allows the use of alkene groups of fatty acids to form polymers as shown in a review of MEIER et al.[128] Another approach to produce bio-based polymers based on unsaturated fatty acids from plant or algae oils are isomerizing

functionalization reactions that convert the internal double bonds of unsaturated fatty acids to a terminal functional group. The produced α,ω-diesters or α,ω-diols can be used for condensation polymerizations to yield bioderived polyesters or polyamides, if α,ω-diamides are used as monomers. The major disadvantage of this method is that only about half of the fatty acids are used in the process. Additionally, unwanted side products are generated.[129] To overcome these problematic issues, the use of selective chemical catalysis to isomerize the internal alkene group to the chain is necessary. Furthermore, an alkoxycarbonylation process is unavoidable to enable near-quantitative production of the desired α,ω-difunctionalized monomers. This was demonstrated by STEMPFLE and WITT et al.[130,131] Bio-based polymers can also be produced by standard polycondensation process as shown based on methyl ω-hydroxytetradecanoic acid, a monomer available by a fermentation process using *Candida tropicalis bacteria*.[132] Enzyme catalysis to form polymers is also possible as a review of GROSS et al. showcases.[133] Despite the variety of possibilities to make use out of vegetable oil-based polymers the low cost of petrochemical-derived polyethylene is still hard to compete with.[3]

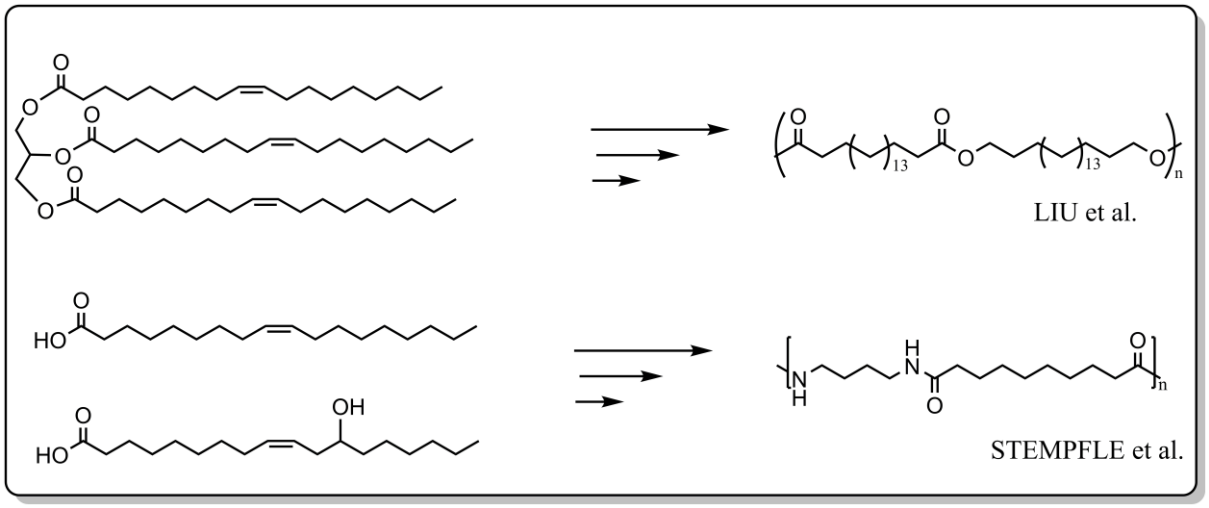


**Figure 7.** Synthesis of bio-based polymers based on vegetable oils. Long-chain aliphatic polyesters can be synthesized by using triglycerides.[132] Starting from fatty acids also polyamides are accessible.[131]

## 6.7 Blends

### 6.7.1 Blends in general

To enhance the mechanical properties of polymers (e.g., PLA), two or more polymers can be mixed to create a new material with improved physical properties. Typically, polymer blends are divided into five groups: thermoplastic–thermoplastic blends, thermoplastic–rubber blends, thermoplastic–thermosetting blends, rubber–thermosetting blends, and polymer–filler blends.[134] Additionally, polymer blends can be categorized into homogenous (miscible) and heterogenous (immiscible blends).[135] Examples for miscible blends are (PS)–poly(2,6-dimethyl-oxide) (PPO) and poly(styrene-acrylonitrile) (SAN)–poly(methyl methacrylate) (PMMA) blends. Examples of immiscible blends are poly(propylene) (PP)–PS and polypropylene–polyethylene (PE) blends.[134] Compatibility between the polymer phases is also an important aspect to consider for blend production because it determines the properties of a heterogenous blend. The Flory-Huggins theory describes the polymer-polymer interactions in terms of miscibility and can predict properties of homogenous or heterogenous blends.[136,137] The advantage of polymer blends lies in the inexpensive production and reduce the time to commercialization.[138] By choosing the right blending partners, the properties can be changed specifically according to requirements.[139] This enables the application of polymer blends in several everyday products (e.g., household plastic products, automotive components, biomedical devices, and aerospace applications).[139]

### 6.7.2 Miscibility and compatibility

Miscibility and compatibility are important key factors for polymer blends because they influence largely morphology, properties, and performance. Miscible blends are homogenous, mechanical properties of their components are average ($\Delta G_m < 0$) and they show a single glass transition temperature. Partially miscible blends are partially phase-separated, mostly keep their mechanical properties of individual component polymers ($\Delta G_m > 0$) and they show two glass transition temperatures, which are intermediate to the component polymers. Immiscible blends show a complete phase separation, mechanical properties are determined by a polymer-polymer interface ($\Delta G_m > 0$) and they show two glass transition temperatures of the component polymers.[140]

Hydrogen bonding, Van-der-Waals interaction, or dipole-dipole interactions are the main forces, which are important in polymer blends, whereas covalent bonds are mainly occurring in copolymers. In comparison to polymer blends, copolymers are polymers, which are made of at least two different monomers. There are different types of copolymers like for example alternating copolymers, random copolymers, block copolymers, or graft polymers. Alternating copolymers are described as polymers in which the different monomer units are alternating. Random copolymers are characterized as copolymers, in which the monomers are repeated randomly. Block copolymers are a combination of repeating blocks of different monomer units. Graft copolymers show structurally different side chains than the main chain. These different structural arrangements of different monomers mainly determine the thermal properties (e.g., glass transition temperature or melting temperatures) or the mechanical properties like for example the *E*-modulus or tensile strength. In a random copolymer, these properties are averaged, whereas block copolymers show properties of both polymers.[141]

One way to describe the polymer miscibility profoundly is to use the "Mean Field Theory" (MFT), which explains the dissolving process of a polymer in a given solvent. Based on the lattice fluid theory, it explains the miscibility of low molar mass liquids.[142] Lattice chain theory, which is the simplest version of this, is called Flory–Huggins solution theory (**Figure 8**).

Using this two-dimensional lattice model allows to describe a system consisting of n sites, with each site occupied by the solvent or a polymer repeating unit. Double occupancy and a vacancy are excluded in this system, so the volume of the polymer ($V_p$) is described as:

$$V_p = \frac{n \cdot \Phi}{N} \quad (1)$$

In this equation, φ is the volume fraction of the polymer and N is the number of sites occupied by a linear polymer with N-1 number of bonds. The volume occupied by the solvent molecules can be described:

$$V_s = n \cdot (1 - \Phi) \quad (2)$$

FLORY is using this mathematical description to calculate the entropy of mixing by counting the number of possible arrangements for the polymer in the molten state and solution. The mixing of two polymers usually leads to a system with complete phase separation due to repulsive interactions between the blend components.[143] If the thermodynamic equation for the GIBBS energy change ($\Delta G_m$) at constant temperature and pressure is fulfilled miscibility can be realized:

(3) $$\Delta G_m = \Delta H_m - T\Delta S_m < 0$$

where $\Delta G_m$ is the free energy of mixing, and $\Delta H_m$ and $\Delta S_m$ are the enthalpy and entropy of mixing at temperature T. A stable one-phase system is described as:

(4) $$\Delta G_m < 0\,, \left(\frac{\delta^2 \Delta G_m}{\delta \Phi^2}\right)_{T,P} > 0$$

If the free Gibbs energy change is negative and the domain size is comparable to the domain size of the macromolecular statistical segment (homogenous even on the molecular level), the polymer blend can be regarded as a miscible polymer blend. A combination of entropy of mixing, interaction energy, free volume, and specific interactions such as hydrogen bonding is mainly responsible for polymer miscibility. Using the FLORY-HUGGINS equation the blend miscibility for nonpolar polymers can be calculated:

(5) $$\frac{\Delta G_m}{RT} = \left(\frac{\Phi_1}{N_1}\ln\Phi_1 + \frac{\Phi_2}{N_2}\ln\Phi_2 + \Phi_1 \cdot \Phi_2 \cdot \chi_{12}\right)$$

where the indices representing each component, $\phi$ the volume part of each component, R the ideal gas constant, T the temperature. and $\chi$ the FLORY-HUGGINS interaction parameter calculated using the Hildebrand solubility parameter. The first two logarithmic terms in this equation representing the combinatoric mixing entropy. The third term in the equation is representing the mixture entropy. Because polymers have a big volume, the first term becomes nearly 0, and the miscibility is mainly influenced by the enthalpy term. The consequence is, that in a homogenous blend hydrogen bonding, dipole-dipole, ionic, van-der-Waals- or $\pi$-$\pi$ interactions are responsible for miscibility.[140]

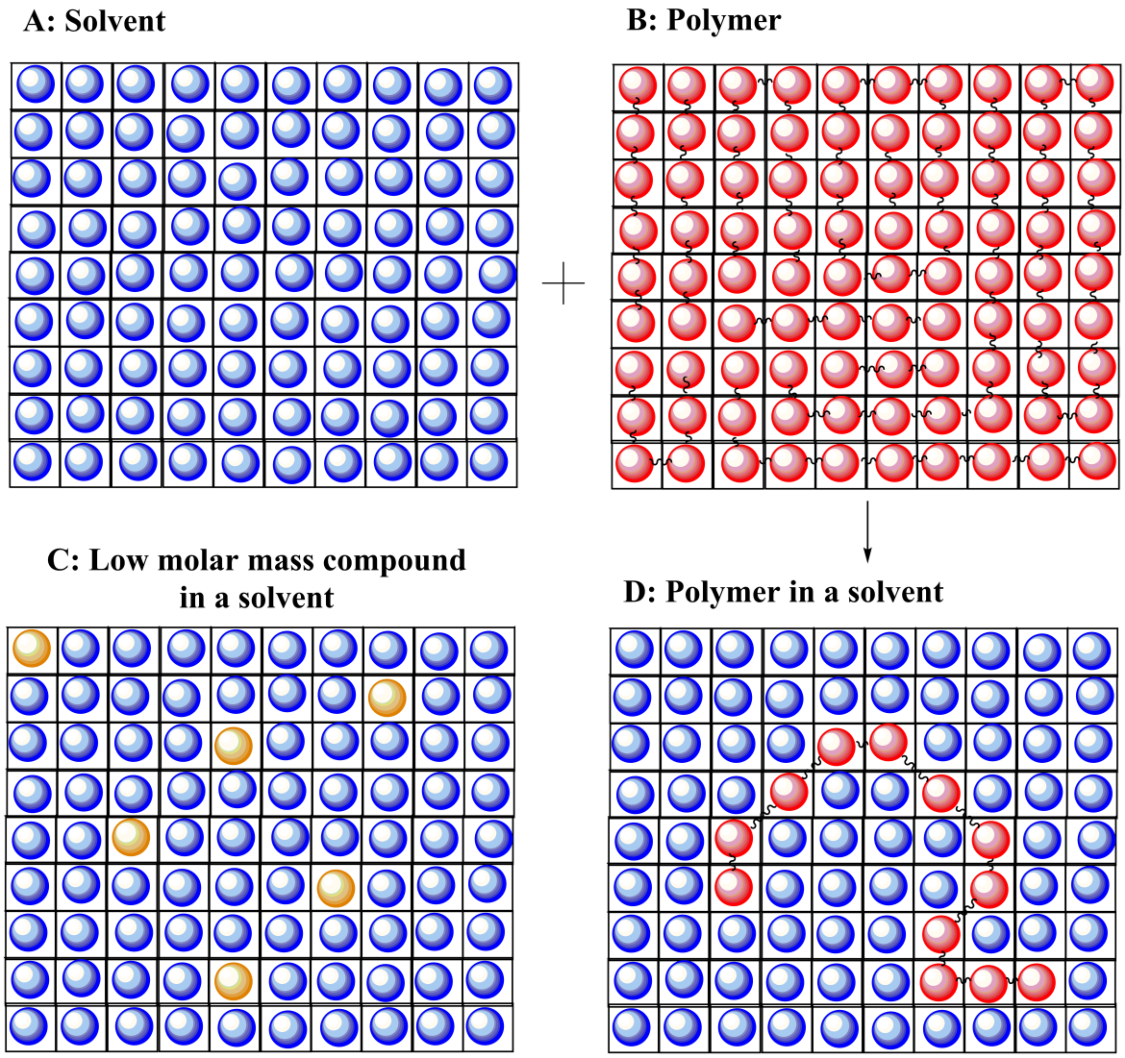


**Figure 8.** The lattice model according to mean-field theory for solvent molecules (A), polymer molecules (B), a low molar mass compound in a solvent (C), and a polymer in a solvent (D). The blue spheres represent the positions occupied by the solvent molecules. The orange spheres represent the positions occupied by a low molar mass compound. The red spheres represent the positions occupied by a polymer compound (adapted from THOMAS et al.[140] with permission of Elsevier © 2014).

A phase diagram can be created by applying the thermodynamic equation for the GIBBS energy change, which displays three different regions with different degrees of miscibility. The miscibility of polymers is also a function of temperature and also the interaction of each polymer must be considered.[143] PS-PPO blends are an excellent example of miscible polymer blends, which have high toughness, heat resistance, and show inflammability.[144] The thermal analysis of this polymer reveals a single glass transition temperature intermediate between those of the individual components. Important phenomena occur if two polymers are mixed at low temperatures and then phase separate on heating. This critical point is called lower critical solution temperature (LCST). Another effect happens if two polymers remain phase-separated at ordinary temperatures and form a single phase at high temperatures. This is called upper

critical solution temperature (UCST) (**Figure 9**). Mathematical, it can be described that the heat of mixing must balance the product of entropy of mixing and absolute temperature at the critical temperature:[140]

$$\left(\frac{\delta^3 \Delta G_m}{\delta \Phi^3}\right)_{T,P} = 0 \quad (6)$$

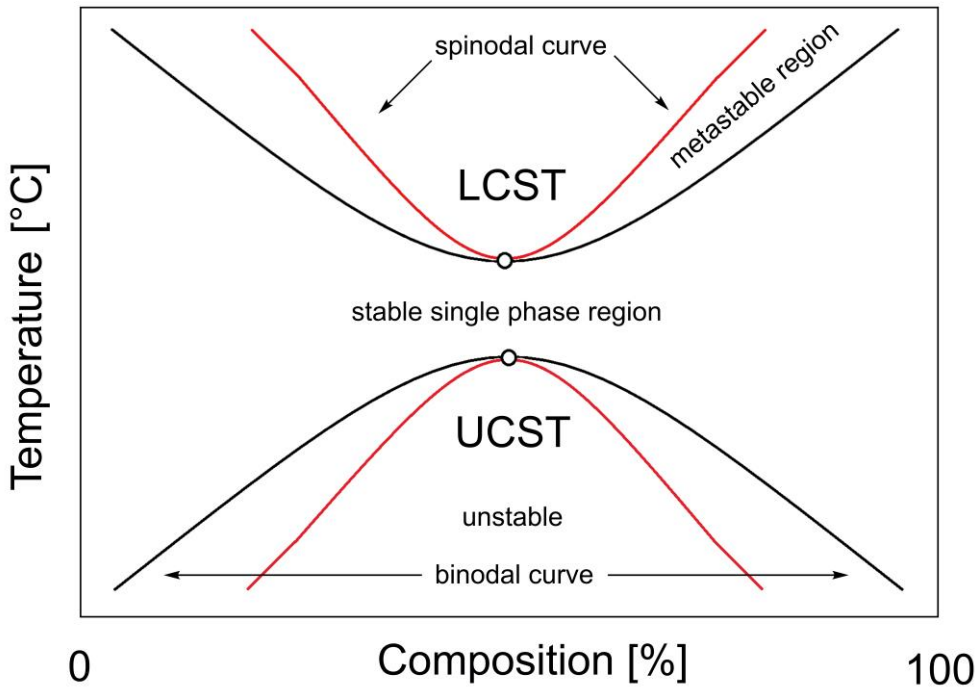


**Figure 9.** The phase diagram is showing the typical behavior and regions of a binary polymer blend. The lower critical solution temperature (LCST) and the upper critical solution temperature (UCST) are highlighted (adapted from KALOGERAS et al.[145] with permission of John Wiley and Sons © 2016).

### 6.7.3 Morphology of polymer blends

The morphology of a polymer blend system is mainly determined by the miscibility of each component, the interfacial tension between the two polymer phases, and as well by surface tension (energy) of the two polymers.[146] Polymers are usually high molecular weight molecules and so they have negligible entropy of mixing. If the enthalpy of mixing is positive if there is no specific interaction and the result of this fact is the immiscibility of polymers. For some deployments, it is necessary to have immiscible blends because the properties of immiscible blends suit more the application. An example of this would be PS and polybutadiene (PBD or BR) blends, which are sold commercially under the name high-impact polystyrene (HIPS).[147] PS is a rather brittle material but blending with PBD leads to improved properties due to the rubber properties of PBD. PBD can absorb more energy under stress, so the immiscible blend

is more robust. It is used in the housings of computers, televisions, fridges, or telephones. Different blend morphologies of binary blends and their tuning potential are displayed in **Figure 10**. An emulsion form of immiscible polymer blends is often used to modify mechanical properties such as toughness and stiffness (**Figure 10A**). Mechanical loading and stress can be easier tolerated by polymer blends in their emulsion form, because of their broad space distribution. The laminar form of polymer blends can be used for example in packaging applications, in which barrier properties are important (**Figure 10C**). For load-bearing applications, oriented structures are interesting due to their increased stability in this direction. Continuous structures can be used for example to enable electrical conductivity (**Figure 10E**).[148]

Interfacial tension and surface tension are the key characteristics in terms of immiscible polymer blends and their properties.[149] Improving mechanical properties usually involves manipulating interface adhesion of immiscible polymer blends. This can be achieved for example by using compatibilizers. On the one hand, compatibilizers allow to decrease the interfacial tension, decrease the size of the dispersed phase or interfere in the dynamic or static coalescence processes. On the other hand, compatibilizers can increase the adhesion between phases and therefore achieve microstructure stabilization.[150–152] There two main ways to improve polymer miscibility. The addition of a copolymer that is mixable or highly compatible with one of the individual polymer components of the blend or to use a compatibilizer during reactive processing. Regarding the first option (addition of copolymer), diblock copolymer, three-block copolymer, branched, or judged copolymers can be used to increase interface adhesion and tune mechanical properties of the corresponding polymer blend system.[153] The other possibility for tune compatibility of polymer blends is to apply a third component that has functional groups, which can react with both phases on the interfaces of the polymer blend. The third component can also have a tail compatible with one of the phases and a functional group that can react with the second phase. On a molecular level, the use of a compatibilizer allows to position molecules on the interface and this, therefore, reduces the interconnected free energy of the system. Oversaturation of compatibilizer is possible if too much compatibilizer is used so that interface adherence between each polymer cannot be influenced anymore. High amounts of compatibilizer lead to micelles in the system.[148] The correlation between morphology and mechanical properties is important for modifying blend properties and ultimately for practical applications.[146,154] Composition, rheological and physical characteristics of the components, relative compatibility, and the nature and intensity of the mixing are features of polymer blends, which have to be considered when tuning blend properties.

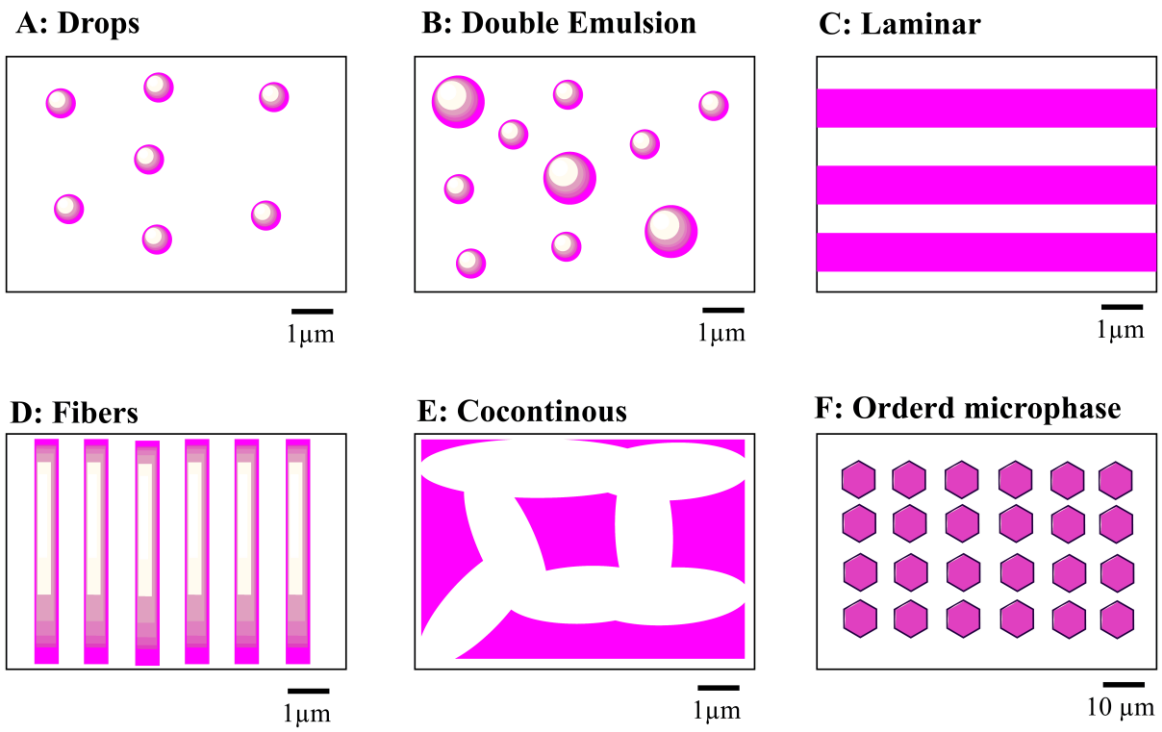


**Figure 10.** An overview over different morphologies of immiscible polymer blends and their potential tuning abilities is displayed: A: drops (toughness and surface modification), B: double emulsion (toughness and stiffness), C: laminar (barrier), D: fibers (strength and thermal expansion), E: concontinous (high flow, electrical conductivity, toughness, stiffness) and F: ordered microphase (adapted from VUKSANOVIĆ and HEINEMANN et al.[148] with permission of Elsevier © 2020).

It is also possible to use different mixers and/or changing mixing parameters to control the phase morphology of an immiscible blend.[155,156] Morphology evolution during processing of granulate/pellets or powder particles is also possible as shown by THOMAS et al.[157] Understanding of mechanisms and kinetics is key for generating suitable mixing procedures. The blend morphology is forming during processing due to stretching into treads or due to the formation of small droplets.[157] On the one side, decomposition is not influenced by the content of the dispersed phase, but on the other side, coalescence is strongly influenced by the composition of the mixture.[157,158] Several publications are dealing with the combination of these factors and the corresponding morphology.[159,160] Not only the mixing process has a strong influence on the blend morphology, but also fillers can have a serious impact on the structure. Electronics, magnets, optics, and photonics are sectors, in which the development of nanomaterial is essential.[161] Polymer characteristics (e.g., mechanical properties) can be improved by the use of fillers, which was shown for example by AVCI et al. In the case of glass fibers.[162] Fillers can also be applied in polymer blends with two or more components as shown by ZHANG et al.[163] The downside of applying fillers is the negative effect on the *E*-modulus. It is usually decreased, which is revealed by Ying et al. with the example of PMMA/Ethyl vinyl

acetate/silica composites.[164] The dispersion of fillers in polymer blend is an interesting subject as well. LE et. al showed that the reciprocated stress of the filler and the relationship to each blend component is a key factor in how the filler is dispersed.[165] Additionally, the filler affects the blend morphology itself. Several factors determine the distribution of fillers inside a polymer blend (e.g., type of polymer, interaction of polymer fillers, or the mixing process).[146] The morphology of immiscible polymer blends is mainly determined by their composition, the properties of individual components, and their corresponding phase structure.[146] For improvement and prediction of mechanical properties the evolution of the phase structure of blend preparation and processing is an essential factor to consider.[166] Rheological properties (viscosity ratio) of the blend of the partner, the composition of the mixture, interfacial tension, and the processing conditions also important key factors in terms of blend morphology as shown by NAMHATA et al.[167] and BÄRWINKEL et al.[168] The use of block or graft copolymer can help to control the morphology of polymer interfaces.[169] Compatibilizers like block or graft copolymer can increase the degree of dispersion and can further stabilize morphology (**Figure 11**). These compatibilizers must be prepared before or can also be prepared in situ by reactive processing. Controlling the size and shape of the dispersed polymer phase of immiscible blends is rather difficult, but very important to achieve desirable properties. [170,171] The complex flow and temperature fields developed during melt processing, the process of droplet elongation, breakdown, and coalescence, or the viscoelastic nature of the phase factors, which make it hard to adjust the blend morphology.[172] Immiscible blends usually showing two major forms of morphology. Either a droplet or a cocontinuous morphology can be observed. A droplet morphology is described as the dispersion of the minor component into the other component in the form of spherical droplets. In the other version, the cocontinuous morphology is displayed by two polymers, which are fully interconnected.[172] Cocontinuity is usually observed for two immiscible polymers with a 50/50 composition. This cocontinuity can be tuned using block copolymers. Applying block copolymers reduces the interfacial tensions and enables an easier formation of cocontinuous morphologies as shown by DEDECKER et al. in the case of polyamide 6 (PA6)/ PMMA.[173] GALLOWAY et al. revealed that tapered block copolymer can stabilize the blend morphology compared to pure block copolymers.[174] This effect was explained by the gradual composition change in the middle of the polymer chains, which are better corresponding to the composition at the interface between the homopolymers. This offers better stabilization during annealing than pure triblock copolymers. Reduced conformational constraints at the interface are the explanation for this better stabilization. TAYLOR et al.[158] and GRACE et al.[175] showed that the size of the dispersed phase of immiscible liquids is determined

by viscosity ratio $\lambda = \eta_d/\eta_m$. In this equation, $\eta_d$ is the viscosity of the dispersed phase and $\eta_m$ is the viscosity of the phase of the matrix. A value close to one increases the probability of a finely dispersed droplet structure. A deviation from this rule was found by WILDES et al., who showed that the average particle size for blends compatibilized with a SAN–amine polymer was approximately half that of uncompatibilized blends and was relatively independent of viscosity ratio and dispersed phase composition.[176] Coalescence or interfacial coarsening are two additional factors, which influence the blend morphology according to TUCKER et al.[177] As a third-factor micro- and nanoparticles can improve mechanical properties and stabilize the morphology.[148]

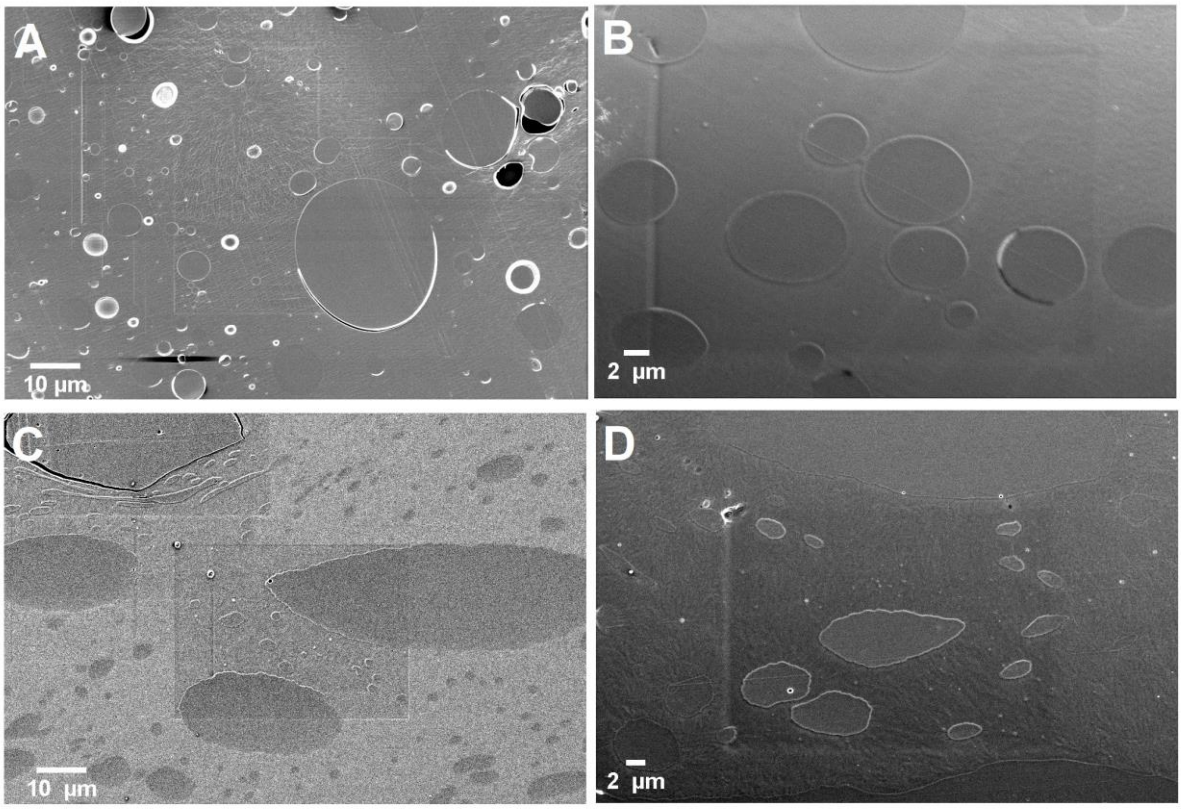


**Figure 11.** SEM of neat PLA/PLimC blends and compatibilized blend. A, B) neat PLA/PLimC = 70/30 w/w. C, D) PLA/PLimC = 70/30 w/w with PLimC-PLA block copolymer (PLimC/PLA = 2/1 n/n%) as compatibilizer (unpublished results, SIMON NEUMANN).

### 6.7.4 Blends based on bio-based and petro-based polymers

Hybrid blends of bio-based and petro-based polymer are quite interesting because they reduce the environmental footprint and at the same time mechanical and optical properties of packaging material could be preserved. Usually, bio-based materials are largely affected by

moisture and show therefore not sufficient gas barrier properties. This can be overcome with hybrid materials.[178] Another important factor for using hybrid materials is that the cost of bio-based polymers is higher than conventional petro-based materials, so combing both products is advantageous. Recyclability is also one important factor to consider. Newly developed bio-based plastics could also interfere with established recycling systems.[179–182] Compostable bioplastics could hinder the stream of recycled conventional petro-based plastics (PP, PE, PET, etc.). Nevertheless, introducing bio-based materials reduce recyclability when compared to conventional petro-based polymers.[183,184] There is a variety of bio-based polymers and materials, which can be used for blending with petro-based polymers.

*Blends based on starch*

Blends of starch and artificial polymers (e.g., PCL, PA, etc.) show potential applications as packaging material.[185,186] Also, chitosan-based polymer blends are interesting due to the nontoxicity, biodegradability, and biocompatibility of chitosan. Blends of chitosan and PVA or PE were investigated by KAUSAR et al.[187] It was shown that chitosan-based blends have potential applications in membrane technology, dye removal, packaging materials, drug delivery, tissue engineering, and biochemical relevance despite the high moisture absorption, low processing temperature, low heat stability and low flame resistance of chitosan-based blends.

*Blends based on cellulose*

Cellulose is also a polysaccharide, which can be used for blends. Advantages of cellulose and its derivatives, (hydroxyl-ethyl, cellulose acetate, and hydroxyl-ethyl cellulose) are commercially available treated celluloses with good toughness, transparency, flexibility, and resistance to fats and oils.[188] For example, methylcellulose/PCL blends showed improved properties. By adding methylcellulose, PCL lowered the water vapor permeability and increases the puncture resistance.[189] Also the usage of cellulose in combination with PET shows positive results. The rate of crystallization of PET could be decreased by 30 %, which results in an improved extrusion process.[190]

*Blends based on PHB*

PHB as a blending material shows the same disadvantages like for example high degree of crystallinity and thermal instability, but it could increase biodegradation like for example in blends PE.[191] For PHB/PET blends DIAS et al., found similar melting temperatures without any significant interaction between them.[192] Investigation of blends of LDPE/PHB blends was also

performed and revealed cylinder-like fibrils of PHB.[193] Thermal, mechanical and morphological properties of PHB and PP blends were investigated by PACHEKOSKI et al. who found out that PHB/PP blends show better mechanical properties than pure PHB and a tendency for lower crystallinity and stiffness of the polymer matrix PHB. Similar degradation pure PHB and blends with 90% PHB and 10% PP.[194]

*Blends based on PLA*

PLA is also a polymer, which is based on polysaccharides. Therefore, its blends with commercial polymers are also interesting. Blends of PLA and poly(ethylene glycol) (PEG) blends were investigated by MCCARTHY et al.[195] It was found out that PLA/PEG blends range from miscible to partially miscible. With an increasing amount of PEG, higher elongations at break and lower *E*-moduli values are observed. Above 50 % PEG, the crystallinity of PEG influences the blend morphology and the mechanical properties. The trend is reversed in that case. Blends of PLA and PVA are also miscible and shown an increased tensile strength and elongation at break if low contents of PVA are added to PLA.[196] Regarding blends of PLA and polyolefins (PP or PE) poor mechanical properties were observed due to the difference in polarity between PLA and polyolefins. Also, LEE et al. used the same principle to improve properties of PLA.[197] Compatibilizers can be applied to overcome these limitations as shown by HILLMYER et. al.[198] PLA/polystyrene (PS) blends are also showing a high incompatibility.[199] Polymethacrylates and PLA show miscibility according to SHEN et al.[200] Also, FERNANDEZ-BERRIDI et al. performed a miscibility study.[201] Drawn films of PMMA/PLA blends are transparent and have high elongation. For blends of PLA and PET, reduced mechanical properties were observed due to PET's high processing temperature (~260–300 °C), which results in a degradation of PLA chains. Additionally, two polymers are not miscible, which was also observed with small amounts of PLA (5wt%).[202] This makes them unappealing for industrial use.[203] Also, the different polarity of PLA and polyolefins is problematic. This results in lesser compatibility. Usually, plasticizers and additives have to be used to overcome this characteristic.[204] PLA and PA blends were investigated to integrate the toughness of PLA into PA.[205,206]

*Blends based on PBS*

Blends on PBS could make use of the biodegradability of PBS in combination with PET, but the mechanical properties of PBS are not sufficient, and immiscibility of PBS/PET blends was found by THREEPOPNATKUL et al.[207] Tensile strength, *E*-modulus, and elongation at break are

decreased by the addition of PBS. In comparison to PBS/PET blends, blends of PE and PBS showing slightly better mechanical properties due to similarities in mechanical properties of the homopolymer according to AONTEE et al.[208] Blends of PVC and PBS are also known an increase in the impact strength, elongation at break, and inclination to biodegrade when compared to the neat PVC.[209]

*Blends based on PBAT*

Blends of PBAT and commercially available polymers could be interesting due to the thermal and mechanical characteristics of the homopolymer like low gas diffusion, chemical resistance, or good transparency. Films of PBAT and PET were investigated by higher PBAT content led to the increment of elongation at break with the sacrifice of modulus of PET thin films by THREEPOPNATKUL et al. that a higher PBAT content leads to the increment of elongation at break of modulus of PET thin films.[210]

## 6.8 Additives and plasticizers

### 6.8.1 Additives and plasticizers in general

Another way to improve mechanical properties besides blending is additive adding. Neat polymer material usually is not possessing suitable properties for a wide range of commercial applications, so additives can be used for tailoring the properties and for influencing processing positively.[211] One of the first effective uses of additives is the use of sulfur as additives for natural rubber in a process called vulcanization by Charles Goodyear in 1839.[212] Additives can be employed in several forms (e.g., solid or liquid). The appearance of the additives depends also on the production method (e.g., extrusion, pelletizing, grinding, spraying, or flaking). Nowadays, a strong environmental shift to more "greener" and safer additives can be observed.[213] Also, the use of additive masterbatches has increased significantly. The advantages of additive masterbatches are better dosability, simplified handling, homogeneous mixing, safety aspects, additive protection, and improvement of performance.[211] The combination of polymer and additive can be performed independently of the production step (e.g., during the manufacturing step of the raw material or directly applied to the finished product).[214] Plasticizers are additives, which can create flexibility, improved processing of certain materials (e.g., polymers).[215] They can decrease the glass transition temperature of polymers, reduce the melt viscosity or lower the elastic modulus of the polymer.[211] One prominent polymer, which is widely used in combination with a plasticizer is poly(vinyl chloride) (PVC). di(2-ethylhexyl) phthalate (DEHP) is mostly used as a plasticizer for PVC.[216] Plasticizers can be divided into two groups: internal plasticizers and external plasticizers.[217] An internal plasticizer lowers the glass transition temperatures and produces flexibility through grafting or copolymerization of softer monomer units. External plasticizers (e.g., DEHP) are mixed with the polymer and do not form covalent bonds.[215] This effect allows the use of PVC as electrical cable insulation, inflatable products, or in packaging.[211] The advantage of external plasticizers is the higher flexibility, easier tunable, no chemical reaction is necessary, and it is usually inexpensive.

### 6.8.2 Lubricity theory

There are different theories, which describe the mechanisms of plasticization. The most prominent theories are for example lubricity theory, gel theory, free volume theory, or mechanistic theory.[211,218]

The concepts of lubricity theory were developed by KRIKPATRICK[219], CLARK[220], and HOUWINK[221]. KRIKPATRICK describes the plasticization process as solvent interaction, lubrication of plastic micelles, and a combination of both. He explains that some of the plasticizer molecules are attached to the polymer, whereas other plasticizer molecules are not attached and act as lubricants between polymer chains. For this theory to work, the presence of groups, which show attractive forces, and the proper orientation of these groups is necessary. Also, the shape of the plasticizer molecule itself is important for this kind of interaction. CLARK explains the plasticization process by plasticizer molecules, which are filling voids in molecular space lattice. Small plasticizer molecules are acting as a lubricant in molecular space lattice so that the planes can glide over one another more easily. HOUWINK supported the concept of gliding planes and plasticizer/polymer polarities and focused on the dissolving and swelling process during plasticization. He postulated two possibilities of gliding in his work: Gliding planes are in the bulk of the plasticizer or at the surface of the polymer (**Figure 12**). In the first case, plasticizer molecules stick to the polymer chains and enable that plasticizer molecules are gliding over each other. In the second case, plasticizer molecules and polymer chains are repelling each other, which results in gliding planes at the surface of the polymer chains. This approach strongly emphasis on the amount of swelling, which depends on the polarities of polymer and plasticizer molecules.[218]

### 6.8.3 Gel theory

The gel theory was established mainly by AIKEN based on plasticized PVC.[222] He used different types of plasticizers (e.g., phosphates, phthalates, etc.) to find correlations between plasticizer effectiveness and softening, compatibility, and molecular structure.[218] In his theory, polar groups in the plasticizer and the polymer are arranging themselves to form solvating dipoles on the polymer chain. Non-polar tails, which are incompatible with PVC, would gather to form small clusters. This results in a large amount of unshielded polar polymer chains, which can form strong polymer-polymer interactions. This intermediate state between solid and liquid is called gel state and is the basis of this theory. Plasticizer molecules, which are located around the polymer chains are responsible for the micro-Brownian motion, according to AIKEN. To

explain polymer flexibility, he used the concept of a three-dimensional gel network structure, which is formed by attachments of the macromolecules along their length **(Figure 12)**. The stiffness of a polymer is the result of weak interactions of interlocked segments along the polymer chains. These points of gel are close together and therefore permitting little movement and represent elastic resistance. Plasticizer molecules reducing the rigidity of a polymer due to the reduced number of polymer-polymer interactions. Van der Waals forces, hydrogen bonding, or crystalline structure of plasticizers and polymers are the origins of these gel sites.[223] By separation of the polymer chains the polymer molecules can move more freely and thus increasing their elasticity and mechanical properties.[218]

### 6.8.4 Free volume theory

A third approach to explain plasticizer and polymer interaction is the free volume theory (**Figure 12**).[224] It was developed after lubricity and gel theory after different properties of polymers as a function of temperature were described in the literature (e.g., specific volume, thermal expansion coefficients, or viscosity).[225–227] A well-known application for this theory is the explanation of the glass transition temperature decline with increasing the plasticizer content. It was first postulated by FOX and FLORY and it is still used to describe the viscoelastic properties of polymers nowadays.[228,229] The glass transition temperature characterizes the range over the gradual and reversible transition in amorphous materials from a hard and relatively brittle "glassy" state into a viscous or rubbery state as the temperature is increased. FOX and FLORY also identified a limiting lower shear viscosity of polymers at their glass transition temperature ($\mu_g = 1 \cdot 10^{12}$ Pa·s)[230] in their work.[228] This applies to all polymers, independently from their chemical structure.[228] Based on this postulate, the viscosity of polymers was correlated to the volume between polymer molecules. Afterward, it was shown by WILLIAMS, LANDEL, and FERRY that the physical state where all materials show the same “fractional free volume” is the glass transition temperature of a polymer.[231] The specific volume of polymers decreases linearly with the temperature until the glass transition temperature is reached. After this point, the decline is happening at a smaller rate according to FOX and FLORY. UEBERREITER revealed the correlation that all the volume-temperature curves of the liquid state above the transition temperature intersect at absolute zero temperature after they are extrapolated.[227,232] This volume is the extant space, where is no moving between atoms and molecules is occurring. It was suggested by KANIG that the volume, which can be detected at absolute zero temperature and the volume measured at the transition temperature were constant for all polymers ($\rho = 0.0646$ cm$^3$/g).[227] This space in amorphous is available for oscillations. Based on these

results, it could be shown that between atoms and molecules there is nothing but the free volume and so the free volume theory can explain polymer flexibility as the difference between the observed volume at absolute zero and the volume measured at a selected temperature.[227] The Williams-Landel-Ferry model (WLF) is usually used for polymer melts or other fluids that have a glass transition temperature and assumes a linear dependence of the fractional free volume on temperature.[231]

$$\log(a_T) = \frac{-C_1(T - T_0)}{C_2 + (T - T_0)} \quad (6)$$

where $a_t$ describes the shift factor, $T_0$ the reference temperature, T the arbitrary temperature, and C universal constants, which are varying from polymer to polymer.[233] SEARS and DARBY summarized the key characteristics of plasticization by indicating that plasticization is increasing the free volume of a polymer system.[234] Different aspects influence the free volume of polymers (e.g., the motion of chain ends, the motion of side chains, or the motion of the main chain) and consequently, plasticization can be achieved by several methods:

1. increasing for example the number of end groups, which can be implemented by using lower molecular weight polymer.[218]
2. increasing the number or the length of side chains, which acts as internal plasticization.[218]
3. inclusion of segments of low steric hindrance and low intermolecular attraction, which acts as internal plasticization.[218]
4. insertion of a compatible compound of lower molecular weight[218]
5. increasing the temperature[218]

By using these principles, plasticization can be explained by the increase in free volume caused by plasticizer molecules. Consequently, the glass transition temperature is lowered. Based on this theory, it can be assumed for example that a branched plasticizer is more efficient than the linear one (considering the same molecular weight) because there is more free volume produced with the branched plasticizer. Also, increasing the molecular size of the plasticizer leads to more free volume, which results in a stronger plasticization.[218] Different mathematical models were established by using free volume theory (e.g., KANIG[232], WOOD[235], or GORDON and TAYLOR[236]). A famous equation, which is based on the work of GORDON and TAYLOR, is the FLORY–FOX equation[237], which describes how a low molecular weight additive (e.g., plasticizer) increases

the free volume of a system and afterward lowers the glass transition temperature, therefore allowing for rubbery properties at lower temperatures:

$$\frac{1}{T_g} = \frac{w_1}{T_{g1}} + \frac{w_2}{T_{g2}} \quad (7)$$

where $T_g$ is the glass transition temperatures of the mixture and $T_{g1}/T_{g2}$ are the individual glass transition temperatures of polymer and plasticizer, respectively. $w_1$, $w_2$ represents the weight fractions of the polymer and the plasticizer, respectively. The FLORY–FOX equation is widely used to predict the glass transition temperature in miscible polymer blends and statistical copolymers.[238]

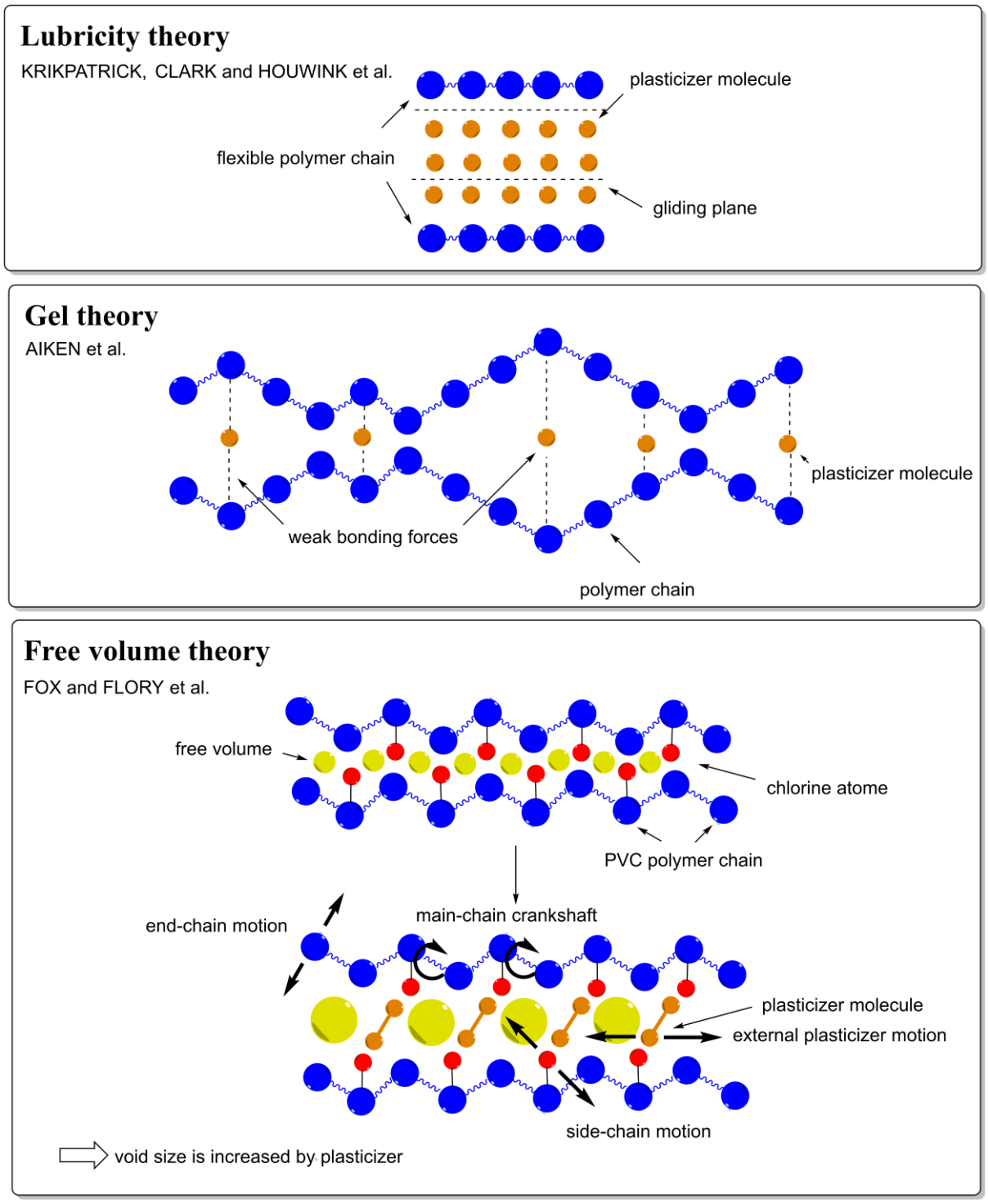


**Figure 12.** Overview of different plasticizer theories. Lubricity theory of KRIKPATRICK[219], CLARK[220], and HOUWINK[221]: Flexible polymer chains (blue) interact with plasticizer molecules (orange). Two possibilities for gliding are depicted according to HOUWINK. Gel theory of AIKEN[222]: Polymers are formed by an internal three-dimensional structure. The plasticizer molecules reduce the polymer-polymer interaction by getting in between the chains and enable more flexibility. Free volume theory of FOX and FLORY: Sources of free volume for plasticization are (1) chain end motion, (2) side chain motion, (3) main chain "Crankshaft", (4) external plasticizer motion. The void size is controlled by plasticizer content and species.[234,239,240] (adapted from MARCILLA and BELTRÁN et al.[241] with permission of Elsevier © 2012).

### 6.8.5 Bio-based plasticizers

Due to the high awareness of sustainability in society and the need for bio-based materials, the interest in bio-based plasticizers is also increasing.[242,243] Bio-based plasticizers should usually possess those characteristics: They should be non-toxic and should not harm the environment. Additionally, it should have good miscibility with the polymer. The efficiency of the plasticizer should also be similar to conventional petro-based plasticizers. Furthermore, it should not leach from the polymer and it should be inexpensive.[223] Natural plasticizers can also be obtained from a bio-based feedstock like bio-based polymers (**Figure 13**).[244]

*Plasticizers based on starches and cellulose*

The basis of polysaccharides and cellulose-based plasticizers starch and cellulose. Starches can be obtained from rice, wheat, maize, and potatoes, whereas cellulose comes from straws and cotton fibers. Monosaccharides like for example mannose, glucose, fructose, sorbitol can be used to make starch films stronger and more stretchable according to HAN et al.[245] Also, glycerol, xylitol, and sorbitol showing positive effects on the physical and mechanical properties of potato starch-based films.[246] Hydroxypropyl Methylcellulose−Beeswax coatings have the potential to extend the shelf life of plums and showing the potential applications of bio-based plasticizers in the food industry.[247] After chemical modifications sugar alcohols or isosorbide can be obtained from monosaccharides.

*Plasticizers based on sugar alcohols*

Sugar alcohols are bio-based polyols, which also can be used for starch plasticization. ADHIKARI et al. for example used glycerol and xylitol to either enhanced or reduced water migration fluxes in low-amylose starch.[248] The study showed that the additional hydroxyl groups of xylitol lead to a better plasticization than glycerol because they can form strong hydrogen bonds with starch molecules. KROCHTA et al. investigated glycerol and sorbitol plasticized whey protein edible films and found out that glycerol films showed significantly higher oxygen permeability with the drawback of a lower elongation at break.[249]

*Plasticizers based on isosorbide esters*

Another interesting bio-based plasticizer is isosorbide, which is non-toxic, biodegradable, and thermally stable. Isosorbide can be synthesized via double dehydration of sorbitol, which itself is available by hydrogenation of glucose. Isosorbide, isomannide, and isoidide are the different isomers, which are based on the chirality of the hydroxyl group.[223] Yin et al. used three different isosorbide esters (oligo(isosorbide adipate) (OSA), oligo(isosorbide suberate) (OSS), and isosorbide dihexanoate (SDH)), which showed potential applications as PVC plasticizers.[250] The isosorbide derivatives lead to PVC films with higher glass transition temperature, lower tensile strain at break, and higher tensile stress at break compared to conventional phthalate plasticizers like diisooctyl phthalate (DIOP). Also, ZHU et al. found out that isosorbide dioctoate was a potential plasticizer to replace phthalate plasticizer.[251] BATTEGAZZORE et al. investigated isosorbide as a plasticizer for thermoplastic starch that does not retrograde.[252] A major disadvantage of isosorbide plasticizer is the hydrophilicity, which can lead to water absorption of the plasticized polymer.[223]

*Glycerol and its derivates as plasticizers*

Glycerol can be obtained and produced from several bio-based sources like for example from biodiesel production or microbial fermentation.[253,254] It consists of three hydroxyl groups, which are responsible for its water solubility. It is used in food-, cosmetic- and pharmaceutical industry due to its properties and its non-toxicity. Additionally, it is approved as a food additive by the FDA (Food and Drug Administration). Glycerol shows good physical and thermal properties for use as a plasticizer like for example a high-temperature tolerance and nonvolatility.[255] Blends of glycerol and starch are commonly used in the food industry due to the three hydroxyl groups, which are creating strong hydrogen bonds.[256] Starch gelatinization in the presence of glycerol was described by FAVIS et al.[257] Glycerol influences the onset of gelatinization positively and as well it increases flexibility.[258] Several applications were developed using glycerol as a plasticizer.[259–261] Glycerol ester can also be used as plasticizers for PVC, as shown by RINCON et al.[262] SAHU et al. also investigated the biodegradation of rosin-glycerol ester derivative and showed that rosin glycerol ester undergoes biodegradation and follows surface erosion mechanism.[263]

*Plasticizers based on vegetable oils*

Vegetable oils, which are available from soybean, linseed, palm, or castor bean can also be applied as bio-based plasticizers (**Figure 13**). An example of this would be tall oil, which is a side product of the kraft process (paper production). Triglycerides or triacylglycerols, which are made of glycerol and various fatty acids, are the main components of vegetable oils. These vegetable oils have two major advantages for their use as plasticizers. Due to the long alky chains, vegetable oils can increase intermolecular space and bring mobility to polymer chains. The other advantage is that the ester groups can interact with polymer chains (via van der Waals interactions) and increase compatibility between plasticizer and polymer. The ester groups and the double bonds are also areas, where chemical modifications are possible. To increase the compatibility of polymer and plasticizer these modifications are necessary. These modifications can be for example trans-esterification of ester groups. By modifying functionalities, glycerol and fatty esters can be used as plasticizers. Epoxidation is another chemical modification, which can be helpful for practical applications. The epoxide structure can absorb released hydrogen chloride, which is produced by poly(vinyl chloride) (PVC) due to light or thermal exposure. Epoxidized esters of palm kernel oil as a plasticizer for PVC would be an example of that.[264] Another example would be epoxidized rice bran oil (ERBO) as a plasticizer for PVC.[265] Another advantage of epoxidized plasticizers is their low toxicity, which makes them ideal for packing, medical and industrial applications.[266,267] A very important bio-based plasticizer for PVC is epoxidized soybean oil (ESO). According to FERRER al. different amounts of ESO can increase compatibility and thermal stability.[268] The thermal properties of epoxy resins can also be influenced by ESO, as shown by PARK et al.[269] Glass transition temperature and thermal stability of the resins are decreasing due to ESO. The explanation for this effect lies in the decreased density of the epoxy network. QU et al. investigated the mechanical and thermal properties of epoxidized soybean oil plasticized PBS blends and found out that the addition of ESO leads to an improved elongation at break (15 times bigger than neat PBS).[270] The use of ESO as a plasticizer for PLA has also been studied by QU et al.[271] It could be shown that 9 wt% ESO increases the elongation at break of PLA by around 63%. Rheological properties of ESO plasticized PLA was also investigated by QU et al. and showed that the blends of PLA/ESO had a higher melt flow index (MFI) than pure PLA.[272] Castor oil or tung oil can also be used as plasticizers for PVC.[273–275] BEPPU et al. revealed that natural polymeric plasticizer obtained through polyesterification of rice fatty acid showed similar properties like commercially available plasticizers.[276] Cardanol is the main component of cashew nutshell liquid, which is a byproduct of cashew nut processing. Based on cardanol several plasticizers can be produced.

Cardanol derivates can be used for the replacement of classical phthalate plasticizers like di-2-ethylhexyl phthalate (DOP). Derivates of cardanol can be synthesized by substitution and epoxidation reactions.[277] Epoxidation of cardanol leads to a plasticizer, which shows similar properties to DOP. Additionally, cardanol-derivatives increases the thermal stability of PVC. Furthermore, it shows no toxicity in comparison to DOP.[278]

*Plasticizers based on citric acid*

The use of citric acid and its derivatives as plasticizers is favorable because they are safe, non-toxic, and show precipitation resistance. Citric acid derivatives can be synthesized by esterification of citric acid, which is obtained from citrus fruits, sugarcane, and beetroots. Due to three carboxylic functionalities, several derivatives can be synthesized. The main advantage of this group of bio-based plasticizers is that they are approved by the FDA as a food additive, so no harm is expected from them.[279] A major disadvantage is the price of citric acid ester. It is three times higher than conventional phthalate-based plasticizers.[278] Nevertheless, the health aspects can overcome the cost like in the case of red blood cells in PVC bags. Citric acid esters can be used as a safe alternative and replacement for DEHP. Also, in food applications, the use of citric acid esters can be useful. Tributyl citrate for example can be used for food-wrapping films because it is thermally stable and does not cause the products to discolor.[280] Cellulose acetate can also be plasticized with triethyl citrate and acetyl triethyl citrate to increase the mechanical properties like for example the elongation at break. The addition of citrate-based plasticizers also increased the biodegradation of cellulose acetate.[281] WESSLÉN et al. investigated the use of tributyl citrate and triacetin for PLA films and recognized a change in crystallinity for PLA.[282] 20 wt% of plasticizer is needed to decrease the glass transition temperature and improve the ductility of PLA. Drug delivery with bio-based citric acid derivatives is also possible. SADEGHI et al. used 20% of triethyl citrate to plasticize copolymer of ethyl acrylate, methyl methacrylate, and low content of methacrylate with quaternary ammonium groups to develop a drug delivery system.[283] Citric acid ester can also use with low-molecular-weight PVC as a plasticizer.[284] Another interesting bio-based plasticizer based on citric acid is itaconic acid. The esters of itaconic acid are called itaconates and can be synthesized by esterification. They also can be used as plasticizers for PVC, as shown by BATZEL et al. BROWN et al. displayed the possibility to use itaconate esters in a copolymerization reaction with allyl starch to obtain films with enhanced flexibility and toughness.[223]

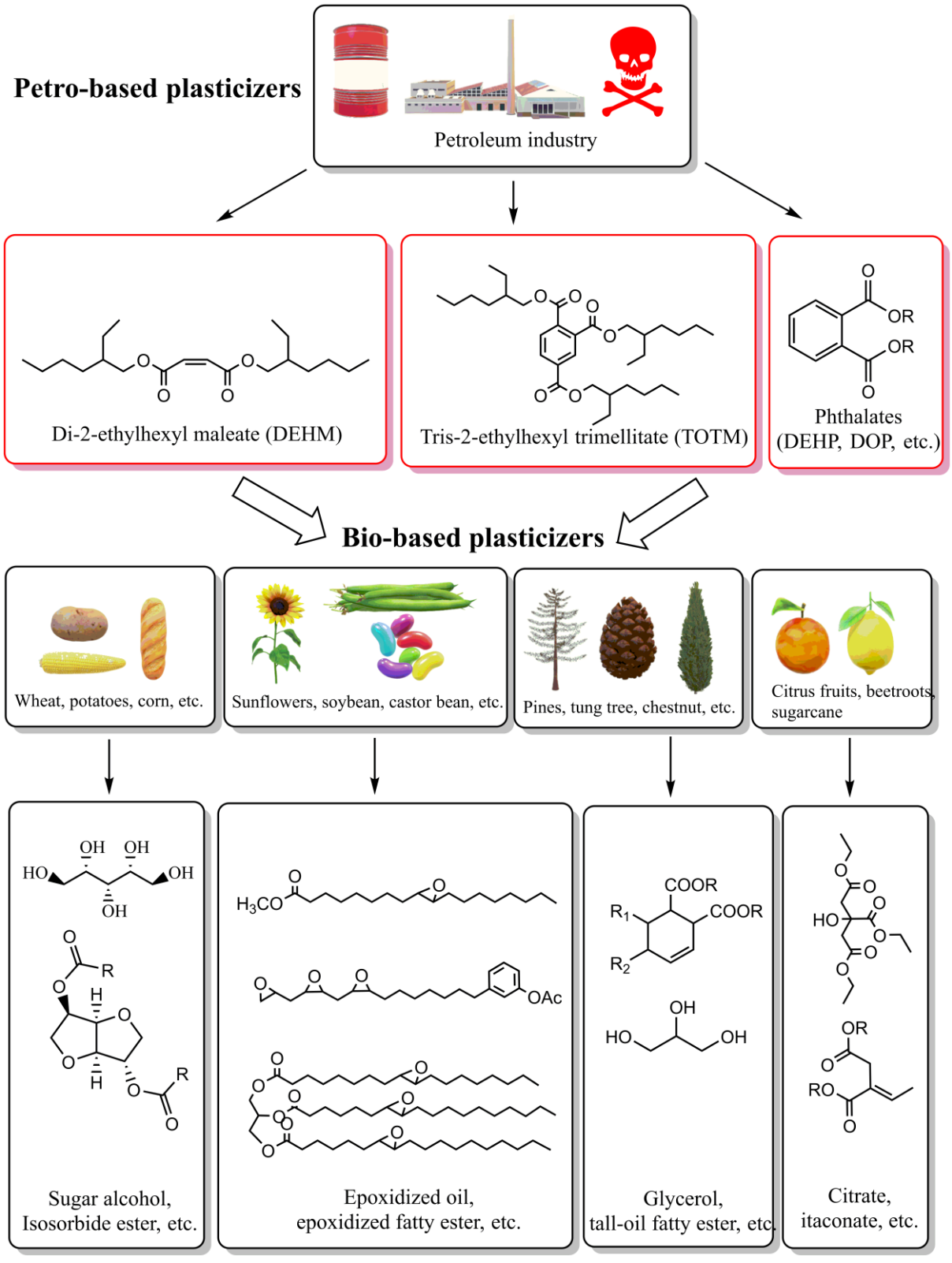


**Figure 13.** Overview of different petro-based plasticizers and potential bio-based alternatives. Toxic and petro-based phthalates (e.g., DEHP) represent 80% of all plasticizers production. Bio-based plasticizers like epoxidized vegetable oils or glycerol esters could be a replacement (adapted from LAPINTE et. al.[223] with permission of John Wiley and Sons © 2015).

# 7 References

(1) D. Schneiderman; M. A. Hillmyer. 50th Anniversary Perspective: There is a great future in sustainable polymers. *Macromolecules* **2017**, *50*, 3733–3749.
(2) X. Zhang; M. Fevre; G. O. Jones; R. M. Waymouth. Catalysis as an Enabling Science for Sustainable Polymers. *Chem. Rev.* **2018**, *118*, 839–885.
(3) Y. Zhu; C. Romain; C. Williams. Sustainable polymers from renewable resources. *Nature* **2016**, *540*, 354–362.
(4) Winkler, M.; Romain, C.; Meier, M. A. R.; Williams, C. K. Renewable polycarbonates and polyesters from 1,4-cyclohexadiene. *Green Chem* **2015**, *17* (1), 300–306. DOI: 10.1039/c4gc01353k.
(5) C. M. Byrne; S. D. Allen; E. B. Lobkovsky; G. W. Coates. Alternating copolymerization of limonene oxide and carbon dioxide. *J. Am. Chem. Soc.* **2004**, *126*, 11404–11405.
(6) O. Hauenstein; M. Reiter; S. Agarwal; B. Rieger; A. Greiner. Bio-based polycarbonate from limonene oxide and CO2 with high molecular weight, excellent thermal resistance, hardness and transparency. *Green Chem.* **2016**, *18*, 760–770.
(7) O. Hauenstein; Md. M. Rahman; M. Elsayed; R. Krause-Rehberg; S. Agarwal; V. Abetz; A. Greiner. Biobased polycarbonate as a gas separation membrane and "breathing glass" for energy saving applications. *Adv. Mater. Technol.* **2017**, *2*, 1700026.
(8) O. Hauenstein; S. Agarwal; A. Greiner. Bio-based polycarbonate as synthetic toolbox. *Nat. Commun.* **2016**, *7*, 11862.
(9) Madbouly, S.; Zhang, C.; Kessler, M. R., Eds. *Bio-based plant oil polymers and composites*; PDL Handbook series; Elsevier, 2016.
(10) Babu, R. P.; O'Connor, K.; Seeram, R. Current progress on bio-based polymers and their future trends. *Progress in biomaterials* **2013**, *2* (1), 8. DOI: 10.1186/2194-0517-2-8.
(11) Bajpai, P. *Biobased polymers*:*Properties and applications in packaging*; Elsevier, 2019.
(12) Patel, M.; Bastioli, C.; Marini, L.; Würdinger, E. *Biopolymers Online: Biology • Chemistry • Biotechnology • Applications*:*Life-cycle Assessment of Bio-based Polymers and Natural Fiber Composites*; Wiley-VCH Verlag GmbH & Co. KGaA., 2005. DOI: 10.1002/3527600035.bpola014.
(13) Soroudi, A.; Jakubowicz, I. Recycling of bioplastics, their blends and biocomposites: A review. *European Polymer Journal* **2013**, *49* (10), 2839–2858. DOI: 10.1016/j.eurpolymj.2013.07.025.
(14) Garrison, T. F.; Murawski, A.; Quirino, R. L. Bio-Based Polymers with Potential for Biodegradability. *Polymers* **2016**, *8* (7). DOI: 10.3390/polym8070262.
(15) Nakajima, H.; Dijkstra, P.; Loos, K. The Recent Developments in Biobased Polymers toward General and Engineering Applications: Polymers that are Upgraded from Biodegradable Polymers, Analogous to Petroleum-Derived Polymers, and Newly Developed. *Polymers* **2017**, *9* (10). DOI: 10.3390/polym9100523.
(16) Kimura, Y. Molecular, Structural, and Material Design of Bio-Based Polymers. *Green Chem* **2009**, *41* (10), 797–807. DOI: 10.1295/polymj.PJ2009154.
(17) Kimura, Y. *Bio-based polymers*; Handbook of R & D information in Japan; CMC Pub, 2013.
(18) Cui, S.; Borgemenke, J.; Qin, Y.; Liu, Z.; Li, Y. Bio-based polycarbonates from renewable feedstocks and carbon dioxide. In ; Advances in Bioenergy; Elsevier, 2019; pp 183–208. DOI: 10.1016/bs.aibe.2019.04.001.
(19) Singh, A. Polycarbonate Synthesis. In *Encyclopedia of Polymeric Nanomaterials*; Kobayashi, S., Müllen, K., Eds.; Springer Berlin Heidelberg, 2015; pp 1793–1796. DOI: 10.1007/978-3-642-29648-2_419.
(20) Brunelle, D. J.; Smigelski, P. M.; Boden, E. P. Evolution of Polycarbonate Process Technologies. In *Advances in polycarbonates*; Brunelle, D. J., Ed.; ACS symposium series, Vol. 898; American Chemical Society, 2005; pp 8–21. DOI: 10.1021/bk-2005-0898.ch002.
(21) Soto, A. M.; Brisken, C.; Schaeberle, C.; Sonnenschein, C. Does Cancer Start in the Womb? Altered Mammary Gland Development and Predisposition to Breast Cancer due to in Utero Exposure

to Endocrine Disruptors. *J Mammary Gland Biol Neoplasia* **2013**, *18* (2), 199–208. DOI: 10.1007/s10911-013-9293-5.
(22) Maia, J.; Cruz, J. M.; Sendón, R.; Bustos, J.; Sanchez, J. J.; Paseiro, P. Effect of detergents in the release of bisphenol A from polycarbonate baby bottles. *Food Research International* **2009**, *42* (10), 1410–1414. DOI: 10.1016/j.foodres.2009.07.003.
(23) Assen, N. von der; Voll, P.; Peters, M.; Bardow, A. Life cycle assessment of CO2 capture and utilization: a tutorial review. *Chemical Society reviews* **2014**, *43* (23), 7982–7994. DOI: 10.1039/C3CS60373C.
(24) Markewitz, P.; Kuckshinrichs, W.; Leitner, W.; Linssen, J.; Zapp, P.; Bongartz, R.; Schreiber, A.; Müller, T. E. Worldwide innovations in the development of carbon capture technologies and the utilization of CO2. *Energy Environ. Sci.* **2012**, *5* (6), 7281. DOI: 10.1039/C2EE03403D.
(25) Chapman, A. M.; Keyworth, C.; Kember, M. R.; Lennox, A. J. J.; Williams, C. K. Adding Value to Power Station Captured CO 2 : Tolerant Zn and Mg Homogeneous Catalysts for Polycarbonate Polyol Production. *ACS Catal.* **2015**, *5* (3), 1581–1588. DOI: 10.1021/cs501798s.
(26) Lee, S. H.; Cyriac, A.; Jeon, J. Y.; Lee, B. Y. Preparation of thermoplastic polyurethanes using in situ generated poly(propylene carbonate)-diols. *Polym. Chem.* **2012**, *3* (5), 1215. DOI: 10.1039/C2PY00010E.
(27) Ren, W.-M.; Liu, Z.-W.; Wen, Y.-Q.; Zhang, R.; Lu, X.-B. Mechanistic aspects of the copolymerization of CO2 with epoxides using a thermally stable single-site cobalt(III) catalyst. *Journal of the American Chemical Society* **2009**, *131* (32), 11509–11518. DOI: 10.1021/ja9033999.
(28) Ellis, W. C.; Jung, Y.; Mulzer, M.; Di Girolamo, R.; Lobkovsky, E. B.; Coates, G. W. Copolymerization of CO 2 and meso epoxides using enantioselective β-diiminate catalysts: a route to highly isotactic polycarbonates. *Chem. Sci.* **2014**, *5* (10), 4004. DOI: 10.1039/C4SC01686F.
(29) Morschbacker, A. Bio-Ethanol Based Ethylene. *Polymer Reviews* **2009**, *49* (2), 79–84. DOI: 10.1080/15583720902834791.
(30) Siracusa, V.; Blanco, I. Bio-Polyethylene (Bio-PE), Bio-Polypropylene (Bio-PP) and Bio-Poly(ethylene terephthalate) (Bio-PET): Recent Developments in Bio-Based Polymers Analogous to Petroleum-Derived Ones for Packaging and Engineering Applications. *Polymers* **2020**, *12* (8). DOI: 10.3390/polym12081641. Published Online: Jul. 23, 2020.
(31) Klemm, D.; Heublein, B.; Fink, H.-P.; Bohn, A. Cellulose: fascinating biopolymer and sustainable raw material. *Angewandte Chemie (International ed. in English)* **2005**, *44* (22), 3358–3393. DOI: 10.1002/anie.200460587.
(32) Pang, J.; Zheng, M.; Sun, R.; Wang, A.; Wang, X.; Zhang, T. Synthesis of ethylene glycol and terephthalic acid from biomass for producing PET. *Green Chem* **2016**, *18* (2), 342–359. DOI: 10.1039/C5GC01771H.
(33) Zhang, M.; Yu, Y. Dehydration of Ethanol to Ethylene. *Ind. Eng. Chem. Res.* **2013**, *52* (28), 9505–9514. DOI: 10.1021/ie401157c.
(34) Welle, F. Twenty years of PET bottle to bottle recycling—An overview. *Resources, Conservation and Recycling* **2011**, *55* (11), 865–875. DOI: 10.1016/j.resconrec.2011.04.009.
(35) Fukushima, K.; Coulembier, O.; Lecuyer, J. M.; Almegren, H. A.; Alabdulrahman, A. M.; Alsewailem, F. D.; Mcneil, M. A.; Dubois, P.; Waymouth, R. M.; Horn, H. W.; Rice, J. E.; Hedrick, J. L. Organocatalytic depolymerization of poly(ethylene terephthalate). *J. Polym. Sci. A Polym. Chem.* **2011**, *49* (5), 1273–1281. DOI: 10.1002/pola.24551.
(36) Gandini, A. Polymers from Renewable Resources: A Challenge for the Future of Macromolecular Materials. *Macromolecules* **2008**, *41* (24), 9491–9504. DOI: 10.1021/ma801735u.
(37) Gandini, A.; Silvestre, A. J. D.; Neto, C. P.; Sousa, A. F.; Gomes, M. The furan counterpart of poly(ethylene terephthalate): An alternative material based on renewable resources. *J. Polym. Sci. A Polym. Chem.* **2009**, *47* (1), 295–298. DOI: 10.1002/pola.23130.
(38) Sousa, A. F.; Vilela, C.; Fonseca, A. C.; Matos, M.; Freire, C. S. R.; Gruter, G.-J. M.; Coelho, J. F. J.; Silvestre, A. J. D. Biobased polyesters and other polymers from 2,5-furandicarboxylic acid: a tribute to furan excellency. *Polym. Chem.* **2015**, *6* (33), 5961–5983. DOI: 10.1039/C5PY00686D.

(39) Knoop, R. J. I.; Vogelzang, W.; van Haveren, J.; van Es, D. S. High molecular weight poly(ethylene-2,5-furanoate); critical aspects in synthesis and mechanical property determination. *J. Polym. Sci. A Polym. Chem.* **2013**, *51* (19), 4191–4199. DOI: 10.1002/pola.26833.
(40) Eerhart, A. J. J. E.; Faaij, A. P. C.; Patel, M. K. Replacing fossil based PET with biobased PEF; process analysis, energy and GHG balance. *Energy Environ. Sci.* **2012**, *5* (4), 6407. DOI: 10.1039/C2EE02480B.
(41) Burgess, S. K.; Leisen, J. E.; Kraftschik, B. E.; Mubarak, C. R.; Kriegel, R. M.; Koros, W. J. Chain Mobility, Thermal, and Mechanical Properties of Poly(ethylene furanoate) Compared to Poly(ethylene terephthalate). *Macromolecules* **2014**, *47* (4), 1383–1391. DOI: 10.1021/ma5000199.
(42) Södergård, A.; Stolt, M. Industrial Production of High Molecular Weight Poly(Lactic Acid). In *Poly(lactic acid)*:*Synthesis, structures, properties, processing, and applications*; Auras, R., Ed.; Wiley series on polymer engineering and technology; Wiley, 2010; pp 27–41. DOI: 10.1002/9780470649848.ch3.
(43) Abdel-Rahman, M. A.; Tashiro, Y.; Sonomoto, K. Recent advances in lactic acid production by microbial fermentation processes. *Biotechnology advances* **2013**, *31* (6), 877–902. DOI: 10.1016/j.biotechadv.2013.04.002. Published Online: Apr. 24, 2013.
(44) Dusselier, M.; van Wouwe, P.; Dewaele, A.; Jacobs, P. A.; Sels, B. F. GREEN CHEMISTRY. Shape-selective zeolite catalysis for bioplastics production. *Science (New York, N.Y.)* **2015**, *349* (6243), 78–80. DOI: 10.1126/science.aaa7169.
(45) Dusselier, M.; van Wouwe, P.; Dewaele, A.; Makshina, E.; Sels, B. F. Lactic acid as a platform chemical in the biobased economy: the role of chemocatalysis. *Energy Environ. Sci.* **2013**, *6* (5), 1415. DOI: 10.1039/C3EE00069A.
(46) Auras, R.; Harte, B.; Selke, S. An overview of polylactides as packaging materials. *Macromolecular bioscience* **2004**, *4* (9), 835–864. DOI: 10.1002/mabi.200400043.
(47) Inkinen, S.; Hakkarainen, M.; Albertsson, A.-C.; Södergård, A. From lactic acid to poly(lactic acid) (PLA): characterization and analysis of PLA and its precursors. *Biomacromolecules* **2011**, *12* (3), 523–532. DOI: 10.1021/bm101302t. Published Online: Feb. 18, 2011.
(48) Ikada, Y.; Jamshidi, K.; Tsuji, H.; Hyon, S. H. Stereocomplex formation between enantiomeric poly(lactides). *Macromolecules* **1987**, *20* (4), 904–906. DOI: 10.1021/ma00170a034.
(49) Shen, L.; Worrell, E.; Patel, M. K. Comparing life cycle energy and GHG emissions of bio-based PET, recycled PET, PLA, and man-made cellulosics. *Biofuels, Bioprod. Bioref.* **2012**, *6* (6), 625–639. DOI: 10.1002/bbb.1368.
(50) Groot, W. J.; Borén, T. Life cycle assessment of the manufacture of lactide and PLA biopolymers from sugarcane in Thailand. *Int J Life Cycle Assess* **2010**, *15* (9), 970–984. DOI: 10.1007/s11367-010-0225-y.
(51) Cosate de Andrade, M. F.; Souza, P. M. S.; Cavalett, O.; Morales, A. R. Life Cycle Assessment of Poly(Lactic Acid) (PLA): Comparison Between Chemical Recycling, Mechanical Recycling and Composting. *J. Polym. Environ.* **2016**, *24* (4), 372–384. DOI: 10.1007/s10924-016-0787-2.
(52) Morão, A.; Bie, F. de. Life Cycle Impact Assessment of Polylactic Acid (PLA) Produced from Sugarcane in Thailand. *J Polym Environ* **2019**, *27* (11), 2523–2539. DOI: 10.1007/s10924-019-01525-9.
(53) Masutani, K.; Kimura, Y. Chapter 1. PLA Synthesis. From the Monomer to the Polymer. In *Poly(lactic acid) Science and Technology*; Jiménez, A., Peltzer, M., Ruseckaite, R., Eds.; Polymer Chemistry Series; Royal Society of Chemistry, 2014; pp 1–36. DOI: 10.1039/9781782624806-00001.
(54) Gupta, A. P.; Kumar, V. New emerging trends in synthetic biodegradable polymers – Polylactide: A critique. *European Polymer Journal* **2007**, *43* (10), 4053–4074. DOI: 10.1016/j.eurpolymj.2007.06.045.
(55) Garlotta, D. *J. Polym. Environ.* **2001**, *9* (2), 63–84. DOI: 10.1023/A:1020200822435.
(56) Madhavan Nampoothiri, K.; Nair, N. R.; John, R. P. An overview of the recent developments in polylactide (PLA) research. *Bioresour. Technol.* **2010**, *101* (22), 8493–8501. DOI: 10.1016/j.biortech.2010.05.092.

(57) Ahmed, J.; Varshney, S. K. Polylactides—Chemistry, Properties and Green Packaging Technology: A Review. *Int. J. Food Prop.* **2011**, *14* (1), 37–58. DOI: 10.1080/10942910903125284.
(58) Mehta, R.; Kumar, V.; Bhunia, H.; Upadhyay, S. N. Synthesis of Poly(Lactic Acid): A Review. *Journal of Macromolecular Science, Part C: Polymer Reviews* **2005**, *45* (4), 325–349. DOI: 10.1080/15321790500304148.
(59) Kowalski, A.; Duda, A.; Penczek, S. Mechanism of Cyclic Ester Polymerization Initiated with Tin(II) Octoate. 2. † Macromolecules Fitted with Tin(II) Alkoxide Species Observed Directly in MALDI−TOF Spectra. *Macromolecules* **2000**, *33* (3), 689–695. DOI: 10.1021/ma9906940.
(60) Moon, S.-I.; Lee, C.-W.; Taniguchi, I.; Miyamoto, M.; Kimura, Y. Melt/solid polycondensation of l -lactic acid: an alternative route to poly(l -lactic acid) with high molecular weight. *Polymer* **2001**, *42* (11), 5059–5062. DOI: 10.1016/S0032-3861(00)00889-2.
(61) Ajioka, M.; Enomoto, K.; Suzuki, K.; Yamaguchi, A. Basic Properties of Polylactic Acid Produced by the Direct Condensation Polymerization of Lactic Acid. *BCSJ* **1995**, *68* (8), 2125–2131. DOI: 10.1246/bcsj.68.2125.
(62) van de Velde, K.; Kiekens, P. Biopolymers: overview of several properties and consequences on their applications. *Polymer Testing* **2002**, *21* (4), 433–442. DOI: 10.1016/S0142-9418(01)00107-6.
(63) Farah, S.; Anderson, D. G.; Langer, R. Physical and mechanical properties of PLA, and their functions in widespread applications - A comprehensive review. *Advanced drug delivery reviews* **2016**, *107*, 367–392. DOI: 10.1016/j.addr.2016.06.012. Published Online: Jun. 26, 2016.
(64) Carrasco, F.; Pagès, P.; Gámez-Pérez, J.; Santana, O. O.; Maspoch, M. L. Processing of poly(lactic acid): Characterization of chemical structure, thermal stability and mechanical properties. *Polymer Degradation and Stability* **2010**, *95* (2), 116–125. DOI: 10.1016/j.polymdegradstab.2009.11.045.
(65) Scaffaro, R.; Morreale, M.; Mirabella, F.; La Mantia, F. P. Preparation and Recycling of Plasticized PLA. *Macromol. Mater. Eng.* **2011**, *296* (2), 141–150. DOI: 10.1002/mame.201000221.
(66) Pillin, I.; Montrelay, N.; Grohens, Y. Thermo-mechanical characterization of plasticized PLA: Is the miscibility the only significant factor? *Polymer* **2006**, *47* (13), 4676–4682. DOI: 10.1016/j.polymer.2006.04.013.
(67) Hamad, K.; Kaseem, M.; Ayyoob, M.; Joo, J.; Deri, F. Polylactic acid blends: The future of green, light and tough. *Prog. Polym. Sci.* **2018**, *85*, 83–127. DOI: 10.1016/j.progpolymsci.2018.07.001.
(68) Saini, P.; Arora, M.; Kumar, M. N. V. R. Poly(lactic acid) blends in biomedical applications. *Advanced drug delivery reviews* **2016**, *107*, 47–59. DOI: 10.1016/j.addr.2016.06.014. Published Online: Jun. 29, 2016.
(69) Murariu, M.; Dubois, P. PLA composites: From production to properties. *Advanced drug delivery reviews* **2016**, *107*, 17–46. DOI: 10.1016/j.addr.2016.04.003. Published Online: Apr. 13, 2016.
(70) Tsuji, H. Poly(lactic acid) stereocomplexes: A decade of progress. *Advanced drug delivery reviews* **2016**, *107*, 97–135. DOI: 10.1016/j.addr.2016.04.017. Published Online: Apr. 25, 2016.
(71) Duan, Y.; Liu, J.; Sato, H.; Zhang, J.; Tsuji, H.; Ozaki, Y.; Yan, S. Molecular weight dependence of the poly(L-lactide)/poly(D-lactide) Stereocomplex at the air-water interface. *Biomacromolecules* **2006**, *7* (10), 2728–2735. DOI: 10.1021/bm060043t.
(72) Corneillie, S.; Smet, M. PLA architectures: the role of branching. *Polym. Chem.* **2015**, *6* (6), 850–867. DOI: 10.1039/C4PY01572J.
(73) Xiao, R. Z.; Zeng, Z. W.; Zhou, G. L.; Wang, J. J.; Li, F. Z.; Wang, A. M. Recent advances in PEG-PLA block copolymer nanoparticles. *Int. J. Nanomed.* **2010**, *5*, 1057–1065. DOI: 10.2147/IJN.S14912.
(74) Cohn, D.; Younes, H. Biodegradable PEO/PLA block copolymers. *J. Biomed. Mater. Res.* **1988**, *22* (11), 993–1009. DOI: 10.1002/jbm.820221104.
(75) Oh, J. K. Polylactide (PLA)-based amphiphilic block copolymers: synthesis, self-assembly, and biomedical applications. *Soft Matter* **2011**, *7* (11), 5096. DOI: 10.1039/C0SM01539C.

(76) Aluthge, D. C.; Xu, C.; Othman, N.; Noroozi, N.; Hatzikiriakos, S. G.; Mehrkhodavandi, P. PLA–PHB–PLA Triblock Copolymers: Synthesis by Sequential Addition and Investigation of Mechanical and Rheological Properties. *Macromolecules* **2013**, *46* (10), 3965–3974. DOI: 10.1021/ma400522n.
(77) Casalini, T.; Rossi, F.; Castrovinci, A.; Perale, G. A Perspective on Polylactic Acid-Based Polymers Use for Nanoparticles Synthesis and Applications. *Front. Bioeng. Biotechnol.* **2019**, *7*, 259. DOI: 10.3389/fbioe.2019.00259.
(78) Hu, Y.; Daoud, W. A.; Cheuk, K. K. L.; Lin, C. S. K. Newly Developed Techniques on Polycondensation, Ring-Opening Polymerization and Polymer Modification: Focus on Poly(Lactic Acid). *Materials (Basel, Switzerland)* **2016**, *9* (3). DOI: 10.3390/ma9030133. Published Online: Feb. 26, 2016.
(79) Müller, H.-M.; Seebach, D. Poly(hydroxyalkanoates): A Fifth Class of Physiologically Important Organic Biopolymers? *Angew. Chem. Int. Ed. Engl.* **1993**, *32* (4), 477–502. DOI: 10.1002/anie.199304771.
(80) Madison, L. L.; Huisman, G. W. Metabolic Engineering of Poly(3-Hydroxyalkanoates): From DNA to Plastic. *Microbiology and Molecular Biology Reviews* **1999**, *63* (1), 21–53.
(81) Doi, Y. Microbial synthesis, physical properties, and biodegradability of polyhydroxyalkanoates. *Macromol. Symp.* **1995**, *98* (1), 585–599. DOI: 10.1002/masy.19950980150.
(82) Morgan-Sagastume, F.; Valentino, F.; Hjort, M.; Cirne, D.; Karabegovic, L.; Gerardin, F.; Johansson, P.; Karlsson, A.; Magnusson, P.; Alexandersson, T.; Bengtsson, S.; Majone, M.; Werker, A. Polyhydroxyalkanoate (PHA) production from sludge and municipal wastewater treatment. *Water science and technology : a journal of the International Association on Water Pollution Research* **2014**, *69* (1), 177–184. DOI: 10.2166/wst.2013.643.
(83) Chatterjee, R.; Yuan, L. Directed evolution of metabolic pathways. *Trends in biotechnology* **2006**, *24* (1), 28–38. DOI: 10.1016/j.tibtech.2005.11.002. Published Online: Nov. 18, 2005.
(84) Witholt, B.; Kessler, B. Perspectives of medium chain length poly(hydroxyalkanoates), a versatile set of bacterial bioplastics. *Current Opinion in Biotechnology* **1999**, *10* (3), 279–285. DOI: 10.1016/S0958-1669(99)80049-4.
(85) Gerngross, T. U.; Martin, D. P. Enzyme-catalyzed synthesis of poly®-(-)-3-hydroxybutyrate: formation of macroscopic granules in vitro. *Proceedings of the National Academy of Sciences of the United States of America* **1995**, *92* (14), 6279–6283.
(86) Ren, Q.; Grubelnik, A.; Hoerler, M.; Ruth, K.; Hartmann, R.; Felber, H.; Zinn, M. Bacterial poly(hydroxyalkanoates) as a source of chiral hydroxyalkanoic acids. *Biomacromolecules* **2005**, *6* (4), 2290–2298. DOI: 10.1021/bm050187s.
(87) Haywood, G. W.; Anderson, A. J.; Roger Williams, D.; Dawes, E. A.; Ewing, D. F. Accumulation of a poly(hydroxyalkanoate) copolymer containing primarily 3-hydroxyvalerate from simple carbohydrate substrates by Rhodococcus sp. NCIMB 40126. *International journal of biological macromolecules* **1991**, *13* (2), 83–88. DOI: 10.1016/0141-8130(91)90053-w.
(88) Matsumoto, K.'i.; Murata, T.; Nagao, R.; Nomura, C. T.; Arai, S.; Arai, Y.; Takase, K.; Nakashita, H.; Taguchi, S.; Shimada, H. Production of short-chain-length/medium-chain-length polyhydroxyalkanoate (PHA) copolymer in the plastid of Arabidopsis thaliana using an engineered 3-ketoacyl-acyl carrier protein synthase III. *Biomacromolecules* **2009**, *10* (4), 686–690. DOI: 10.1021/bm8013878.
(89) Chen, G.-Q.; Patel, M. K. Plastics derived from biological sources: present and future: a technical and environmental review. *Chem. Rev.* **2012**, *112* (4), 2082–2099. DOI: 10.1021/cr200162d.
(90) Thakker, C.; Martínez, I.; San, K.-Y.; Bennett, G. N. Succinate production in Escherichia coli. *Biotechnology journal* **2012**, *7* (2), 213–224. DOI: 10.1002/biot.201100061. Published Online: Sep. 20, 2011.
(91) Zeikus, J. G.; Jain, M. K.; Elankovan, P. Biotechnology of succinic acid production and markets for derived industrial products. *Applied Microbiology and Biotechnology* **1999**, *51* (5), 545–552. DOI: 10.1007/s002530051431.

(92) Xu, J.; Guo, B.-H. Poly(butylene succinate) and its copolymers: research, development and industrialization. *Biotechnology journal* **2010**, *5* (11), 1149–1163. DOI: 10.1002/biot.201000136.
(93) Niaounakis, M. *Biopolymers*:*Applications and trends*; PDL Handbook series; Elsevier, 2015.
(94) Siracusa, V.; Genovese, L.; Munari, A.; Lotti, N. How Stress Treatments Influence the Performance of Biodegradable Poly(Butylene Succinate)-Based Copolymers with Thioether Linkages for Food Packaging Applications. *Materials (Basel, Switzerland)* **2017**, *10* (9). DOI: 10.3390/ma10091009. Published Online: Aug. 30, 2017.
(95) Luo, S.; Li, F.; Yu, J.; Cao, A. Synthesis of poly(butylene succinate- co -butylene terephthalate) (PBST) copolyesters with high molecular weights via direct esterification and polycondensation. *J.Appl. Polym. Sci.* **2010**, *115* (4), 2203–2211. DOI: 10.1002/app.31346.
(96) Wu, L.; Mincheva, R.; Xu, Y.; Raquez, J.-M.; Dubois, P. High molecular weight poly(butylene succinate-co-butylene furandicarboxylate) copolyesters: from catalyzed polycondensation reaction to thermomechanical properties. *Biomacromolecules* **2012**, *13* (9), 2973–2981. DOI: 10.1021/bm301044f. Published Online: Aug. 16, 2012.
(97) H. Nakajima; P. Dijkstra; K. Loos. The recent developments in biobased polymers toward general and engineering applications: polymers that are upgraded from biodegradable polymers, analogous to petroleum-derived polymers, and newly developed. *Polymers* **2017**, *9*, 523.
(98) Winnacker, M.; Rieger, B. Recent progress in sustainable polymers obtained from cyclic terpenes: synthesis, properties, and application potential. *ChemSusChem* **2015**, *8* (15), 2455–2471. DOI: 10.1002/cssc.201500421. Published Online: Jun. 30, 2015.
(99) Gandini, A.; Lacerda, T. M. From monomers to polymers from renewable resources: Recent advances. *Progress in Polymer Science* **2015**, *48*, 1–39. DOI: 10.1016/j.progpolymsci.2014.11.002.
(100) Gandini, A. The irruption of polymers from renewable resources on the scene of macromolecular science and technology. *Green Chem* **2011**, *13* (5), 1061. DOI: 10.1039/C0GC00789G.
(101) Ciriminna, R.; Lomeli-Rodriguez, M.; Demma Carà, P.; Lopez-Sanchez, J. A.; Pagliaro, M. Limonene: a versatile chemical of the bioeconomy. *Chemical communications (Cambridge, England)* **2014**, *50* (97), 15288–15296. DOI: 10.1039/C4CC06147K. Published Online: Oct. 24, 2014.
(102) Satoh, K. Controlled/living polymerization of renewable vinyl monomers into bio-based polymers. *Polym J* **2015**, *47* (8), 527–536. DOI: 10.1038/pj.2015.31.
(103) Satoh, K.; Nakahara, A.; Mukunoki, K.; Sugiyama, H.; Saito, H.; Kamigaito, M. Sustainable cycloolefin polymer from pine tree oil for optoelectronics material: living cationic polymerization of β-pinene and catalytic hydrogenation of high-molecular-weight hydrogenated poly(β-pinene). *Polym. Chem.* **2014**, *5* (9), 3222–3230. DOI: 10.1039/C3PY01320K.
(104) Satoh, K.; Sugiyama, H.; Kamigaito, M. Biomass-derived heat-resistant alicyclic hydrocarbon polymers: poly(terpenes) and their hydrogenated derivatives. *Green Chem* **2006**, *8* (10), 878. DOI: 10.1039/B607789G.
(105) Grignard, B.; Gennen, S.; Jérôme, C.; Kleij, A. W.; Detrembleur, C. Advances in the use of CO2 as a renewable feedstock for the synthesis of polymers. *Chemical Society reviews* **2019**, *48* (16), 4466–4514. DOI: 10.1039/C9CS00047J.
(106) Miyaji, H.; Satoh, K.; Kamigaito, M. Bio-Based Polyketones by Selective Ring-Opening Radical Polymerization of α-Pinene-Derived Pinocarvone. *Angew. Chem. Int. Ed. Engl.* **2016**, *55* (4), 1372–1376. DOI: 10.1002/anie.201509379. Published Online: Dec. 11, 2015.
(107) Poland, S. J.; Darensbourg, D. J. A quest for polycarbonates provided via sustainable epoxide/CO 2 copolymerization processes. *Green Chem.* **2017**, *19* (21), 4990–5011. DOI: 10.1039/c7gc02560b.
(108) Singh, A.; Kamal, M. Synthesis and characterization of polylimonene: Polymer of an optically active terpene. *J. Appl. Polym. Sci.* **2012**, *125* (2), 1456–1459. DOI: 10.1002/app.36250.
(109) Sharma, S.; Srivastava, A. K. Radical co-polymerization of limonene with N-vinyl pyrrolidone: synthesis and characterization. *Designed Monomers and Polymers* **2006**, *9* (5), 503–516. DOI: 10.1163/156855506778538001.

(110) Wilbon, P. A.; Chu, F.; Tang, C. Progress in renewable polymers from natural terpenes, terpenoids, and rosin. *Macromolecular rapid communications* **2013**, *34* (1), 8–37. DOI: 10.1002/marc.201200513. Published Online: Oct. 15, 2012.
(111) Sharma, S.; Srivastava, A. K. Alternating Copolymers of Limonene with Methyl Methacrylate: Kinetics and Mechanism. *Journal of Macromolecular Science, Part A* **2003**, *40* (6), 593–603. DOI: 10.1081/MA-120020867.
(112) C. Martín; A. Kleij. Terpolymers derived from limonene oxide and carbon dioxide: access to cross-linked polycarbonates with improved thermal properties. *Macromolecules* **2016**, *49*, 6285–6295.
(113) Auriemma, F.; Rosa, C. de; Di Caprio, M. R.; Di Girolamo, R.; Ellis, W. C.; Coates, G. W. Stereocomplexed poly(limonene carbonate): a unique example of the cocrystallization of amorphous enantiomeric polymers. *Angew. Chem., Int. Ed.* **2015**, *54* (4), 1215–1218. DOI: 10.1002/anie.201410211.
(114) Auriemma, F.; Rosa, C. de; Di Caprio, M. R.; Di Girolamo, R.; Coates, G. W. Crystallization of Alternating Limonene Oxide/Carbon Dioxide Copolymers: Determination of the Crystal Structure of Stereocomplex Poly(limonene carbonate). *Macromolecules* **2015**, *48* (8), 2534–2550. DOI: 10.1021/acs.macromol.5b00157.
(115) Wambach, A.; Agarwal, S.; Greiner, A. Synthesis of Biobased Polycarbonate by Copolymerization of Menth-2-ene Oxide and CO 2 with Exceptional Thermal Stability. *Sustain. Chem. Eng.* **2020**, *8* (39), 14690–14693. DOI: 10.1021/acssuschemeng.0c04335.
(116) Zoghbi, M. G. B.; Andrade, E. H. A.; Da Silva, M. H. L.; Carreira, L. M. M.; Maia, J. G. S. Current awareness in flavour and fragrance. *Flavour Fragr. J.* **2003**, *18* (6), 543–550. DOI: 10.1002/ffj.1212.
(117) Burwell, R. L. The Mechanism of the Pyrolyses of Pinenes. *J. Am. Chem. Soc.* **1951**, *73* (9), 4461–4462. DOI: 10.1021/ja01153a508.
(118) Kobayashi, S.; Lu, C.; Hoye, T. R.; Hillmyer, M. A. Controlled polymerization of a cyclic diene prepared from the ring-closing metathesis of a naturally occurring monoterpene. *Journal of the American Chemical Society* **2009**, *131* (23), 7960–7961. DOI: 10.1021/ja9027567.
(119) Sarkar, P.; Bhowmick, A. K. Green Approach toward Sustainable Polymer: Synthesis and Characterization of Poly(myrcene- co -dibutyl itaconate). *ACS Sustainable Chem. Eng.* **2016**, *4* (4), 2129–2141. DOI: 10.1021/acssuschemeng.5b01591.
(120) Albertsson, A.-C.; Voepel, J.; Edlund, U.; Dahlman, O.; Söderqvist-Lindblad, M. Design of renewable hydrogel release systems from fiberboard mill wastewater. *Biomacromolecules* **2010**, *11* (5), 1406–1411. DOI: 10.1021/bm100253e.
(121) Shin, J.; Lee, Y.; Tolman, W. B.; Hillmyer, M. A. Thermoplastic elastomers derived from menthide and tulipalin A. *Biomacromolecules* **2012**, *13* (11), 3833–3840. DOI: 10.1021/bm3012852. Published Online: Oct. 12, 2012.
(122) Bolton, J. M.; Hillmyer, M. A.; Hoye, T. R. Sustainable Thermoplastic Elastomers from Terpene-Derived Monomers. *ACS Macro Lett.* **2014**, *3* (8), 717–720. DOI: 10.1021/mz500339h.
(123) Adekunle, K. F. A Review of Vegetable Oil-Based Polymers: Synthesis and Applications. *OJPChem* **2015**, *05* (03), 34–40. DOI: 10.4236/ojpchem.2015.53004.
(124) Stempfle, F.; Ortmann, P.; Mecking, S. Long-Chain Aliphatic Polymers To Bridge the Gap between Semicrystalline Polyolefins and Traditional Polycondensates. *Chemical reviews* **2016**, *116* (7), 4597–4641. DOI: 10.1021/acs.chemrev.5b00705. Published Online: Mar. 29, 2016.
(125) Santacesaria, E.; Vitiello, R.; Tesser, R.; Russo, V.; Turco, R.; Di Serio, M. Chemical and Technical Aspects of the Synthesis of Chlorohydrins from Glycerol. *Ind. Eng. Chem. Res.* **2014**, *53* (22), 8939–8962. DOI: 10.1021/ie403268b.
(126) Sharninghausen, L. S.; Campos, J.; Manas, M. G.; Crabtree, R. H. Efficient selective and atom economic catalytic conversion of glycerol to lactic acid. *Nature communications* **2014**, *5*, 5084. DOI: 10.1038/ncomms6084. Published Online: Oct. 3, 2014.
(127) Haun, W.; Coffman, A.; Clasen, B. M.; Demorest, Z. L.; Lowy, A.; Ray, E.; Retterath, A.; Stoddard, T.; Juillerat, A.; Cedrone, F.; Mathis, L.; Voytas, D. F.; Zhang, F. Improved soybean oil

quality by targeted mutagenesis of the fatty acid desaturase 2 gene family. *Plant biotechnology journal* **2014**, *12* (7), 934–940. DOI: 10.1111/pbi.12201. Published Online: May. 23, 2014.
(128) Meier, M. A. R.; Metzger, J. O.; Schubert, U. S. Plant oil renewable resources as green alternatives in polymer science. *Chemical Society reviews* **2007**, *36* (11), 1788–1802. DOI: 10.1039/B703294C.
(129) Goldbach, V.; Roesle, P.; Mecking, S. Catalytic Isomerizing ω-Functionalization of Fatty Acids. *ACS Catal.* **2015**, *5* (10), 5951–5972. DOI: 10.1021/acscatal.5b01508.
(130) Stempfle, F.; Ritter, B. S.; Mülhaupt, R.; Mecking, S. Long-chain aliphatic polyesters from plant oils for injection molding, film extrusion and electrospinning. *Green Chem* **2014**, *16* (4), 2008. DOI: 10.1039/C4GC00114A.
(131) Witt, T.; Stempfle, F.; Roesle, P.; Häußler, M.; Mecking, S. Unsymmetrical α,ω-Difunctionalized Long-Chain Compounds via Full Molecular Incorporation of Fatty Acids. *ACS Catal.* **2015**, *5* (8), 4519–4529. DOI: 10.1021/acscatal.5b00825.
(132) Liu, C.; Liu, F.; Cai, J.; Xie, W.; Long, T. E.; Turner, S. R.; Lyons, A.; Gross, R. A. Polymers from fatty acids: poly(ω-hydroxyl tetradecanoic acid) synthesis and physico-mechanical studies. *Biomacromolecules* **2011**, *12* (9), 3291–3298. DOI: 10.1021/bm2007554. Published Online: Aug. 9, 2011.
(133) Gross, R. A.; Ganesh, M.; Lu, W. Enzyme-catalysis breathes new life into polyester condensation polymerizations. *Trends in biotechnology* **2010**, *28* (8), 435–443. DOI: 10.1016/j.tibtech.2010.05.004. Published Online: Jul. 1, 2010.
(134) Thomas, S.; Grohens, Y.; Jyotishkumar, P. *Characterization of Polymer Blends*; Wiley-VCH Verlag GmbH & Co. KGaA, 2014. DOI: 10.1002/9783527645602.
(135) Meaurio, E.; Sanchez-Rexach, E.; Zuza, E.; Lejardi, A.; Sanchez-Camargo, A. d. P.; Sarasua, J.-R. Predicting miscibility in polymer blends using the Bagley plot: Blends with poly(ethylene oxide). *Polymer* **2017**, *113*, 295–309. DOI: 10.1016/j.polymer.2017.01.041.
(136) Manias, E.; Utracki, L. A. Thermodynamics of Polymer Blends. In *Polymer Blends Handbook*; Utracki, L. A., Wilkie, C. A., Eds.; Springer Netherlands, 2014; pp 171–289. DOI: 10.1007/978-94-007-6064-6_4.
(137) Flory, P. J. *Principles of polymer chemistry*, 19. print; Cornell Univ. Press, ca. 2006.
(138) Scobbo, J. J.; Goettler, L. A. Applications of Polymer Alloys and Blends. In *Polymer Blends Handbook*; Utracki, L. A., Ed.; Springer Netherlands, 2003; pp 951–976. DOI: 10.1007/0-306-48244-4_13.
(139) Paul, D. R. Control of Phase Structure in Polymer Blends. In *Functional Polymers*; Bergbreiter, D. E., Martin, C. R., Eds.; Springer US, 1989; pp 1–18. DOI: 10.1007/978-1-4613-0815-7_1.
(140) Sarath, C. C.; Shanks, R. A.; Thomas, S. Polymer Blends. In *Nanostructured Polymer Blends*; Elsevier, 2014; pp 1–14. DOI: 10.1016/B978-1-4557-3159-6.00001-8.
(141) Kenney, J. F. Properties of block versus random copolymers. *Polym. Eng. Sci.* **1968**, *8* (3), 216–226. DOI: 10.1002/pen.760080307.
(142) Flory, P. J. Thermodynamics of High Polymer Solutions. *The Journal of Chemical Physics* **1942**, *10* (1), 51–61. DOI: 10.1063/1.1723621.
(143) Eitouni, H. B.; Balsara, N. P. Thermodynamics of Polymer Blends. In *Physical Properties of Polymers Handbook*; Mark, J. E., Ed.; Springer New York, 2007; pp 339–356. DOI: 10.1007/978-0-387-69002-5_19.
(144) Rai, B.; Keller, J. M.; Bajpai, R. Structural – Morphological relative study of polyphenylene oxide and polystyrene (PS: PPO) polymer blends. In ; AIP Publishing, 2020; p 20139. DOI: 10.1063/5.0002547.
(145) Kalogeras, I. M. Glass-Transition Phenomena in Polymer Blends. In *Encyclopedia of Polymer Blends*; Isayev, A. I., Ed.; Wiley-VCH Verlag GmbH & Co. KGaA, 2016; pp 1–134. DOI: 10.1002/9783527653966.ch1.
(146) Paul, D. R., Ed. *Polymer blends*; Wiley, 2000.
(147) Craver, C. D.; Carraher, C. E. *Applied polymer science*:*21st century*, 1. ed.; Elsevier, 2000.

(148) Vuksanović, M. M.; Jančić Heinemann, R. Micro and nanoscale morphology characterization of compatibilized polymer blends by microscopy. In *Compatibilization of Polymer Blends*; Elsevier, 2020; pp 299–330. DOI: 10.1016/B978-0-12-816006-0.00010-4.
(149) Liang, H.; Favis, B. D.; Yu, Y. S.; Eisenberg, A. Correlation between the Interfacial Tension and Dispersed Phase Morphology in Interfacially Modified Blends of LLDPE and PVC. *Macromolecules* **1999**, *32* (5), 1637–1642. DOI: 10.1021/ma9805553.
(150) Macosko, C. W.; Guégan, P.; Khandpur, A. K.; Nakayama, A.; Marechal, P.; Inoue, T. Compatibilizers for Melt Blending: Premade Block Copolymers †. *Macromolecules* **1996**, *29* (17), 5590–5598. DOI: 10.1021/ma9602482.
(151) Lepers, J.-C.; Favis, B. D. Interfacial tension reduction and coalescence suppression in compatibilized polymer blends. *AIChE J.* **1999**, *45* (4), 887–895. DOI: 10.1002/aic.690450419.
(152) Cerclé, C.; Favis, B. D. Generalizing interfacial modification in polymer blends. *Polymer* **2012**, *53* (20), 4338–4343. DOI: 10.1016/j.polymer.2012.07.027.
(153) Fayt, R.; Jérôme, R.; Teyssié, P. Molecular design of multicomponent polymer systems. XIV. Control of the mechanical properties of polyethylene–polystyrene blends by block copolymers. *J. Polym. Sci. B Polym. Phys.* **1989**, *27* (4), 775–793. DOI: 10.1002/polb.1989.090270405.
(154) Feldman, D. Two-phase polymer systems, L. A. Utracki, Ed. Hanser Publishers, Munich, 1991, pp. 421. Price: $84.00. *J. Polym. Sci. A Polym. Chem.* **1993**, *31* (1), 297. DOI: 10.1002/pola.1993.080310138.
(155) Sundararaj, U.; Macosko, C. W. Drop Breakup and Coalescence in Polymer Blends: The Effects of Concentration and Compatibilization. *Macromolecules* **1995**, *28* (8), 2647–2657. DOI: 10.1021/ma00112a009.
(156) Utracki, L. A.; Shi, Z. H. Development of polymer blend morphology during compounding in a twin-screw extruder. Part I: Droplet dispersion and coalescence?a review. *Polym. Eng. Sci.* **1992**, *32* (24), 1824–1833. DOI: 10.1002/pen.760322405.
(157) Joseph, S.; Thomas, S. Morphology, morphology development and mechanical properties of polystyrene/polybutadiene blends. *European Polymer Journal* **2003**, *39* (1), 115–125. DOI: 10.1016/S0014-3057(02)00180-5.
(158) Taylor, G. I. The viscosity of a fluid containing small drops of another fluid. *Proc. R. Soc. Lond. A* **1932**, *138* (834), 41–48. DOI: 10.1098/rspa.1932.0169.
(159) Elmendorp, J. J.; van der Vegt, A. K. A study on polymer blending microrheology: Part IV. The influence of coalescence on blend morphology origination. *Polym. Eng. Sci.* **1986**, *26* (19), 1332–1338. DOI: 10.1002/pen.760261908.
(160) Varghese, H.; Bhagawan, S. S.; Rao, S.S.; Thomas, S. Morphology, mechanical and viscoelastic behaviour of blends of nitrile rubber and ethylene-vinyl acetate copolymer. *European Polymer Journal* **1995**, *31* (10), 957–967. DOI: 10.1016/0014-3057(95)00056-9.
(161) Mendez-Vilas, A.; Díaz, J. *Microscopy*:*Science, technology, applications and education*; Formatex Microscopy Series, No. 4; Formatex, 2010.
(162) Avci, A.; Arikan, H.; Akdemir, A. Fracture behavior of glass fiber reinforced polymer composite. *Cement and Concrete Research* **2004**, *34* (3), 429–434. DOI: 10.1016/j.cemconres.2003.08.027.
(163) Zhang, L. M.; Dai, G. C. Effect of interfacial treatment on the thermal properties of thermal conductive plastics. *Express Polym. Lett.* **2007**, *1* (9), 608–615. DOI: 10.3144/expresspolymlett.2007.83.
(164) Ying, T. P.; Rahman, R.; Ab. Wahab, M. K.; Du Uy Lan, N. Effect of Phase Selective Localization of Silica on Mechanical Properties of Polymethyl Methacrylate/Ethyl Vinyl Acetate/Silica Composites. *Macromol. Symp.* **2017**, *371* (1), 16–21. DOI: 10.1002/masy.201600031.
(165) Le, H. H.; Ilisch, S.; Heidenreich, D.; Wutzler, A.; Radusch, H.-J. Kinetics of the phase selective localization of silica in rubber blends. *Polym Compos* **2010**, *31* (10), 1701–1711. DOI: 10.1002/pc.20960.

(166) Charef, H.; Sabu, T.; Gabriel, G. *Micro- and nanostructured multiphase polymer blend systems*:*Phase morphology*; CRC Press, 2019.
(167) Namhata, S.; Guest, M. J.; Aerts, L. M. Blend morphology development during melt flow: Correlation of a model concept based on dynamic phase volume with practical observations. *J. Appl. Polym. Sci.* **1999**, *71* (2), 311–318. DOI: 10.1002/(SICI)1097-4628(19990110)71:2<311:AID-APP15>3.0.CO;2-3.
(168) Bärwinkel, S.; Seidel, A.; Hobeika, S.; Hufen, R.; Mörl, M.; Altstädt, V. Morphology Formation in PC/ABS Blends during Thermal Processing and the Effect of the Viscosity Ratio of Blend Partners. *Materials (Basel, Switzerland)* **2016**, *9* (8). DOI: 10.3390/ma9080659. Published Online: Aug. 5, 2016.
(169) Sperling, L. H. Polymer alloys and blends thermodynamics and rheology, by L. A. Utracki, Hanser, Munich, 1989, 356 pp. Price: $90.00. *J. Polym. Sci. B Polym. Lett. Ed.* **1990**, *28* (12), 387. DOI: 10.1002/pol.1990.140281208.
(170) Utracki, L. A., Ed. *Polymer Blends Handbook*; Springer Netherlands, 2003. DOI: 10.1007/0-306-48244-4.
(171) Delaby, I.; Froelich, D.; Muller, R. Drop deformation in polymer blends during uniaxial elongational flow. *Macromol. Symp.* **1995**, *100* (1), 131–135. DOI: 10.1002/masy.19951000121.
(172) Jianming, L.; Pei Lian, M.; Basil, D. F. The Role of the Blend Interface Type on Morphology in Cocontinuous Polymer Blends. *Macromolecules* **2002**, *35* (6), 2005–2016.
(173) Dedecker, K.; Groeninckx, G. Reactive compatibilisation of A/(B/C) polymer blends. Part 2. Analysis of the phase inversion region and the co-continuous phase morphology. *Polymer* **1998**, *39* (21), 4993–5000. DOI: 10.1016/S0032-3861(97)10089-1.
(174) Galloway, J. A.; Jeon, H. K.; Bell, J. R.; Macosko, C. W. Block copolymer compatibilization of cocontinuous polymer blends. *Polymer* **2005**, *46* (1), 183–191. DOI: 10.1016/j.polymer.2004.10.061.
(175) Grace, H. P. Dispersion phenomena in high viscosity immiscible fluid systems and application of static mixers as dispersion devices in such systems. *Chemical Engineering Communications* **1982**, *14* (3-6), 225–277. DOI: 10.1080/00986448208911047.
(176) Wildes, G.; Keskkula, H.; Paul, D. R. Morphology of PC/SAN blends: effect of reactive compatibilization, SAN concentration, processing, and viscosity ratio. *J. Polym. Sci. B Polym. Phys.* **1999**, *37* (1), 71–82. DOI: 10.1002/(SICI)1099-0488(19990101)37:1<71:AID-POLB7>3.0.CO;2-7.
(177) Tucker III, C. L.; Moldenaers, P. Microstructural evolution in polymer blends. *Annu. Rev. Fluid Mech.* **2002**, *34* (1), 177–210. DOI: 10.1146/annurev.fluid.34.082301.144051.
(178) Chiellini, E. *Environmentally compatible food packaging*; Woodhead Publishing in food science, technology and nutrition; CRC, 2008.
(179) Lackner, M. Bioplastics. In *Kirk-Othmer Encyclopedia of Chemical Technology*; Inc, J. W. & S., Ed.; John Wiley & Sons, Inc, 2000; pp 1–41. DOI: 10.1002/0471238961.koe00006.
(180) Alaerts, L.; Augustinus, M.; van Acker, K. Impact of Bio-Based Plastics on Current Recycling of Plastics. *Sustainability* **2018**, *10* (5), 1487. DOI: 10.3390/su10051487.
(181) Lambert, S.; Wagner, M. Environmental performance of bio-based and biodegradable plastics: the road ahead. *Chemical Society reviews* **2017**, *46* (22), 6855–6871. DOI: 10.1039/C7CS00149E.
(182) Gironi, F.; Piemonte, V. Bioplastics and Petroleum-based Plastics: Strengths and Weaknesses. *Energy Sources, Part A: Recovery, Utilization, and Environmental Effects* **2011**, *33* (21), 1949–1959. DOI: 10.1080/15567030903436830.
(183) Peres, A. M.; Pires, R. R.; Oréfice, R. L. Evaluation of the effect of reprocessing on the structure and properties of low density polyethylene/thermoplastic starch blends. *Carbohydrate Polymers* **2016**, *136*, 210–215. DOI: 10.1016/j.carbpol.2015.09.047. Published Online: Sep. 15, 2015.
(184) Okan, M.; Aydin, H. M.; Barsbay, M. Current approaches to waste polymer utilization and minimization: a review. *J. Chem. Technol. Biotechnol.* **2019**, *94* (1), 8–21. DOI: 10.1002/jctb.5778.
(185) Khan, B.; Bilal Khan Niazi, M.; Samin, G.; Jahan, Z. Thermoplastic Starch: A Possible Biodegradable Food Packaging Material-A Review. *Journal of Food Process Engineering* **2017**, *40* (3), e12447. DOI: 10.1111/jfpe.12447.

(186) Tabasum, S.; Younas, M.; Zaeem, M. A.; Majeed, I.; Majeed, M.; Noreen, A.; Iqbal, M. N.; Zia, K. M. A review on blending of corn starch with natural and synthetic polymers, and inorganic nanoparticles with mathematical modeling. *International journal of biological macromolecules* **2019**, *122*, 969–996. DOI: 10.1016/j.ijbiomac.2018.10.092. Published Online: Oct. 18, 2018.
(187) Kausar, A. Scientific potential of chitosan blending with different polymeric materials: A review. *Journal of Plastic Film & Sheeting* **2017**, *33* (4), 384–412. DOI: 10.1177/8756087916679691.
(188) Campos, C. A.; Gerschenson, L. N.; Flores, S. K. Development of Edible Films and Coatings with Antimicrobial Activity. *Food Bioprocess Technol* **2011**, *4* (6), 849–875. DOI: 10.1007/s11947-010-0434-1.
(189) Khan, R. A.; Salmieri, S.; Dussault, D.; Sharmin, N.; Lacroix, M. Mechanical, barrier, and interfacial properties of biodegradable composite films made of methylcellulose and poly(caprolactone). *J. Appl. Polym. Sci.* **2012**, *123* (3), 1690–1697. DOI: 10.1002/app.34655.
(190) Nabar, Y. U.; Gupta, A.; Narayan, R. Isothermal Crystallization Kinetics of Poly (Ethylene Terephthalate) ? Cellulose Acetate Blends. *Polym. Bull.* **2005**, *53* (2), 117–125. DOI: 10.1007/s00289-004-0318-5.
(191) Burlein, G. A. D.; Rocha, M. C. G. Mechanical and morphological properties of LDPE/ PHB blends filled with castor oil pressed cake. *Macromol. Symp.* **2014**, *17* (1), 97–105. DOI: 10.1590/S1516-14392013005000196.
(192) Dias, D. S.; Crespi, M. S.; Kobelnik, M.; Ribeiro, C. A. Calorimetric and SEM studies of PHB–PET polymeric blends. *J Therm Anal Calorim* **2009**, *97* (2), 581–584. DOI: 10.1007/s10973-009-0328-5.
(193) Ol'khov, A. A.; Iordanskii, A. L.; Zaikov, G. E.; Shibryaeva, L. S.; Litwinov, I. A.; Vlasov, S. V. Morphological Features of Poly (3-Hydroxybutyrate)/Low Density Polyethylene Blends. *International Journal of Polymeric Materials and Polymeric Biomaterials* **2000**, *47* (2-3), 457–468. DOI: 10.1080/00914030008035079.
(194) Pachekoski, W. M.; Agnelli, J. A. M.; Belem, L. P. Thermal, mechanical and morphological properties of poly (hydroxybutyrate) and polypropylene blends after processing. *Polymer* **2009**, *12* (2), 159–164. DOI: 10.1590/S1516-14392009000200008.
(195) Sheth, M.; Kumar, R. A.; Dav, V.; Gross, R. A.; McCarthy, S. P. Biodegradable polymer blends of poly(lactic acid) and poly(ethylene glycol). *J. Appl. Polym. Sci.* **1997**, *66* (8), 1495–1505. DOI: 10.1002/(SICI)1097-4628(19971121)66:8<1495:AID-APP10>3.0.CO;2-3.
(196) Gajria, A. M.; Davé, V.; Gross, R. A.; P. McCarthy, S. Miscibility and biodegradability of blends of poly(lactic acid) and poly(vinyl acetate). *Polymer* **1996**, *37* (3), 437–444. DOI: 10.1016/0032-3861(96)82913-2.
(197) Kim, Y. F.; Choi, C. N.; Kim, Y. D.; Lee, K. Y.; Lee, M. S. Compatibilization of immiscible poly(l-lactide) and low density polyethylene blends. *Fibers Polym* **2004**, *5* (4), 270–274. DOI: 10.1007/BF02875524.
(198) Anderson, K. S.; Hillmyer, M. A. The influence of block copolymer microstructure on the toughness of compatibilized polylactide/polyethylene blends. *Polymer* **2004**, *45* (26), 8809–8823. DOI: 10.1016/j.polymer.2004.10.047.
(199) Biresaw, G.; Carriere, C. J. Interfacial tension of poly(lactic acid)/polystyrene blends. *J. Polym. Sci. B Polym. Phys.* **2002**, *40* (19), 2248–2258. DOI: 10.1002/polb.10290.
(200) Zhang, G.; Zhang, J.; Wang, S.; Shen, D. Miscibility and phase structure of binary blends of polylactide and poly(methyl methacrylate). *J. Polym. Sci. B Polym. Phys.* **2003**, *41* (1), 23–30. DOI: 10.1002/polb.10353.
(201) Eguiburu, J. L.; Iruin, J. J.; Fernandez-Berridi, M. J.; San Román, J. Blends of amorphous and crystalline polylactides with poly(methyl methacrylate) and poly(methyl acrylate): a miscibility study. *Polymer* **1998**, *39* (26), 6891–6897. DOI: 10.1016/S0032-3861(98)00182-7.
(202) McLauchlin, A. R.; Ghita, O. R. Studies on the thermal and mechanical behavior of PLA-PET blends. *J. Appl. Polym. Sci.* **2016**, *133* (43), 2839. DOI: 10.1002/app.44147.

(203) You, X.; Snowdon, M. R.; Misra, M.; Mohanty, A. K. Biobased Poly(ethylene terephthalate)/Poly(lactic acid) Blends Tailored with Epoxide Compatibilizers. *ACS Omega* **2018**, *3* (9), 11759–11769. DOI: 10.1021/acsomega.8b01353. Published Online: Sep. 24, 2018.
(204) Sangermano, M.; Marchi, S.; Valentini, L.; Bon, S. B.; Fabbri, P. Transparent and Conductive Graphene Oxide/Poly(ethylene glycol) diacrylate Coatings Obtained by Photopolymerization. *Macromol. Mater. Eng.* **2011**, *296* (5), 401–407. DOI: 10.1002/mame.201000372.
(205) Feng, F.; Ye, L. Structure and Property of Polylactide/Polyamide Blends. *Journal of Macromolecular Science, Part B* **2010**, *49* (6), 1117–1127. DOI: 10.1080/00222341003609179.
(206) Luzi, F.; Torre, L.; Kenny, J. M.; Puglia, D. Bio- and Fossil-Based Polymeric Blends and Nanocomposites for Packaging: Structure–Property Relationship. *Materials (Basel, Switzerland)* **2019**, *12* (3). DOI: 10.3390/ma12030471. Published Online: Feb. 3, 2019.
(207) Threepopnatkul, P.; Wongnarat, C.; Intolo, W.; Suato, S.; Kulsetthanchalee, C. Effect of TiO2 and ZnO on Thin Film Properties of PET/PBS Blend for Food Packaging Applications. *Energy Procedia* **2014**, *56*, 102–111. DOI: 10.1016/j.egypro.2014.07.137.
(208) Aontee, A.; Sutapun, W. Effect of Blend Ratio on Phase Morphology and Mechanical Properties of High Density Polyethylene and Poly (Butylene Succinate) Blend. *AMR* **2013**, *747*, 555–559. DOI: 10.4028/www.scientific.net/AMR.747.555.
(209) Chuayjuljit, S.; Kongthan, J.; Chaiwutthinan, P.; Boonmahitthisud, A. Poly(vinyl chloride)/Poly(butylene succinate)/wood flour composites: Physical properties and biodegradability. *Polym Compos* **2018**, *39* (5), 1543–1552. DOI: 10.1002/pc.24098.
(210) Thongsong, W.; Kulsetthanchalee, C.; Threepopnatkul, P. Effect of polybutylene adipate- co -terephthalate on properties of polyethylene terephthalate thin films. *Materials Today: Proceedings* **2017**, *4* (5), 6597–6604. DOI: 10.1016/j.matpr.2017.06.173.
(211) Marturano, V.; Cerruti, P.; Ambrogi, V. Polymer additives. *Physical Sciences Reviews* **2017**, *2* (6), 3197. DOI: 10.1515/psr-2016-0130.
(212) Akiba, M. Vulcanization and crosslinking in elastomers. *Progress in Polymer Science* **1997**, *22* (3), 475–521. DOI: 10.1016/S0079-6700(96)00015-9.
(213) Weinekötter, R.; Gericke, H. *Mixing of Solids*; Particle Technology Series, Vol. 12; Springer, 2000. DOI: 10.1007/978-94-015-9580-3.
(214) Zweifel, H., Ed. *Plastics additives handbook*, 5. ed.; Hanser, 2001.
(215) Jamarani, R.; Erythropel, H. C.; Nicell, J. A.; Leask, R. L.; Marić, M. How Green is Your Plasticizer? *Polymers* **2018**, *10* (8). DOI: 10.3390/polym10080834.
(216) Wilkes, C. E.; Summers, J. W.; Daniels, C. A.; Berard, M. T., Eds. *PVC handbook*, 1. ed.; Hanser; Hanser Gardner, 2005.
(217) Braun, D.; Cherdron, H.; Rehahn, M.; Ritter, H.; Voit, B. *Polymer Synthesis: Theory and Practice*:*Fundamentals, Methods, Experiments*, 5th ed. 2013; Springer, 2013. DOI: 10.1007/978-3-642-28980-4.
(218) *Handbook of Plasticizers*; Elsevier, 2012.
(219) Arnold Kirkpatrick. Some Relations Between Molecular Structure and Plasticizing Effect. *Journal of Applied Physics* **2004**, *11* (4), 255. DOI: 10.1063/1.1712768.
(220) Clark, F. W. *Chem. Ind.* **1941** (60), 225.
(221) Houwink, R. *Proceedings of the XI congress of pure and applied chemistry* **1947**, 575–583.
(222) Aiken, W.; Alfrey, T.; Janssen, A.; Mark, H. Creep behavior of plasticized vinylite VYNW. *J. Polym. Sci.* **1947**, *2* (2), 178–198. DOI: 10.1002/pol.1947.120020206.
(223) Bocqué, M.; Voirin, C.; Lapinte, V.; Caillol, S.; Robin, J.-J. Petro-based and bio-based plasticizers: Chemical structures to plasticizing properties. *J. Polym. Sci. A Polym. Chem.* **2016**, *54* (1), 11–33. DOI: 10.1002/pola.27917.
(224) Ramos-Devalle, L.; Gilbert, M. PVC/plasticizer compatibility: Evaluation and its relation to processing. *J. Vinyl Addit. Technol.* **1990**, *12* (4), 222–225. DOI: 10.1002/vnl.730120409.
(225) Flory, P. J. Viscosities of Linear Polyesters. An Exact Relationship between Viscosity and Chain Length. *J. Am. Chem. Soc.* **1940**, *62* (5), 1057–1070. DOI: 10.1021/ja01862a020.

(226) Fox, T. G.; Flory, P. J. Viscosity—Molecular Weight and Viscosity—Temperature Relationships for Polystyrene and Polyisobutylene 1,2. *J. Am. Chem. Soc.* **1948**, *70* (7), 2384–2395. DOI: 10.1021/ja01187a021.
(227) Ueberreiter, K.; Kanig, G. Self-plasticization of polymers. *Journal of Colloid Science* **1952**, *7* (6), 569–583. DOI: 10.1016/0095-8522(52)90040-8.
(228) Fox, T. G.; Flory, P. J. Second-Order Transition Temperatures and Related Properties of Polystyrene. I. Influence of Molecular Weight. *Journal of Applied Physics* **1950**, *21* (6), 581–591. DOI: 10.1063/1.1699711.
(229) Ferry, J. D. *Viscoelastic properties of polymers*, Third edition; John Wiley & Sons, 1980.
(230) Bair, S. The viscosity at the glass transition of a liquid lubricant. *Friction* **2019**, *7* (1), 86–91. DOI: 10.1007/s40544-018-0210-1.
(231) Williams, M. L.; Landel, R. F.; Ferry, J. D. The Temperature Dependence of Relaxation Mechanisms in Amorphous Polymers and Other Glass-forming Liquids. *J. Am. Chem. Soc.* **1955**, *77* (14), 3701–3707. DOI: 10.1021/ja01619a008.
(232) Ueberreiter, K.; Kanig, G. Die Kettenlängenabhängigkeit des Volumens, des Ausdehnungskoeffizienten und der Einfriertemperatur von fraktionierten Polystyrolen. *Zeitschrift für Naturforschung A* **1951**, *6* (10), 551–559. DOI: 10.1515/zna-1951-1006.
(233) Ashter, S. A. Mechanics of Materials. In *Thermoforming of Single and Multilayer Laminates*; Elsevier, 2014; pp 123–145. DOI: 10.1016/B978-1-4557-3172-5.00006-2.
(234) Platzer, N. The technology of plasticizers, J. Kern Sears and Joseph R. Darby, SPE Monograph Series, Wiley, New York, 1982, 1166 pp. Price: $130.00. *J. Polym. Sci. B Polym. Lett. Ed.* **1982**, *20* (8), 459. DOI: 10.1002/pol.1982.130200810.
(235) Wood, L. A. Glass transition temperatures of copolymers. *J. Polym. Sci.* **1958**, *28* (117), 319–330. DOI: 10.1002/pol.1958.1202811707.
(236) Gordon, M.; Taylor, J. S. Ideal copolymers and the second-order transitions of synthetic rubbers. i. non-crystalline copolymers. *J. Appl. Chem.* **1952**, *2* (9), 493–500. DOI: 10.1002/jctb.5010020901.
(237) Fox, T. G. Influence of Diluent and of Copolymer Composition on the Glass Temperature of a Polymer System. *Bull. Am. Phys. Soc.* **1956** (1), 123.
(238) Hiemenz, P. C.; Lodge, T. P. *Polymer Chemistry, Second Edition*, 2nd ed.; CRC Press, 2007.
(239) Langer, E.; Bortel, K.; Waskiewicz, S.; Lenartowicz-Klik, M. *Plasticizers Derived from Post-Consumer PET*; Elsevier, 2020. DOI: 10.1016/C2015-0-05915-9.
(240) Fong, R. J.; Robertson, A.; Mallon, P. E.; Thompson, R. L. The Impact of Plasticizer and Degree of Hydrolysis on Free Volume of Poly(vinyl alcohol) Films. *Polymers* **2018**, *10* (9). DOI: 10.3390/polym10091036. Published Online: Sep. 18, 2018.
(241) Marcilla, A.; Beltrán, M. Mechanisms of plasticizers action. In *Handbook of Plasticizers*; Elsevier, 2012; pp 119–133. DOI: 10.1016/b978-1-895198-50-8.50007-2.
(242) Kumar, S. Recent Developments of Biobased Plasticizers and Their Effect on Mechanical and Thermal Properties of Poly(vinyl chloride): A Review. *Ind. Eng. Chem. Res.* **2019**, *58* (27), 11659–11672. DOI: 10.1021/acs.iecr.9b02080.
(243) Vieira, M. G. A.; da Silva, M. A.; dos Santos, L. O.; Beppu, M. M. Natural-based plasticizers and biopolymer films: A review. *European Polymer Journal* **2011**, *47* (3), 254–263. DOI: 10.1016/j.eurpolymj.2010.12.011.
(244) McCormick, K.; Kautto, N. The Bioeconomy in Europe: An Overview. *Sustainability* **2013**, *5* (6), 2589–2608. DOI: 10.3390/su5062589.
(245) Zhang, Y.; Han, J. H. Mechanical and Thermal Characteristics of Pea Starch Films Plasticized with Monosaccharides and Polyols. *Journal of Food Science* **2006**, *71* (2), E109-E118. DOI: 10.1111/j.1365-2621.2006.tb08891.x.
(246) Talja, R. A.; Helén, H.; Roos, Y. H.; Jouppila, K. Effect of various polyols and polyol contents on physical and mechanical properties of potato starch-based films. *Carbohydrate Polymers* **2007**, *67* (3), 288–295. DOI: 10.1016/j.carbpol.2006.05.019.

(247) Navarro-Tarazaga, M. L.; Sothornvit, R.; Pérez-Gago, M. B. Effect of plasticizer type and amount on hydroxypropyl methylcellulose-beeswax edible film properties and postharvest quality of coated plums (cv. Angeleno). *Journal of agricultural and food chemistry* **2008**, *56* (20), 9502–9509. DOI: 10.1021/jf801708k. Published Online: Sep. 30, 2008.
(248) Adhikari, B.; Chaudhary, D. S.; Clerfeuille, E. Effect of Plasticizers on the Moisture Migration Behavior of Low-Amylose Starch Films during Drying. *Drying Technology* **2010**, *28* (4), 468–480. DOI: 10.1080/07373931003613593.
(249) McHugh, T. H.; Krochta, J. M. Sorbitol- vs Glycerol-Plasticized Whey Protein Edible Films: Integrated Oxygen Permeability and Tensile Property Evaluation. *J. Agric. Food Chem.* **1994**, *42* (4), 841–845. DOI: 10.1021/jf00040a001.
(250) Yin, B.; Hakkarainen, M. Oligomeric isosorbide esters as alternative renewable resource plasticizers for PVC. *J. Appl. Polym. Sci.* **2011**, *119* (4), 2400–2407. DOI: 10.1002/app.32913.
(251) Yang, Y.; Xiong, Z.; Zhang, L.; Tang, Z.; Zhang, R.; Zhu, J. Isosorbide dioctoate as a "green" plasticizer for poly(lactic acid). *Materials & Design* **2016**, *91*, 262–268. DOI: 10.1016/j.matdes.2015.11.065.
(252) Battegazzore, D.; Bocchini, S.; Nicola, G.; Martini, E.; Frache, A. Isosorbide, a green plasticizer for thermoplastic starch that does not retrogradate. *Carbohydrate Polymers* **2015**, *119*, 78–84. DOI: 10.1016/j.carbpol.2014.11.030. Published Online: Nov. 20, 2014.
(253) Vaidya, P. D.; Rodrigues, A. E. Glycerol Reforming for Hydrogen Production: A Review. *Chem. Eng. Technol.* **2009**, *32* (10), 1463–1469. DOI: 10.1002/ceat.200900120.
(254) Wang, Z.; Zhuge, J.; Fang, H.; Prior, B. A. Glycerol production by microbial fermentation. *Biotechnology advances* **2001**, *19* (3), 201–223. DOI: 10.1016/s0734-9750(01)00060-x.
(255) Banker, G. S. Film coating theory and practice. *Journal of pharmaceutical sciences* **1966**, *55* (1), 81–89. DOI: 10.1002/jps.2600550118.
(256) Avérous, L. Biodegradable Multiphase Systems Based on Plasticized Starch: A Review. *Journal of Macromolecular Science, Part C: Polymer Reviews* **2004**, *44* (3), 231–274. DOI: 10.1081/MC-200029326.
(257) Taghizadeh, A.; Favis, B. D. Effect of high molecular weight plasticizers on the gelatinization of starch under static and shear conditions. *Carbohydrate Polymers* **2013**, *92* (2), 1799–1808. DOI: 10.1016/j.carbpol.2012.11.018. Published Online: Nov. 14, 2012.
(258) Nashed, G.; Rutgers, R. P. G.; Sopade, P. A. The Plasticisation Effect of Glycerol and Water on the Gelatinisation of Wheat Starch. *Starch/Stärke* **2003**, *55* (34), 131–137. DOI: 10.1002/star.200390027.
(259) Ma, X.; Chang, P. R.; Yang, J.; Yu, J. Preparation and properties of glycerol plasticized-pea starch/zinc oxide-starch bionanocomposites. *Carbohydrate Polymers* **2009**, *75* (3), 472–478. DOI: 10.1016/j.carbpol.2008.08.007.
(260) Yu, J.; Yang, J.; Liu, B.; Ma, X. Preparation and characterization of glycerol plasticized-pea starch/ZnO-carboxymethylcellulose sodium nanocomposites. *Bioresource technology* **2009**, *100* (11), 2832–2841. DOI: 10.1016/j.biortech.2008.12.045. Published Online: Feb. 13, 2009.
(261) Chang, P. R.; Wu, D.; Anderson, D. P.; Ma, X. Nanocomposites based on plasticized starch and rectorite clay: structure and properties. *Carbohydrate Polymers* **2012**, *89* (2), 687–693. DOI: 10.1016/j.carbpol.2012.03.076. Published Online: Apr. 3, 2012.
(262) Suárez Palacios, O. Y.; Narváez Rincón, P. C.; Corriou, J.-P.; Camargo Pardo, M.; Fonteix, C. Low-molecular-weight glycerol esters as plasticizers for poly(vinyl chloride). *J. Vinyl Addit. Technol.* **2014**, *20* (2), 65–71. DOI: 10.1002/vnl.21351.
(263) Sahu, N. H.; Mandaogade, P. M.; Deshmukh, A. M.; Meghre, V. S.; Dorle, A. K. Biodegradation Studies of Rosin-Glycerol Ester Derivative. *Journal of Bioactive and Compatible Polymers* **1999**, *14* (4), 344–360. DOI: 10.1177/088391159901400405.
(264) Dutta, K.; Das, S.; Kundu, P. P. Epoxidized Esters of Palm Kernel Oil as an Effective Plasticizer for PVC: A Study of Mechanical Properties and Effect of Processing Conditions. *IPP* **2014**, *29* (4), 495–506. DOI: 10.3139/217.2922.

(265) Nihul, P. G.; Mhaske, S. T.; Shertukde, V. V. Epoxidized rice bran oil (ERBO) as a plasticizer for poly(vinyl chloride) (PVC). *Iran Polym J* **2014**, *23* (8), 599–608. DOI: 10.1007/s13726-014-0254-7.
(266) Rodríguez, M. T.; García, S. J.; Cabello, R.; Suay, J. J.; Gracenea, J. J. Effect of plasticizer on the thermal, mechanical, and anticorrosion properties of an epoxy primer. *J Coat. Technol. Res.* **2005**, *2* (7), 557–564. DOI: 10.1007/s11998-005-0015-9.
(267) Tan, S. G.; Chow, W. S. Biobased Epoxidized Vegetable Oils and Its Greener Epoxy Blends: A Review. *Polymer-Plastics Technology and Engineering* **2010**, *49* (15), 1581–1590. DOI: 10.1080/03602559.2010.512338.
(268) Bueno-Ferrer, C.; Garrigós, M. C.; Jiménez, A. Characterization and thermal stability of poly(vinyl chloride) plasticized with epoxidized soybean oil for food packaging. *Polymer Degradation and Stability* **2010**, *95* (11), 2207–2212. DOI: 10.1016/j.polymdegradstab.2010.01.027.
(269) Park, S.-J.; Jin, F.-L.; Lee, J.-R. Thermal and mechanical properties of tetrafunctional epoxy resin toughened with epoxidized soybean oil. *Materials Science and Engineering: A* **2004**, *374* (1-2), 109–114. DOI: 10.1016/j.msea.2004.01.002.
(270) Zhao, Y.; Qu, J.; Feng, Y.; Wu, Z.; Chen, F.; Tang, H. Mechanical and thermal properties of epoxidized soybean oil plasticized polybutylene succinate blends. *Polym. Adv. Technol.* **2012**, *23* (3), 632–638. DOI: 10.1002/pat.1937.
(271) Xu, Y.-Q.; Qu, J.-P. Mechanical and rheological properties of epoxidized soybean oil plasticized poly(lactic acid). *J. Appl. Polym. Sci.* **2009**, *112* (6), 3185–3191. DOI: 10.1002/app.29797.
(272) Xu, Y.; You, M.; Qu, J. Melt rheology of poly (lactic acid) plasticized by epoxidized soybean oil. *Wuhan Univ. J. Nat. Sci.* **2009**, *14* (4), 349–354. DOI: 10.1007/s11859-009-0413-4.
(273) Jia, P.; Zhang, M.; Hu, L.; Feng, G.; Bo, C.; Zhou, Y. Synthesis and Application of Environmental Castor Oil Based Polyol Ester Plasticizers for Poly(vinyl chloride). *ACS Sustainable Chem. Eng.* **2015**, *3* (9), 2187–2193. DOI: 10.1021/acssuschemeng.5b00449.
(274) Jia, P.; Ma, Y.; Xia, H.; Zheng, M.; Feng, G.; Hu, L.; Zhang, M.; Zhou, Y. Clean Synthesis of Epoxidized Tung Oil Derivatives via Phase Transfer Catalyst and Thiol–ene Reaction: A Detailed Study. *ACS Sustainable Chem. Eng.* **2018**, *6* (11), 13983–13994. DOI: 10.1021/acssuschemeng.8b02446.
(275) Jia, P.; Zhang, M.; Hu, L.; Zhou, Y. Green plasticizers derived from soybean oil for poly(vinyl chloride) as a renewable resource material. *Korean J. Chem. Eng.* **2016**, *33* (3), 1080–1087. DOI: 10.1007/s11814-015-0213-9.
(276) Vieira, M. G. A.; Silva, M. A. d.; Maçumoto, A. C. G.; Santos, L. O. d.; Beppu, M. M. Synthesis and application of natural polymeric plasticizer obtained through polyesterification of rice fatty acid. *J. Appl. Polym. Sci.* **2014**, *17* (2), 386–391. DOI: 10.1590/S1516-14392014005000017.
(277) Chen, J.; Liu, Z.; Jiang, J.; Nie, X.; Zhou, Y.; Murray, R. E. A novel biobased plasticizer of epoxidized cardanol glycidyl ether: synthesis and application in soft poly(vinyl chloride) films. *RSC Adv.* **2015**, *5* (69), 56171–56180. DOI: 10.1039/C5RA07096A.
(278) Jia, P.; Xia, H.; Tang, K.; Zhou, Y. Plasticizers Derived from Biomass Resources: A Short Review. *Polymers* **2018**, *10* (12). DOI: 10.3390/polym10121303. Published Online: Nov. 24, 2018.
(279) Johnson, W. Final report on the safety assessment of acetyl triethyl citrate, acetyl tributyl citrate, acetyl trihexyl citrate, and acetyl trioctyl citrate. *International journal of toxicology* **2002**, *21 Suppl 2*, 1–17. DOI: 10.1080/10915810290096504.
(280) Pritchard, G. *Plastics additives*:*A Rapra market report*; Rapra market report; Rapra Technology Ltd, 2005.
(281) Ghiya, V. P.; Dave, V.; Gross, R. A.; McCarthy, S. P. Biodegradability of Cellulose Acetate Plasticized with Citrate Esters. *Journal of Macromolecular Science, Part A* **1996**, *33* (5), 627–638. DOI: 10.1080/10601329608010883.
(282) Ljungberg, N.; Andersson, T.; Wesslén, B. Film extrusion and film weldability of poly(lactic acid) plasticized with triacetine and tributyl citrate. *J. Appl. Polym. Sci.* **2003**, *88* (14), 3239–3247. DOI: 10.1002/app.12106.

(283) Khodaverdi, E.; Tekie, F. S. M.; Amoli, S. S.; Sadeghi, F. Comparison of plasticizer effect on thermo-responsive properties of Eudragit RS films. *AAPS PharmSciTech* **2012**, *13* (3), 1024–1030. DOI: 10.1208/s12249-012-9827-y. Published Online: Jul. 28, 2012.
(284) Heinze, D.; Mang, T.; Peter, K.; Möller, M.; Weichold, O. Synthesis of low molecular weight poly(vinyl acetate) and its application as plasticizer. *J. Appl. Polym. Sci.* **2014**, *131* (9), n/a-n/a. DOI: 10.1002/app.40226.
(285) L. P. Carrodeguas; J. G. lez-Fabra; F. Castro-Gûmez; C. Bo. AlIII-Catalysed Formation of Poly(limonene carbonate: DFT Analysis of the Origin of Stereoregularity. *Chem. Eur. J.* **2015**, *21* (21), 6115–6122.
(286) T. Stößer; C. Li; J. Unruangsri; P. Saini; R.Sablong; M. Meier; C. Williams; C. Koning. Bio-derived polymers for coating applications: comparing poly(limonene carbonate) and poly(cyclohexadiene carbonate). *Polym. Chem.* **2017**, *8*, 6099–6105.
(287) J. Bailer; S. Feth; F. Bretschneider; S. Rosenfeldt; M. Drechsler; V. Abetz; H. Schmalz; A. Greiner. Synthesis and self-assembly of biobased poly-(limonene carbonate block-poly(cyclohexene carbonate) diblock copolymers prepared by sequential ring-opening copolymerization. *Green Chem.* **2019**, *21*, 2266.
(288) Neumann, S.; Leitner, L.-C.; Schmalz, H.; Agarwal, S.; Greiner, A. Unlocking the Processability and Recyclability of Biobased Poly(limonene carbonate). *Sustain. Chem. Eng.* **2020**, *8* (16), 6442–6448. DOI: 10.1021/acssuschemeng.0c00895.
(289) Weiss, P. Block copolymers – overview and critical survey, Allen Noshay and James E. Mcgrath, Academic, New York, 1977, 516 pp. *J. Polym. Sci. B Polym. Lett. Ed.* **1978**, *16* (3), 151–152. DOI: 10.1002/pol.1978.130160313.
(290) Chauvel, A.; Lefebvre, G. *Major oxygenated, chlorinated and nitrated derivates*; Institut Français du Pétrole publications, technical and economic characteristics / Alain Chauvel; Gilles Lefebvre ; 2; Éditions Technip, 1989.

# 8 Synopsis

## 8.1 Aim and motivation

The focus of this thesis is the bio-based polymer PLimC and its further development. It was first discovered by COATES et. al.[5] and further improved by GREINER et al.[6] Methyl iodide was used to mask hydroxyl groups impurities within the monomer LO and so the molecular weight of PLimC could be increased significantly (~ 100.000 Da).[6] KLEJI et al. demonstrated PLimC synthesis with other catalytic systems besides [(BDI)Zn-(μ-OAc)] like for example Al(III)-Amino-trisphenolate complexes.[112,285] GREINER et al. found also a way to modify the properties of PLimC by using the exocyclic double bond of PLimC with polymer analogous reactions.[8] Applications like a breathing glass are also possible with PLimC.[7,286] Block copolymerization of cyclohexene oxide (CHO) and LO was performed also performed by GREINER et al.[287] Despite possessing excellent properties and a broad modification range for applications, it is only usable when it is cast as a film from solvents. Processing of neat PLimC is rather difficult and leads to polymer with poor mechanical and optical properties.[288] The reason for this processing problems lies in its high viscosity in the melt ($\eta_0$ = 0.89 MPa·s), its high onset of the viscous flow (~ $T_{onset}$ = 167 °C), and its low degradation temperature (~ $T_{degr}$ = 180 °C).

The motivation for this thesis is to overcome these processing issues and to find suitable ways to process PLimC. Processing and property modifications of bio-based polymers are key necessities for sustainable applications and a "greener" future. In this thesis three different ways are pursued to enable PLimC processing and property tuning: Additives, blending, and copolymerization (**Figure 14**).

**Additives**

Additives are an easy and cost-efficient method for tuning polymer properties. A well-known example of that are phthalate-based plasticizers in PVC (e.g., DEHP, DOP). They are acting as softening agents and improve mechanical properties. The same approach can also be transferred to PLimC. However, commercially available plasticizers are petro-based and causing health issues. This can be avoided by applying a bio-based and non-toxic plasticizer. In this thesis, ethyl oleate (EtOL) is used as a low-cost, bio-based plasticizer for PLimC (**Chapter 9.1)**. EtOL is a fatty acid ester, which displays good plasticizing properties due to its long alkyl chains. EtOL reduces the viscosity in melt and the onset of the viscous flow of PLimC efficiently. So, PLimC/EtOL compounds can be processed at lower temperatures and without decomposition.

Also, the addition of 7.5 wt% EtOL improves the mechanical properties of PLimC significantly so that processed PLimC can now be used for sustainable applications. Additionally, PLimC/EtOL compounds can also be recycled at least once by melt reprocessing, which also leads to more sustainability and applicability for PLimC/EtOL compounds.

**Blending**

Another way to reduce the environmental footprint and to process PLimC lies in blending. Blending is also a cost-efficient and already applied method in the industry. The main objective of blending in this thesis is to reduce the amount of petro-based polymers in use and to investigate the properties of PLimC in blends (**Chapter 9.2)**. Interesting blending partners for PLimC are commodity polymers like for example PS, PA, or PMMA because they are applied in large quantities in the industry, and so a partial replacement with bio-based PLimC seems reasonable in terms of sustainability. The produced hybrid blends of bio-based and petro-based polymers are usually phase-separated and showing moderate mechanical properties. However, in the case of PLimC/COPE or PLimC/PBAT blends a strong increase in the *E*-modulus could be observed due to PLimC. This could be interesting for practical and sustainable applications.

**Copolymerization**

PLimC and PLA are bio-based polymers, which provide an interesting potential for sustainable applications. Also, blends of PLimC and PLA could be appealing for applications. The mechanical properties of PLimC/PLA blends are quite moderate due to the phase separation (**Chapter 9.2)**. To improve the performance and properties of these promising sustainable blends, compatibilizers can be applied. Compatibilizers interact with the two phases of the blend to make the morphology more homogenous. This could lead to better mechanical properties. In the case of PLimC/PLA blends, block copolymers of PLimC and PLA could be employed. The advantage of block copolymers of PLimC and PLA lies again in their bio-based origin and their tunability. Because of these interesting aspects, copolymerization of PLimC and PLA was explored (**Chapter 9.3)**. One-pot and sequential reactions were investigated to understand the polymerization behavior of PLimC and PLA in detail. The so obtained block copolymers can be applied as sustainable and tunable compatibilizers. SEM measurements of compatibilized PLimC/PLA blends showed an influence on the morphology, which could be an indicator for a better performance (**Figure 11**). For improving the performance of PLimC, also lactide derivatives (e.g., diHLA) are interesting because their polymerizability gives access to rubber-like polymers (e.g., poly(diHLA)). Poly(diHLA) is a bio-based and biodegradable

polymer with a low glass transition temperature ($T_g$ = -30 °C). The rubber-like properties of poly(diHLA) could be advantageous for improving the properties of PLimC (e.g., processing, impact strength, or elongation at break). In this thesis, PLimC/PdiHLA block copolymers with high transparency and elastic properties were synthesized. These flexible block copolymers could find a potential use for example in the packaging industry. Due to the feasibility of the copolymerization of PLimC and lactide derivatives, the synthesis of bio-based thermoplastic elastomers (TPE) based on PLimC and lactide derivatives seems also possible now.

## 8.2 Individual aspects of each publication

### Additives

In the first publication (**Chapter 9.1**) the difficult processing behavior of neat PLimC is discussed. PLimC possesses relatively poor stability at higher temperatures (> 180 °C). Additionally, the high zero-shear viscosity ($\eta_0$ = 0.89 MPa·s) and the onset of the viscous flow ($T$ = 167 °C) of PLimC make injection molding or hot-pressing problematic. To overcome these limitations additives can be used to tune the processing behavior. This additive should be bio-based, non-toxic, and environmentally friendly to strengthen the "green" character of PLimC. One suitable candidate for that role is ethyl oleate (EtOL), which is the ω-9-fatty acid ester of oleic acid. Adding EtOL to PLimC has certain positive effects on the processing behavior and as well on mechanical properties. PLimC compounds with EtOL show lower glass transition temperatures ($T_g$) than neat PLimC ($T_g$ = 130 °C). This is the effect is induced by EtOL, which possesses two long alky chains to influence the entanglement of the PLimC polymer chains. By adding different amounts of EtOL (2.5 - 25 wt%) to PLimC the glass transition temperatures can be varied over a broad area ($T_g$ = 130 °C – 30 °C). PLimC/EtOL compounds with contents of below 7.5 wt% could not be processed in the desired temperature window (~ $T$ = 170°C), so PLimC/EtOL compounds with > 7.5 wt% EtOL were further investigated. In terms of rheological properties, PLimC/EtOL compound with 7.5 wt% EtOL showed a reduced zero-shear viscosity ($\eta_0$ = 0.12 MPa·s) and the reduced onset of the viscous flow ($T$ = 136 °C). Increasing the EtOL content (15 wt%) leads to lower a lower value for zero-shear viscosity ($\eta_0$ = 0.07 MPa·s) and onset of the viscous flow ($T$ = 125 °C), respectively. PlimC/EtOL compounds are showing improved mechanical properties in comparison to neat PLimC. For compounds with 7.5 wt% EtOL the $E$-modulus ($E$ = 2.1 ± 0.19 GPa) and the elongation at break ($\varepsilon_{br}$ = 28 ± 9.3%) are drastically increased in comparison to neat PLimC. Regarding optical properties of PLimC/EtOL compounds (7.5 wt%), a high transmission (90 ± 0.5 %) and high

clarity (85 ± 0.3 %) can be observed. This is comparable with commercially available bisphenol A polycarbonate (BPA-PC). To take the term sustainability even more into account, the recycling properties of PLimC/EtOL compounds were investigated. The observed values for *E*-modulus ($E$ = 1.94 ± 0.10 GPa) and tensile strength ($\sigma_{max}$ = 22 ± 8.0 MPa) are very close to the values observed for the one-time processed compound. However, the elongation at break decreased to 9 ± 15%. This can be explained by defects, which were introduced by hot pressing the used tensile specimens for a second time. No significant shift of the respective GPC trace to lower molecular weights could be observed after recycling PLimC/EtOL compounds (7.5 wt% EtOL), so chain degradation can be excluded.

**Blending**

Processing of PLimC is also a strong objective in the second publication (**Chapter 9.2**). The second publication is about the blending process of commodity polymers and PLimC to form binary blends with PLimC as the minority component. Using PLimC as a blending partner increases the sustainability of commercially available polymers. For the blending process, polymers with a similar structure to PLimC were chosen to confirm a good combability (e.g., poly (*L*-lactic acid) (PLA), polyamide 12 (PA12), poly(butylene adipate-*co*-terephthalate) (PBAT, EcoFlex®) or a segmented polyether ester (COPE, Arnitel EM400®). PLimC was also blended with commodity plastics with a similar glass transition temperature (e.g., poly(methyl methacrylate) (PMMA) or polystyrene (PS)), but the blends showed either high brittleness or high incompatibility and were not investigated further. The investigated blends were characterized by their thermal properties, their morphology, and as well by their mechanical properties. All produced blends showed opaque strands, which indicates the formation of phase-separated blends. This was confirmed by SEM and Raman imaging. For PLimC/PLA blends a monomodal distribution of spherical PLimC domains was identified, whereas PLimC/PBAT, PLimC/COPE, and PLimC/PA12 blends are showing a bimodal distribution of PLimC. The explanation for lies in the high incompatibility and the huge difference in zero shear viscosity of PLimC and the blending partner. PLimC possesses a quite high zero shear viscosity ($\eta_0$ = 890 kPa·s), whereas the zero shear viscosity of the blending partners is three orders of magnitudes below PLimC, so the shear forces during processing are not sufficient to deform or split the domains further, which resulted in a bimodal distribution. Regarding thermal properties, all investigated blends showed no change in glass transition temperature by the addition of PLimC but blending usually leads to an increased crystallization temperature ($T_c$) of the matrix polymer due to the nucleation effect of PLimC domains. Comparison of

thermogravimetric measurements (TGA) show an increased stability of PLimC (~ $T_{5\%}$ = 250 °C) within the matrix polymer compared to neat PLimC ($T_{5\%}$ = 230 °C). In terms of mechanical properties, the most pronounced effect of PLimC in blends is the strong increase of *E*-modulus, as it was observed in the case of PLimC/PBAT or PLimC/COPE blends. Blending with 30 wt% PLimC increases the *E*-modulus of PBAT four times (from 0.06 MPa to 0.25 MPa). However, the elongation at break is suffering, but still acceptable for applications (~ $\varepsilon_{br}$ = 200 %).

**Copolymerization**

Also, in the third publication, the processing is an extended aim. To improve the mechanical properties of PLimC/PLA blends for applications, PLimC/PLA block copolymers were synthesized (**Chapter 9.3**). These can be applied as compatibilizers in immiscible PLimC/PLA blends and can enhance the blend performance in terms of mechanical properties. Lactides (LA) and their derivatives are suitable candidates as comonomers for LO because the corresponding polymers (e.g., PLA or PdiHLA) are also bio-based, show biodegradability, and displaying interesting mechanical properties. Due to all these reasons, living ring-opening copolymerization (ROCOP) of LO, and $CO_2$, and LA was investigated in detail. First, polymerizations of LO, $CO_2$, and *D,L*-lactide (DLLA) were performed to clarify the polymer architecture in one-pot reactions. The successful copolymerization was identified by observing characteristic protons for PLimC (5.06 ppm) and (PDLLA) (5.20 ppm) with $^{1}$H NMR spectroscopy. Also, $^{13}$C NMR reveals the formation of PLimC and poly((*D/L*))-lactide acid) (PDLLA). By comparing feed composition (LO: DLLA) and polymer composition with $^{1}$H-NMR, a fast polymerization rate of DLLA in presence of LO could be observed. High molecular weight (~ $M_n$ = 70 – 80 kDa) polymers with two distinctive glass transition temperatures ($T_g$ = 122 °C and $T_g$ = 50 °C) were obtained from one-pot reactions. Observing two glass transition temperatures would lead to the assumption, that either homopolymers or block copolymers are forming. TGA measurements of copolymers are showing a mainly PLimC dominated degradation for all the different copolymer compositions (~ $T_{5\%}$ = 228 °C). To differentiate between homopolymers and block copolymers, 2D NMR spectroscopy ($^{1}$H-$^{1}$H NOESY NMR) was used to identify cross-peaks of PLimC and PDLLA. To confirm block copolymer structure the morphology of the copolymers was studied by transmission electron microscopy (TEM). A mixture of spherical, cylindrical, hexagonally perforated lamellar structure and lamellar morphology was observed for PLimC/PLA copolymers. This indicates the formation of PLimC and PLA copolymers with different chain lengths. The reactivity of a PLimC terminated polymer chain was demonstrated by sequential polymerization of LO, $CO_2$, and *L*-lactide (LLA)

to form PLimC-*block*-poly((*L*)-lactide acid). To improve mechanical properties of PLimC without the use of additives or plasticizers, sequential ROCOP of LO, $CO_2$, and dihexyl-substituted lactide (diHLA) was performed to give PlimC-*block*-PdiHLA block copolymers. PdiHLA as a soft block should influence elongation at break and impact strength positively due to its flexible chains. That toughness of brittle rigid polymer can be improved by block copolymerization is well-known and demonstrated by styrene-butadiene-styrene block copolymers or epoxy-polycaprolactone thermosetting block copolymers.[289] Using diHLA as a monomer possesses also other advantages. It is based on non-food and bio-based materials like for example heptaldehyde, which can be obtained from castor oil or ricinoleic acid ester.[290] Additionally, it shows biodegradability and can be used drug delivery system. Three different block copolymers with different ratios of PLimC and PdiHLA were synthesized. $^1$H-NMR spectroscopy confirms the synthesis by showing the characteristic protons for PLimC (5.06 ppm) and PdiHLA (5.20 ppm). Moderate molecular weights (~ $M_n$ = 35.000 Da) and low glass transition temperatures (~ $T_g$ = - 39 °C) were obtained. The decomposition of PLimC-*block*-PdiHLA copolymers (~ $T_{5\%}$ = 225 °C) is occurring in the same temperature region as PLimC-*block*-PLA copolymers. By using ROCOP of diHLA and LO a window for PLimC modification can be opened.


**Figure 14.** Overview of the different aspects of this thesis: Additives, blending, and copolymerization. Additives like EtOL can influence the processing behavior of PLimC significantly (marked in red). Blending of PLimC and commodity polymers (e.g., PBAT, PA12) can reduce the environmental footprint of petro-based polymers (marked in yellow). The copolymerization of LO, $CO_2$ and LA derivatives results in block copolymers, which have potential use as compatibilizers in blends or can be used for property tuning.

## 8.3 Individual contribution to joint publications

Several MCII scientists under the supervision of Holger Schmalz, Seema Agarwal, and Andreas Greiner contributed to this thesis and the corresponding manuscripts and publications. In this chapter, the individual contributions of all authors are given.

### 8.3.1 Unlocking the processability and recyclability of the biobased poly(limonene carbonate)

*Simon Neumann, Lisa-Cathrin Leitner, Holger Schmalz, Seema Agarwal and Andreas Greiner*

**ACS Sustainable Chem. Eng. 2020, 8, 6442−6448**

Received: February 3, 2020
Revised: March 22, 2020
Published: April 7, 2020

https://dx.doi.org/10.1021/acssuschemeng.0c00895

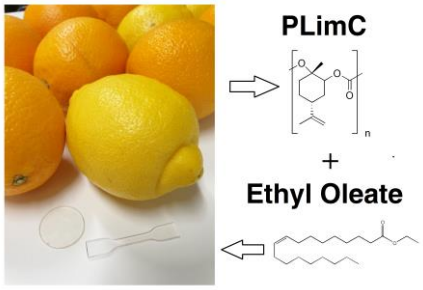


#### Author Contributions

Simon Neumann performed experiments and wrote the manuscript. Lisa-Cathrin Leitner performed hot-pressing and tensile testing of PLimC/EtOL compounds during her lab course. Holger Schmalz performed the melt rheology experiments and cowrote the manuscript. Seema Agarwal and Andreas Greiner guided the project and cowrote the manuscript.

### 8.3.2 Blends of bio-based poly(limonene carbonate) with commodity polymers

*Simon Neumann, Pin Hu, Felix Bretschneider, Holger Schmalz and Andreas Greiner*

**Macromol. Mater. Eng. 2021, 2100090**

Received: February 7, 2021
Revised: April 11, 2021
Published: June 12, 2021

https://doi.org/10.1002/mame.202100090

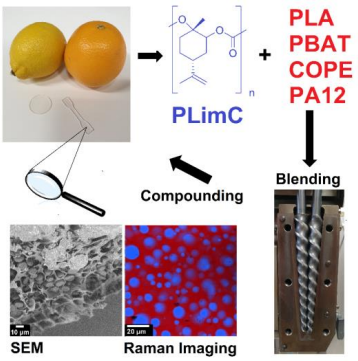


## Author Contributions

Simon Neumann performed analytical experiments and wrote the manuscript. Pin Hu performed extrusion of PLimC/PBAT, PLimC/COPE and PLimC/PA12 blends and the corresponding tensile testing. Felix Bretschneider performed extrusion of PLimC/PLA blends and the corresponding tensile testing during his bachelor thesis. Holger Schmalz performed Raman imaging and cowrote the manuscript. Andreas Greiner guided the project and cowrote the manuscript.

### 8.3.3 Sustainable block copolymers of poly(limonene carbonate)

*Simon Neumann, Sophia Barbara Däbritz, Sophie Edith Fritze, Lisa-Cathrin Leitner, Aneesha Anand, Andreas Greiner and Seema Agarwal*

**RSC Polym. Chem., 2021,12, 903-910**

Received: December 09, 2020
Accepted: January 09, 2021
Published: January 22, 2021

https://doi.org/10.1039/D0PY01685C

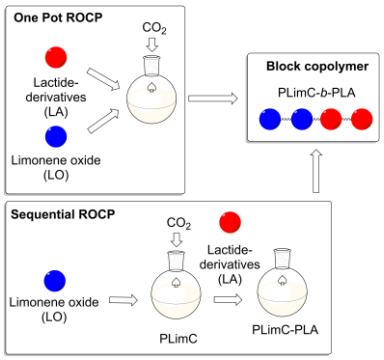


## Author Contributions

Simon Neumann performed experiments, supervised all experiments, and wrote the manuscript. Aneesha Anand performed synthesis of PLimC-*block*-PLA copolymers during her internship. Sophia Däbritz performed the synthesis of PLimC-*block*-PDLLA copolymers during her bachelor thesis. Lisa-Cathrin Leitner performed the synthesis of PLimC-*block*-PLLA copolymers during her lab course. Sophie Fritze performed the synthesis of PLimC-*block*-diHLA copolymers during her lab course. Seema Agarwal and Andreas Greiner guided the project and cowrote the manuscript.

# 9 Reprints of publications

## 9.1 Unlocking the processability and recyclability of biobased poly(limonene carbonate)

Simon Neumann, Lisa-Cathrin Leitner, Holger Schmalz, Seema Agarwal, and Andreas Greiner*

Macromolecular Chemistry II, University of Bayreuth, 95440 Bayreuth, Germany

in

Received: February 3, 2020

Revised: March 22, 2020

Published: April 7, 2020

https://dx.doi.org/10.1021/acssuschemeng.0c00895

**ACS Sustainable Chem. Eng. 2020, 8, 6442−6448**



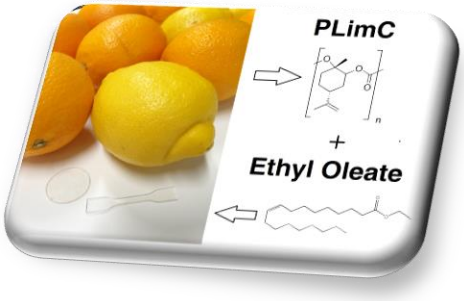

ABSTRACT

Poly(limonene carbonate) (PLimC) has a huge potential as a sustainable biobased polymer due to its promising property profile and the availability of the raw materials from nonedible resources, e.g.,, limonene from orange peel. PLimC and related terpene-based polycarbonates have not been processed from the melt state successfully due to their comparably low decomposition temperatures. Indeed, melt-processed PLimC samples are brittle and colorized. To change the paradigm, we have investigated compounds of PLimC with biobased ethyl oleate (EtOL). The glass transition temperature ($T_g$) and melt viscosity of these compounds can be readily controlled by the EtOL content. The melt-processed PLimC/EtOL compounds showed improved mechanical properties without significant loss in optical properties as compared to neat PLimC. Interestingly, the PLimC/EtOL compounds could be melt-processed a second time without significant loss of mechanical and optical properties, which could mark an important step toward recyclability.

KEYWORDS: biobased, poly(limonene carbonate), fatty acid, additive, processing, recycling

## INTRODUCTION

Biobased polymers are of utmost importance for the sustainable circular economy, which is essential for future materials. The importance of biobased synthetic polymers has been highlighted in several excellent reviews.[1–3] Polymers from relevant nonfood resources could become a cornerstone for sustainability if some inherent problems are solved, which could be nicely illustrated by poly(limonene carbonate) (PLimC). PLimC made by ring-opening copolymerization (ROCOP) of *trans*-limonene oxide (LO) and $CO_2$ was introduced by Coates et al.[4] It has received significant scientific attention but has not yet being applied in technically relevant applications due to problems related to melt processing. The versatility of different catalysts and reaction parameters for the copolymerization of LO and $CO_2$,[5–7] derivatives of PLimC,[8–11] block copolymers,[12] and applications[13–15] were investigated by several teams. The production of high-molecular-weight PLimC on a kg scale was achieved by the purification of the monomer, which was an important step toward applications. The potential of PLimC for applications was shown by Koning et al. for coatings[13,14] and by us for membranes.[15] Interestingly, even the evaluation of the availability of limonene16 and life cycle assessments of PLimC[17,18] gave a promising outlook for the technical application of PLimC. Unfortunately, the onset of degradation ($T_{5\%}$ = 225 °C, $T_{5\%}$ = temperature at 5% weight loss) of PLimC is rather close to its glass transition temperature ($T_g \approx 130$ °C).[7] Additionally, its melt viscosity is

very high, which restricts most engineering applications of this promising biobased polymer, like compression molding or extrusion. Consequently, melt processing of PLimC results only in brittle and colorized samples. If this problem could be resolved by a "green" approach, PLimC and many related polymers could be utilized for sustainable engineering applications. Recent progress in improving the melt processability of biobased polymers was made by Fu et al., who developed a low temperature sintering method for melt processing of stereo complex-type polylactide or employed polymers with a bimodal melting temperature distribution.[19–23] An alternative method involves the use of polymers with ultrabroad molecular weight distribution, as shown by Mülhaupt et al. for high density polyethylene (HDPE) employing a reactor blend of nanophase-separated ultrahigh-molecular-weight polyethylene (UHMWPE) in a low-molecular-weight PE wax as an additive.[24] To improve the melt processability of PLimC, we have investigated compounds of PLimC and a low-molecular weight additive with the expectation that these compounds will have lower $T_g$ and thereby allow melt processing without decomposition. We have selected the biobased ethyl oleate (EtOL) made from ethanol and the ω-9-fatty-acid oleic acid due to its chemical similarity (polar ester group, long aliphatic chain) to PLimC. Oleic acid based polyesters have for example already been used to improve the melt processability of polyethylene and polypropylene.[25] In addition, EtOL is nontoxic and is used as a regulated food additive (code of federal regulations: 21CFR172.515) and as a solvent for intramuscular drug delivery.[26] Moreover, some phthalates, which are still commonly used in commodity polymers, are suspected to be responsible for several health issues, e.g., they are suspected to act as teratogens or endocrine disruptors. Thus, there is an ongoing need to find nontoxic alternatives to improve the melt processability of commodities as well as engineering polymers. Here, we studied the effect of EtOL on the rheological and mechanical properties of melt-processed PLimC/EtOL compounds, as well as on their optical properties and recyclability.

RESULTS AND DISCUSSION

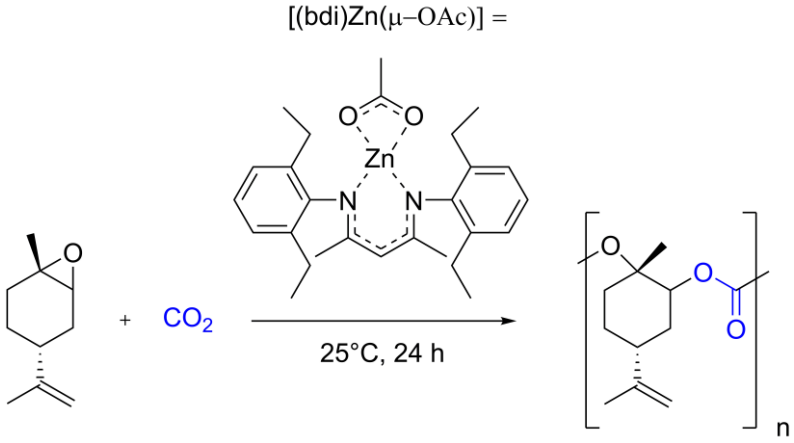


**Scheme 1.** Synthesis of PLimC *via* ring-opening copolymerization (ROCOP) of *trans*-LO and $CO_2$ (10 bar) employing (bdi)Zn($\mu$-OAc) as catalyst (ca. 30 vol% *trans*-LO in toluene).

PLimC was synthesized by ring-opening copolymerization (ROCOP) of *trans*-LO and $CO_2$ catalyzed by the β-diiminate zinc catalyst (bdi)Zn($\mu$-OAc) (**Scheme 1**), following a previously published procedure (details of the synthesis can be found in the Supporting Information).[7] Gel permeation chromatography (GPC; **Figure S1**) showed a unimodal molecular weight distribution, with an apparent number average molecular weight of $M_{n,app}$ = 50 000 g mol$^{-1}$ ($Đ$ = 1.15). A solvent-related approach with dichloromethane (DCM) was chosen for the preparation of PLimC/EtOL compounds to achieve a homogeneous distribution of the additive in the polymer matrix, which was proven by Raman imaging (**Figure S2**). This solvent-related approach could be improved in terms of sustainability by, e.g., spray coating of EtOL onto PLimC powder employing a more sustainable solvent like ethanol.

### Rheological Properties of Neat PLimC

Until now, all attempts to process pure PLimC without decomposition have failed because the glass transition temperature ($T_g$) of PLimC ($T_g$ = 130 °C) is rather close to its decomposition temperature of $T_{5\%}$ = 225 °C[7] ($T_{5\%}$ = temperature at 5% weight loss), and it shows gradual degradation under isothermal conditions at 180 °C (**Figure S3**). A processing temperature window of 160−170 °C (above $T_g$, but below decomposition temperature) is too low to induce sufficient flow of the sample, and at temperatures above 170 °C, PLimC starts to degrade, resulting in brittle, yellowish pellets with bubbles (**Figure S4**). To gain quantitative data about

the processing of PLimC, we first investigated the rheological properties of neat PLimC. The temperature ramp (**Figure 1A**) reveals the onset of viscous flow at about 170 °C (crossover of $G'$ and $G''$), which is close to the decomposition temperature of 180 °C. In addition, the zero shear viscosity of PLimC is rather high at 170 °C ($\eta_0$ = 0.89 MPa·s, **Figure 1B**). This results in high shear forces required for processing, which also contributes to the degradation of PLimC. The zero shear viscosity of PLimC is significantly higher in comparison to the value of 3.4 kPa·s (at a processing temperature of 270 °C) for the commercial polycarbonate Lexan 141.[27] The small processing window of 170−180 °C combined with the high melt viscosity of PLimC makes thermal processing of PLimC impossible. To overcome these limitations, biobased EtOL was used to reduce the $T_g$ and to lower the onset of the viscous flow of PLimC.

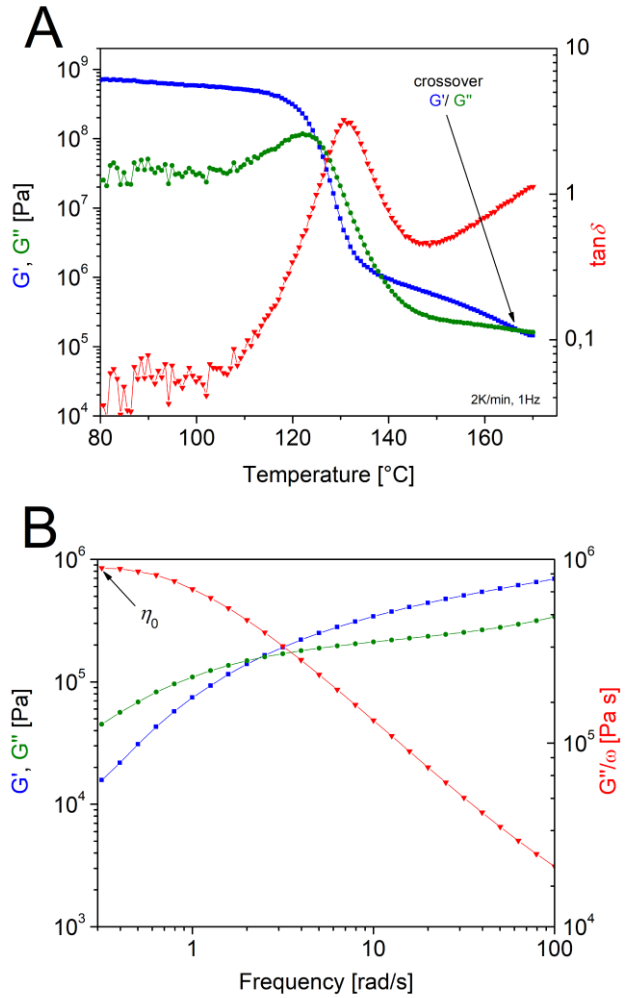


**Figure 1.** A) Temperature-dependent dynamic moduli for neat PLimC. B) Frequency sweep for neat PLimC at 170 °C. The zero shear viscosity of $\eta_0$ = 0.89 MPa·s was calculated from $G''/\omega$ for the lowest measured frequency.

**Thermal and Rheological Properties of PLimC/EtOL Compounds**

PLimC/EtOL compounds with different weight fractions of EtOL were studied to understand the effect of EtOL on the $T_g$ and the rheological properties (**Table S1**). The EtOL content in the compounds was verified by proton nuclear magnetic resonance ($^1$H NMR) spectroscopy (**Figures S5** and **S6** and **Table S1**) and $T_g$ was determined by differential scanning calorimetry (DSC; **Figure S7**). The $T_g$ of the PLimC/EtOL compounds decreases continuously with the EtOL content from 128 °C (neat PLimC) to 32 °C (PLimC/EtOL compound with 25 wt % EtOL), which also indicates molecular miscibility of PLimC and EtOL over a wide composition range (**Figure 2**). This effect can be explained by the free volume theory of Fox and Flory. Here, the plasticization effect is explained by the introduction of small plasticizer molecules into the polymer matrix, which possesses not only a $T_g$ lower than the polymer matrix itself, but the small molecules significantly increase the free volume of the system and, thus, diminish the $T_g$ and the melt viscosity.[28]

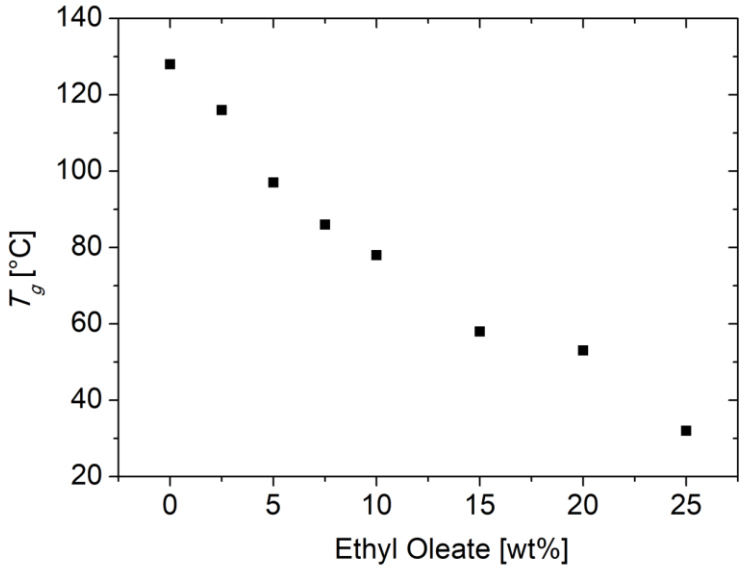


**Figure 2.** Dependence of $T_g$ on the amount of EtOL in PLimC/EtOL compounds. Determined by $^1$H-NMR spectroscopy ($CDCl_3$) and DSC (10 K min$^{-1}$).

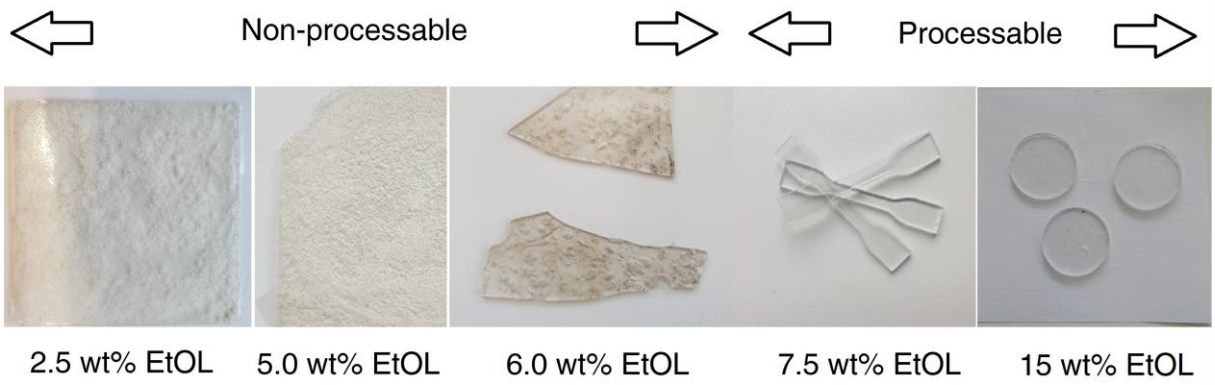


**Figure 3.** Optical appearance of hot pressed PLimC/EtOL compounds with different EtOL contents. The respective EtOL contents and processing temperatures are given below the images.

PLimC/EtOL compounds with EtOL contents below 7.5 wt% could not be hot-pressed in the desired temperature window of 170−180 °C despite their lowered $T_g$. Temperatures up to 210 °C were necessary to completely melt the sample, and as a result, the prepared specimens showed clear signs of beginning PLimC degradation (brownish color, the formation of bubbles; **Figure 3**). In contrast, compounds with higher EtOL contents (7.5−15 wt % EtOL) were well processable already at 160 °C, yielding clear, colorless disks and dog-bone-shaped samples (**Figure 3**). Consequently, PLimC/EtOL compounds with EtOL contents of 7.5, 10, and 15 wt % were selected to further study their rheological properties. EtOL has not only an effect on the $T_g$ of the PLimC/EtOL compounds but also on the onset of viscous flow, which is one of the key factors for processing. The onset of viscous flow is decreased from 167 °C (neat PLimC) to 136 °C for an EtOL content of 7.5 wt % (**Figure 4A**). This widens the small processing window of PLimC and, therefore, decomposition during melt processing can be efficiently prevented. Furthermore, the zero shear viscosity is lowered by a factor of ≈7 from $\eta_0$ = 0.89 MPa·s for neat PLimC to 0.12 MPa·s for the compound with 7.5 wt % EtOL, respectively (**Figure 4B**). Upon further increasing the EtOL content in the compounds, the onset of viscous flow and the zero shear viscosity are further shifted to lower values (**Figures S8** and **S9** and **Table 1),** yielding an onset of viscous flow of 125 °C and a zero shear viscosity of $\eta_0$ = 0.07 MPa·s for the compound with the highest EtOL content of 15 wt %, respectively.

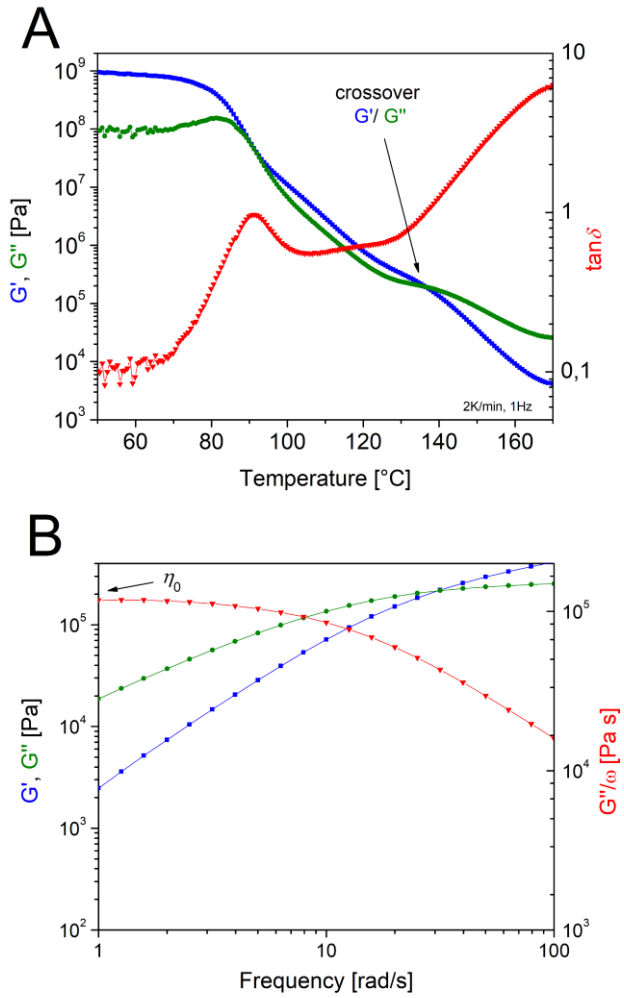


**Figure 4.** A) Temperature-dependent dynamic moduli for a PLimC/EtOL compound with 7.5 wt% EtOL and B) corresponding frequency sweep at 170 °C. The zero shear viscosity $\eta_0$ = 0.12 MPa·s was calculated from $G''/\omega$ for the lowest measured frequency.

## Mechanical and Optical Properties of PLimC/EtOL Compounds

**Figure 5** shows the representative stress−strain traces for PLimC/EtOL compounds with 7.5, 10, and 15 wt % EtOL, and the respective mechanical properties (Young′s modulus, tensile strength, and elongation at break) are compared to that of neat PLimC in **Table 1**. Due to the improved melt processability of PLimC/EtOL compounds, a significant enhancement in the mechanical performance can be achieved for the compound with 7.5 wt % EtOL. Young′s modulus ($E$ = 2.1 ± 0.19 GPa) and elongation at break ($\varepsilon_{br}$ = 28 ± 9.3%) are doubled compared to the values observed for neat PLimC ($E$ = 0.95 GPa, $\varepsilon_{br}$ = 15%)[7] and the sample shows a Charpy impact strength of 2.10 ± 0.09 kJ m$^{-2}$. Due to the plasticizing effect of EtOL, the tensile

strength is lowered from 55 to 22 ± 8 MPa for the PLimC/EtOL compound. With higher amounts of EtOL (10 and 15 wt %; **Table 1**), a decrease in certain mechanical properties was observed. The Young′s modulus as well as elongation at break are lowered to $E$ = 1.60 ± 0.35 GPa and $\varepsilon_{br}$ = 13 ± 7.1%, respectively, for the compound with the highest EtOL content of 15 wt %. In contrast, the tensile strength is not significantly altered and the Charpy impact strength is more than doubled (4.90 ± 0.03 kJ $m^{-2}$). This effect can again be explained by the free volume model of Fox and Flory.[28] The addition of EtOL results in a significant increase in the free volume of the system. Consequently, the interactions between the PLimC chains are reduced and, thus, chain mobility is increased, as manifested in the decreased melt viscosity of PLimC/EtOL compounds (**Table 1**). This, on one hand, is the prerequisite for melt processing of PLimC/EtOL compounds, as otherwise, the high melt viscosity requires high processing temperatures resulting in decomposition of PLimC. On the other hand, polymer−polymer interactions that hold the polymer chains together are increasingly reduced upon the addition of EtOL. As a result, there is an optimum EtOL content of 7.5 wt %, where melt processing is enhanced without significantly deteriorating mechanical properties, like Young′s modulus and elongation at break. Similar results in terms of mechanical properties were found with epoxidized vegetable oils as additives for polylactide[30] and poly(vinyl chloride).[31]

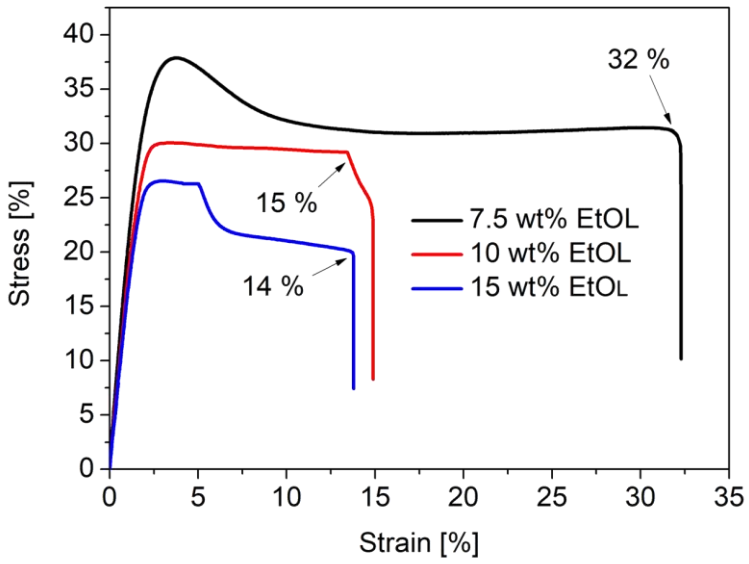


**Figure 5.** Representative stress-strain curves of PLimC/EtOL compounds with different EtOL contents.

With respect to optical properties (**Table 1**), high transmission and clarity of about 90 and 85%, respectively, can be reached even for the compound with 15 wt % EtOL, which are comparable to those for commercial polycarbonate (BPA-PC, Lexan 141). Besides, the addition of EtOL results in an increase in the haze, with values ≤15%. Consequently, PLimC/EtOL compounds have performance comparable to that of Lexan 141 in terms of Young′s modulus and optical transparency but still show some limitations with respect to elongation at break and impact strength. Processed PLimC/EtOL (7.5 wt % EtOL) was recycled by hot pressing to study the impact of repeated processing on mechanical and optical properties (**Figure S10** and **Table S6**). Tensile strength ($\sigma_{max}$ = 22 ± 13 MPa) and Young′s modulus ($E$ = 1.94 ± 0.10 GPa) are very close to the values observed for the one-time processed compound ($\sigma_{max}$ = 22 ± 8.0 MPa, $E$ = 2.10 ± 0.09 GPa; **Table 1**). The elongation at break, however, dropped to 9 ± 15%. This might be explained by defects, which were introduced by hot pressing the used tensile specimens for a second time. The elongation at break is very sensitive to small defects in the tensile specimens. For the recycling test, the used tensile specimens were cut into small pieces for compression molding (**Figure S10**). In contrast, the initial test specimens were prepared by compression molding of a powderlike sample, which ensures a much more homogeneous melt. It is noted that chain degradation is not a major issue, as no significant shift of the respective GPC trace to lower molecular weights could be observed after recycling (**Figure S11**). Concerning the optical properties of the recycled PLimC/EtOL compound, no significant changes induced by recycling could be observed (**Table S6**).

**Table 1.** Summary of rheological, mechanical and optical properties of pure PLimC, PLimC/EtOL compounds and the commercial polycarbonate Lexan 141.

| | Unit | PLimC neat | PLimC 7.5 wt% EtOL | PLimC 10 wt% EtOL | PLimC 15 wt% EtOL | Lexan 141 | Method |
|---|---|---|---|---|---|---|---|
| **Thermal/rheological** | | | | | | | |
| Glass transition temperature | °C | 128/131 | 86/91 | 78/70 | 58/62 | 150/n.d.[29] | DSC/Rheo-meter[a] |
| Zero shear viscosity | MPa s | 0.89 | 0.12 | 0.12 | 0.07 | 0.0034[27] | Rheometer[b] |
| Onset of viscous flow | °C | 167 | 136 | 130 | 125 | n.d. | Rheometer[a] |
| **Mechanical** | | | | | | | |
| Tensile strength | MPa | 55[7] | 22 ± 8.0 | 21 ± 2.2 | 19 ± 2.1 | 49 ± 5.8 | Tensile tester[c] |
| Elongation at break | % | 15[7] | 28 ± 9.3 | 11 ± 10 | 13 ± 7.1 | 61 ± 46 | Tensile tester[c] |
| E-modulus | GPa | 0.95[7] | 2.10 ± 0.19 | 1.70 ± 0.18 | 1.60 ± 0.35 | 1.80 ± 0.20 | Tensile tester[c] |
| Charpy impact strength | kJ $m^{-2}$ | n.d. | 2.10 ± 0.09 | n.d. | 4.90 ± 0.03 | 12.0 ± 1.10 | Impact strength tester[d] |
| **Optical** | | | | | | | |
| Transmission | % | 94[5] | 90 ± 0.5 | 85 ± 1.2 | 91 ± 0.5 | 92 ± 1.2 | Haze meter |
| Haze | % | 0.75[5] | 13 ± 0.4 | 15 ± 1.1 | 14 ± 0.4 | 5.0 ± 1.4 | Haze meter |
| Clarity | % | 99.8[7] | 85 ± 0.3 | 97 ± 1.5 | 85 ± 0.4 | 89 ± 1.3 | Haze meter |

[a] DSC: $T_g$ was determined from the second heating traces (scanning rate 10 K $min^{-1}$, **Figure S7**); rheology: $T_g$ und onset of viscous flow (cross over of $G'$ and $G''$) were determined from temperature ramp tests at 2 K $min^{-1}$ employing a frequency of 1 Hz.

[b] Zero shear viscosities were determined from frequency sweeps at 170 °C and were calculated from $G''/\omega$ at the lowest measured frequency.

[c] A test speed of 0.5 mm $min^{-1}$ was used to determine the Young´s modulus and 2.0 mm $min^{-1}$ for tensile strength and elongation at break, respectively. Given values (standard deviations in brackets) correspond to average value of 9-10 samples. Experimental data for single measurements can be found in the supporting information (**Tables S2-S5**).

[d] Impact strength was measured according to ISO 179-2

## EXPERIMENTAL SECTION

Materials. R-Limonene (97%), *N*-bromosuccinimide (NBS) (97%), sodium hydride (60% dispersion in mineral oil) and iodomethane (99%, stabilized with silver) were used as received. Carbon dioxide (5.0, Linde Gase) was dried by passing through a column packed with molecular sieves (pore size 3 Å). *trans*-Limonene oxide (LO) was synthesized from R-limonene via the endo-cyclic bromohydrin formed by the reaction with *N*-bromosuccinimide (NBS) and conversion to the corresponding epoxide in the presence of aqueous sodium hydroxide. LO was further reacted with sodium hydride and methyl iodide to mask the OH groups of impurities that act as chain-transfer agents during polymerization. The β-diiminate zinc catalyst (bdi)Zn($\mu$-OAc)[4] and PLimC[7] were synthesized according to literature procedures. In short, PLimC was prepared by ring-opening copolymerization (ROCOP) of LO and $CO_2$, employing (bdi)Zn($\mu$-OAc) as a catalyst in toluene. The obtained PLimC was purified by several precipitations from methanol. Ethyl oleate (98%, mixture of isomers, clear liquid, maximum acid content of 0.5 mg KOH $g^{-1}$) was used as received from Acros Organics. Dichloromethane (DCM) was supplied by Carl Roth Chemicals and distilled prior to use. Polycarbonate Lexan 141 was supplied by Sabic.

### PLimC/EtOL Compounds

The preparation of a PLimC/EtOL compound with 15 wt % EtOL is given as a representative procedure for all of the prepared PLimC/EtOL compounds. Five hundred milligrams of PLimC were dissolved in 20 mL of DCM until a clear solution was generated. To this solution, 0.058 mL of EtOL were added. After 30 min, the DCM was removed using a rotary evaporator. The obtained PLimC/EtOL compound was dried under high vacuum ($2 \cdot 10^{-2}$ mbar) for 16 h and characterized by $^1$H NMR and DSC measurements.

### Melt Processing of PLimC/EtOL Compounds.

A hot press from Carver (model 2518) with a temperature setting of 160−210 °C was used for processing. Powderlike samples of the respective PLimC/EtOL compounds were filled in a metal frame (13 cm × 13 cm) with a thickness of 1.0 mm and hot-pressed for 5 min by applying a force of 10 kN. After obtaining the hot-pressed polymer plates, dogbone-shaped specimens were punched for tensile testing according to DIN53504S3A, employing a Coesfeld Material punching machine (model 951617).

## METHODS

NMR spectra were recorded on a Bruker Avance-300 NMR spectrometer operating at 300 MHz, using deuterated chloroform ($CDCl_3$) as a solvent. Chemical shifts δ are indicated in parts per million (ppm) with respect to residual solvent signals. Differential scanning calorimetry (DSC) was performed on a Mettler Toledo DSC 3+ Star systems using a scanning rate of 10 K $min^{-1}$ under N2 atmosphere. For GPC analyses an Agilent 1200 system equipped with a SDV precolumn (particle size 5 μm; PSS Mainz), a SDV linear XL column (particle size 5 μm, PSS Mainz) and a refractive index detector (G1362A, Agilent Technologies) was used. $CHCl_3$ (high-performance liquid chromatography (HPLC) grade) was used as a solvent at a flow rate of 0.5 mL $min^{-1}$ at room temperature. The calibration was done with narrowly distributed polystyrene standards (PSS calibration kit) and toluene (HPLC grade) was used as the internal standard. Raman imaging was performed with a WITec Alpha 300 RA+ imaging system equipped with an UHTS 300 spectrometer and a back-illuminated Andor Newton 970 EMCCD camera. The measurement was conducted with an excitation wavelength of λ = 352 nm and an integration time of 0.6 s per pixel using a laser power of 15 mW (100× objective, NA = 0.9, step width 100 nm per pixel). All spectra were subjected to a cosmic ray removal routine and baseline correction using the WITec project 5.2 software. The spatial distribution of the components was extracted from the Raman imaging data employing the Raman spectra of the neat components, employing the True Component Analysis in the WITec project 5.2 software. An Anton Paar MCR 302 rheometer equipped with a parallel-plate Peltier device and a Peltier hood was used for rheological studies, employing a plate−plate geometry with D = 12 mm. Prior to the measurements, a strain sweep was conducted to ensure that the measurements were performed in the linear viscoelastic regime. Glass transition temperatures ($T_g$) were determined from the maximum of tan δ. The onset of the viscous flow was determined from the crossover of G′ and G″. Zero shear viscosities were calculated from G″/ω, using the lowest frequency measured. A Gardner Haze-Gard Plus haze meter was used for testing the optical properties. A tensile tester (Instron 5565) with 0.5 and 2 mm $min^{-1}$ test speeds and a 10 kN load cell was used for tensile testing. Charpy impact properties were tested with a Zwick 5113 testing machine/50 J Hammer according to ISO 179-2.

## CONCLUSIONS

In this contribution, we introduced a concept for meltprocessable, biobased PLimC employing biobased ethyl oleate (EtOL) as an additive. EtOL was selected as a suitable additive because it is readily available, inexpensive, nontoxic, and shows chemical similarity to PLimC. Neat PLimC suffers from decomposition during thermal processing starting at 180 °C according to our thermogravimetric analysis (TGA) study. Taking into consideration that the viscous flow starts at around 170 °C for pure PLimC, processing is not possible without decomposition of the polymer. The addition of the biobased, nontoxic EtOL lowers the $T_g$ and melt viscosity, which significantly widens the accessible temperature window for processing without thermal degradation and reduces shearinduced degradation of PLimC. Additionally, the mechanical properties improved significantly without colorization or a significant loss of transparency of the samples. It should be mentioned that the addition of larger amounts of EtOL could lead to compounds with too low $T_g$ for engineering applications. Interestingly, the compounds could be meltprocessed a second time without a significant change of the mechanical and optical properties. This could be an important step toward melt recycling and displays a highly relevant alternative to the already published chemical recycling of PLimC. The promising results of this investigation could pave the way toward sustainable engineering and application of PLimC and unlock the important class of terpene-based polycarbonates for real-world applications.

## ASSOCIATED CONTENT

### Supporting Information

The Supporting Information is available free of charge at https://pubs.acs.org/doi/10.1021/acssuschemeng.0c00895.

$^1$H NMR and GPC of PLimC and PLimC/EtOL compounds as well as Raman imaging; TGA; DSC; and rheology and detailed mechanical data of PLimC/EtOL compounds (PDF)

AUTHOR INFORMATION


## Corresponding Author

**Andreas Greiner** − Macromolecular Chemistry and Bavarian Polymer Institute, University of Bayreuth, 95440 Bayreuth, Germany; orcid.org/0000-0002-5310-3850;

Email: greiner@uni-bayreuth.de

## Authors

**Simon Neumann** − Macromolecular Chemistry, University of Bayreuth, 95440 Bayreuth, Germany

**Lisa-Cathrin Leitner** − Macromolecular Chemistry, University of Bayreuth, 95440 Bayreuth, Germany

**Holger Schmalz** − Macromolecular Chemistry and Bavarian Polymer Institute, University of Bayreuth, 95440 Bayreuth, Germany; orcid.org/0000-0002-4876-0450

**Seema Agarwal** − Macromolecular Chemistry and Bavarian Polymer Institute, University of Bayreuth, 95440 Bayreuth, Germany; orcid.org/0000-0002-3174-3152

Complete contact information is available at:

https://pubs.acs.org/10.1021/acssuschemeng.0c00895

## Author Contributions

S.N. performed the experiments and cowrote the manuscript. L.-C.L. performed the experiments. H.S. was involved in project management, performed the melt rheology measurements and cowrote the manuscript. S.A. and A.G. guided the project and cowrote the manuscript.

## Notes

The authors declare no competing financial interest.

**ACKNOWLEDGMENTS**

We thank Simon Bard (Polymer Engineering, University of Bayreuth) for Charpy impact strength measurements. We gratefully acknowledge the use of equipment and assistance offered in the Keylab "Small Scale Polymer Processing" of the Bavarian Polymer Institute at the University of Bayreuth.

**REFERENCES**

(1) Zhu, Y.; Romain, C.; Williams, C. K. Sustainable polymers from renewable resources. Nature 2016, 540, 354−362.

(2) Nakajima, H.; Dijkstra, P.; Loos, K. The recent developments in biobased polymers toward general and engineering applications: Polymers that are upgraded from biodegradable polymers, analogous to petroleum-derived polymers, and newly developed. Polymers 2017, 9, 523.

(3) Schneiderman, D. K.; Hillmyer, M. A. 50th Anniversary Perspective: There is a great future in sustainable polymers. Macromolecules 2017, 50, 3733−3749.

(4) Byrne, C. M.; Allen, S. D.; Lobkovsky, E. B.; Coates, G. W. Alternating copolymerization of limonene oxide and carbon dioxide. J. Am. Chem. Soc. 2004, 126, 11404−11405.

(5) Auriemma, F.; de Rosa, C.; Di Caprio, M. R.; Di Girolamo, R.; Ellis, W. C.; Coates, G. W. Stereocomplexed poly(limonene carbonate): A unique example of the cocrystallization of amorphous enantiomeric polymers. Angew. Chem., Int. Ed. 2015, 54, 1215−1218.

(6) Peña Carrodeguas, L.; González-Fabra, J.; Castro-Gómez, F.; Bo, C.; Kleij, A. W. Al(III)-catalysed formation of poly(limonene)-carbonate: DFT analysis of the origin of stereoregularity. Chem. - Eur. J. 2015, 21, 6115−6122.

(7) Hauenstein, O.; Reiter, M.; Agarwal, S.; Rieger, B.; Greiner, A. Bio-based polycarbonate from limonene oxide and CO2 with high molecular weight, excellent thermal resistance, hardness and transparency. Green Chem. 2016, 18, 760−770.

(8) Martín, C.; Kleij, A. Terpolymers derived from limonene oxide and carbon dioxide: Access to cross-linked polycarbonates with improved thermal properties. Macromolecules 2016, 49, 6285−6295.

(9) Hauenstein, O.; Agarwal, S.; Greiner, A. Bio-based polycarbonate as synthetic toolbox. Nat. Commun. 2016, 7, No. 11862.

(10) Li, C.; Sablong, R. J.; Koning, C. Chemoselective alternating copolymerization of limonene dioxide and carbon dioxide: A new highly functional aliphatic epoxy polycarbonate. Angew. Chem., Int. Ed. 2016, 55, 11572−11576.

(11) Kindermann, N.; Cristòfol, À.; Kleij, A. W. Access to biorenewable polycarbonates with unusual glass-transition temperature (Tg) modulation. ACS Catal. 2017, 7, 3860−3863.

(12) Bailer, J.; Feth, S.; Bretschneider, F.; Rosenfeldt, S.; Drechsler, M.; Abetz, V.; Schmalz, H.; Greiner, A. Synthesis and self-assembly of biobased poly(limonene carbonate)-block-poly(cyclohexene carbonate) diblock copolymers prepared by sequential ring-opening copolymerization. Green Chem. 2019, 21, 2266−2272.

(13) Li, C.; Sablong, R. J.; Koning, C. E. Synthesis and characterization of fully-biobased α,ω-dihydroxyl poly(limonene carbonate)s and their initial evaluation in coating applications. Eur. Polym. J. 2015, 67, 449−458.

(14) Stößer, T.; Li, C.; Unruangsri, J.; Saini, P. K.; Sablong, R. J.; Meier, M. A. R.; Williams, C. K.; Koning, C. Bio-derived polymers for coating applications: Comparing poly(limonene carbonate) and poly(cyclohexadiene carbonate). Polym. Chem. 2017, 8, 6099−6105.

(15) Hauenstein, O.; Rahman, M. M.; Elsayed, M.; Krause-Rehberg, R.; Agarwal, S.; Abetz, V.; Greiner, A. Biobased polycarbonate as a gas separation membrane and “breathing glass” for energy saving applications. Adv. Mater. Technol. 2017, 2, No. 1700026.

(16) Parrino, F.; Fidalgo, A.; Palmisano, L.; Ilharco, L. M.; Pagliaro, M.; Ciriminna, R. Polymers of limonene oxide and carbon dioxide: Polycarbonates of the solar economy. ACS Omega 2018, 3, 4884−4890.

(17) Zhang, D.; del Rio-Chanona, E. A.; Wagner, J. L.; Shah, N. Life cycle assessments of bio-based sustainable polylimonene carbonate production process. Sustainable Prod. Consumption 2018, 14, 152−160.

(18) Durkin, A.; Taptygin, I.; Kong, Q.; Gunam Resul, M. F. M.; Rehman, A.; Fernández, A. M. L.; Harvey, A. P.; Shah, N.; Guo, M. Scale-up and sustainability evaluation of biopolymer production from citrus waste offering carbon capture and utilisation pathway. ChemistryOpen 2019, 8, 668−688.

(19) Bai, D.; Liu, H.; Bai, H.; Zhang, Q.; Fu, Q. Low-temperature sintering of stereocomplex-type polylactide nascent powder: Effect of crystallinity. Macromolecules 2017, 50, 7611−7619.

(20) Bai, H.; Deng, S.; Bai, D.; Zhang, Q.; Fu, Q. Recent advances in processing of stereocomplex-type polylactide. Macromol. Rapid Commun. 2017, 38, No. 1700454.

(21) Fu, M.; Liu, Z.; Bai, D.; Ling, F.; Bai, H.; Zhang, Q.; Fu, Q. Low-temperature sintering of stereocomplex-type polylactide nascent powder: From compression molding to injection molding. Macromol. Mater. Eng. 2018, 303, No. 1800178.

(22) Bai, D.; Liu, H.; Bai, H.; Zhang, Q.; Fu, Q. Powder metallurgy inspired low-temperature fabrication of high-performance stereocomplexed polylactide products with good optical transparency. Sci. Rep. 2016, 6, No. 20260.

(23) Liu, Z.; Fu, M.; Ling, F.; Sui, G.; Bai, H.; Zhang, Q.; Fu, Q. Stereocomplex-type polylactide with bimodal melting temperature distribution: Toward desirable melt processability and thermomechanical performance. Polymer 2019, 169, 21−28.

(24) Hofmann, D.; Kurek, A.; Thomann, R.; Schwabe, J.; Mark, S.; Enders, M.; Hees, T.; Mülhaupt, R. Tailored nanostructured HDPE Wax/UHMWPE reactor blends as additives for melt-processable allpolyethylene composites and in situ UHMWPE fiber reinforcement. Macromolecules 2017, 50, 8129−8139.

(25) Sander, M. M.; Nicolau, A.; Guzatto, R.; Samios, D. Plasticiser effect of oleic acid polyester on polyethylene and polypropylene. Polym. Test. 2012, 31, 1077−1082.

(26) Eenink, M. J. D.; Feijen, J.; Olijslager, J.; Albers, J. H. M.; Rieke, A. J. C.; Greidanus, P. J. Biodegradable hollow fibres for controlled release of hormones. J. Controlled Release 1987, 6, 225−247.

(27) Lomellini, P. Viscosity-temperature relationships of a polycarbonate melt: Williams-Landel-Ferry versus Arrhenius behaviour. Makromol. Chem. 1992, 193, 69−79.

(28) Marcilla, A.; Beltrán, M. Mechanisms of Plasticizers Action. In Handbook of Plasticizers; Elsevier, 2012; pp 119−133.

(29) Delbreilh, L.; Dargent, E.; Grenet, J.; Saiter, J.-M.; Bernès, A.; Lacabanne, C. Study of poly(bisphenol A carbonate) relaxation kinetics at the glass transition temperature. Eur. Polym. J. 2007, 43, 249−254.

(30) Chieng, B. W.; Ibrahim, N. A.; Then, Y. Y.; Loo, Y. Y. Epoxidized vegetable oils plasticized poly(lactic acid) biocomposites: Mechanical, thermal and morphology properties. Molecules 2014, 19, 16024−16038.

(31) Bouchoul, B.; Benaniba, M. T.; Massardier, V. Thermal and mechanical properties of bio-based plasticizers mixtures on poly(vinyl chloride). Polıḿ eros 2017, 27, 237−246.

# Supporting Information

to

# Unlocking the processability and recyclability of biobased poly(limonene carbonate)

Simon Neumann, † Lisa-Cathrin Leitner, † Holger Schmalz, †,‡ Seema Agarwal, †,‡ Andreas Greiner †,‡, *

† University of Bayreuth, Macromolecular Chemistry II, Universitätsstrasse 30, 95440 Bayreuth, Germany.

‡ University of Bayreuth, Bavarian Polymer Institute, Universitätsstrasse 30, 95440 Bayreuth, Germany.

Corresponding author: greiner@uni-bayreuth.de

Total pages: 18 Total number of Figures: 11 Total number of Tables: 6

**Table of Contents**

**Table S2.** Mechanical properties of PLimC/EtOL compounds with 7.5 wt% EtOL

**Table S3.** Mechanical properties of PLimC/EtOL compounds with 10.0 wt% EtOL

**Table S4.** Mechanical properties of PLimC/EtOL compounds with 15 wt% EtOL

**Table S5.** Mechanical properties of polycarbonate Lexan 141 (Sabic)

**Table S6.** Mechanical and optical properties of the recycled PLimC/EtOL compound with 7.5 wt% EtOL

**$CHCl_3$-GPC trace of neat PLimC**

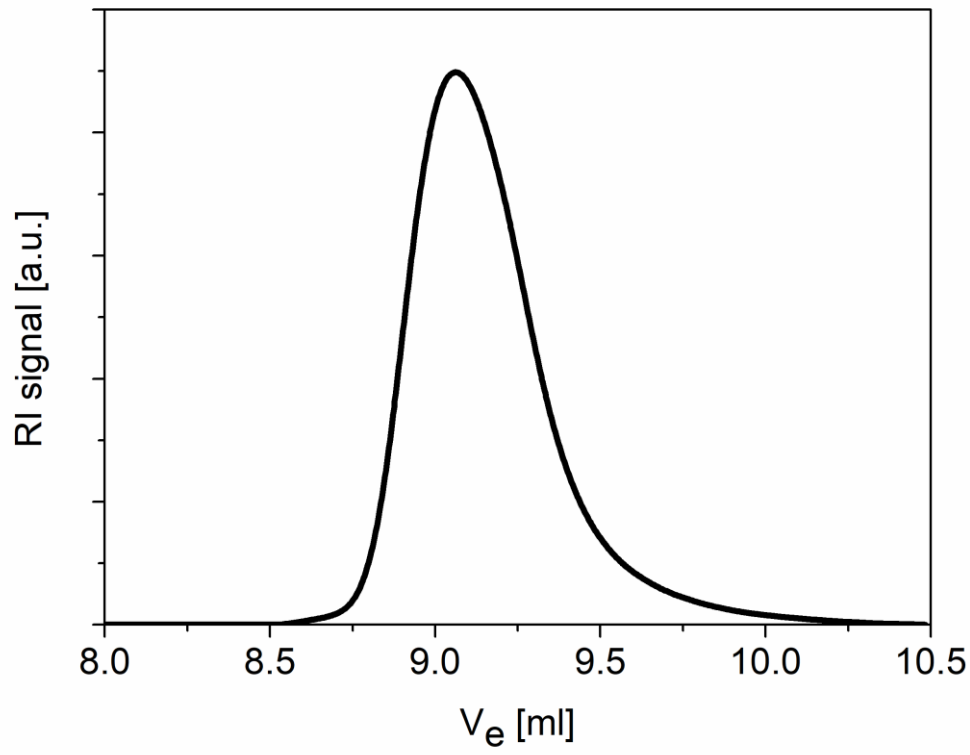


**Figure S1.** $CHCl_3$-GPC trace of the employed PLimC ($M_{n,\,app}$ = 50 000 g/mol, $Đ$ = 1.15).

**Raman imaging on a PLimC/EtOL compound**

**A)**

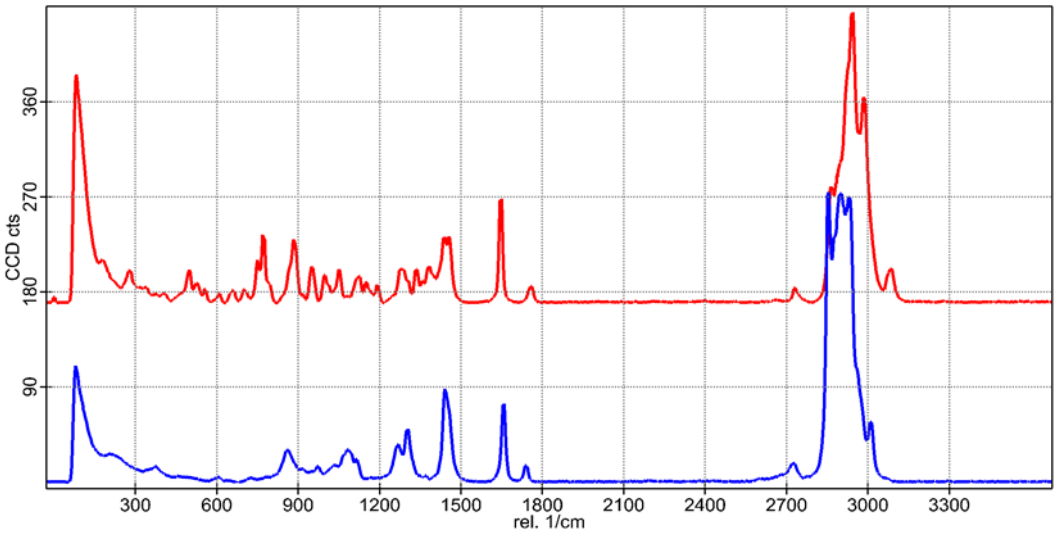


**B)**

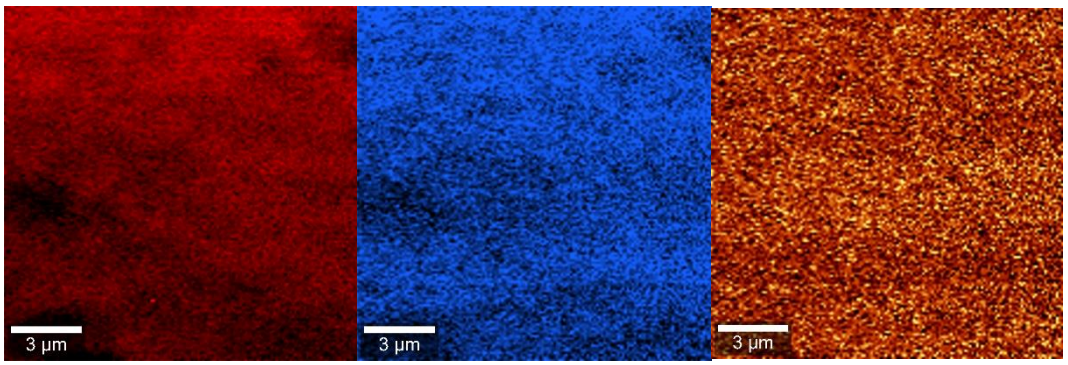


**Figure S2.** A) Raman spectra of PLimC (red) and EtOL (blue). B) Raman x,y-imaging on a PLimC/EtOL compound with 15wt% EtOL (λ = 532 nm, step width 100 nm pixel$^{-1}$ , 100x objective with NA = 0.9): PLimC distribution (left image); ethyl oleate distribution (middle image); ratio between PLimC and ethyl oleate (right image). A homogenous distribution of ethyl oleate in the polymer matrix could be detected in the limit of lateral resolution for the employed 100x objective (ca. 350 nm).

**TGA of PLimC**

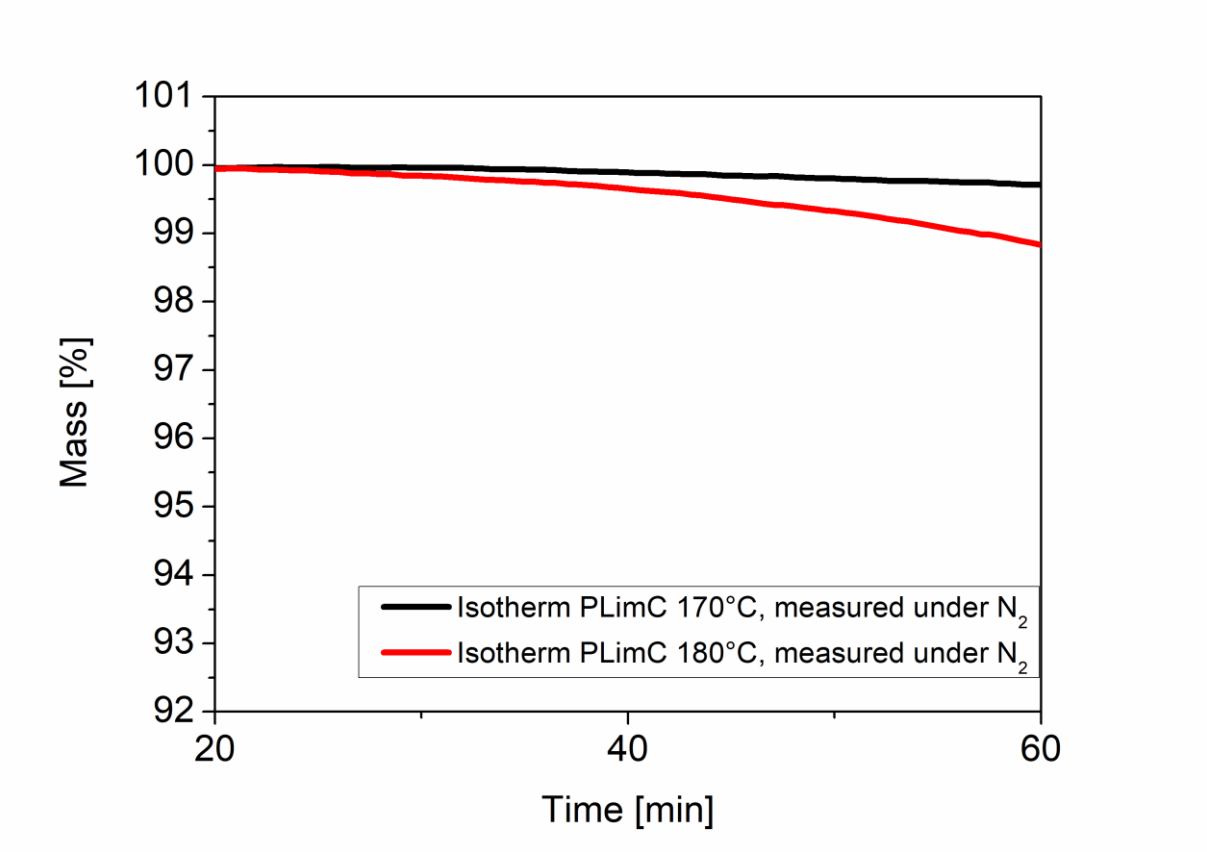


**Figure S3.** TGA isotherms of PLimC at two different temperatures (170 °C and 180 °C, measured under nitrogen).

**Melt processability of neat PLimC**

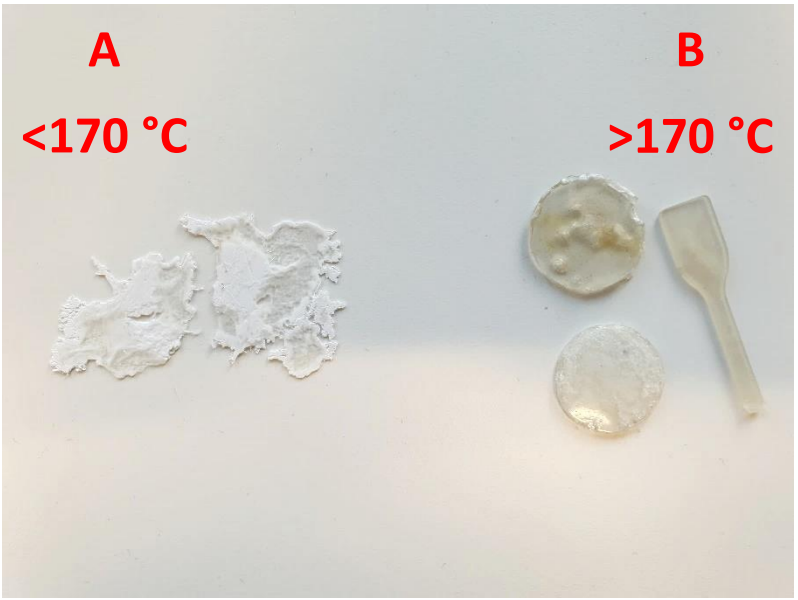


**Figure S4.** Melt processability of neat PLimC at different temperatures. Digital images of samples compression molded at 160 °C (A) and at temperatures above 170 °C (B).

## $^{1}$H-NMR of PLimC/EtOL compounds

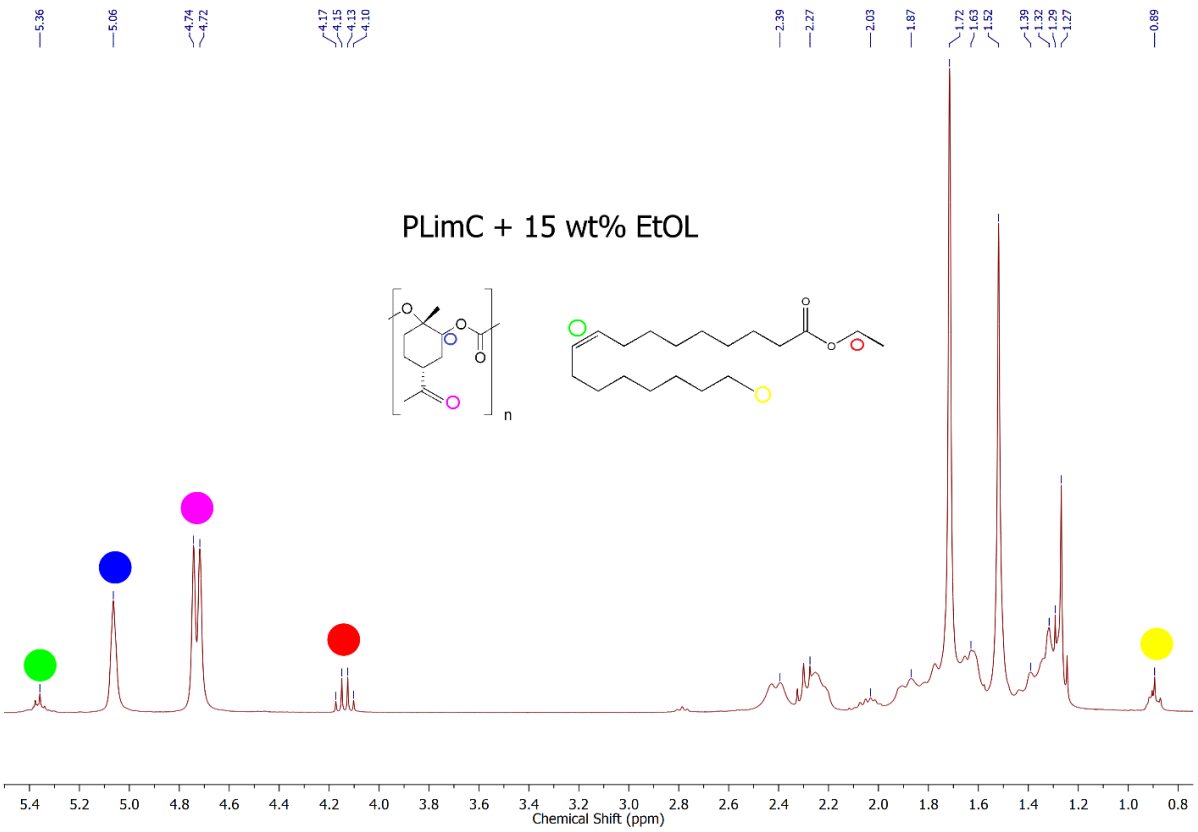


**Figure S5.** $^{1}$H-NMR spectrum (CDCl3, 300 MHz) of PLimC with 15 wt% EtOL. The EtOL content in mol% was calculated by using the characteristic quartet of the methylene group of EtOL (marked in red). The reference proton for PLimC is marked in blue. The methylene group of EtOL represents two protons, whereas the reference proton for PLimC is one, resulting in 10 mol% EtOL. Using the molar masses of EtOL and the repetition unit of PLimC, respectively, the weight fraction of EtOL in PLimC was then calculated to 14.9 wt%. For all other PLimC/EtOL compounds the same procedure was used.

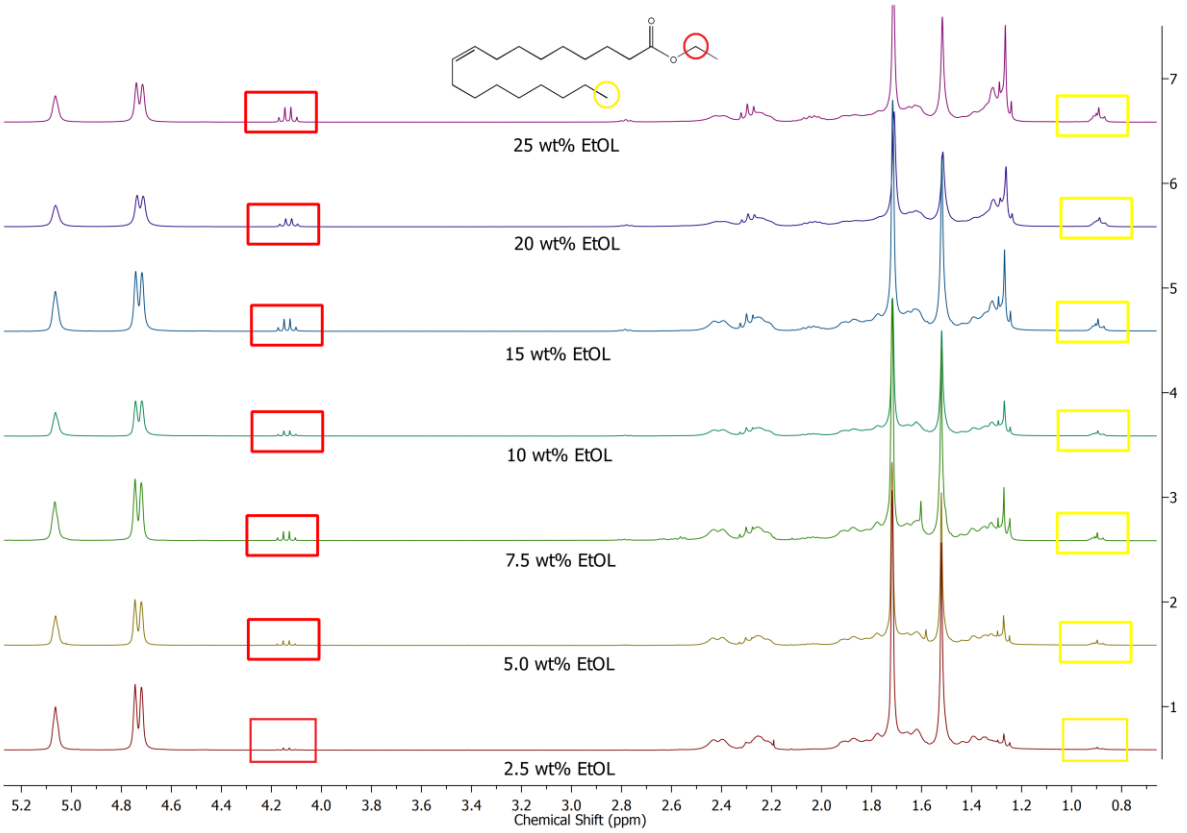


**Figure S6.** $^{1}$H-NMR spectra ($CDCl_3$, 300 MHz) of PLimC/EtOL compounds with different EtOL contents from 2.5 wt% – 25 wt%. The increasing amount of EtOL can be identified in the characteristic quartet of the methylene group (marked in red) or in the methyl group of EtOL (marked in yellow).

**DSC of PLimC/EtOL compounds**

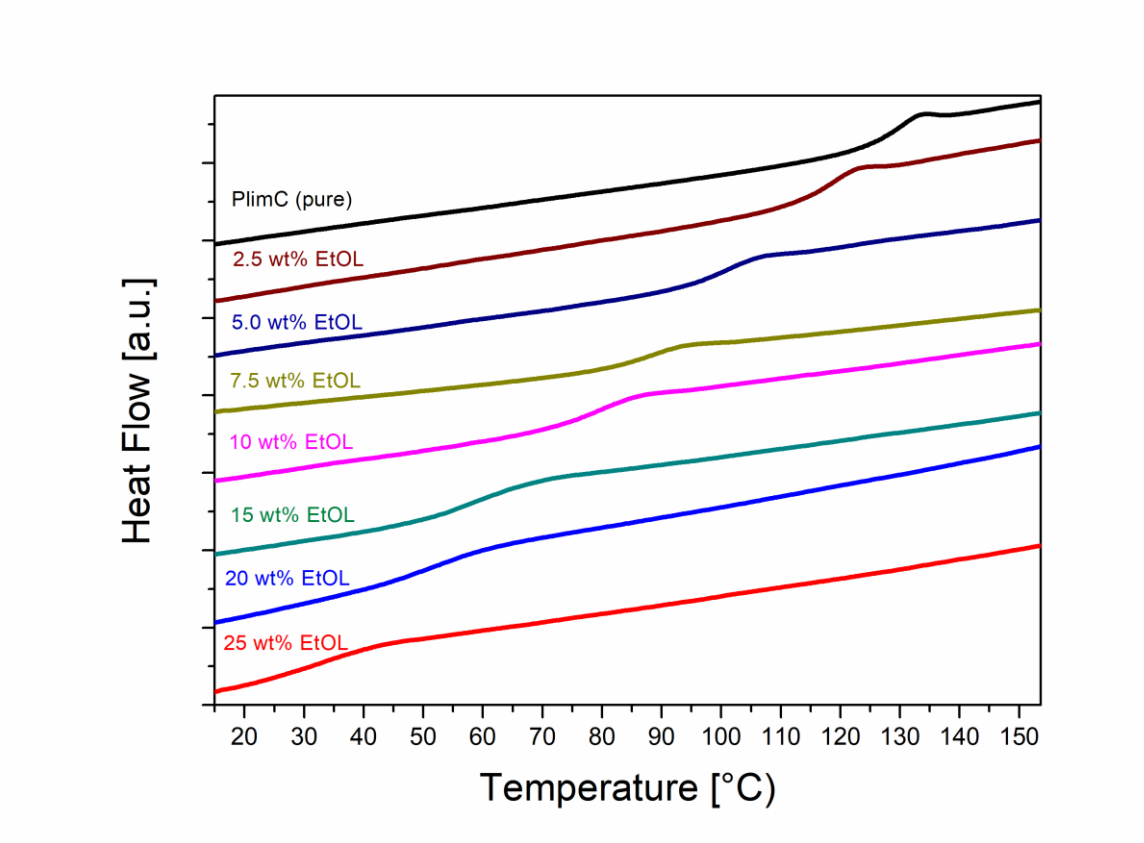


**Figure S7.** DSC thermograms of PLimC with different EtOL contents. The displayed traces correspond to the second heating curve measured at 10 K $min^{-1}$.

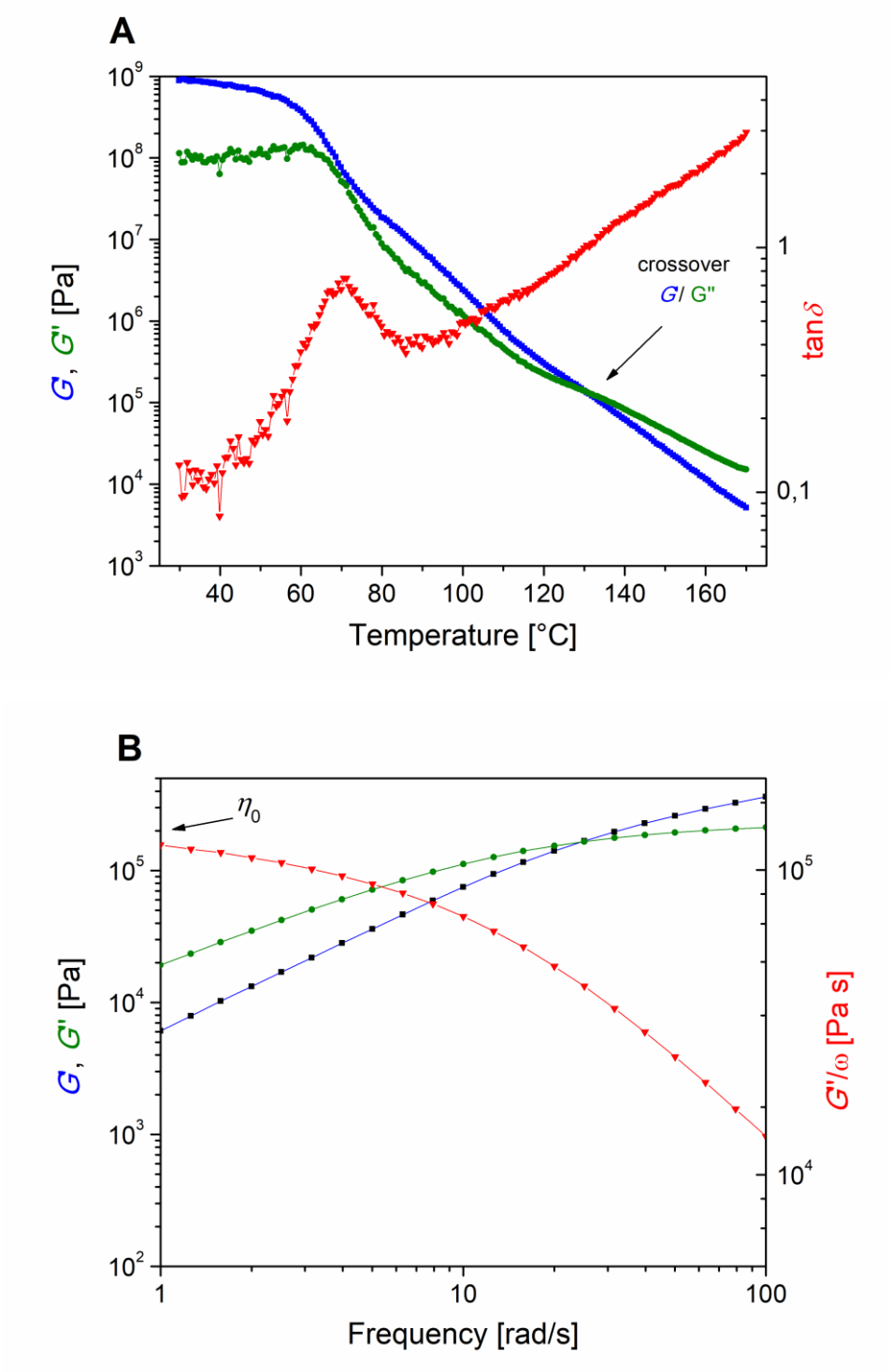


**Figure S8.** A) Temperature-dependent dynamic moduli for a PLimC/EtOL compound with 10% EtOL and B) corresponding frequency sweep at 170 °C. The zero shear viscosity $\eta_0$ = 0.12 MPa s was calculated from $G''/\omega$ for the lowest measured frequency.

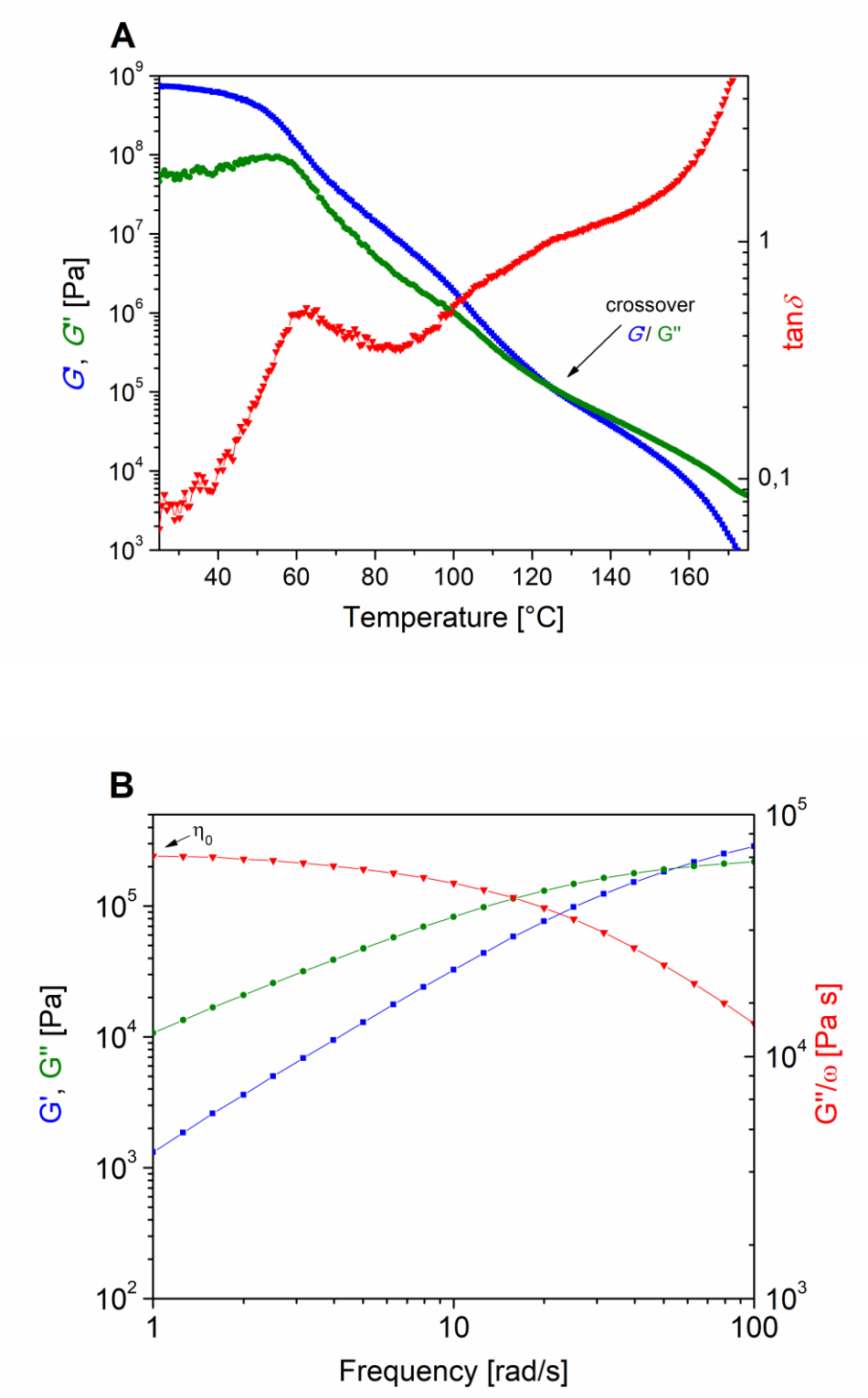


**Figure S9.** A) Temperature-dependent dynamic moduli for a PLimC/EtOL compound with 15 wt% EtOL and B) corresponding frequency sweep at 170 °C. The zero shear viscosity $\eta_0$ = 0.07 MPa s was calculated from $G''/\omega$ for the lowest measured frequency.

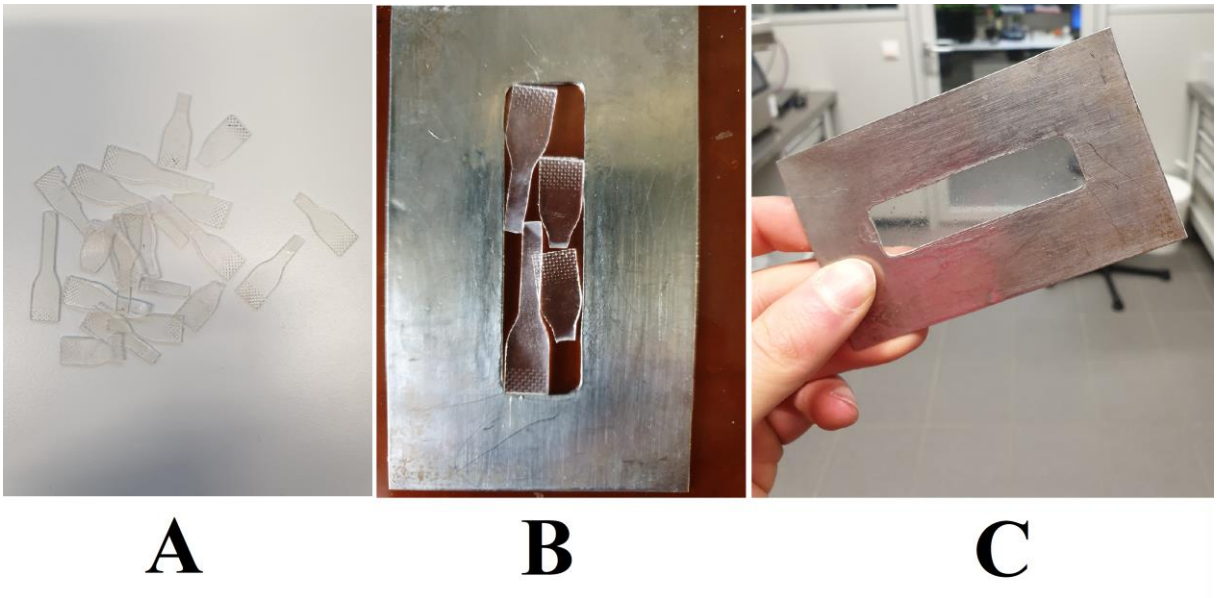


**Figure S10.** Fragments of the dog bone-shaped tensile specimens of the PLimC/EtOL compound with 7.5 wt% EtOL (A) were put into a frame (6 cm x 1.5 cm x 1mm) for recycling (B). The sample was again compression molded at 160 °C, yielding a clear and transparent recycled PLimC/EtOL plate (C).

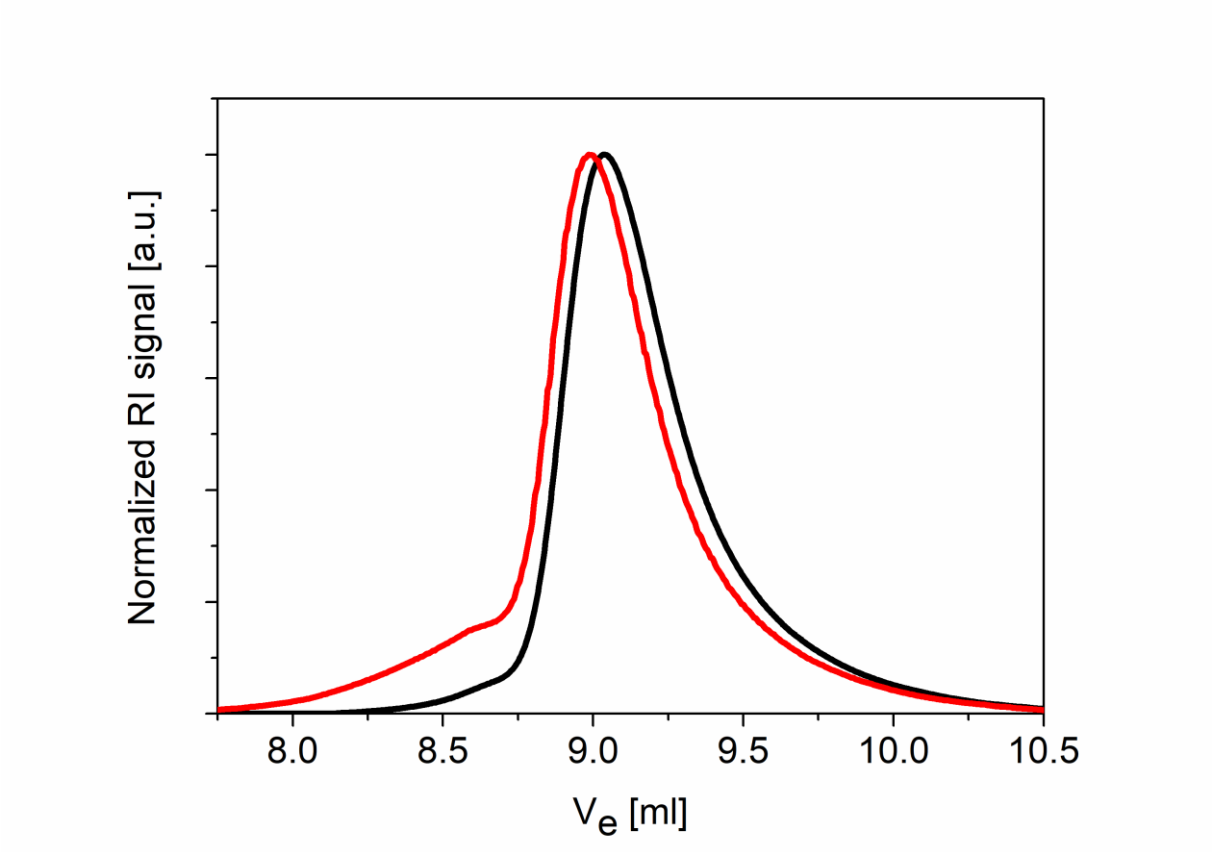


**Figure S11.** $CHCl_3$-GPC traces of the PLimC/EtOL compound with 7.5 wt% EtOL after hot pressing for one (black) and two times (red).

**Table S1.** Composition of PLimC/EtOL compounds

| Sample | PLimC [mg] | EtOL [mg] | EtOL [ml] | DCM [ml] | EtOL loading [wt%] | EtOL content [wt%] [a] | EtOL content [mol%][a] | $T_g$ [°C][b] |
|---|---|---|---|---|---|---|---|---|
| Reference | 500.0 | 0 | 0 | 0 | 0 | 0 | 0 | 128 |
| 1 | 527.1 | 8.7 | 0.010 | 15 | 2.5 | 3.1 | 2.0 | 116 |
| 2 | 502.3 | 25 | 0.029 | 15 | 5.0 | 5.4 | 3.5 | 97 |
| 3 | 500.0 | 37.5 | 0.043 | 15 | 7.5 | 8.4 | 5.5 | 86 |
| 4 | 513.7 | 50 | 0.058 | 15 | 10.0 | 10.6 | 7.0 | 78 |
| 5 | 499.8 | 75 | 0.086 | 15 | 15.0 | 14.9 | 10.0 | 58 |
| 6 | 502.0 | 100 | 0.115 | 15 | 20.0 | 19.8 | 13.5 | 53 |
| 7 | 509.3 | 125 | 0.144 | 15 | 25.0 | 24.4 | 17.0 | 32 |

[a] Determined by $^1$H-NMR spectroscopy.

[b] The glass transition temperature ($T_g$) was determined by DSC from the second heating traces measured at 10 K min$^{-1}$.

**Table S2.** Mechanical properties of PLimC/EtOL compounds (7.5 wt% loading)

| | Unit | Sample 1 | Sample 2 | Sample 3 | Sample 4 | Sample 5 | Sample 6 | Sample 7 | Sample 8 | Sample 9 | Sample 10 | **Average ø** | Standard Deviation σ |
|---|---|---|---|---|---|---|---|---|---|---|---|---|---|
| Length | mm | 3.9 | 4 | 4 | 4 | 4 | 4 | 4 | 4 | 4 | 4 | | |
| Width | mm | 15 | 15 | 15 | 15 | 15 | 15 | 15 | 15 | 15 | 15 | | |
| Thickness | mm | 1.13 | 1.16 | 1.19 | 1.12 | 1.09 | 1.17 | 1.1 | 1.11 | 1.11 | 1.13 | | |
| | | | | | | | | | | | | | |
| Tensile strength | MPa | 10 | 20 | 29 | 27 | 28 | 5 | 29 | 22 | 22 | 28 | **22** | 8 |
| Elongation at break | % | 16 | 35 | 19 | 32 | 19 | 20 | 20 | 39 | 39 | 40 | **28** | 9 |
| E-modulus | MPa | 2148 | 2181 | 2499 | 2197 | 1966 | 1738 | 2138 | 1946 | 2163 | 2146 | **2113** | 189 |

0.5 mm min$^{-1}$ test speed was used to measure the elastic modulus. 2.0 mm min$^{-1}$ test speed was used for tensile strength and elongation at break determination.

**Table S3.** Mechanical properties of PLimC/EtOL compounds with 10.0 wt% EtOL

| | Unit | Sample 1 | Sample 2 | Sample 3 | Sample 4 | Sample 5 | Sample 6 | Sample 7 | Sample 8 | Sample 9 | Sample 10 | **Average ø** | Standard Deviation σ |
|---|---|---|---|---|---|---|---|---|---|---|---|---|---|
| Length | mm | 15 | 15 | 15 | 15 | 15 | 15 | 15 | 15 | 15 | 15 | | |
| Width | mm | 3.9 | 3.91 | 3.92 | 3.9 | 3.9 | 3.92 | 3.9 | 3.88 | 3.92 | 3.87 | | |
| Thickness | mm | 1.16 | 1.19 | 1.06 | 1.17 | 1.1 | 1.08 | 1.08 | 1.07 | 1.14 | 1.07 | | |
| | | | | | | | | | | | | | |
| Tensile strength | MPa | 18 | 20 | 21 | 25 | 20 | 23 | 17 | 20 | 20 | 21 | 21 | 2 |
| Elongation at break | % | 7 | 1 | 26 | 2 | 4 | 15 | 11 | 6 | 6 | 34 | 11 | 10 |
| E-modulus | MPa | 1799 | 1756 | 1867 | 1981 | 1562 | 1774 | 1337 | 1528 | 1723 | 1889 | 1722 | 184 |

0.5 mm $min^{-1}$ test speed was used to measure the elastic modulus. 2.0 mm $min^{-1}$ test speed was used for tensile strength and elongation at break determination.

**Table S4.** Mechanical properties of PLimC/EtOL compounds (15 wt% loading)

| | Unit | Sample 1 | Sample 2 | Sample 3 | Sample 4 | Sample 5 | Sample 6 | Sample 7 | Sample 8 | Sample 9 | **Average ø** | Standard Deviation σ |
|---|---|---|---|---|---|---|---|---|---|---|---|---|
| Length | mm | 4 | 4 | 4 | 4 | 4 | 4 | 4 | 4 | 4 | | |
| Width | mm | 15 | 15 | 15 | 15 | 15 | 15 | 15 | 15 | 15 | | |
| Thickness | mm | 1.16 | 1.16 | 1.13 | 1.08 | 1.16 | 1.22 | 1.28 | 1.27 | 1.27 | | |
| | | | | | | | | | | | | |
| Tensile strength | MPa | 20 | 19 | 25 | 20 | 20 | 18 | 17 | 18 | 19 | **19** | 2 |
| Elongation at break | % | 13 | 8 | 9 | 12 | 14 | 29 | 6 | 19 | 5 | **13** | 7 |
| E-modulus | MPa | 1969 | 1650 | 1880 | 1920 | 1675 | 1745 | 716 | 1631 | 1661 | **1650** | 351 |

0.5 mm $min^{-1}$ test speed was used to measure the elastic modulus. 2.0 mm $min^{-1}$ test speed was used for tensile strength and elongation at break determination.

**Table S5.** Mechanical properties of polycarbonate Lexan 141 (Sabic)

| | Unit | Sample 1 | Sample 2 | Sample 3 | Sample 4 | Sample 5 | Sample 6 | Sample 7 | Sample 8 | Sample 9 | Sample 10 | **Average ø** | Standard Deviation σ |
|---|---|---|---|---|---|---|---|---|---|---|---|---|---|
| Length | mm | 4 | 4 | 4 | 4 | 4 | 4 | 4 | 4 | 4 | 4 | | |
| Width | mm | 15 | 15 | 15 | 15 | 15 | 15 | 15 | 15 | 15 | 15 | | |
| Thickness | mm | 1.54 | 1.55 | 1.88 | 1.88 | 1.4 | 1.79 | 1.54 | 1.47 | 1.57 | 1.75 | | |
| | | | | | | | | | | | | | |
| Tensile strength | MPa | 38 | 50 | 46 | 45 | 46 | 56 | 47 | 55 | 55 | 54 | **49** | 6 |
| Elongation at break | % | 5 | 10 | 100 | 6 | 7 | 98 | 93 | 92 | 97 | 99 | **61** | 46 |
| E-modulus | MPa | 1813 | 1955 | 1608 | 2225 | 1771 | 1711 | 1531 | 1681 | 1944 | 1842 | **1808** | 200 |

0.5 mm $min^{-1}$ test speed was used to measure the elastic modulus. 2.0 mm $min^{-1}$ test speed was used for tensile strength and elongation at break determination.

**Table S6:** Mechanical and optical properties of recycled PLimC-EtOL

| | Unit | Sample 1 | Sample 2 | Sample 3 | Sample 4 | Sample 5 | **Average ø** | Standard Deviation σ |
|---|---|---|---|---|---|---|---|---|
| **Mechanical** | | | | | | | | |
| Tensile strength | MPa | 32 | 7 | 5 | 33 | 31 | **22** | 13 |
| Elongation at break | % | 2 | 1 | 2 | 3 | 39 | **9** | 15 |
| E-modulus | MPa | 2030 | 1762 | 2011 | 1874 | 2004 | **1936** | 103 |
| **Optical** | | | | | | | | |
| Transmission | % | 93 | 92 | 94 | - | - | **93** | 1 |
| Haze | % | 18 | 17 | 16 | - | - | **17** | 1 |
| Clarity | % | 93 | 92 | 93 | - | - | **93** | 1 |

0.5 mm $min^{-1}$ test speed was used to measure the elastic modulus. 2.0 mm $min^{-1}$ test speed was used for tensile strength and elongation at break determination.

# 9.2 Blends of bio-based poly(limonene carbonate) with commodity polymers

Simon Neumann, Pin Hu, Felix Bretschneider, Holger Schmalz, Andreas Greiner*

University of Bayreuth, Macromolecular Chemistry and Bavarian Polymer Institute, Universitätsstraße 30, 95440 Bayreuth, Germany

E-mail: greiner@uni-bayreuth.de

in

Macromolecular Materials and Engineering

Received: February 7, 2021

Revised: April 11, 2021

Published: June 12, 2021

https://doi.org/10.1002/mame.202100090

**Macromol. Mater. Eng. 2021, 2100090**



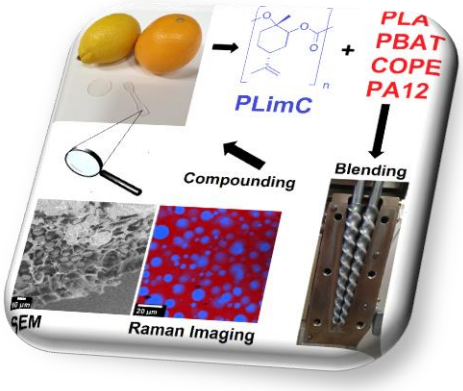


WILEY

ABSTRACT

In this study, blends of the biobased poly(limonene carbonate) (PLimC) with different commodity polymers were investigated in order to explore the potential of PLimC toward generating more sustainable polymer materials by reducing the amount of petro- or food-based polymers. PLimC was employed as minority component in the blends. Next to the morphology and thermal properties of the blends the impact of PLimC on the mechanical properties of the matrix polymers was studied. The interplay of incompatibility and zero-shear melt viscosity contrast determined the blend morphology, leading for all blends to a dispersed droplet morphology for PLimC. Blends with polymers of similar structure to PLimC (*e.g.*, aliphatic/aromatic polyester) showed the best performance with respect to mechanical properties, whereas blends with polystyrene or poly(methyl methacrylate) were too brittle and polyamide 12 blends showed very low elongations at break. In blends with Ecoflex (poly(butylene adipate-*co*-terephthalate)) and Arnitel EM400 (copolyetherester) with poly(butylene terephthalate) hard and polytetrahydrofuran soft segments) a threefold increase in *E*-modulus could be achieved, while keeping the elongation at break at reasonable high values of about 200%, making these blends highly interesting for applications.

## 1. INTRODUCTION

Based on the limitation of fossil resources, the development of bio-based and sustainable polymers and their corresponding blends is a highly relevant and intensively studied field of research.[1] Several bio-based synthetic polymers are made from naturally derived monomers and show biodegradability, like poly(hydroxy alkanoates) (PHAs), poly(butylene succinate) (PBS) or poly(*L*-lactic acid) (PLA).[2] $CO_2$ is one of the interesting candidates as a sustainable C1 building block for polymers, because it is non-toxic, cheap, and highly available. It can react with epoxides *via* alternating ring-opening copolymerization (ROCOP) to polycarbonates.[3, 4] Limonene oxide (LO) is next to menth-2-ene oxide (Men2C) one of the few bio-based epoxides and can be directly produced by oxidizing naturally occurring limonene (main component from citrus oil) to yield bio-based polycarbonates *via* ROCOP with $CO_2$.[5, 6] About 57000 t/a[7] of citrus oil are gathered as side product from the orange juice production, representing a significant non-food based feedstock for LO production.[4] Synthesis of poly(limonene carbonate) (PLimC) by ROCOP of *trans*-limonene oxide (*trans*-LO) and $CO_2$ was first introduced by Coates et al.[8], employing a $\beta$-diiminate zinc complex ([(bdi)Zn($\mu$-OAc)]. Further on, in 2015 Kleij et. al. developed an Al(III) aminotriphenolate complex for the

synthesis of PLimC.[9, 10] In the last 5 years, lot of research efforts have been focused on PLimC.[9, 10, 11] The synthesis of high molar mass PLimC ($M_n$ ~ 100 kg·mol$^{-1}$) by using [(bdi)Zn($\mu$-OAc)] as catalyst was achieved by masking hydroxyl impurities in *trans*-LO, as demonstrated by Hauenstein et al.[6] This high molar mass PLimC features a high glass transition temperature ($T_g$ = 130 °C), high transparency (99.8%), high light transmission (95%) and Young´s modulus ($E$ = 0.95 GPa). PLimC has also a high gas permeability for oxygen and $CO_2$, which can be made use of in "breathing glass" applications.[12] A highly versatile and efficient route for PLimC modification is based on thiol-ene click chemistry, which allows to tailor properties like solubility, $T_g$ or subsequent crosslinking for coating applications.[13] Moreover, the living character of ROCOP catalyzed by [(bdi)Zn($\mu$-OAc)] allows the synthesis of well-defined PLimC-*block*-poly(cyclohexene carbonate) diblock copolymers, showing an interesting phase behaviour with a rather broad stability range for the HPL (hexagonal perforated lamella) morphology.[14] The market potential of PLimC has been recently assessed by Parrino et al.[15] and Zhang et al.[16] They show that PLimC can be an useful non-toxic, bio-based alternative for bisphenol A based polycarbonates (BPA-PC), which use highly toxic monomers, such as phosgene and bisphenol A. According to Zhang et al., PLimC is a potential replacement for fossil based polystyrene (PS), because the production costs of both polymers are quite similar (ca. \$1.36-\$1.51 kg$^{-1}$).[16] An easy and cost-efficient method to produce materials with new properties is blending. The currently technically used bio-based polymers, such as PLA, are mainly used in the form of blends (e.g. in blends with polyglycols[17], poly(vinyl acetate)[18], polypropylene[19] or styrene resins[20]). Also blends of biodegradable poly(butylene adipate-*co*-terephthalate) (PBAT, EcoFlex®) and PLA with improved mechanical properties were established.[21] The importance of PAH[22] and PBS[23] blends as well as bio-based blends in general have been highlighted in several publications and reviews.[24] One advantage of employing PLimC in blends, next to its sustainability, is its high glass transition temperature ($T_g$ = 130 °C), which can lead to blends with increased heat resistance. Besides, due to its high glass transition temperature neat PLimC is usually rather brittle and exhibits a comparably low elongation at break. Together with the high melt viscosity of PLimC, which is inherently attributed to its stiff polymer backbone, melt processing of neat PLimC usually requires the use of additives like bio-based ethyl oleate.[25] Hence, the use of bio-based PLimC as minority component in polymer blends represents an elegant method to harness its high glass transition temperature without encountering difficulties in melt processing due to its high melt viscosity and the need to use additional additives.

In this contribution PLimC blends (10 – 30 wt% PLimC) with engineering or commodity plastics have been explored with the aim to gain an basic understanding of PLimC blends which could lead to future sustainable polymer materials. As matrix polymers for blending with PLimC we considered polymers with similar structure, like aliphatic/aromatic polyesters and polyamides, to ensure a good combability (e.g., PLA, PBAT, polyamide 12 (PA12), segmented copoly(ether ester)s (COPE, Arnitel EM400®). Additionally, commodity plastics with similar glass transition temperatures (e.g., poly(methyl methacrylate) (PMMA) or PS) were also employed. The different blend systems were investigated with respect to their morphology, thermal and mechanical properties. The outcome of the basic understanding of the present PLimC blends with selected commodity polymers should be the starting point for future developments for tuning of blends properties towards more sustainable und useful polymer materials.

## 2. RESULTS AND DISCUSSION

### 2.1 Selection and specifications of blend components

Poly(*L*-lactic acid) (PLA), polyamide 12 (PA12), poly(butylene adipate-*co*-terephthalate) (PBAT, EcoFlex®) and a segmented copoly(ether ester) (COPE, Arnitel EM400®) were selected as matrix polymers for PLimC blends because of their similar chemical structure (polyesters, polyamides) to PLimC. PS ($T_g$ = 100 °C) and PMMA ($T_g$ = 117 °C) were chosen as polymers with glass transition temperatures close to that of PLimC ($T_g$ = 130 °C). Compatibility of the used polymers with PLimC can be estimated by comparing the polymer solubility parameters ($\delta$). As the solubility parameters are significantly different from PLimC (**Table 1**), phase separation is expected for all blend systems. Melt viscosity and molecular weight of the investigated polymers are also playing a significant role in the blending process, because PLimC has by far the highest zero-shear melt viscosity (**Table 1**). Consequently, at the employed weight fractions (10 – 30 wt%) PLimC is expected to form the dispersed phase in the blend and the matrix will be formed by the polymer with the lower melt viscosity. Characteristics of the employed polymers and processing parameters for blending are summarized in **Table 1**.

**Table 1**. Characteristics of the employed polymers and processing conditions for blend preparation.

| Polymer | Grade | Supplier | $M_n$ / $Đ$ [a] | δ [b] | $\eta_0$ [c] | Processing temperature |
|---|---|---|---|---|---|---|
| | | | [kDa] / - | [$MPa^{1/2}$] | [kPa·s] | [°C] |
| **PLimC** | - | - | 65/1.1 | 17.6[14] | 890[25] | - |
| **PLA** | Inego 4060D | Nature Works | 64/1.7 | 20.7[26] | 4.2[27] | 190 |
| **PBAT** | EcoFlex, BASF F Blend A1200 | BASF SE | 45/1.3 | 22.3[28] | 2.7[29] | 180 |
| **COPE** | Arnitel EM400 | DSM | 75/1.5 | 19.2[30] | 0.275[31] | 200 |
| **PA12** | Vestamid Typ L1600 | Evonik Industries | 40/1.4 | 20.8[30] | 0.390[32] | 185 |
| **PMMA** | PLEXIGLAS® 8N | Evonik Industries | 57/1.6 | 18.6[33] | 0.071[34] | 180 |
| **PS** | BASF 143E | BASF SE | 121/2.0 | 18.7[33] | - | 180 |

[a] Number average molecular weight ($M_n$) and dispersity ($Đ$) were determined by $CHCl_3$-GPC and HFIP-GPC, calibrated with narrowly distributed PS ($CHCl_3$-GPC) and PMMA (HFIP-GPC) standards.
[b] Solubility parameter.
[c] Zero-shear melt viscosity.

Blends with PS and PMMA were found to be inhomogeneous and/or very brittle and, thus, were not pursued further. An overview of these blend systems and their mechanical data can be found in the supporting information **(Figure S1, Table S1)**. In the following, the morphology and thermal/mechanical properties of the other blend systems will be discussed starting with PLA (aliphatic polyester), followed by PBAT (aromatic/aliphatic polyester), Arnitel EM400 (segmented aromatic copoly(ether ester)) and PA12 (aliphatic polyamide).

### 2.2 Blends with poly(*L*-lactic acid) (PLA, aliphatic polyester)

The effect of blending PLA with bio-based PLimC is addressed in the following. PLA/PLimC blends are opaque in comparison to neat PLA, which is transparent (**Figure S2)**, indicating phase-separation in PLA/PLimC blends. Morphology investigation with scanning electron microscopy (SEM) reveals a homogenous dispersion of spherical PLimC droplets in the PLA matrix for blends with 10 and 30 wt% PLimC, respectively (**Figure 1**). PLimC is forming the dispersed phase, because it is the minority component and the melt viscosity of PLimC ($\eta_0$ =

890 kPa·s)[25] is significantly higher compared to that of PLA ($\eta_0$ = 4.2 kPa·s)[27] (**Table 1**). As a result, the shear forces during melt processing are not sufficient to deform or split the PLimC droplets further. From SEM measurements, an average PLimC droplet diameter of $D$ = 3.6 ± 3.9 µm (PLA/PLimC = 90/10 w/w) and $D$ = 6.0 ± 6.1 µm (PLA/PLimC = 70/30 w/w) from surface fractures can be extracted (**Table 2, Figure S3**). For the calculation of the droplet size, the area of each PLimC droplet was measured using the ImageJ software.[35] Then, assuming that droplets are fully spherical particles and the fracture have gone through the middle of each droplet, the diameter corresponding to the area was back calculated. Of course, these assumptions cannot be 100% fulfilled, hence resulting in the relatively high standard deviations. PLimC and PLA can be nicely distinguished based on their Raman spectra (**Figure S4**), which enables the use of Raman imaging for morphological studies. Comparing SEM with Raman imaging shows values for the PLimC droplet diameters in the same order of magnitude (PLA/PLimC = 90/10 w/w: $D$ = 2.8 ± 3.0 µm, PLA/PLimC = 70/30 w/w: $D$ = 7.1 ± 7.2 µm). The corresponding domain size distributions are presented in the Supporting Information (**Figure S5, Table S2)**.

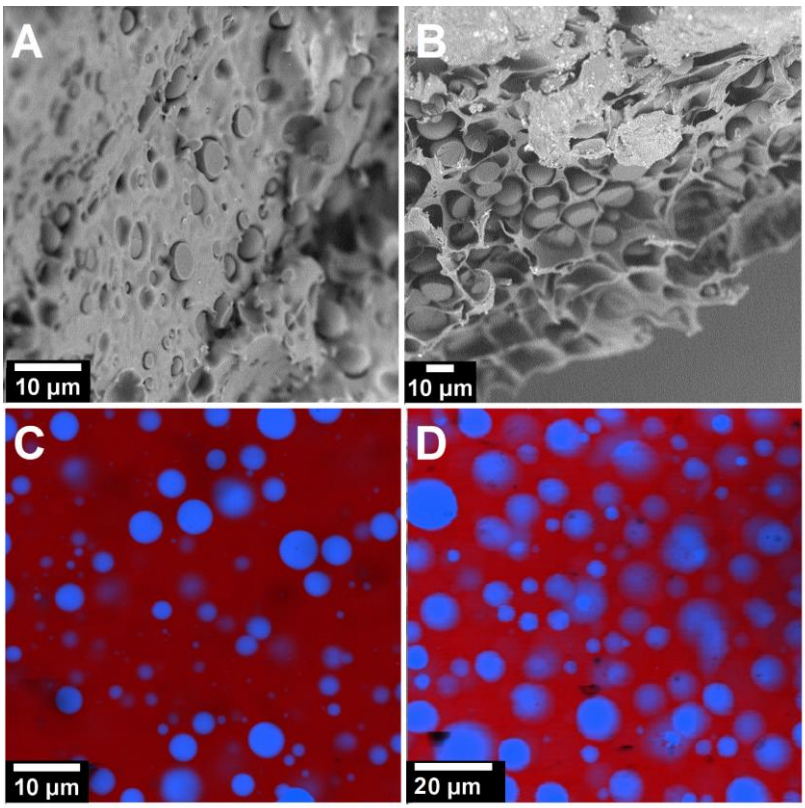


**Figure 15.** SEM and Raman imaging of PLA/PLimC blends: A, C) PLA/PLimC = 90/10 w/w; B, D) PLA/PLimC = 70/30 w/w. In C, D) the domains coloured in blue represent PLimC droplets that are embedded in the PLA matrix (coloured in red). The Raman spectra of each component are given in **Figure S4**.

Thermal properties of PLA/PLimC blends (**Table 2, Figure 2**) were investigated by differential scanning calorimetry (DSC) and thermogravimetric analysis (TGA). Comparing the glass transition temperatures ($T_g$) of PLA in PLA/PLimC blend systems with neat PLA shows similar values at around 60 °C, as it would be expected from a phase-separated blend. The $T_g$ of PLimC ($T_g$ = 128 °C, **Figure S6**) could not be recognized, because $T_g$ is superimposed with the cold crystallization of PLA at $T_{cc} \approx 120$ °C (**Figure 2A**) and the PLimC fraction is very low, so the sensitivity limit of the DSC is reached.

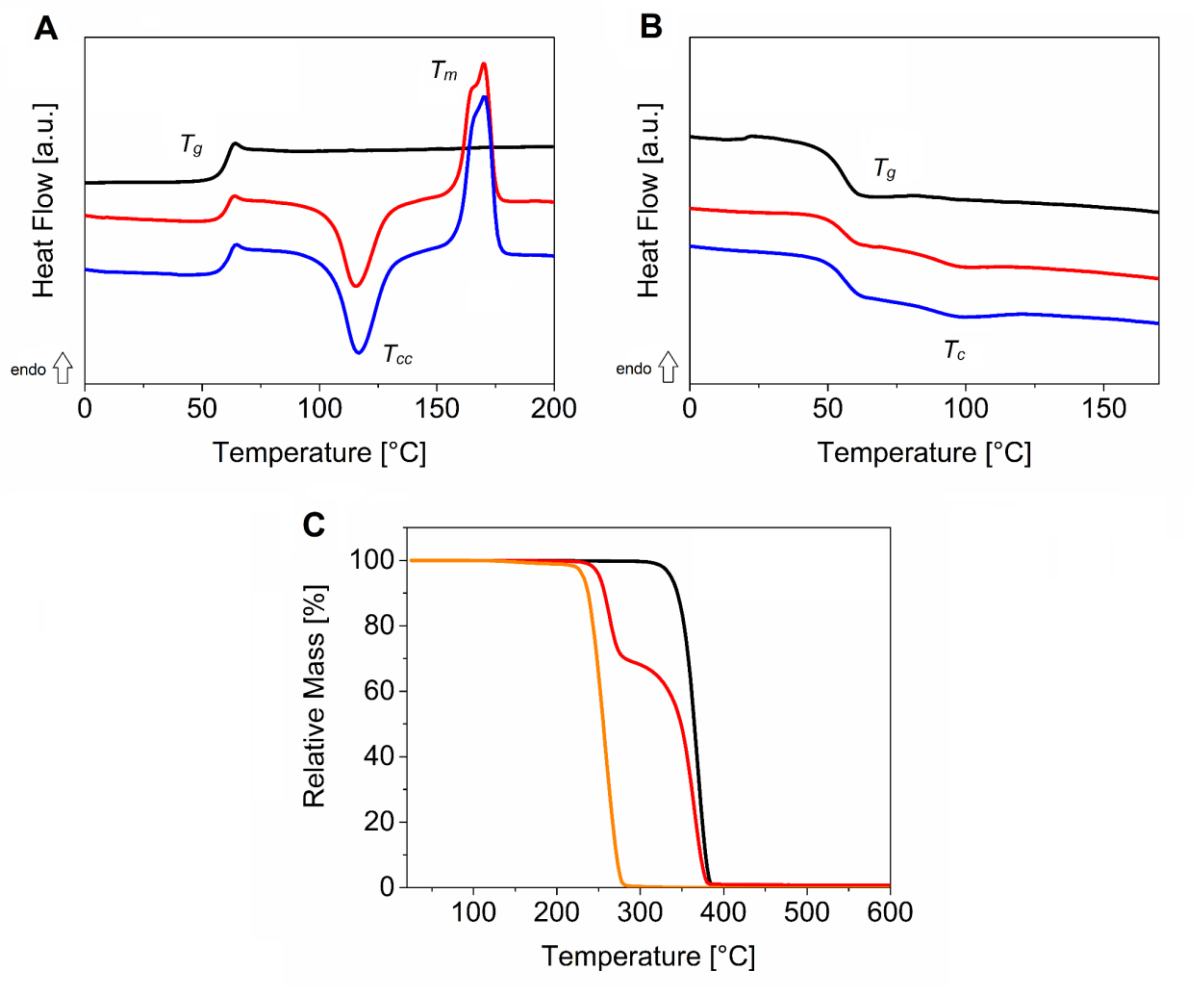


**Figure 16.** A) DSC second heating and B) cooling traces of PLA/PLimC blends (scanning rate 10 K·min$^{-1}$). C) TGA of PLA/PLimC blends. PLA/PLimC = 100/0 w/w (black); PLA/PLimC = 90/10 w/w (red); PLA/PLimC = 70/30 w/w (blue); PLA/PLimC = 0/100 w/w (orange).

**Table 2.** PLimC droplet sizes and thermal/mechanical properties of the produced blends.

| | **PLimC droplet sizes[a)] SEM/Raman imaging** | | **Thermal[b)]** | | | | | **Mechanical[c)]** | | |
|---|---|---|---|---|---|---|---|---|---|---|
| | Domain area | Equivalent diameter | $T_g$ | $T_{cc}$ | $T_m$ | $T_c$ | $T_{5\%}$ | $\sigma_m$ | $\varepsilon_{br}$ | *E-modulus* |
| | [µm²] | [µm] | [°C] | | | | | [MPa] | [%] | [MPa] |
| **PLimC (neat)** | - | - | 130 | - | - | - | 230 | 42 ± 0.37 | 15 ± 4 | 972 ± 95 |
| | | | **PLA blends** | | | | | | | |
| **PLA (neat)** | - | - | 61 | - | - | - | 335 | 58 ± 3 | 2.7 ± 0.2 | 3520 ± 112 |
| **10 wt% PLimC** | 10.3 ± 6 / 6.2 ± 13 | 3.6 ± 3.9 / 2.8 ± 3.0 | 60 | 116 | 170 | - | n-d. | 57 ± 0.3 | 2.1 ± 0.1 | 3454 ± 22 |
| **30 wt% PLimC** | 28 ± 24 / 40 ± 14 | 6.0 ± 6.1 / 7.1 ± 7.3 | 61 | 117 | 172 | 100 | 250/ 335 | 36 ± 1 | 1.39 ± 0.1 | 3050 ± 56 |
| | | | **PBAT blends** | | | | | | | |
| **PBAT (neat)** | - | - | -30 | - | 122 | 42 | 370 | 36 ± 3.0 | 1376 ± 103 | 92 ± 19 |
| **10 wt% PLimC** | 1.9 ± 2.4 / 1.4 ± 1.0 | 1.6 ± 1.7 / 1.3 ± 1.9 | -28 | - | 128 | 84 | n.d. | 17 ± 1.2 | 659 ± 43 | 99 ± 3.0 |
| **30 wt% PLimC** | 1.0 ± 0.7 / 0.6 ± 0.5 | 1.1 ± 1.8 / 0.90 ± 1.8 | -28 | - | 131 | 89 | 253/ 370 | 10 ± 0.19 | 184 ± 50 | 247 ± 12 |
| | | | **COPE blends** | | | | | | | |
| **COPE (neat)** | - | - | -72 | - | 0.9/ 197 | -30/ 122 | 377 | 25 ± 1.5 | 1013 ± 111 | 34.3 ± 5.8 |
| **10 wt% PLimC** | 0.1 ± 0.1 / 0.3 ± 0.2 | 0.4 ± 1.3/ 0.6 ± 1.8 | -70 | - | 4.9/ 200 | -28/ 173 | n.d. | 21 ± 0.70 | 930 ± 76 | 49.7 ± 5.4 |
| **30 wt% PLimC** | 1.9 ± 3.8 / 0.49 ± 0.25 | 1.5 ± 1.7 / 0.8 ± 1.9 | -70 | - | 5.5/ 199 | -30/ 178 | 250/ 377 | 14 ± 1.2 | 193 ± 44 | 146 ± 11 |
| | | | **PA12 blends** | | | | | | | |
| **PA12 (neat)** | - | - | 53 | - | 180 | 148 | 420 | 36 ± 1.0 | 223 ± 85 | 1170 ± 37 |
| **10 wt% PLimC** | 9.8 ± 5.1 / 0.39 ± 0.29 | 3.5 ± 3.8 / 0.7 ± 1.0 | 53 | - | 179 | 155 | n.d. | 32 ± 2.0 | 11 ± 1.7 | 1143 ± 50 |
| **30 wt% PLimC** | 39 ± 23/ 4.3 ± 3.8 | 7.1 ± 7.2/ 2.3 ± 2.4 | 53 | - | 179 | 154 | 250/ 420 | 19 ± 4.0 | 1.5 ± 0.3 | 1580 ± 109 |

[a)] SEM (top values): Average area (µm²) was calculated from min. 100 domains (Table S2).
Raman (bottom values): Average area (µm²) was calculated from min. 60 domains (PA12 blends ca. 30 domains) (Table S2). The given diameters correspond to the area of an equivalent circle. For bimodal distributions only the average values for smaller droplets are given, values for larger droplets are presented in Table S2.

Interestingly, PLA/PLimC blends show cold crystallization ($T_{cc}$ ≈ 120 °C) and melting ($T_m$ ≈ 170 °C) in the second heating runs (**Table 2, Figure 2A**), whereas pure PLA displays these characteristics only in the first heating trace (not shown). In the corresponding cooling traces a weak exothermic peak at $T_c$ ≈ 100 °C can be detected (**Figure 2B**), which can be attributed to a partial crystallization of PLA and is also in the same range where cold crystallization ($T_{cc}$ ≈ 120 °C) was observed in the second heating traces. This might point to a nucleation effect of the PLimC droplets on PLA crystallization, an effect that has also been observed for the matrix of the other blend systems studied (see discussion in following sections). Strong nucleation effects were also found by Rizzuto et al., who investigated PLA/poly(ε-caprolactone) (PCL) blends.[36] TGA shows a distinct two-step degradation, with temperatures at 5% mass loss of $T_{5\%}$ = 250 °C for PLimC and $T_{5\%}$ = 335 °C for PLA, respectively (**Figure 2C**). Mass loss at each stage correlates with the weight percentages of the respective polymers in the blend. In PLA/PLimC blends $T_{5\%}$ for PLimC is significantly higher than in neat PLimC ($T_{5\%}$ = 230 °C), whereas the $T_{5\%}$ of the PLA matrix is hardly influenced (**Table 2**). Here, the assumption is that the PLA matrix protects the encapsulated PLimC, resulting in an increased thermal stability of the dispersed PLimC phase. The *E*-modulus of heterogenous blends with a dispersed droplet morphology can be estimated by the well-established series model ($E^{-1} = \Phi_1/E_1 + \Phi_2/E_2$, $\Phi_i$ = volume fraction of blend components), which describes the lower limit of the modulus, and the parallel model ($E = \Phi_1 E_1 + \Phi_2 E_2$), describing the upper limit, respectively.[37] Representative stress-strain curves for neat PLA and PLA/PLimC blends are shown in **Figure 3A**. The results from tensile testing show that the *E*-moduli are more predictable using the parallel model than the series model, but still higher than the parallel model would suggest (**Figure 3B**, **Table 2**). Tensile strength ($\sigma_m$ = 36 ± 1 MPa) and elongation at break ($\varepsilon_{br}$ = 2.7 ± 0.2 %) were slightly decreased by the addition of PLimC, but still acceptable in comparison to neat PLA.

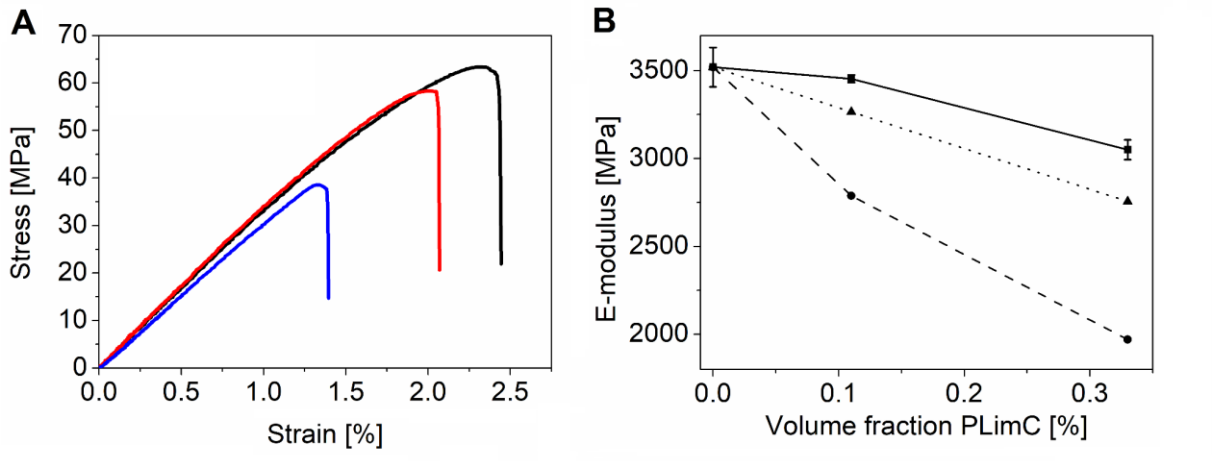


**Figure 17.** A) Representative stress-strain curves for neat PLA (black) and PLA/PLimC blends (PLA/PLimC = 90/10 w/w (red), PLA/PLimC = 70/30 w/w (blue). B) *E*-moduli of PLA/PLimC blends (solid) in dependence of the volume fraction of PLimC and estimated *E*-moduli of the blends employing the series (dashed) and parallel (dotted) model, respectively.

A possible reason for the comparably hight *E*-moduli of the blends could be transesterification, which occurred during the blending process and increased the adhesion between PLimC and PLA. Gel permeation chromatography (GPC) of the produced blends showed on the one hand a significant broadening with a shift of the molar mass distribution towards both smaller and higher molar masses (especially in the blend with 30 wt% PLimC) in comparison to the GPCs of the pure blend components **(Figure S7)**. This indicates transesterification reactions and, thus, the formation of block-type copolymer structures during melt processing. Similar results were found by Wacharawichanant *et al.*, who investigated PLA/poly(ethylene-*co*-methyl acrylate) (EMAC)/clay blends.[38] The *E*-modulus of PLA/EMAC blends increased significantly by the addition of clay, whereas tensile strength was slightly decreased. An increased adhesion between PLA and EMAC due to the clay was suggested as an explanation.

## 2.3 Blends with poly(butylene adipate-*co*-terephthalate) (PBAT, aliphatic/aromatic polyester)

The produced PBAT/PLimC blends show opaque strands after processing, which points again to phase-separated, immiscible blends (**Figure S8**), which is confirmed by morphological studies. SEM and Raman imaging show the presence of dispersed PLimC droplets with a bimodal size distribution, consisting of small PLimC droplets in the µm-range and significantly larger PLimC domains with diameters of $D > 10$ µm (**Figure 4**, **S10**). The respective histograms for PLimC droplet size distributions are given in **Figure S9**. For the smaller PLimC droplets average diameters of $D = 1.6 \pm 1.7$ µm (from SEM) and $D = 1.3 \pm 1.9$ µm (from Raman imaging) were determined for the PBAT/PLimC = 90/10 w/w blend, and $D = 1.1 \pm 1.8$ µm (from SEM) and $D = 0.9 \pm 1.8$ µm (from Raman imaging) for the PBAT/PLimC = 70/30 w/w blend, respectively (**Table 2**). The bimodal size distribution of PLimC droplets can be explained by the high melt viscosity contrast between both polymers (PLimC: $\eta_0 = 890$ kPa·s,[25] PBAT: $\eta_0 = 2.7$ kPa·s[29]) in combination with the significantly stronger incompatibility (difference in solubility parameters; PBAT: $\delta = 22.3$ MPa$^{1/2}$ [28], PLimC: $\delta = 17.6$ MPa$^{1/2}$ [14]) between PBAT/PLimC with respect to PLA/PLimC (**Table 1**). Consequently, the shear forces during compounding are not high enough to break up the PLimC droplets effectively, resulting in the observed bimodal size distribution.

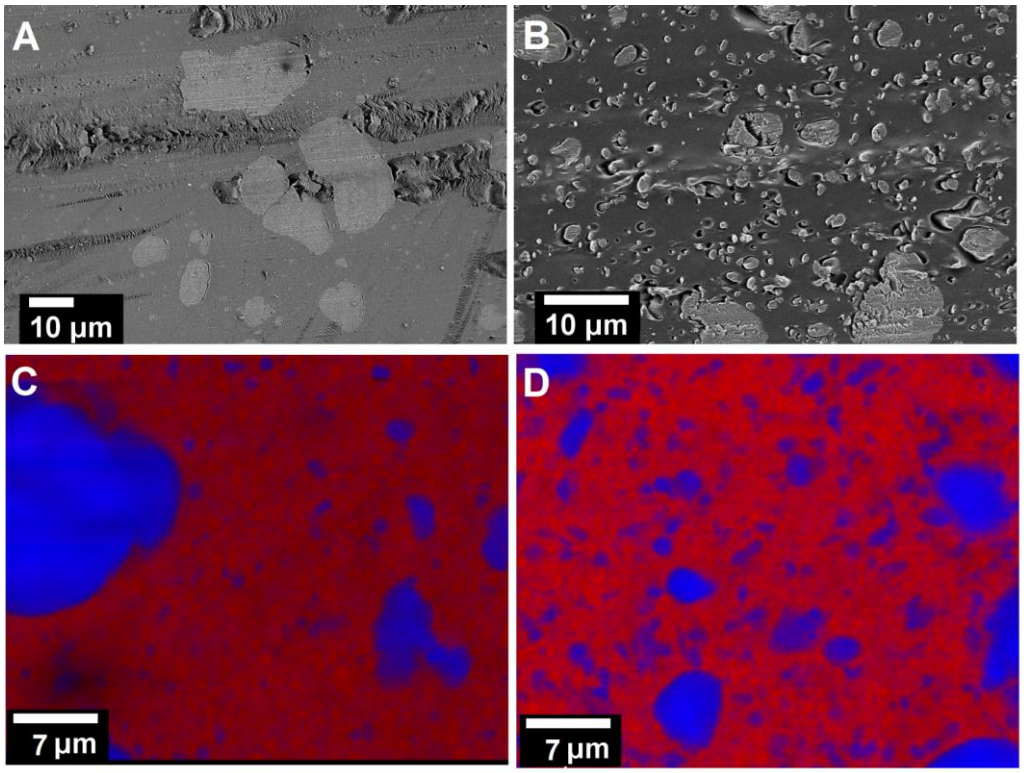


**Figure 18.** SEM (PLimC appears bright) and Raman imaging (PLimC domains are coloured in blue) of PBAT/PLimC blends: A, C) PBAT/PLimC = 90/10 w/w, B, D) PBAT/PLimC = 70/30 w/w. The corresponding Raman spectra of each component are given in **Figure S4**.

The observed phase separation is also reflected in the thermal properties of the blends (**Figure 5A, B**, **Table 2**), showing a glass transition temperature for the PBAT matrix of $T_g$ = - 28 °C, being almost identical to that of neat PBAT ($T_g$ = - 30 °C). The $T_g$ of pure PLimC is 128 °C (**Figure S6**) and is hidden underneath the melting transition of PBAT. The crystallization temperature of neat PBAT ($T_c$ = 42 °C) is increased significantly in PBAT/PLimC blends (~ $T_c$ = 84 °C). The same behaviour was observed for PLA/PLimC blends and might be attributed to a nucleating effect of the interface between PLimC and the matrix polymer. TGA also reveals an increased stability of PLimC ($T_{5\%}$ = 253 °C) in the PBAT matrix, like it was observed for PLA/PLimC blends (**Figure S11**).

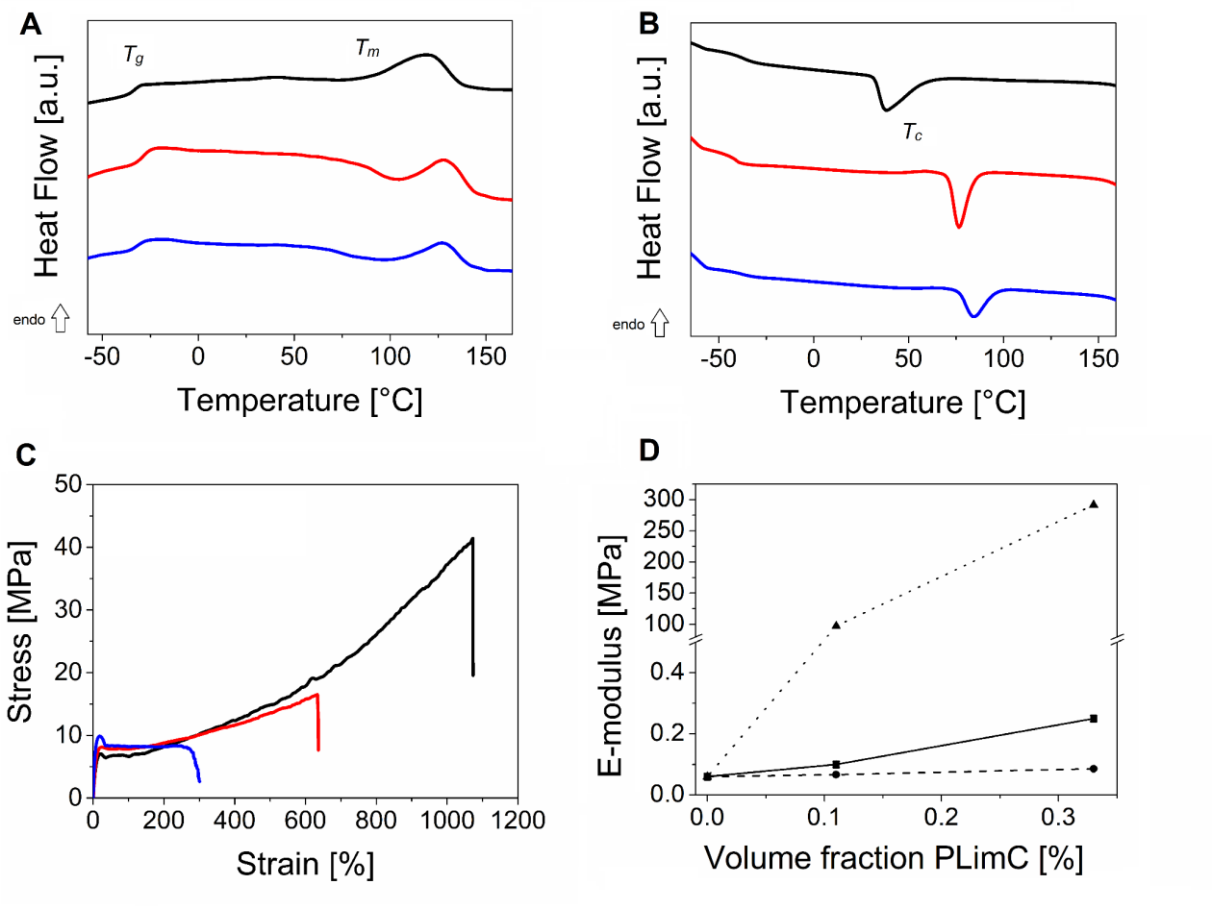


**Figure 19.** A) DSC second heating and B) cooling traces (scanning rate 10 K·min$^{-1}$), and C) representative stress-strain curves for neat PBAT (black) and PBAT/PLimC blends (PBAT/PLimC = 90/10 w/w (red), PBAT/PLimC = 70/30 w/w (blue)). D) *E*-moduli of PBAT/PLimC blends (solid) in dependence of the volume fraction of PLimC. Estimated *E*-moduli of the blends employing the series (dashed) and parallel (dotted) model, respectively.

Focusing on the mechanical properties of PBAT/PLimC blends, the influence of PLimC on the *E*-modulus is most pronounced (**Figure 5C, D**, **Table 2**). Blending PBAT with 30 wt% PLimC increases the *E*-modulus about three times from $E = 92 \pm 19$ MPa for neat PBAT to $E = 247 \pm 12$ MPa for the blend. At the same time, elongation at break is decreased, but still shows reasonably high values of $\varepsilon_{br} \approx 200$ %. This combination of an increased *E*-modulus with high elongation at break makes PBAT/PLimC blends interesting for applications, despite their inhomogeneous blend morphology with a bimodal PLimC droplet distribution. In general, the *E*-moduli of the blends are close to the prediction from the series model (**Figure 5D**). This is reasonable, because the *E*-modulus of the PBAT matrix is substantially lower compared to that of the dispersed PLimC phase and due to the incompatibility of the blend partners the interfacial interactions are expected to be rather weak.

### 2.4 Blends with Arnitel EM400 (copoly(ether ester), COPE)

Arnitel EM400 is a copoly(ether ester) with PBT hard segments and PTHF soft segments (PBT/PTHF = 40/60 w/w), which shows similarities in structure to PBAT and of all investigated polymers its solubility parameter is closest to that of PLimC **(Table 1)**. SEM and Raman imaging clearly show that the produced COPE/PLimC blends (optical photographs in **Figure S12**) are phase-separated with a bimodal distribution of PLimC domains dispersed in the COPE matrix, *e.g.*, similar to the morphology observed for the PBAT/PLimC blends. This is quite reasonable, because COPE and PBAT have similarities in structure. The small PLimC domains are finely distributed over the whole COPE matrix, showing average diameters of $D = 0.4 \pm 1.3$ µm (COPE/PLimC = 90/10 w/w) and $D = 1.5 \pm 1.7$ µm (COPE/PLimC = 70/30 w/w) as determined by SEM (**Figure 6**, **Figure S13, S14**). It is noted that PLimC droplet size of the COPE blend with 10 wt% PLimC is smaller compared to that of the respective PBAT/PLimC blend, which might be attributed to the higher compatibility (smaller difference in solubility parameters). Raman imaging confirms the measured values with an average size of $D = 0.6 \pm 1.8$ µm (COPE/PLimC = 90/10 w/w) and $D = 0.8 \pm 1.9$ µm (COPE/PLimC = 70/30 w/w). The larger PLimC domains show sizes of $D \approx 10$ µm, being slightly lower compared to that in PBAT/PLimC blends. Despite the better compatibility of COPE and PLimC a bimodal size distribution can be found. This is due to the greater viscosity contrast between PLimC and COPE (**Table 1**).

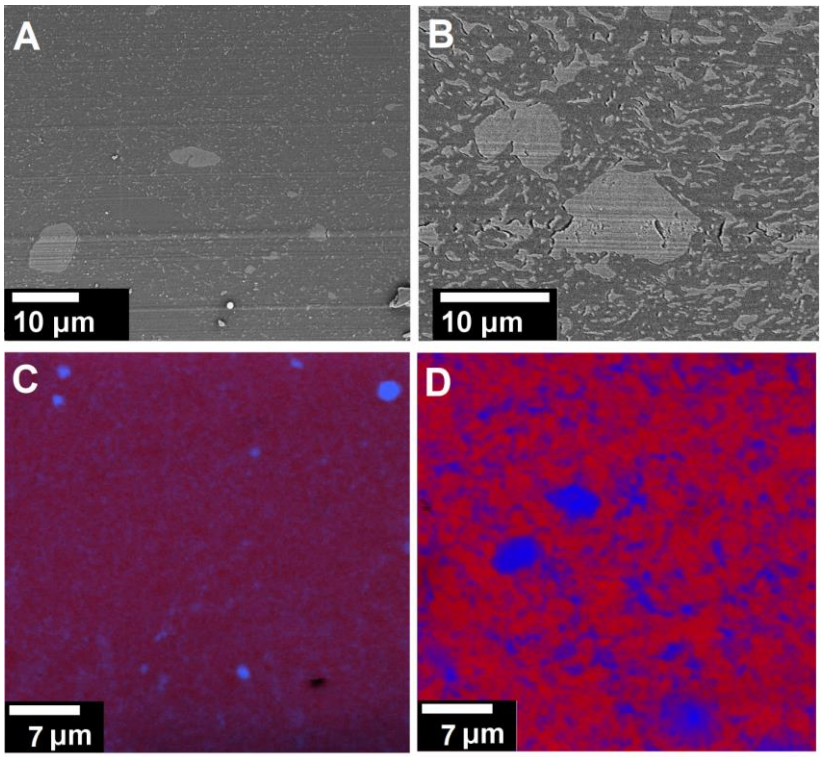


**Figure 20.** SEM (PLimC appears bright) and Raman imaging (PLimC domains are coloured in blue) of COPE/PLimC blends: A, C) COPE/PLimC = 90/10 w/w, B, D) COPE/PLimC = 70/30 w/w. The corresponding Raman spectra of each component are given in **Figure S4**.

The investigation of thermal properties of neat COPE and COPE/PLimC blends revealed similar glass transition temperatures for the PTHF soft segment ($T_g \approx$ -70 °C) (**Figure 7A)**. The influence of PLimC on $T_c$ and $T_m$ of the PTHF soft segment was negligible, whereas $T_c$ of the PBT hard segment ($T_c \approx$ 175 °C) was significantly increased in comparison to neat COPE ($T_c \approx$ 122 °C) (**Figure 7B**, **Table 2**). This might again be attributed to a nucleation effect of the COPE/PLimC domain interface. In line with the TGA results of the above discussed blends PLimC showed an increased temperature stability ($T_{5\%}$ = 253 °C) in COPE/PLimC blends (**Figure S15**).

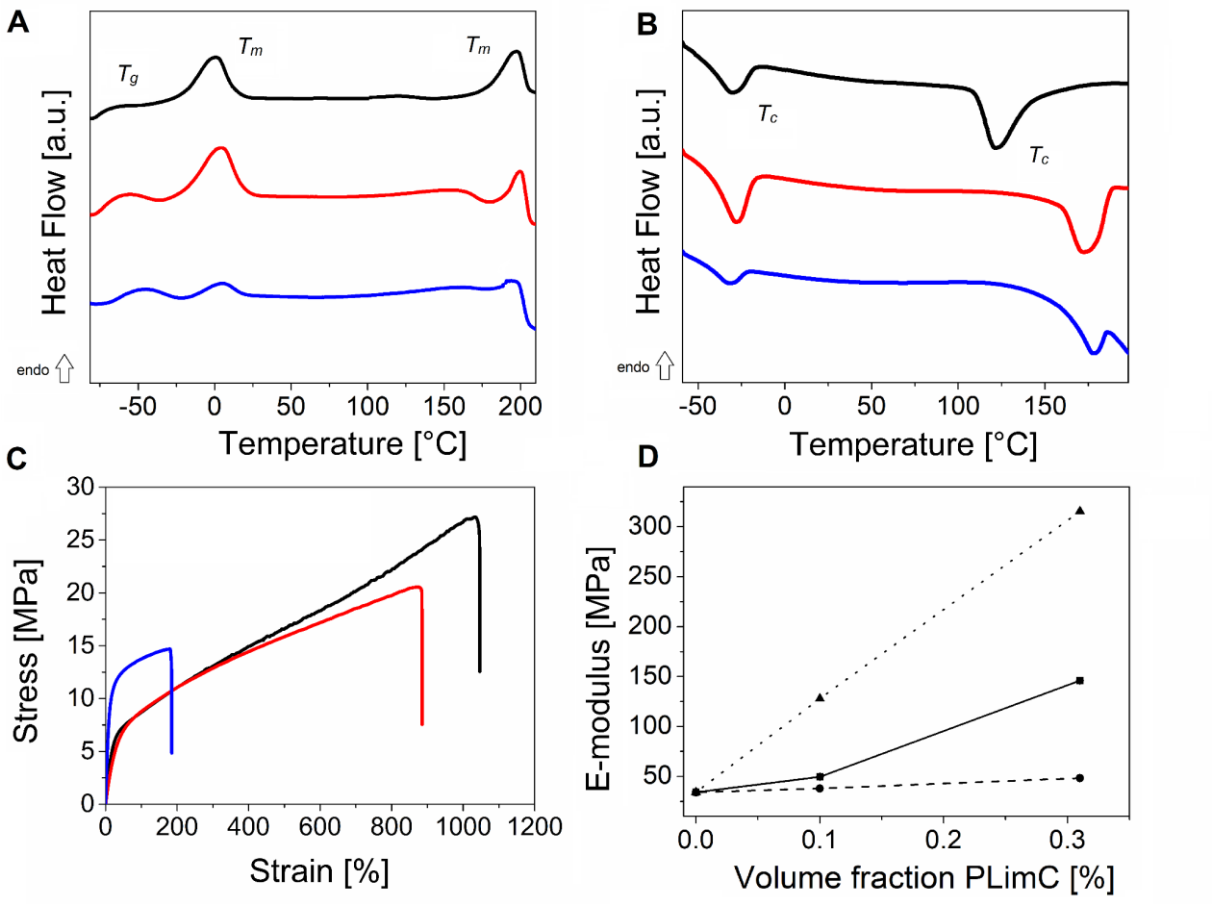


**Figure 21.** A) DSC second heating and B) cooling traces of COPE/PLimC blends (scanning rate 10 K·min$^{-1}$). C) Representative stress-strain curves for neat COPE (black) and COPE/PLimC blends (COPE/PLimC = 90/10 w/w (red); COPE/PLimC = 70/30 w/w (blue). D) *E*-moduli of COPE/PLimC blends (solid) in dependence of the volume fraction of PLimC. Estimated *E*-moduli of the blends employing the series (dashed) and parallel (dotted) model, respectively.

Due to similarities in structure of PBAT and COPE and the respective blend morphologies comparable mechanical properties were observed (**Figure 7C, D**, **Table 2**). The *E*-modulus showed a fourfold increase from $E = 34 \pm 5.8$ MPa for neat COPE to $E = 146 \pm 11$ MPa for the COPE/PLimC = 70/30 w/w blend, while the elongation at break decreased but still stayed in an acceptable range for applications ($\varepsilon_{br} \approx 200$ %). The *E*-moduli of the blends are closer to the values predicted from the series model rather than the parallel model, in analogy to PBAT/PLimC blends (**Figure 5D**). This might be ascribed to the rather high difference in *E*-modulus of both homopolymers (**Table 2**) and a weak interfacial adhesion between the blend partners.

### 2.5 Blends with polyamide 12 (PA12, aliphatic polyamide)

The last explored blend partner, the aliphatic polyamide PA12, shows a fundamentally different chemical structure than the above investigated polyesters, so different results for PA12/PLimC blends might be expected (optical photographs of the produced blends are displayed in **Figure S16**). Morphology investigations with SEM and Raman imaging revealed a bimodal size distribution also for this type of blend system **(Figure 8**, **S17**, **S18)**. However, the average PLimC domain sizes were significantly higher compared to that of the other blend systems studied (**Table 2, S2**). For PA12 blends with 10 wt% PLimC average PLimC droplet sizes of $D$ = 3.5 ± 3.8 µm and $D$ = 11 ± 11 µm were obtained from SEM image evaluation, and $D$ = 7.1 ± 7.2 µm and $D$ = 20 ± 20 µm for the blend with 30 wt% PLimC, respectively. Raman imaging, where mostly the small droplets were probed, *e.g.*, the lower size fraction of the bimodal distribution, showed PLimC droplets in the same order of magnitude ($D$ = 0.7 ± 1.0 µm for PA12/PLimC = 90/10 w/w and $D$ = 2.3 ± 2.4 µm for PA12/PLimC = 70/30 w/w). The comparably broad bimodal size distribution in PA12/PLimC blends most likely originates from the low melt viscosity of PA12 in combination with its rather high incompatibility (large difference in solubility parameters, **Table 1**) to PLimC. Consequently, the shear forces during processing might be not high enough to split the PLimC droplets further, resulting in larger PLimC domains. The strongly phase-separated structure of the blends is also manifested in the thermal properties, revealing similar glass transition temperatures for PA12 in the PA12/PLimC blends with respect to neat PA12 ($T_g$ ≈ 53 °C, **Table 2**). It is noted that in this case glass transition temperatures could only be detected in the first heating run (**Figure S19A**). The crystallization temperature is only slightly increased by 7 °C from $T_c$ = 148 °C for neat PA12 to $T_c$ = 155 °C for the PA12/PLimC blend with 30 wt% PLimC, whereby the PA12 melting temperature is hardly influenced (**Figure 9A, B**). This indicates that the nucleation effect of the PLimC domains, respective the PA12/PLimC interface, is not as strong as in PLA, PBAT or COPE blends. TGA analysis also shows the stabilizing effect of the polymer matrix on PLimC with an observed increase in $T_{5\%}$ (PLimC) by about 20 °C (**Figure S19B)**.

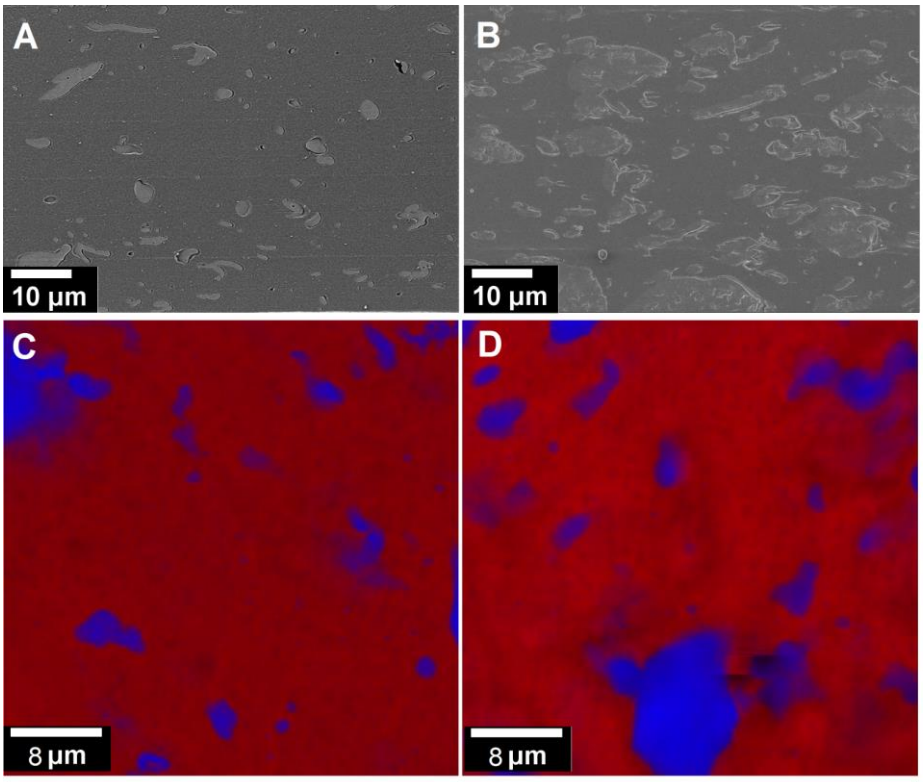


**Figure 22.** SEM (PLimC appears bright) and Raman imaging (PLimC domains are coloured in blue) of PA12/PLimC blends. A, C) PA12/PLimC = 90/10 w/w, B, D) PA12/PLimC = 70/30 w/w. The corresponding Raman spectra of each component are given in **Figure S4**.

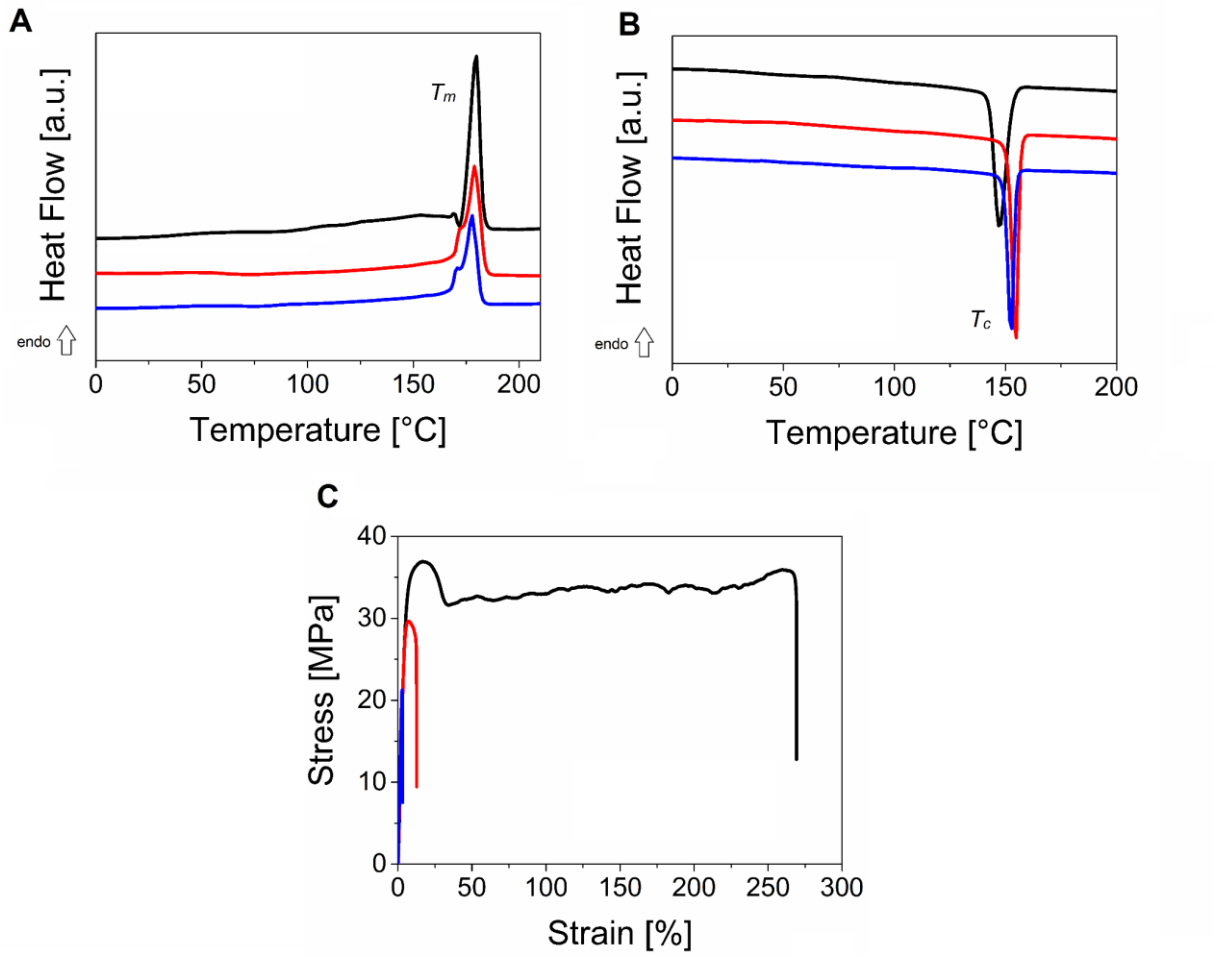


**Figure 23.** A) DSC second heating and B) cooling traces of PA12/PLimC blends (scanning rate 10 K·min$^{-1}$). C) Representative stress-strain curves for neat PA12 (black) and PA12/PLimC blends (PA12/PLimC = 90/10 w/w (red); PA12PLimC = 70/30 w/w (blue).

As the *E*-moduli of both blend components (PA12 and PLimC) are quite similar (~ 1000 MPa), no significant effect of composition on the *E*-modulus of the blends is expected and also predicted by both the series and parallel model **(Figure S19C)**. The observed deviation in the *E*-modulus of the PA12/PLimC = 70/30 w/w blend, which showed a much higher value than predicted, can be attributed to the very inhomogeneous blend morphology giving rise to a very high standard deviation for this blend composition. The stress-strain traces presented in **Figure 9C** clearly show that the addition of PLimC has a detrimental effect on the elongation at break, which was drastically reduced down to $\varepsilon_{br} \approx 2\%$ for the PA12/PLimC = 70/30 w/w blend. This in turn makes this blend system rather unattractive for applications.

# 3. EXPERIMANTAL SECTION

## 3.1 Materials and blend processing

The used PLimC ($M_n$ = 65 kDa, $Đ$ = 1.09) was synthesized according to literature procedures.[6] In general, the blends were produced as follows. Polymers were pre-dried at 0.1 mbar and 80 °C for 16 h. In a double screw compounder (DSM Micro 15cc Twin Screw Compounder, Company: Xplore) 8 g - 14 g polymer were processed to form binary blends. Blending was performed at 50 rpm for 4 min. PLimC was used as minority blend component with contents of 10 wt% and 30 wt%. The neat blending partners (matrix polymers) were also processed as a reference. Specifications of the employed matrix polymers and the processing parameters, like rotational speed or processing time can be found in **Table 1**. The solubility parameter of Arnitel EM400 was calculated from the composition of the copoly(ether ester): PBT/PTHF 40/60 w/w (PBT 22.7[30], PTHF 16.8[30]).

## 3.2 Methods

*Scanning electron microscopy (SEM)* images were taken with a Zeiss LEO 1530 (FE-SEM with Schottky-field-emission cathode and In-lens detector) using an accelerating voltage of 3-10 kV. Small fragments of the samples were mounted on a standard sample holder by conductive adhesion graphite-pad (Plano) for SEM examination. For cyro-microtomy of polymer blends a Leica EM VC7 microtome was used. The ultrathin sections were treated with $OsO_4$ vapour overnight in order to selectively stain the PLimC domains (appear bright in the SEM micrographs). SEM was performed on microtome cuts and as well on the surface of small sample fragments.

The average domain sizes were determined by measuring at least 100 (SEM) and 30 (Raman imaging) particles using ImageJ software (1.52a).[35] Detailed overview over all analysed particles can be found in the supporting information. For the calculation of the particle diameters, the area of each PLimC domain was measured using the ImageJ software. Then, assuming that droplets are fully spherical particles and the cuts have gone through the middle of each droplet, the diameter corresponding to the area was back calculated. Of course, these assumptions cannot be 100% fulfilled, hence resulting in the relatively large standard deviations.

*Differential scanning calorimetry (DSC)* was performed on a Netzsch 204 F1 Phoenix using a scanning rate of 10 K·min $^{-1}$ under $N_2$ atmosphere. Glass transition temperature ($T_g$), cold crystallization temperature ($T_{cc}$), melting temperature ($T_m$) and crystallization temperature ($T_c$) were determined from the 2$^{nd}$ heating or cooling traces (scanning rate 10 K·min$^{-1}$ under nitrogen) except for PA12, where the 1$^{st}$ heating trace was used.

*Thermogravimetric analysis (TGA)* was conducted on a Netzsch TG 209 F1 Libra at a scanning rate of 10 K·min$^{-1}$ under $N_2$ atmosphere. Temperature at 5% weight loss ($T_{5\%}$) was determined by TGA measurements at 10 K min$^{-1}$ under nitrogen. In **Table 2**, the first value refers to PLimC, whereas the second value refers to the matrix polymer.

For *$CHCl_3$-GPC* analyses an Agilent 1200 system equipped with a SDV precolumn (particle size 5 µm; PSS Mainz), a SDV linear XL column (particle size 5 µm, PSS Mainz) and a refractive index detector (Agilent Technologies 1260 Infinity) was used. Toluene (HPLC grade) was used as internal standard and $CHCl_3$ (HPLC grade) was used as solvent at a flow rate of 0.5 mL·min$^{-1}$ at room temperature. Calibration was based on narrowly distributed PS standards.

*HFIP-GPC* was conducted with an Agilent 1200 system equipped with a SDV precolumn (particle size 7 µm; PSS Mainz), a SDV linear XL column (particle size 7 µm, PSS Mainz) and a refractive index detector (RI, Gynotek SE-61, Agilent Technologies). Toluene (HPLC grade) was used as internal standard. Calibration was done with narrowly distributed poly(methyl methacrylate) standards from the company PSS Mainz. HFIP with potassium trifluoroacetate ($c$ = 8 g L$^{-1}$) was used as solvent at a flow rate of 0.5 mL·min$^{-1}$ at room temperature.

For *Raman imaging* a WITec alpha 300 RA+ imaging system equipped with an UHTS 300 spectrometer and a back-illuminated Andor Newton 970 EMCCD (electron multiplying charge-coupled device) camera was employed. The measurements were conducted with an excitation wavelength of $\lambda$ = 352 nm and a typical integration time of 0.35 s pixel$^{-1}$ using a laser power of 10 mW (100x objective, NA = 0.9, step size 100 nm pixel$^{-1}$). All spectra were subjected to a cosmic ray removal routine and baseline correction using WITec project 5.2. The spatial distribution of the components was extracted from the Raman imaging data employing the Raman spectra of the neat components **(Figure S4)**, employing the True Component Analysis in WITec project 5.2.

*Samples for mechanical testing* were prepared from extruded polymer strands, which were filled in a metal frame (13 cm × 13 cm) with a thickness of 1.0 mm and hot-pressed for 5 min by applying a force of 10 kN. After obtaining the hot-pressed polymer plates, dogbone-shaped

specimens were punched for tensile testing according to DIN53504S3A, employing a Coesfeld Material punching machine (model 951617).

A Zwick/Roell Z0.5 tensile tester was used for *tensile testing*. The pre-load for all blends was 0.02 MPa. A test speed of 0.5 mm·min$^{-1}$ was used to determine the tensile strength ($\sigma_m$), elongation at break ($\varepsilon_{br}$) and *E*-modulus of all blends besides PBAT. For PBAT a test speed of 40 mm·min$^{-1}$ was employed to determine tensile strength and elongation at break, respectively. Given values correspond to the average of 3 measurements.

## 4. CONCLUSION

In this paper, blends of various commodity polymers with PLimC as minority component (10 – 30 wt%) were investigated. Blends with PS and PMMA (similar glass transition temperature to PLimC) were very brittle and blends with PA12 showed very low elongation at break. The most promising results were obtained for blends with polymers exhibiting a similar chemical structure to PLimC, *e.g.*, PLA, PBAT and COPE (aliphatic/aromatic polyester). The most homogeneous morphology was observed for PLA/PLimC blends, probably due to transesterification and formation of PLA/PLimC block-type structures during processing (acting as compatibilizers). In terms of mechanical properties PBAT and COPE blends were the most promising, as they combine a comparably high *E*-modulus (to pure PBAT and COPE) with reasonably high elongations at break up to 200%. These results show the potential of PLimC for the production of more sustainable polymer blends *via* blending with petrol- or food-based polymers, having similar chemical structures compared to PLimC. For the other polymers the use of compatibilizers like block copolymers could improve the phase connectivity. Besides, the observed increased thermal stability of PLimC in the investigated blends together with the nucleation effect of the matrix/PLimC interface for semicrystalline matrix polymers (increase in crystallization temperature) can add additional benefits to PLimC blends, resulting for example in lower cycle times for PLA/PLimC blends due to improved PLA crystallization.

## Supporting Information

Supporting Information is available from the Wiley Online Library or from the author.

## Acknowledgements

Financial support by DFG for the project 438886960 is gratefully acknowledged. We would like to thank Carmen Kunert for sample preparation and conducting the SEM measurements. We gratefully acknowledge the use of equipment and assistance offered by the Keylab "Small Scale Polymer Processing" and "Electron and Optical Microscopy" of the Bavarian Polymer Institute at the University of Bayreuth.

Keywords: poly(limonene carbonate), bio-based, blend, morphology, sustainability

Received: ((will be filled in by the editorial staff))

Revised: ((will be filled in by the editorial staff))

Published online: ((will be filled in by the editorial staff))

## References

[1] a) Y. Zhu, C. Romain, C. Williams, *Nature.* **2016**, *540*, 354; b) H. Nakajima, P. Dijkstra, K. Loos, *Polymers* **2017**, *9*, 523; c) D. Schneiderman, M. A. Hillmyer, *Macromolecules.* **2017**, *50*, 3733; d) X. Zhang, M. Fevre, G. O. Jones, R. M. Waymouth, *Chem. Rev.* **2018**, *118*, 839; e) G.-Q. Chen, M. K. Patel, *Chem. Rev.* **2012**, *112*, 2082; f) S. Spierling, E. Knüpffer, H. Behnsen, M. Mudersbach, H. Krieg, S. Springer, S. Albrecht, C. Herrmann, H.-J. Endres, *J. Cleaner Prod.* **2018**, *185*, 476.

[2] S. A. Attaran, A. Hassan, M. U. Wahit, *J. Thermoplast. Compos. Mater*. **2017**, *30*, 143.

[3] a) D. J. Darensbourg, *Chem. Rev*. **2007**, *107*, 2388; b) A. J. Kamphuis, F. Picchioni, P. P. Pescarmona, *Green Chem.* **2019**, *21*, 406; c) M. Scharfenberg, J. Hilf, H. Frey, *Adv. Funct. Mater*. **2018**, *28*, 1704302.

[4] S. J. Poland, D. J. Darensbourg, *Green Chem.* **2017**, *19*, 4990.

[5] A. Wambach, S. Agarwal, A. Greiner, *Sustain. Chem. Eng.* **2020**, *8*, 14690.

[6] O. Hauenstein, M. Reiter, S. Agarwal, B. Rieger, A. Greiner, *Green Chem.* **2016**, *18*, 760.

[7] M. Winkler, C. Romain, M. A. R. Meier, C. K. Williams, *Green Chem.* **2015**, *17*, 300.

[8] C. M. Byrne, S. D. Allen, E. B. Lobkovsky, G. W. Coates, *J. Am. Chem. Soc.* **2004**, *126*, 11404.

[9] C. Martín, A. Kleij, *Macromolecules.* **2016**, *49*, 6285.

[10] L. Peña Carrodeguas, J. González-Fabra, F. Castro-Gómez, C. Bo, A. W. Kleij, *Chemistry.* **2015**, *21*, 6115.

[11] a) N. Kindermann, À. Cristòfol, A. W. Kleij, *ACS Catal.* **2017**, *7*, 3860; b) F. Auriemma, C. de Rosa, M. R. Di Caprio, R. Di Girolamo, W. C. Ellis, G. W. Coates, *Angew. Chem., Int. Ed.* **2015**, *54*, 1215; c) C. Li, R. J. Sablong, C. Koning, *Angew. Chem. Int. Ed.* **2016**, *55*, 11572; d) C. Li, R. J. Sablong, C. Koning, *Eur. Polym. J.* **2015**, *67*, 449.

[12] O. Hauenstein, Md. M. Rahman, M. Elsayed, R. Krause-Rehberg, S. Agarwal, V. Abetz, A. Greiner, *Adv. Mater. Technol.* **2017**, *2*, 1700026.

[13] a) O. Hauenstein, S. Agarwal, A. Greiner, *Nat. Commun.* **2016**, *7*, 11862; b) T. Stößer, C. Li, J. Unruangsri, P. Saini, R.Sablong, M. Meier, C. Williams, C. Koning, *Polym. Chem.* **2017**, *8*, 6099; c) C. Li, R. J. Sablong, R. A. T. M. van Benthem, C. E. Koning, *ACS Macro Lett.* **2017**, *6*, 684.

[14] J. Bailer, S. Feth, F. Bretschneider, S. Rosenfeldt, M. Drechsler, V. Abetz, H. Schmalz, A. Greiner, *Green Chem.* **2019**, *21*, 2266.

[15] F. Parrino, A. Fidalgo, L. Palmisano, L. M. Ilharco, M. Pagliaro, R. Ciriminna, *ACS Omega* **2018**, *3*, 4884.

[16] D. Zhang, E. A. del Rio-Chanona, J. L. Wagner, N. Shah, *Sus. Prod. Consum.* **2018**, *14*, 152.

[17] M. Sheth, R. A. Kumar, V. Dav, R. A. Gross, S. P. McCarthy, *J. Appl. Polym. Sci.* **1997**, *66*, 1495.

[18] A. M. Gajria, V. Davé, R. A. Gross, S. P. McCarthy, *Polymer.* **1996**, *37*, 437.

[19] Y. F. Kim, C. N. Choi, Y. D. Kim, K. Y. Lee, M. S. Lee, *Fibers Polym.* **2004**, *5*, 270.

[20] G. Biresaw, C. J. Carriere, *J. Polym. Sci. B Polym. Phys.* **2002**, *40*, 2248.

[21] M. Evstatiev, S. Simeonova, K. Friedrich, X.-Q. Pei, P. Formanek, *J. Mater. Sci.* **2013**, *48*, 6312.

[22] a) M. Larsson, O. Markbo, P. Jannasch, *RSC Adv.* **2016**, *6*, 44354; b) Y. Ke, X. Y. Zhang, S. Ramakrishna, L. M. He, G. Wu, *Mater. Sci. Eng. C* **2017**, *70*, 1107; c) E. Renard, M. Walls, P. Guérin, V. Langlois, *Polym. Degrad. Stab.* **2004**, *85*, 779.

[23] a) M. Harada, T. Ohya, K. Iida, H. Hayashi, K. Hirano, H. Fukuda, *J. Appl. Polym. Sci.* **2007**, *106*, 1813; b) M. Shibata, Y. Inoue, M. Miyoshi, *Polymer.* **2006**, *47*, 3557; c) Z. Qiu, T. Ikehara, T. Nishi, *Polymer.* **2003**, *44*, 2799.

[24] a) B. Imre, B. Pukánszky, *Eur. Polym. J.* **2013**, *49*, 1215; b) K. M. Zia, A. Noreen, M. Zuber, S. Tabasum, M. Mujahid, *Int. J. Biol. Macromol.* **2016**, *82*, 1028; c) J. J. Koh, X. Zhang, C. He, *Int. J. Biol. Macromol.* **2018**, *109*, 99.

[25] S. Neumann, L.-C. Leitner, H. Schmalz, S. Agarwal, A. Greiner, *Sustain. Chem. Eng.* **2020**, *8*, 6442.

[26] E. Meaurio, E. Sanchez-Rexach, E. Zuza, A. Lejardi, A. d. P. Sanchez-Camargo, J.-R. Sarasua, *Polymer.* **2017**, *113*, 295.

[27] T. Standau, H. Long, S. Murillo Castellón, C. Brütting, C. Bonten, V. Altstädt, *Materials.* **2020**, *13*.

[28] R. Muthuraj, M. Misra, A. K. Mohanty, *J. Polym. Environ.* **2014**, *2014*, 336.

[29] D. Kanev, E. Takacs, J. Vlachopoulos, *Int. Polym. Process.* **2007**, *22*, 395.

[30] C. Wohlfarth, Lechner, K. F., Arndt K. F., *Polymers Subvolume D Polymer Solutions Part 2: Physical Properties and their Relations I (Thermodynamic Properties: PVT-Data and Miscellaneous Properties of Polymer Solutions*, Springer. **2010**.

[31] H. Veenstra, B. Norder, J. van Dam, A. Posthuma de Boer, *Polymer.* **1999**, *40*, 5223.

[32] B. Haworth, N. Hopkinson, D. Hitt, X. Zhong, *Rapid Prototyp. J.* **2013**, *19*, 28.

[33] J. E. Mark, *Polymer Data Book*, New York, Oxford University Press. **1990**.

[34] C. J. Carriere, A. Cohen, *J. Rheol.* **1991**, *35*, 205.

[35] W. S. Rasband, *ImageJ*, U. S. National Institutes of Health, Bethesda, Maryland, USA,. **1997-2018**.

[36] M. Rizzuto, L. Marinetti, D. Caretti, A. Mugica, M. Zubitur, A. J. Müller, *CrystEngComm* **2017**, *19*, 3178.

[37] H. Ruckdäschel, J. K.W. Sandler, V. Altstädt, H. Schmalz, V. Abetz, A. H.E. Müller, *Polymer.* **2007**, *48*, 2700.

[38] S. Wacharawichanant, S. Ratchawong, P. Hoysang, M. Phankokkruad, *MATEC Web Conf.* **2017**, *130*, 7006.

## Table of contents

In this study, we investigate the blending process between bio-based poly(limonene carbonate) (PLimC) and different commercially available polymers like poly (L-lactic acid) (PLA), polyamide 12 (P12), poly(butylene adipate-co-terephthalate) (PBAT, EcoFlex®) and a segmented polyether ester (COPE, Arnitel EM400®) to the showcase potential of PLimC in terms of sustainability.

Simon Neumann, Pin Hu, Felix Bretschneider, Holger Schmalz, and Andreas Greiner*

## Blends of bio-based poly(limonene carbonate) with commodity polymers

## TOC Figure

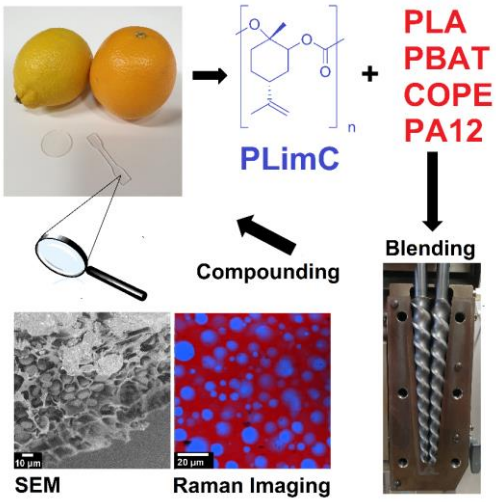

# Supporting Information

**Blends of bio-based poly(limonene carbonate) with commodity polymers**

Simon Neumann, Pin Hu, Felix Bretschneider, Holger Schmalz and Andreas Greiner*

University of Bayreuth, Macromolecular Chemistry and Bavarian Polymer Institute, Universitätsstraße 30, 95440 Bayreuth, Germany

Total pages: 22

Total number of Figures: 19

Total number of Tables: 2

## Poly(methyl methacrylate) (PMMA) and polystyrene (PS) blends

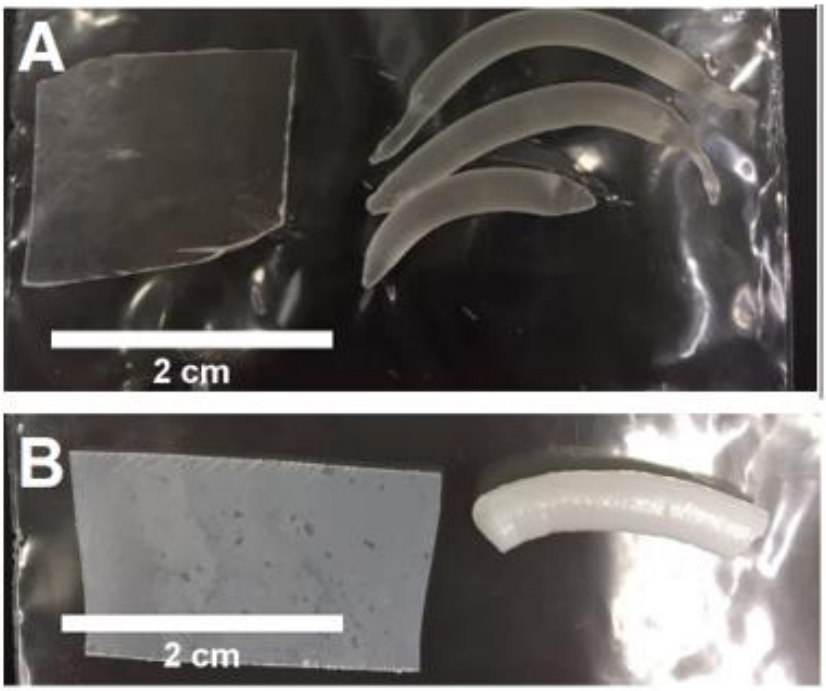


**Figure S24.** Digital photographs of the produced PMMA/PLimC and PS/PLimC blends. A) PMMA/PLimC = 90/10 w/w; 190 °C, 2 min, 50 rpm. B) PS/PLimC = 90/10 w/w; 180 °C, 2 min, 50 rpm.

**Table S3.** Mechanical properties of PMMA/PLimC and PS/PLimC blends.*

| Sample | Processing temperature | *E*-modulus | Tensile strength | Elongation at break |
|---|---|---|---|---|
| | [°C] | [GPa] | [MPa] | [%] |
| **PMMA** | 190 | 1.47 ± 0.01 | 60.17 ± 3.36 | 5.07 ± 0.42 |
| **PMMA +10 wt% PLimC** | 190 | 1.27 ± 0.02 | 25.65 ± 0.70 | 2.67 ± 0.26 |
| **PS** | 180 | 1.31 ± 0.06 | 29.80 ± 2.78 | 2.7 ± 0.33 |
| **PS +10 wt% PLimC** | 180 | 1.41 ± 0.07 | 15.24 ± 3.03 | 1.47 ± 0.26 |

* Samples were processed at the given temperature for 2 min at 50 rpm. A test speed of 5.0 $mm \cdot min^{-1}$ was used for tensile tests.

## Aliphatic polyester (poly(*L*-lactic acid), PLA) blends

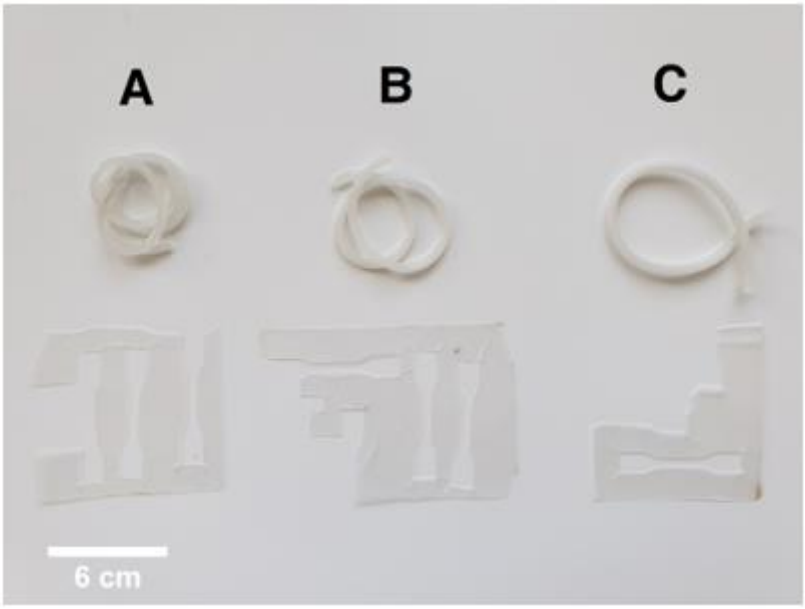


**Figure S25.** Digital photograph of the produced PLA/PLimC blends. A) PLA/PLimC = 100/0 w/w, B) PLA/PLimC = 90/10 w/w, C) PLA/PLimC = 70/30 w/w. All blends were processed for 4 min at 190 °C and 50 rpm.

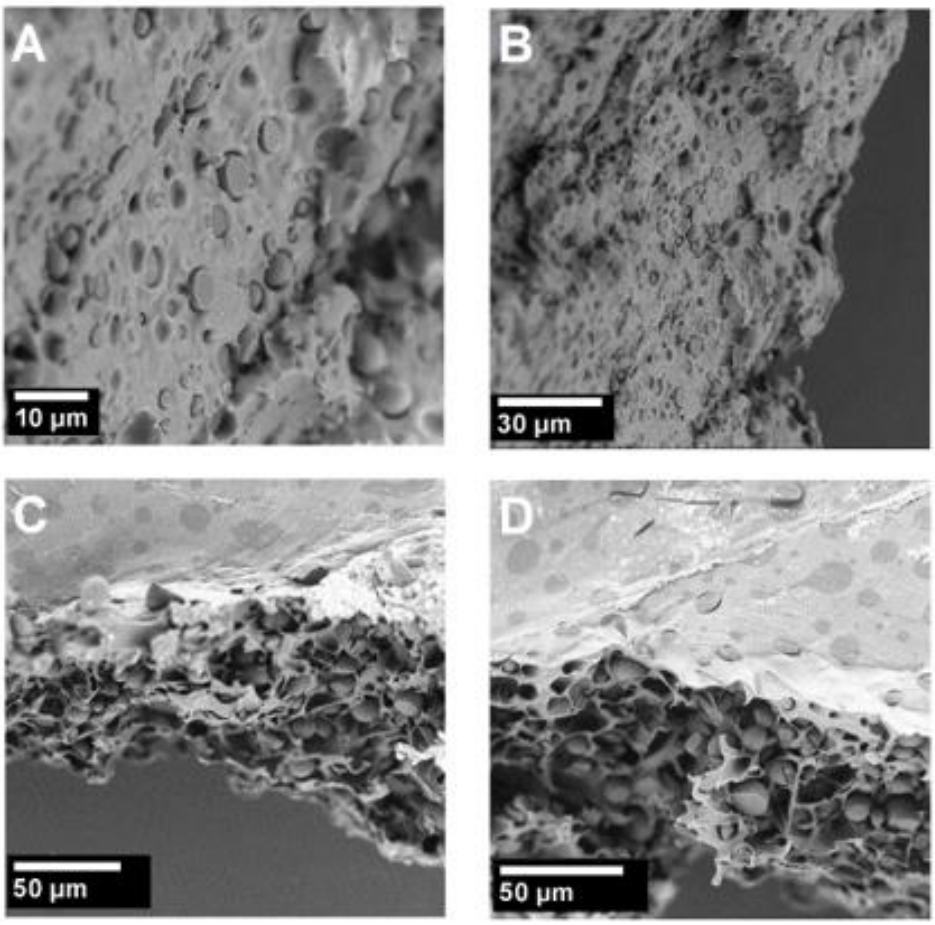


**Figure S26.** SEM images of A, B) PLA/PLimC = 90/10 w/w and C, D) PLA/PLimC = 70/30 w/w blends in different magnifications.

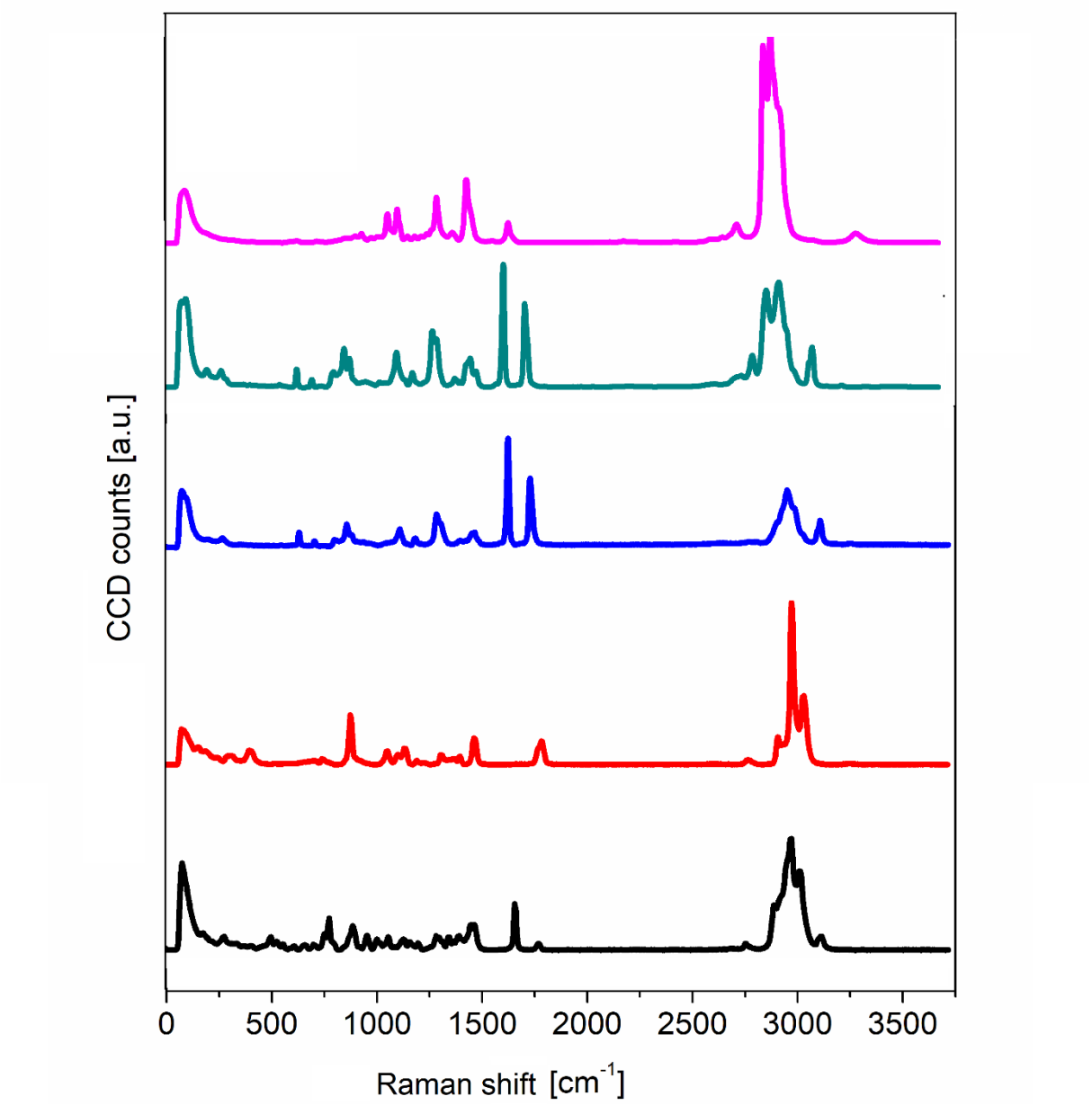


**Figure S27.** Raman spectra of neat PLimC (black), PLA (red), PBAT (blue), COPE (green) and PA12 (pink).

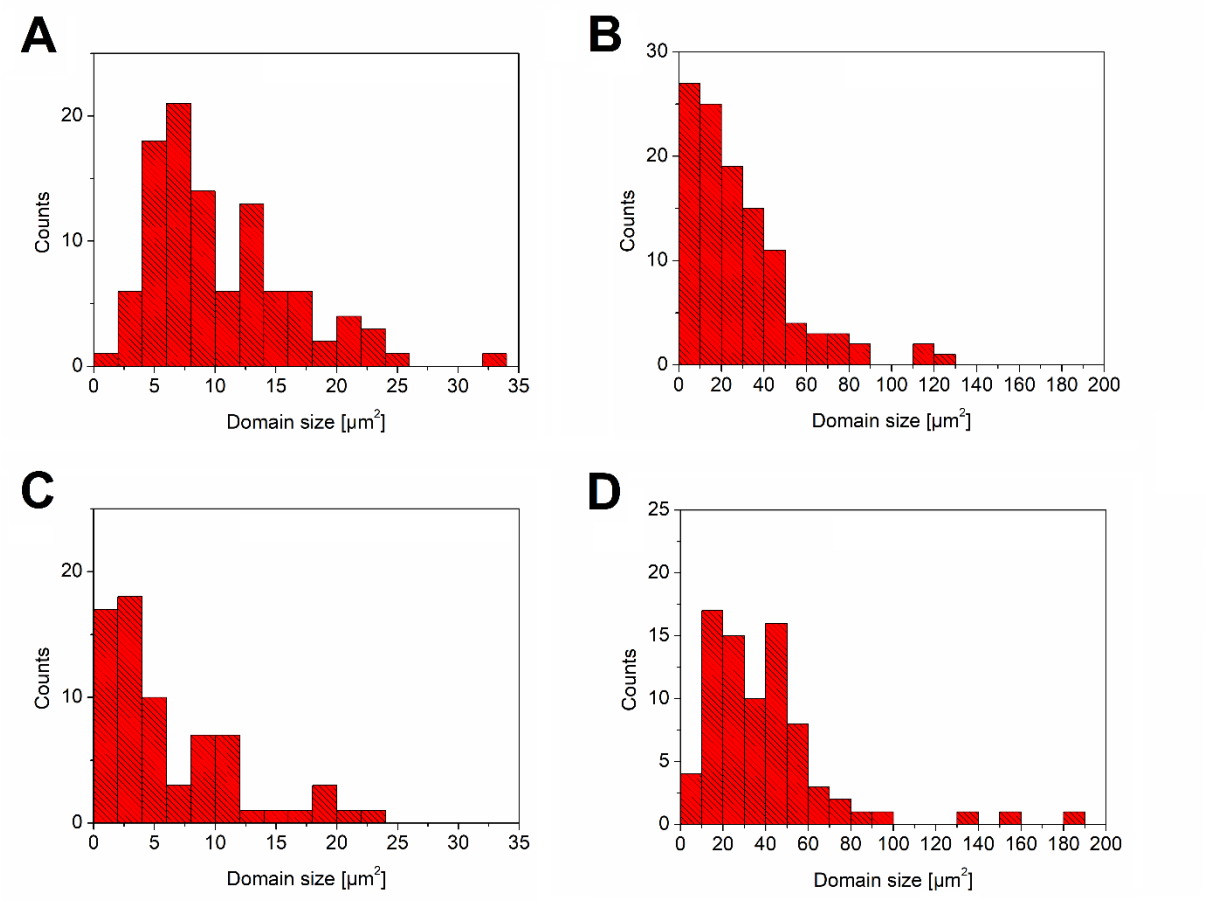


**Figure S28.** Histograms of PLimC domain sizes in PLA/PLimC blends determined by SEM: A) PLA/PLimC = 90/10 w/w; B) PLA/PLimC = 70/30 w/w and Raman imaging: C) PLA/PLimC = 90/10 w/w; D) PLA/PLimC = 70/30 w/w.

**Table S4.** Average PLimC domain areas and corresponding PLimC droplet sizes for the investigated PLimC blends.

| PLimC | Average area | Average diameter[a] | Domains[b] | Method |
|---|---|---|---|---|
| | [µm$^2$] | [µm] | | |
| **PLA Blends** | | | | |
| **10wt%** | 10.3 ± 5.9 | 3.6 ± 3.9 | 102 | SEM |
| **10wt%** | 6.2 ± 5.4 | 2.8 ± 3.0 | 70 | Raman |
| **30wt%** | 28 ± 24 | 6.0 ± 6.1 | 112 | SEM |
| **30wt%** | 39.5 ± 30.4 | 7.1 ± 7.3 | 80 | Raman |
| **PBAT Blends[c]** | | | | |
| **10wt%** | 1.9 ± 2.4 | 1.6 ± 1.7 | 114 | SEM |
| **10wt%** | 170 ± 149 | 15 ±29 | 40 | SEM |
| **10wt%** | 1.4 ± 0.9 | 1.3 ± 1.9 | 64 | Raman |
| **30wt%** | 0.9 ± 0.7 | 1.1 ± 1.8 | 127 | SEM |
| **30wt%** | 137 ± 137 | 13 ± 13 | 33 | SEM |
| **30wt%** | 0.6 ± 0.3 | 0.9 ± 1.8 | 10 | Raman |
| **COPE Blends[c]** | | | | |
| **10wt%** | 0.14 ± 0.05 | 0.4 ± 1.3 | 102 | SEM |
| **10wt%** | 44 ± 26 | 7.5 ± 10 | 32 | SEM |
| **10wt%** | 0.26 ± 0.17 | 0.6 ± 1.8 | 112 | Raman |
| **30wt%** | 1.9 ± 3.8 | 1.5 ± 1.7 | 121 | SEM |
| **30wt%** | 88 ± 56 | 11 ± 11 | 32 | SEM |
| **30wt%** | 0.49 ± 0.24 | 0.8 ± 1.9 | 124 | Raman |
| **PA12 Blends[c]** | | | | |
| **10wt%** | 9.8 ± 5.1 | 3.5 ± 3.8 | 114 | SEM |
| **10wt%** | 93 ± 67 | 11 ± 11 | 40 | SEM |
| **10wt%** | 0.38 ± 0.28 | 0.7 ± 1.0 | 64 | Raman |
| **30wt%** | 39 ± 23 | 7.1 ± 7.2 | 116 | SEM |
| **30wt%** | 311 ± 366 | 20 ± 20 | 30 | SEM |
| **30wt%** | 4.32 ± 3.76 | 2.3 ± 2.4 | 28 | Raman |

[a] Diameter was calculated from the area of an equivalent circle.
[b] Number of PLimC domains used for area calculation.
[c] Bimodal PLimC droplet distribution, given values from SEM represent average values for the lower and higher domain area distributions, respectively.

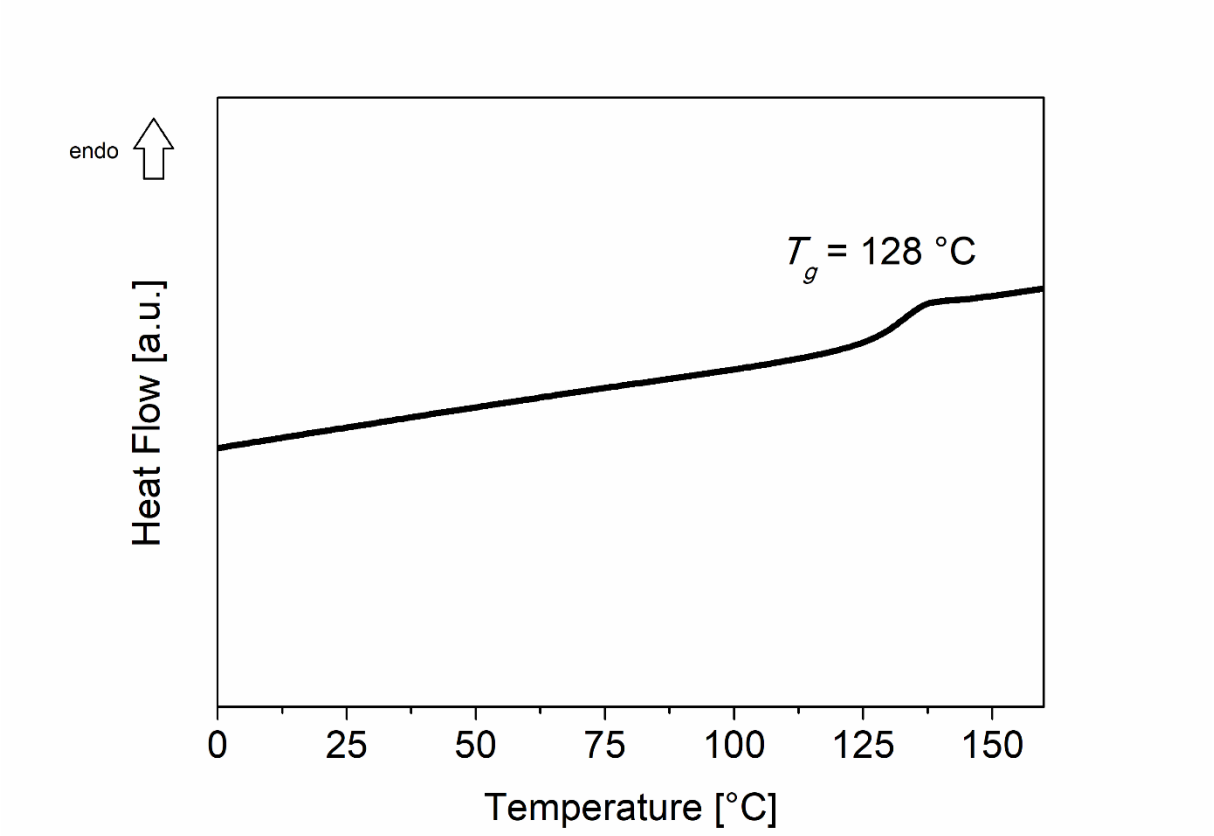


**Figure S29.** DSC heating trace of neat PLimC (2nd heating, scanning rate: 10 K·min$^{-1}$).

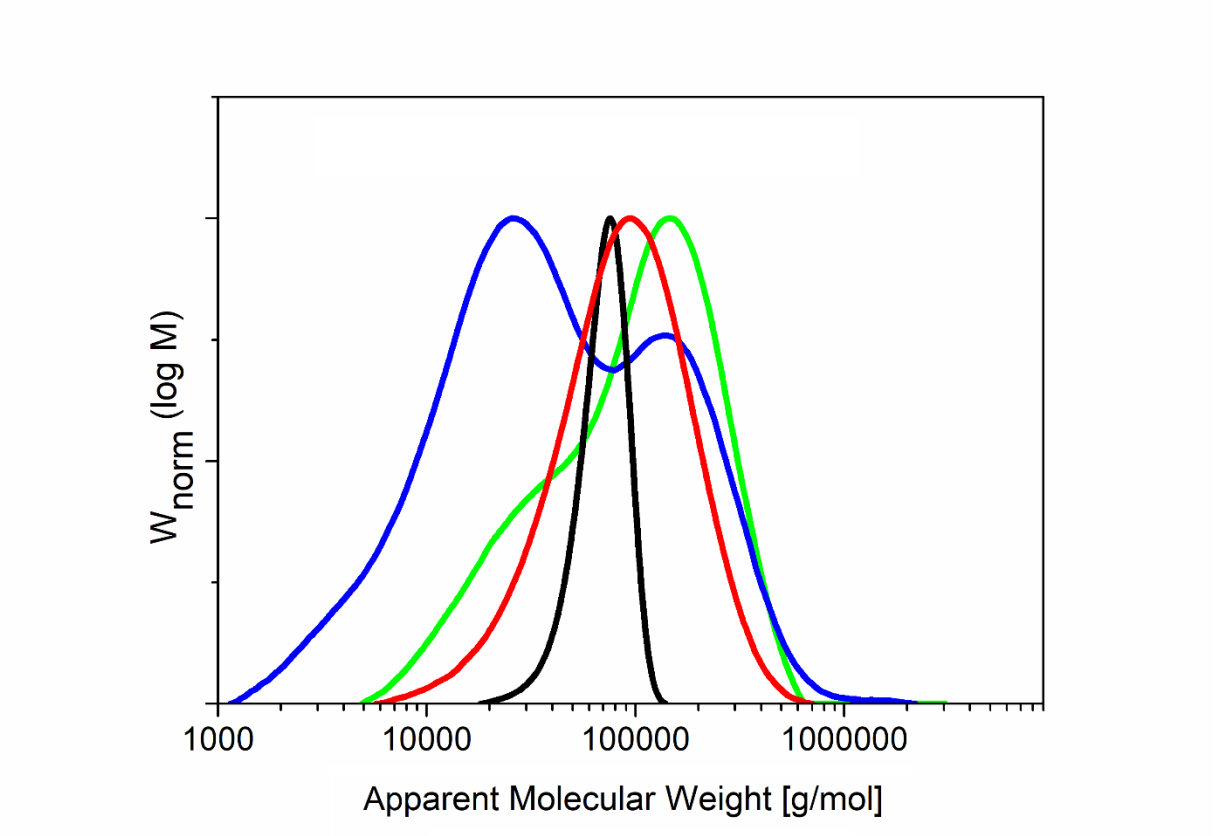


**Figure S30.** $CHCl_3$-GPC traces of neat PLA (red), neat PLimC (black), PLA/PLimC = 90/10 w/w (green) and PLA/PLimC = 70/30 w/w (blue). Toluene (HPLC grade) was used as internal standard and calibration was based on narrowly distributed PS standards.

## Aliphatic/aromatic polyester (poly(butylene adipate-*co*-terephthalate), PBAT) blends

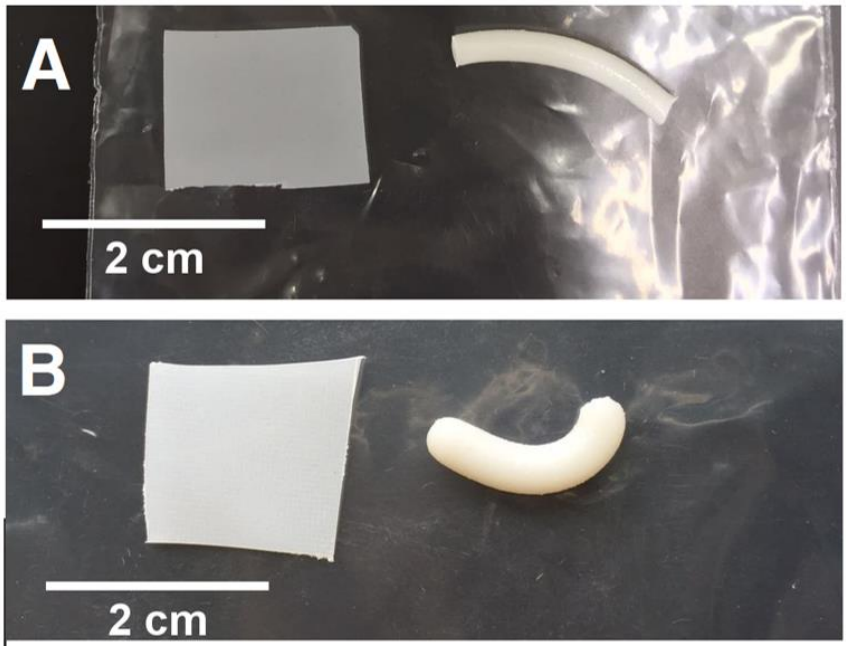


**Figure S31.** Digital photographs of the produced PBAT/PLimC blends. A) PBAT/PLimC = 90/10 w/w, B) PBAT/PLimC = 70/30 w/w. All blends were processed for 4 min at 180 °C and 50 rpm.

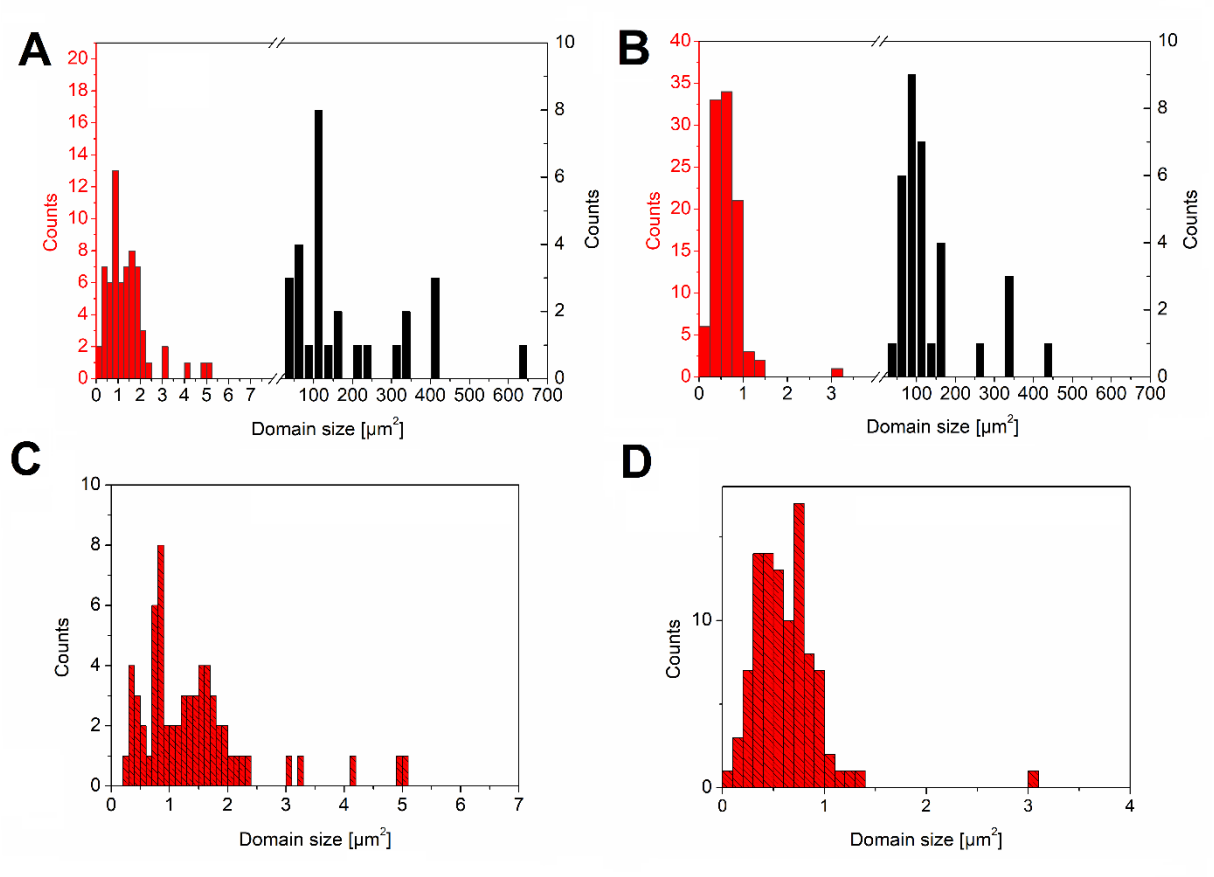


**Figure S32.** Histograms of PLimC domain sizes in PBAT/PLimC blends determined by SEM: A) PBAT/PLimC = 90/10 w/w, B) PBAT/PLimC = 70/30 w/w and Raman imaging: C) PBAT/PLimC = 90/10 w/w, D) PBAT/PLimC = 70/30 w/w. Smaller PLimC domains are depicted in red and larger PLimC domains in black.

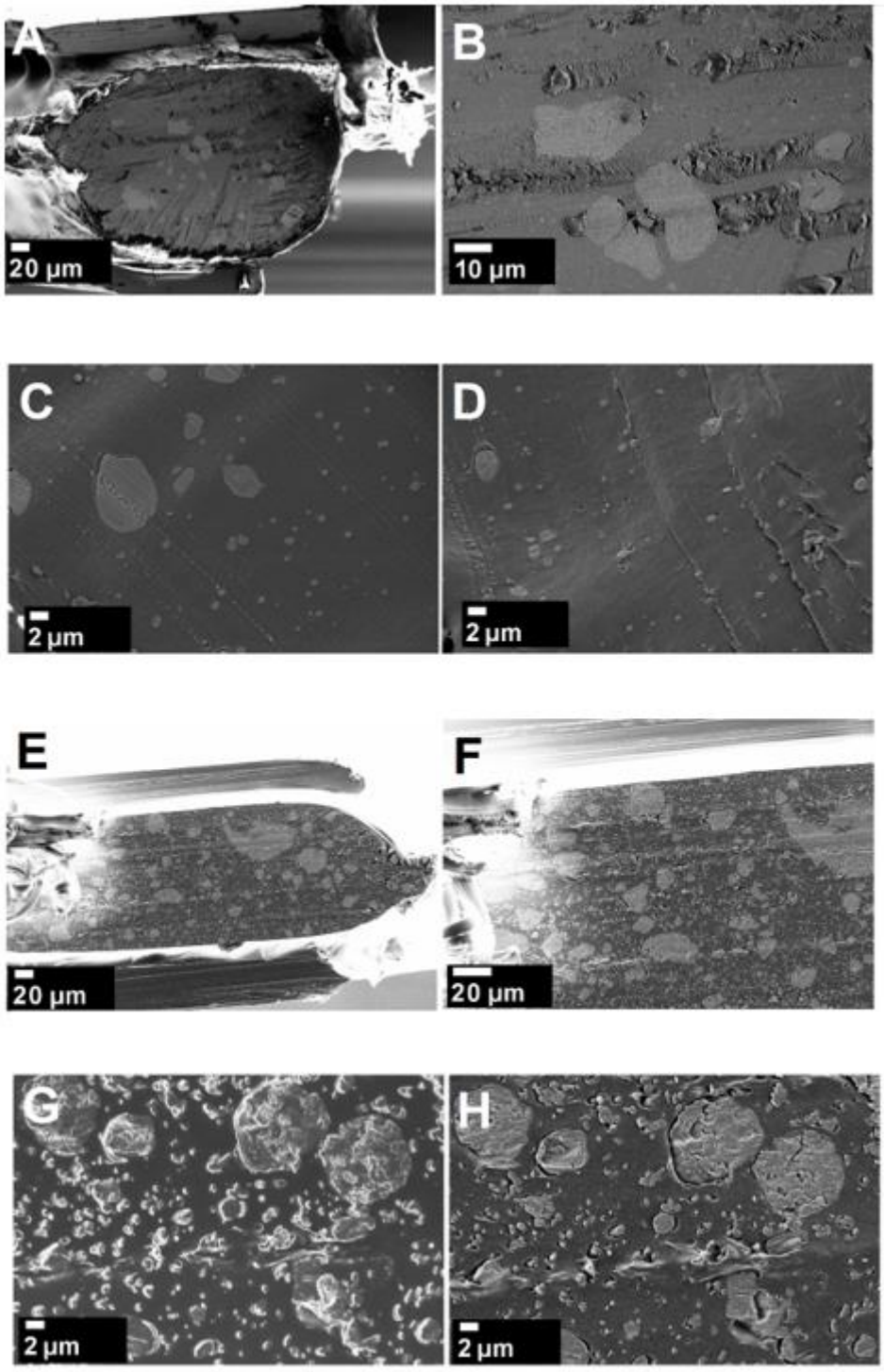


**Figure S33.** SEM images of A-D) PBAT/PLimC = 90/10 w/w and E-H) PBAT/PLimC = 70/30 w/w blends in different magnifications.

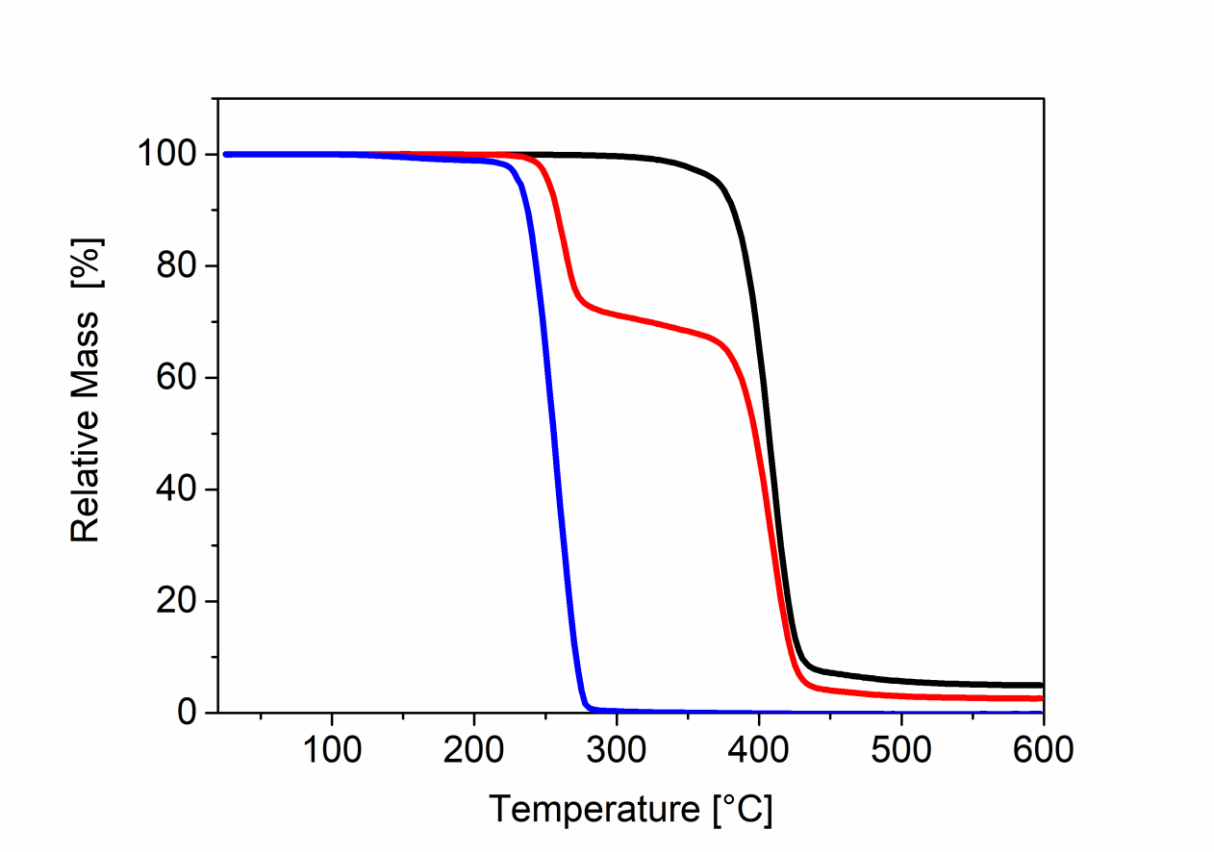


**Figure S34.** TGA traces of neat PLimC (blue), neat PBAT (black) and a PBAT/PLimC 70/30 w/w blend (red), measured under nitrogen at 10 $K \cdot min^{-1}$.

## Copoly(ether ester) (Arnitel EM400, COPE) blends

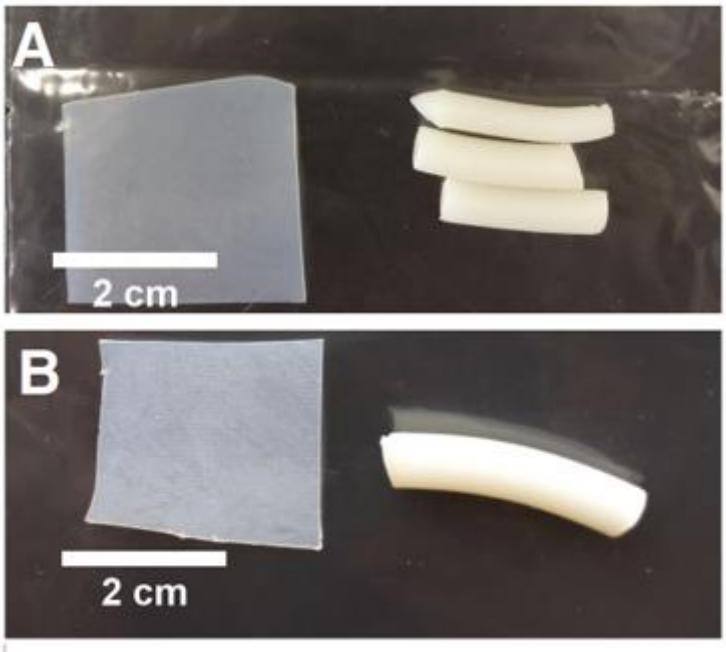


**Figure S35.** Digital photographs of the produced COPE/PLimC blends. A) COPE/PLimC = 90/10 w/w, B) COPE/PLimC = 70/30 w/w. All blends were processed for 4 min at 200 °C and 50 rpm.

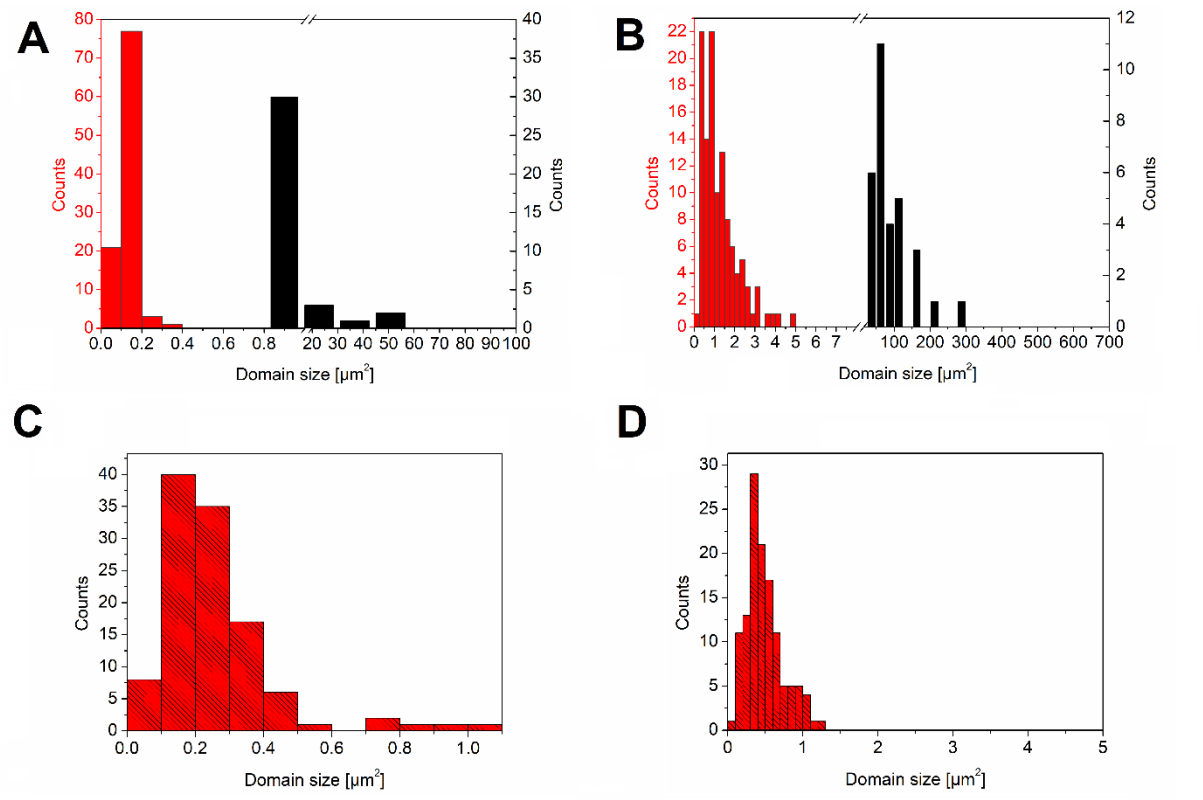


**Figure S36.** Histograms of PLimC domain sizes in COPE/PLimC blends determined by SEM: A) COPE/PLimC = 90/10 w/w, B) COPE/PLimC = 70/30 w/w and Raman imaging: C) COPE/PLimC = 90/10 w/w, D) COPE/PLimC = 70/30 w/w. Smaller PLimC domains are depicted in red and larger PLimC domains in black.

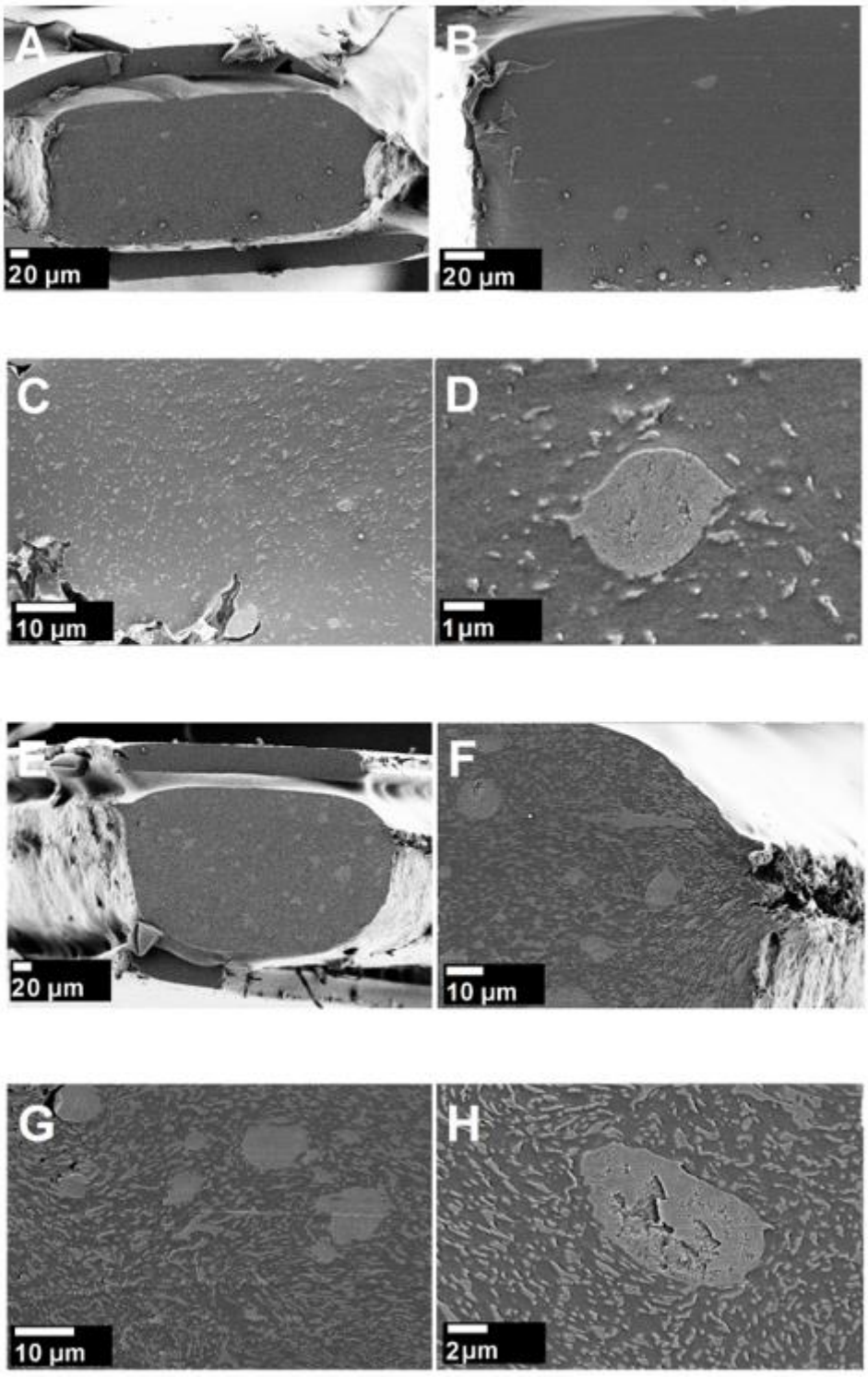


**Figure S37.** SEM images of A-D) COPE/PLimC = 90/10 w/w and E-H) COPE/PLimC = 70/30 w/w blends in different magnifications.

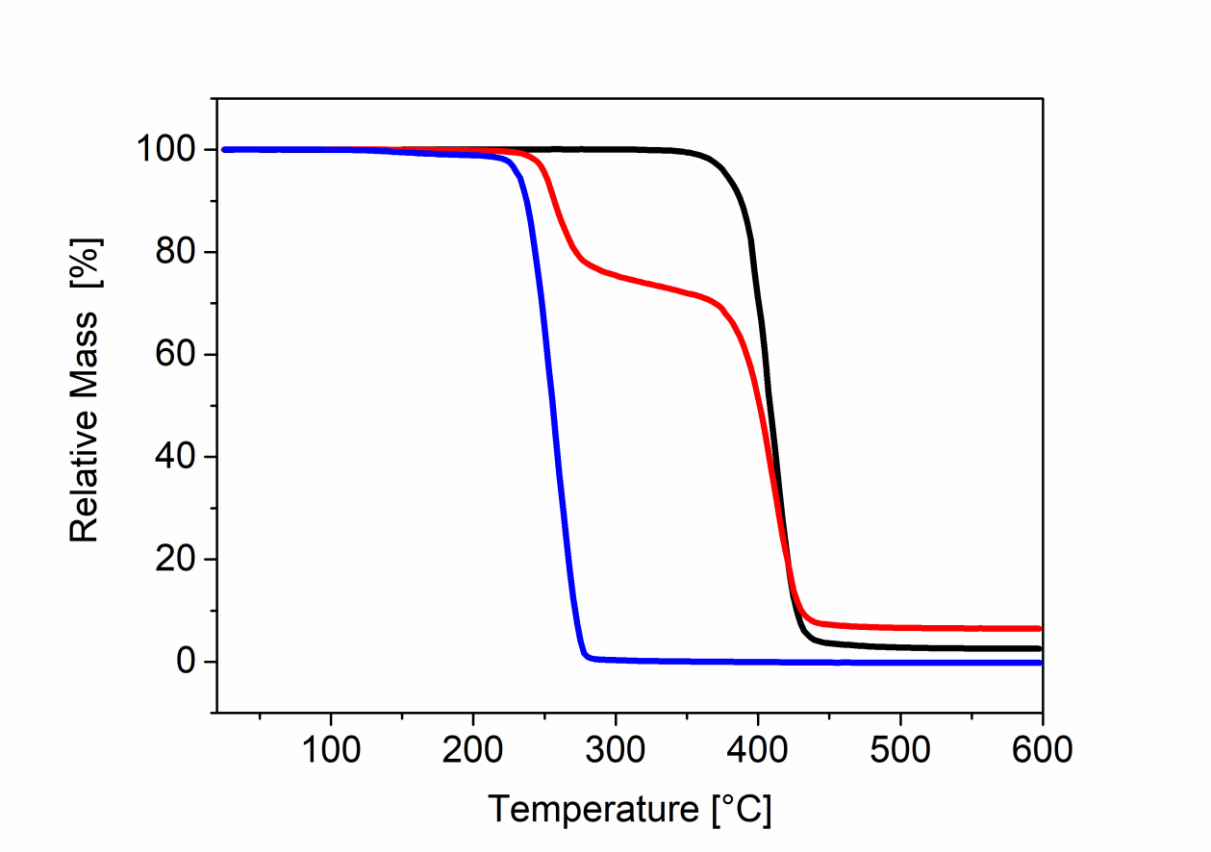


**Figure S38.** TGA traces of neat PLimC (blue), neat COPE (black) and a COPE/PLimC 70/30 w/w blend (red), measured under nitrogen at 10 $K \cdot min^{-1}$.

## Aliphatic polyamide (polyamide 12, PA12) blends

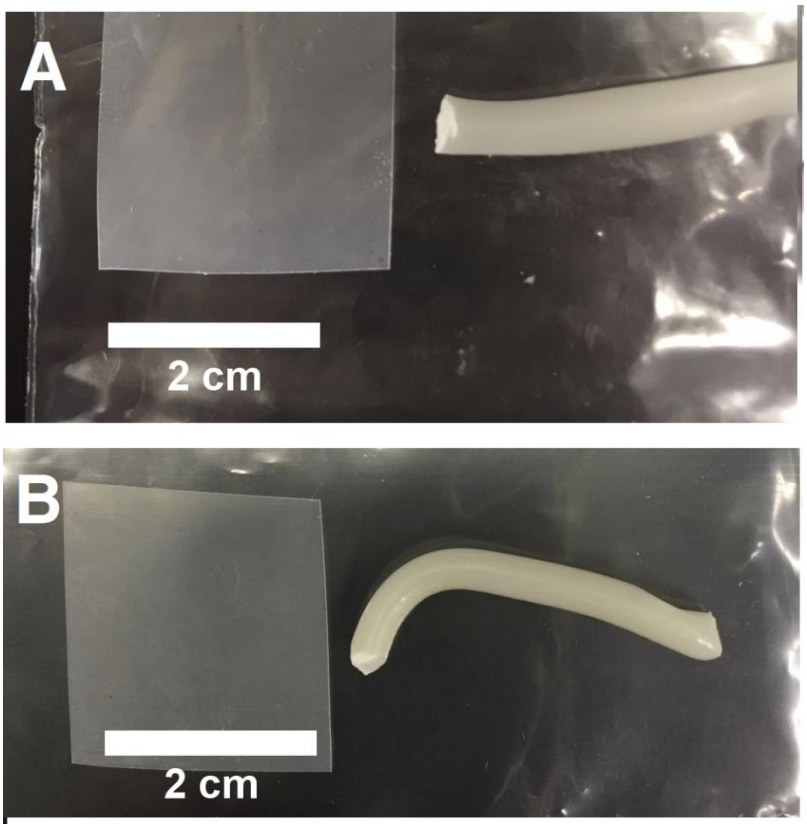


**Figure S39.** Digital photographs of the produced PA12/PLimC blends. A) PA12/PLimC = 90/10 w/w, B) PA12/PLimC = 70/30 w/w. All blends were processed for 4 min at 185 °C and 50 rpm.

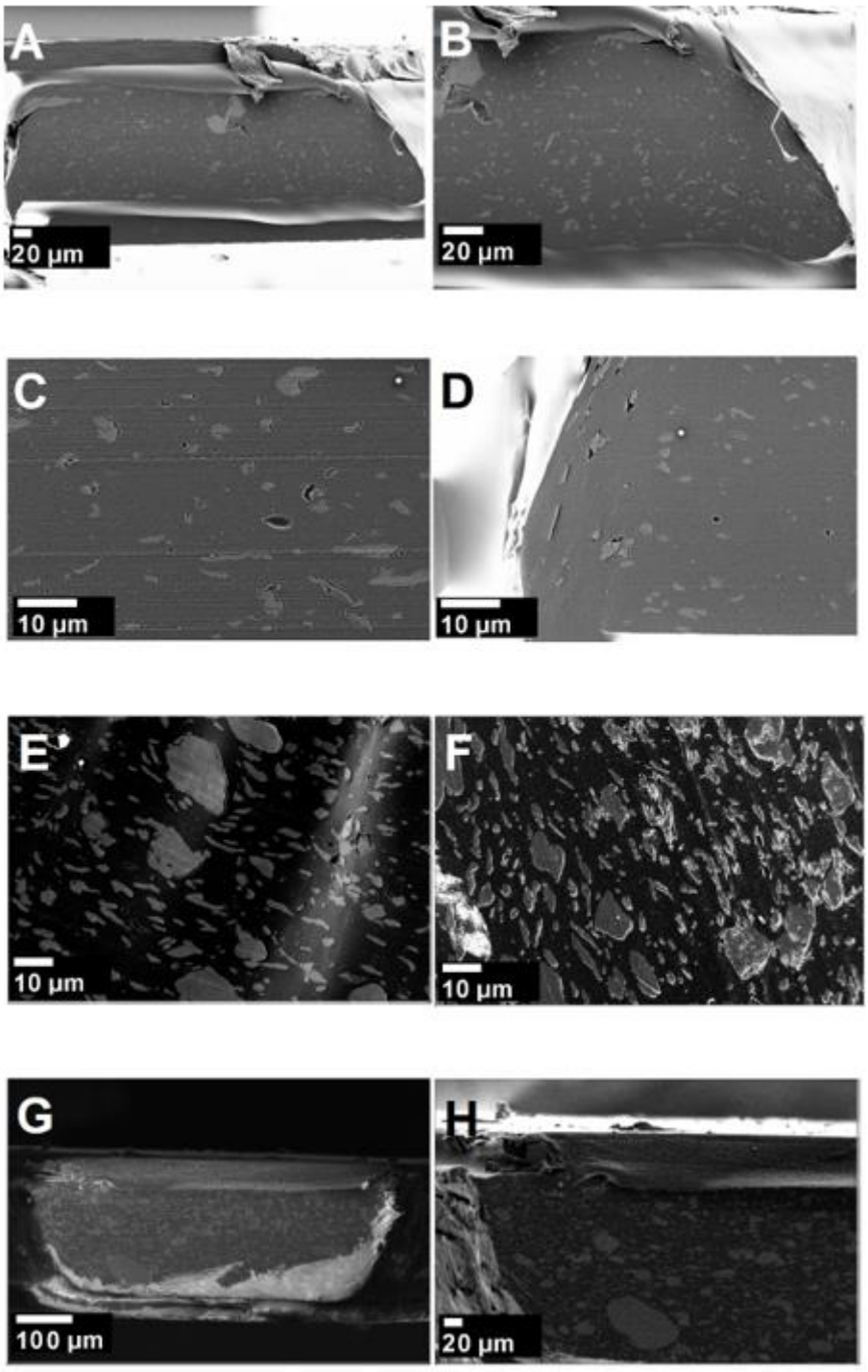


**Figure S40.** SEM images of A-D) PA12/PLimC = 90/10 w/w and E-H) PA12/PLimC = 70/30 w/w blends in different magnifications.

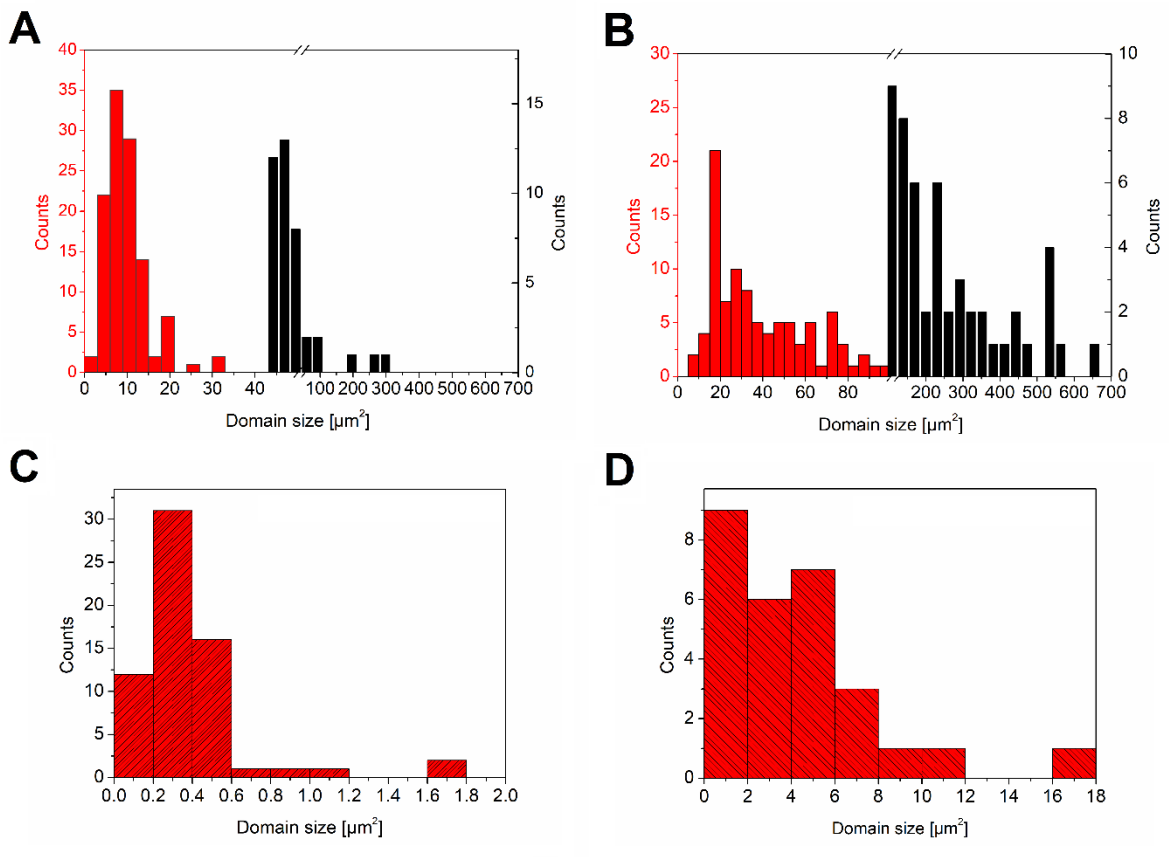


**Figure S41.** Histograms of PLimC domain sizes in PA12/PLimC blends determined by SEM: A) PA12/PLimC = 90/10 w/w, B) PA12/PLimC = 70/30 w/w and Raman imaging: C) PA12/PLimC = 90/10 w/w, D) PA12/PLimC = 70/30 w/w. Smaller PLimC domains are depicted in red and larger PLimC domains in black.

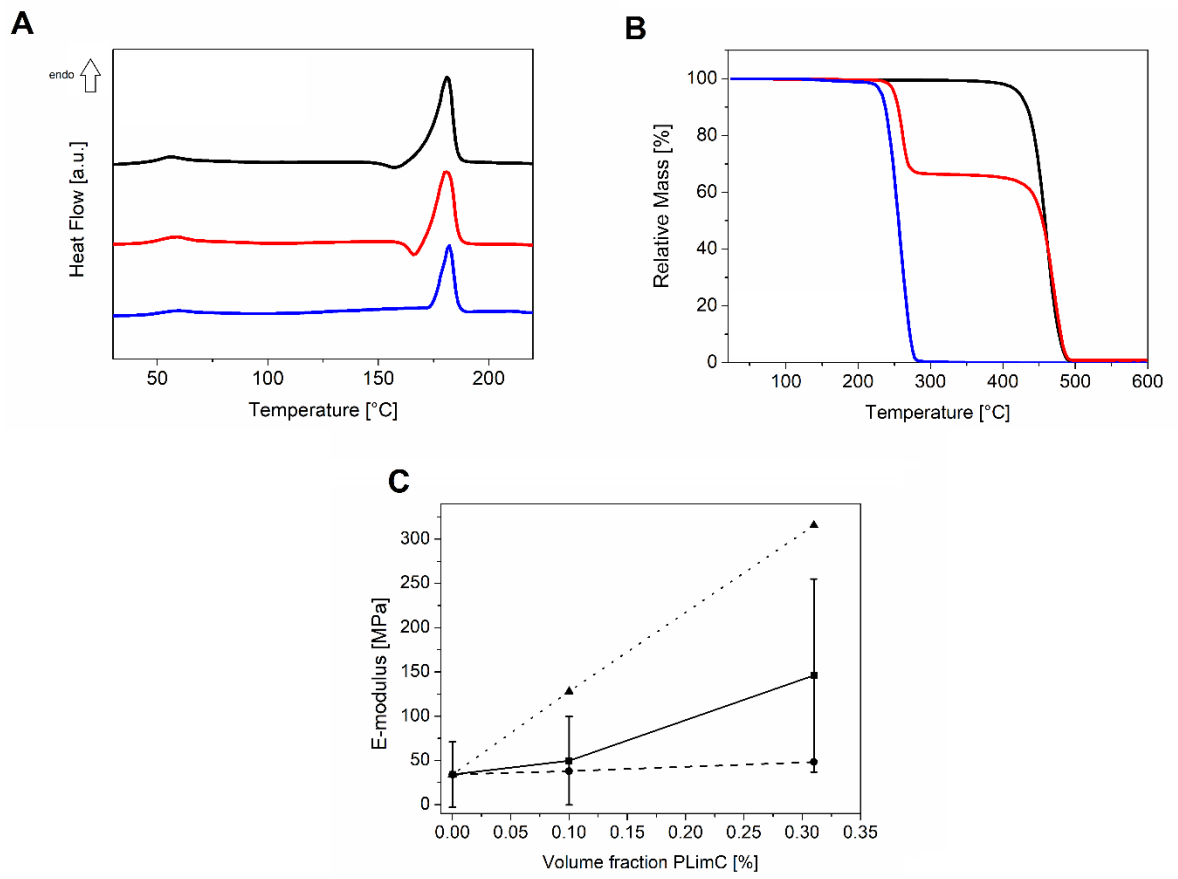


**Figure S42.** A) First heating runs for PA12/PLimC blends, measured under nitrogen at 10 K·min$^{-1}$ (PA12/PLimC = 100/0 w/w (black), PA12/PLimC = 90/10 w/w (red), PA12/PLimC = 70/30 w/w (blue)). B) TGA comparison of neat PLimC (blue), neat PA12 (black) and a PA12/PLimC 70/30 w/w blend (red), measured under nitrogen at 10 K·min$^{-1}$. C) *E*-moduli of PA12/PLimC blends (solid) in dependence of the volume fraction of PLimC and estimated *E*-moduli of the blends employing the series (dashed) and parallel (dotted) model, respectively.

## 9.3 Sustainable block copolymers of poly(limonene carbonate)

Simon Neumann,[a] Sophia Barbara Däbritz,[a] Sophie Edith Fritze,[a] Lisa-Cathrin Leitner,[a] Aneesha Anand,[a] Andreas Greiner [a,b] and Seema Agarwal *[a,b]

[a]University of Bayreuth, Macromolecular Chemistry II, Universitätsstraße 30, 95440 Bayreuth, Germany. E-mail: agarwal@uni-bayreuth.de

[b]University of Bayreuth, Bavarian Polymer Institute (BPI), Universitätsstraße 30, 95440 Bayreuth, Germany

in

Polymer Chemistry

Received: December 09, 2020

Accepted: January 09, 2021

Published: January 22, 2021

https://doi.org/10.1039/D0PY01685C

**Polym. Chem., 2021,12, 903-910**



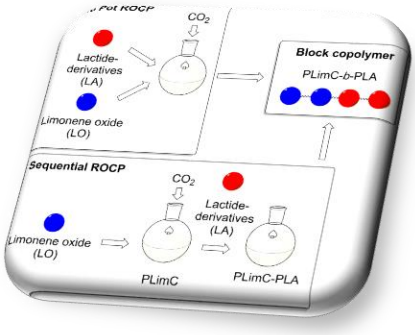

ABSTRACT

Poly(limonene carbonate) (PLimC) is a bio-based, non-food-based polymer produced by copolymerization of limonene oxide (LO) with carbon dioxide ($CO_2$). It can be a potential candidate for the replacement of toxic state-of-the-art polycarbonates only after improvement of its mechanical properties. An elegant way to tune and improve the mechanical properties of PLimC lies in copolymerization. For this, we present the basic studies regarding the copolymerization behaviour of LO/$CO_2$ with the lactide monomer and its derivatives using a catalyst [(BDI)Zn-($\mu$-OAc)]. The simultaneous copolymerization of LO/$CO_2$ with lactide in one pot did not provide a random copolymer. Advanced characterization methods were used to study the polymer structure, and it was proved to be a block copolymer (poly(limonene carbonate)- *block*-poly(lactide) (PLimC-*b*-PLA)) with inhomogeneous macromolecular chain compositions. A sequential living ring-opening copolymerization method provided precise block copolymers. The mechanical characteristics could be altered by the use of lactide derivatives with a low glass transition temperature. The use of lactide with long hexyl alkyl chains during sequential copolymerization provided block copolymers with polyester soft blocks with a very low glass transition temperature ($T_g = -38$ °C) showing rubber-like behavior. Upscaling of the method, processing and detailed characterization of the mechanical properties will be carried out in the future based on the present work.

## INTRODUCTION

Sustainability is one of the keywords of our decade. Many types of research show the interest in bio-based polymers.[1] Poly(limonene carbonate) (PLimC), discovered by Coates et al. when he used a μ-bis-diiminato zinc complex catalyst for the polymerization of limonene oxide (LO),[2] is one of the interesting and potentially useful bio-based polymers.[3] It is based on the monomer trans-limonene oxide, which can be directly produced by oxidizing naturally occurring limonene as the main component from citrus oil. 57 000 t $a^{-1}$ of citrus oil is collected from orange juice production.[4] The polymerization method was modified by Hauenstein et al., who increased the molecular weight of PLimC to was demonstrated by Kleij et al., who further developed the synthesis.[7] PLimC features excellent properties when it is cast as a film. High optical transparency (99%) and strong tensile strength of 40 MPa are characteristics of PLimC.[5] PLimC can also be modified by thiol click chemistry for adjusting the properties.[8] Also, block copolymerization with cyclohexane oxide is possible.[9] PLimC can also be used as a coating

material or as a breathing glass due to its high gas permeability.[10] The life cycle assessment of limonene and the economic potential of PLimC were shown by several groups.[11] Due to the economic potential, PLimC offers an interesting perspective for applications as thermoplastic polymer. One of the disadvantages of PLimC is its low impact and mechanical properties. Recently, the improvement in the mechanical properties of PLimC has been shown by the use of additives (e.g., ethyl oleate).[12] Although simple to use, the additive approach is disadvantageous due to the leaching of the additive with time. Copolymerization is one of the oldest methods of polymer property improvement. Depending upon the origin of the comonomer (petro-based/bio-based), either complete or partly bio-based copolymers can be prepared by this method. Recently, Williams et al. published a study on the modification of PLimC using bio-based cyclic ester ε-decalactone as a comonomer to selectively form thermoplastic ABA elastomers (A = high $T_g$ polycarbonate, B = low $T_g$ polyester), which can improve the mechanical properties of PLimC.[13] The synthesis of triblock copolymers required two different catalysts to cope with the different reactivities of comonomers in two different step ringopening polymerization (ROP) of lactone, chain-end-modification and then ring-opening copolymerization of limonene oxide (LO) and carbon dioxide ($CO_2$) carried out sequentially. Other cyclic diesters, such as lactide and its derivatives, are interesting comonomers for property modification as they can provide PLimC copolymer segments with different glass transition temperatures and, therefore, different mechanical characteristics dependent upon either the stereospecificity or the side chain. Two variants of PLA are well known: poly(*L*-lactide) (PLLA) and poly(*D/L*-lactide acid) (PDLLA) prepared by ring-opening polymerization.[14] They are created with different stereospecific monomers of lactide. *L,L*-Lactide is a bio-based cyclic ester prepared by the fermentation of plants, such as corn or sugar beet pulp.[15] PDLLA is an amorphous polymer,[15] whereas PLLA shows semi-crystallinity.[16] The crystallinity of PLLA is advantageous in terms of mechanical properties, but amorphous PDLLA shows better biodegradability in aqueous systems. Its derivatives, such as dihexyllactide (diHLA), can easily be prepared by a condensation reaction of 2-hydroxyoctanoic acid.[18–20] The starting material heptaldehyde is a bio-based material.[17] Therefore, in the present study, we focused on one-pot and sequential ring-opening copolymerization (ROCOP) of LO/$CO_2$ with lactide and its derivative, dihexyllactide (diHLA), using a single monozinc catalyst [BDI-Zn-$\mu$-OAc] for the formation of an AB-type block copolymer, which complements nicely the recently published work of Williams et al. using a two-catalyst system for ABA block copolymer formation.[13] We study the details of copolymerization, both in one pot by the simultaneous addition of the monomers and by the

sequential addition of the monomers without changing the catalyst. Detailed microstructure characterization of the polymers, thermal properties and phase-separation behavior of the polymers was performed to prove the polymer architecture.

## RESULTS AND DISCUSSION

Terpolymerziation of trans-limonene oxide, (*D/L*)-lactide and $CO_2$ (one-pot ROCP) First, one-pot reactions of (*D/L*)-lactide (DLLA), trans-limonene oxide (LO), and $CO_2$ in the presence of a catalyst [(BDI)Zn-(μOAc)] were investigated to clarify the polymer structure in onepot reactions (**Scheme 1**). The feed ratio (LO/DLLA) was varied to explore the polymerization behaviour of lactide (DLLA) in the presence of LO (**Table S1†**). The polymer structure in onepot reactions was identified by $^{1}$H-NMR spectroscopy (**Fig. S1** and **S2†**). The NMR spectrum shows characteristic peaks from both types of repeat units. The peak at 5.06 ppm is distinct for the proton close to the carbonate group, marked in the red circle in Fig. S2†, originating from the ring opening of LO (r-LO). The multiplet at 5.20 ppm indicates the presence of ring-opened DLLA units (r-DLLA) in the copolymer. Determination of LO/LA conversion would need $CO_2$ pressure release and repressurizing, which would influence onepot reactions due to the highly sensitive reactants and the vulnerable catalytic system, so the polymer composition was focused upon. The polymer composition was determined by using the peak ratio of these two peaks. For DLLA/LO = 9/91 mol% in the feed, a polymer with the composition of 21 mol% r-DLLA and 79 mol% r-LO was identified by $^{1}$H-NMR spectroscopy. A copolymer prepared from a feed molar ratio of DLLA/LO = 17/83 mol% and a polymer with 39 mol% r-DLLA and 61 mol% r-LO could be obtained. Increasing the amount of DLLA in the feed increased the corresponding r-DLLA in the product. A systematic study by varying the feed molar ratio of the two components, DLLA and LO, also revealed that the amount of r-DLLA in the product was always higher than the amount used in the feed (**Table 1**, **Fig. S2†**). $^{13}$C-NMR also reveals the presence of both r-DLLA and r-LO units in the product (**Fig. S3†**).

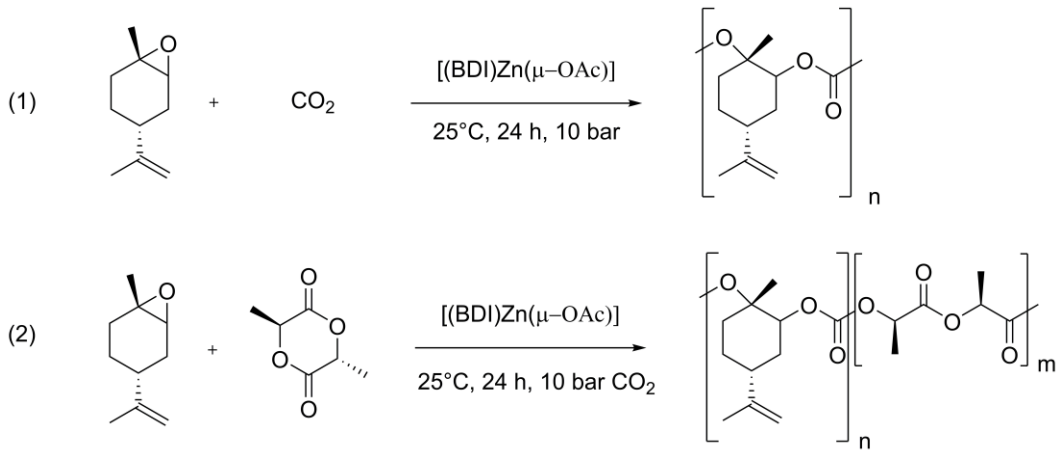


**Scheme 1** (1) PLimC is synthesized by using LO, $CO_2$, and the catalyst [(BDI)Zn-($\mu$-OAc)]. (2) DLLA and LO are reacted to synthesize a PLimC-*b*-PDLLA block copolymer in a one-pot reaction.

GPC measurements reveal high-molecular-weight polymers (~$M_n$ = 70–80 kDa) for all different polymer compositions (**Table 1**). All copolymer compositions show a small shoulder at higher molecular weights (**Fig. S4†).** This is due to the expected formation of a faster catalytic species of [(BDI)Zn-($\mu$-OAc)] that shows the typical expected GPC of PLimC.[15] The copolymerization product showed low molar mass dispersity. Thermogravimetric analysis (TGA) of copolymers reveals similar degradation steps for all the different copolymer compositions (~$T_{5\%}$ = 228 °C) except for polymers with 100 mol% PDLLA (~$T_{5\%}$ = 280 °C) (**Fig. S5†**). Focusing on differential scanning calorimetry (DSC) measurements for copolymerization products, all polymers showed two glass transition temperatures ($T_g$), close to the respective $T_g$ values of neat PLimC and PDLLA of around 122 °C and 50 °C, respectively (**Table 1**, **Fig. S6†**). The observation of two glass transition temperatures would lead to the assumption that during the one-pot reaction, either two homopolymers or incompatible PLimC and PDLLA block copolymers are formed. 2D NMR spectroscopy provided a way to distinguish between the two scenarios: formation of homopolymers or copolymers (**Fig. 1**). $^1$H–$^1$H-NOESY NMR analysis of the copolymer with a feed ratio of DLLA/LO = 34/ 66 mol% shows evidence for the formation of copolymers. The methyl group of PDLLA (H14) shows cross-peaks with PLimC related groups. In the lower field region, cross-peaks with

**Table 1** Overview of the synthesized copolymers by one-pot simultaneous polymerization of DLLA, LO and $CO_2$ in terms of feed ratio, polymer composition, molecular weight, and thermal properties.

| Sample | Feed Ratio DLLA:LO | Copolymer Composition[a] r-DLLA/r-LO | $M_n$[b] | $Đ$[b] | $T_{g1}$[c] | $T_{g2}$[c] | $T_{5\%}$[d] | $T_{max,1}$[d] |
|---|---|---|---|---|---|---|---|---|
| | [mol%] | [mol%] | [kDa] | | [°C] | [°C] | [°C] | [°C] |
| **1** | 9/91 | 21/79 | 75 | 1.18 | 122 | - | 225 | - |
| **2** | 17/83 | 39/61 | 75 | 1.18 | 124 | 48 | 235 | 257 |
| **3** | 23/77 | 41/59 | 77 | 1.19 | 123 | 49 | 232 | 260 |
| **4** | 29/71 | 54/46 | 80 | 1.24 | 124 | 50 | 224 | 257 |
| **5** | 34/66 | 60/40 | 72 | 1.26 | 121 | 51 | 222 | 257 |
| **6** | 77/23 | 99/1 | 45 | 1.64 | - | 48 | 229 | 254 |
| **7** | 91/9 | 100/0 | 75 | 1.18 | - | 46 | 280 | - |

[a]determined via integration of characteristic r-LO and r-DLLA protons ($CDCl_3$, 300 MHz) [b]GPC: $M_n$ and $Đ$ were determined by $CHCl_3$-GPC, calibrated with narrowly distributed polystyrene standards. [c]DSC: $T_g$ was determined from the second heating trace (scanning rate 10 K $min^{-1}$ under $N_2$ atmosphere). [d]TGA: $T_{5\%}$ was determined with a heating rate of 10 K $min^{-1}$ under $N_2$ atmosphere. [e]TGA: $T_{max,1}$ and $T_{max,2}$ were determined from the 1st derivative of the TGA trace.

characteristic PLimC protons (H5 and H8) can be identified. In the higher field region, cross-peaks with the PLimC ring system (H1, H2 and H5) can be observed. Also, the methyl group (H10) close to the carbonate interacts with the methyl group of the PDLLA block (**Fig. 1**). The observation of cross peaks is a strong hint for the bonding of PLimC and PDLLA units. A second experiment was performed to prove the formation of block copolymers. PLimC and PDLLA show different solubilities in THF. PLimC is not soluble in THF, whereas PDLLA shows good solubility. By using THF and multiple centrifugation steps, it should be possible to separate homopolymers from each other. After multiple centrifugation cycles, a 43 wt% THF-soluble fraction and a 57 wt% THF-insoluble fraction from crude polymers with a feed ratio of DLLA/LO = 34/ 66 mol% were obtained. The $^1$H-NMR analysis (**Fig. S7†**) of the two fractions shows peaks from both r-DLLA and r-LO in both fractions. As expected, the content of r-LO was higher in the THF-insoluble fraction (PDLLA/PLimC = 18 : 82 mol%), whereas the THF-soluble fraction showed more r-DLLA (PDLLA/PLimC = 87 : 13 mol%). DSC analysis (**Fig. S8†**) of the two fractions reveals a glass transition temperature ($\sim T_g$ =50 °C) close to that of the crude sample, which shows the presence of PDLLA in both fractions. Thermal investigation with TGA reveals mainly PLimC-dominated thermal degradation for the THF-insoluble

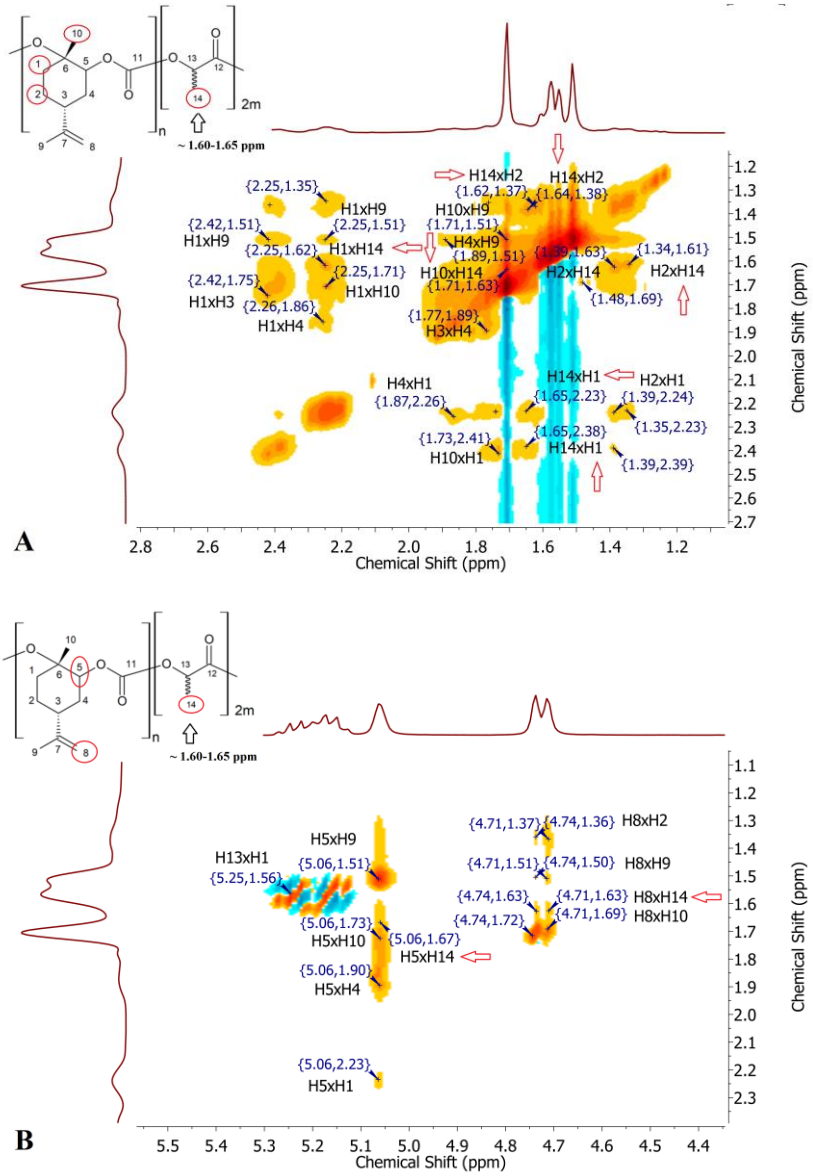


**Fig. 1** Two-dimensional $^{1}H$–$^{1}H$-NOESY NMR spectra of copolymers with a feed ratio of DLLA/LO = 34 : 66 mol% in $CDCl_3$. (A) High-field region (2.8–1.0 ppm) and (B) low-field region (4.4–5.5 ppm). The crosspeaks (marked in blue) are assigned to the corresponding protons (marked in black). Cross-peaks of ring-opened LO and DLLA are circled in red and highlighted with an arrow.

fraction, whereas the THF-soluble fraction is mainly dominated by the thermal degradation of PDLLA (**Fig. S9†**). The $CHCl_3$-GPC trace of the THF-insoluble fraction displays a monomodal curve with a small shoulder at a higher molecular weight (**Fig. S10†**). This resembles the $CHCl_3$-GPCtraces of the crude sample with a feed ratio of DLLA/LO = 34/66 mol%. The THF-soluble fraction shows a broad monomodal curve, which shows similarities to the copolymer with a nearly 100 mol% PDLLA content. Summarizing the obtained results leads to the conclusion that the formation of block copolymers during a one-pot reaction has happened. Using the knowledge of all experiments and the fact that the copolymer composition always

shows r-LO less in the copolymers compared to the feed, the presence of different types of copolymer chains with long and short sequences of PLimC can be confirmed in the product (**Fig. 2**). For the terpolymerization of (rac)- β-butyrolactone (BBL), cyclohexene oxide (CHO), and carbon dioxide utilizing a Lewis acid BDICF$_3$-Zn-N(SiMe$_3$)$_2$ catalyst, the tendency of polycarbonate formation by the reaction of an epoxide with CO2 over polyester formation was shown by Kernbichl et al.[21] In our case, most probably, the polymerization started by the ring opening of LO and its copolymerization with $CO_2$ for the formation of PLimC. As we used an excess of $CO_2$, it would lead to a carbonato chain end by the insertion of $CO_2$ into the Zn–O bond. Carbonato chain-ends, although weak like alkali carboxylate, can start ROP of lactide, as demonstrated by Kernbichl et al.[21]

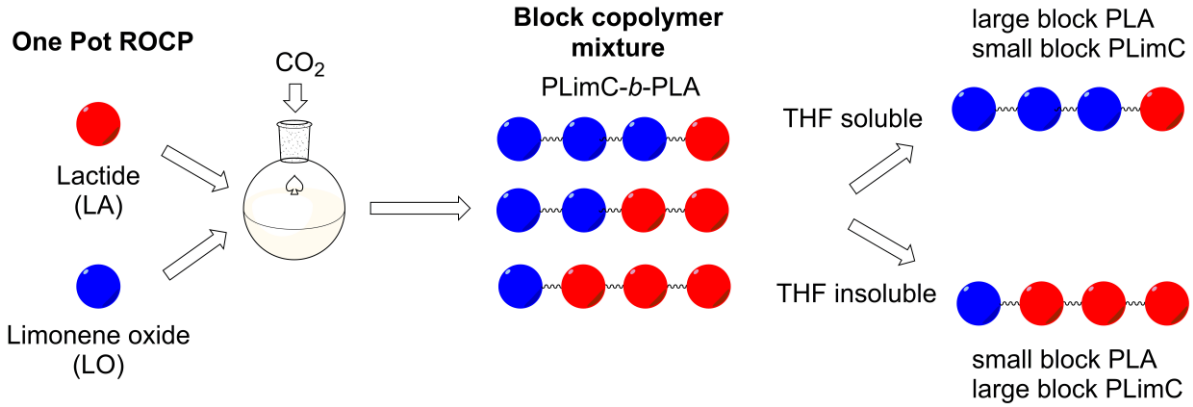


**Fig. 2** Schematic illustration of the mechanism of a one-pot ring-opening copolymerization of LA and LO.

In our case, most probably, the polymerization started by the ring opening of LO and its copolymerization with $CO_2$ for the formation of PLimC. As we used an excess of $CO_2$, it would lead to a carbonato chain end by the insertion of $CO_2$ into the Zn–O bond. Carbonato chain-ends, although weak like alkali carboxylate, can start ROP of lactide, as demonstrated by Kernbichl et al.[21] Once lactide starts polymerizing, it seems that the Zn–O–CH(CH$_3$)– chain-end does not support ring opening of LO.[5] Furthermore, the morphology of the copolymers was studied by transmission electron microscopy (TEM). According to the difference in their structures, PLimC and PDLLA should show incompatibility, and so microphase separation is expected for PLimC/PDLLA block copolymers. To address and emphasize the incompatibility of PLimC and PDLLA blocks, the Hansen solubility parameters (δ) of both blocks employing the group contribution method of Hoftyzer–van Krevelen (HVK)[22] were used, which resulted in $\delta = 17.6$ MPa$^{1/2}$ for PLimC and $\delta = 20.7$ MPa$^{1/2}$ for PDLLA. For morphological investigation,

we chose PLimC-*b*-PDLLA block copolymers with a composition of PDLLA/PLimC = 41/59 mol% and PDLLA/PLimC = 54/46 mol% because with a more symmetric composition, a lamellar morphology is predicted by the theoretical phase diagram[23] and mean-field theory.[24] The TEM samples were prepared by slowly casting thin films (thickness ca. 1 mm) of the copolymers from dichloromethane over 6 days, followed by vacuum drying at room temperature for 1 day. PLimC was selectively stained with $OsO_4$ vapor so that PDLLA (not stained by $OsO_4$) appeared bright in the dark, showing a PLimC matrix. Analysis of the TEM samples shows a mixture of spherical, cylindrical, hexagonally perforated lamellar structures and lamellar morphologies (**Fig. 3**, **Fig. S11–S14†**). To avoid the influence of the sample preparation, the samples were annealed to 140 °C for 3 days under nitrogen and measured again to verify a stable morphology. Crystallization of the lactide part can be excluded due to the use of PDLLA, which is amorphous and shows no melting/crystallization peaks in DSC (**Fig. S6†**). A mixture of different morphologies appears because different block copolymers of PLimC and PDLLA with different chain lengths are formed. With an increasing volume fraction of PDLLA ($f_{PLA}$), the morphology changes from a spherical to a lamellar morphology. This indicates the formation of block copolymers during a one-pot reaction with different chain lengths. Investigation of samples with a feed ratio with a higher amount of DLLA (PDLLA/PLimC = 60/40 mol%) also shows spherical, cylindrical, and lamellar morphologies and confirms the formation of block copolymers (**Fig. S14†**).

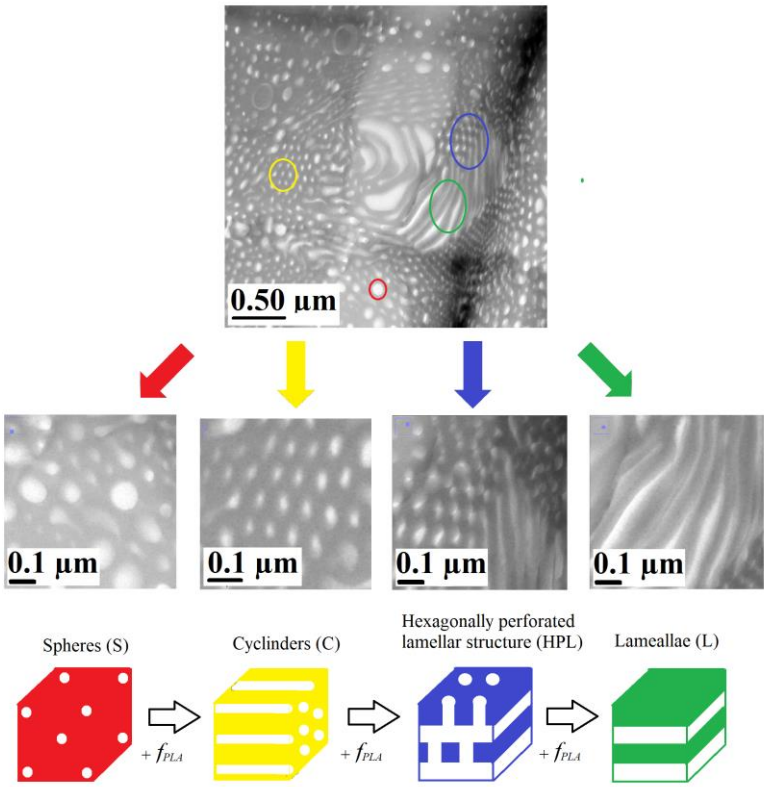


**Fig. 3** TEM micrographs of PLimC-*b*-PDLLA block copolymers (PLimC/ PDLLA = 59/41 mol%). The different morphologies are magnified and highlighted in color. PLimC is selectively stained with $OsO_4$ vapor.

### Sequential terpolymerziation of *trans*-limonene oxide, (*L*)- lactide and $CO_2$

To confirm the reactivity of chain-ends as observed during terpolymerization above in one pot, sequential living ringopening copolymerization (ROCOP) of LO, $CO_2$ and (*L*)-lactide (LLA) was investigated (**Scheme 2**). First, LO was copolymerized with CO2 in toluene to produce a block of PLimC. Afterward, (*L*)-lactide in toluene was added to produce the polymer, as investigated by $^{1}$H-NMR, and the corresponding second block of poly(*L*-lactide acid) (PLLA). The obtained protons for PLimC and PLLA could be identified **(Fig. 4**). The characteristic quartet for PLLA is located at 5.17 ppm. $^{13}$C-NMR spectroscopy also reveals the formation of PLimC and PLLA units in the copolymers (**Fig. S15**†). These experiments showed that block copolymerization of lactide is possible in sequential living ROCOP. GPC analysis of the obtained polymers showed high molecular-weight copolymers with ~$M_n$ = 50.000 Da (**Fig. S16**†). Thermal analysis with DSC reveals two glass transition temperatures as expected for block copolymers: PLimC: ($T_g$ = 121 °C) and PLLA: ($T_g$ = 56 °C) **(Fig. S17**†). A melting peak of PLLA can also be identified at $T_m$ = 173 °C. TGA analysis (**Fig. S18**†) of PLimC/PLLA copolymers synthesized by a sequential approach shows a similar decomposition temperature

to that observed for PLimC/PDLLA copolymers (~$T_{5\%}$ = 225 °C). The first derivative of the TGA trace shows two maxima (~$T_{5\%}$ = 228 °C) besides the polymer with 100 mol% PDLLA (~$T_{5\%}$ = 280 °C). The first derivative of the TGA trace shows one maximum that can be identified as the decomposition of PLimC (~$T_{max,1}$ = 257 °C). TEM analysis of PLimC-*b*-PLLA block copolymers reveals a spherical morphology for this block copolymer composition (**Fig. S19†**). This is expected because the content of PLLA (PLLA/PLimC = 29/71 mol%) in the block copolymer is lower in comparison with that in PLimC-*b*-PDLLA block copolymers. The sequential polymerization experiment also confirms the mechanism of formation of block copolymers in situ in one pot as described in the previous section.

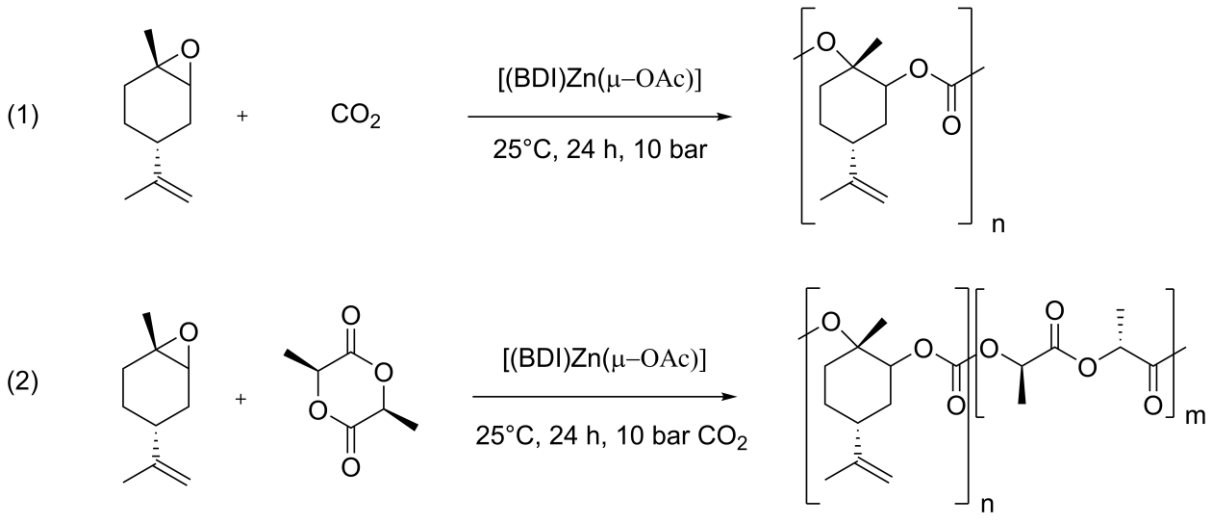


**Scheme 1** LLA and LO are reacted to synthesize a PLimC-*b*-PLLA block copolymer in a sequential ring-opening copolymerization.

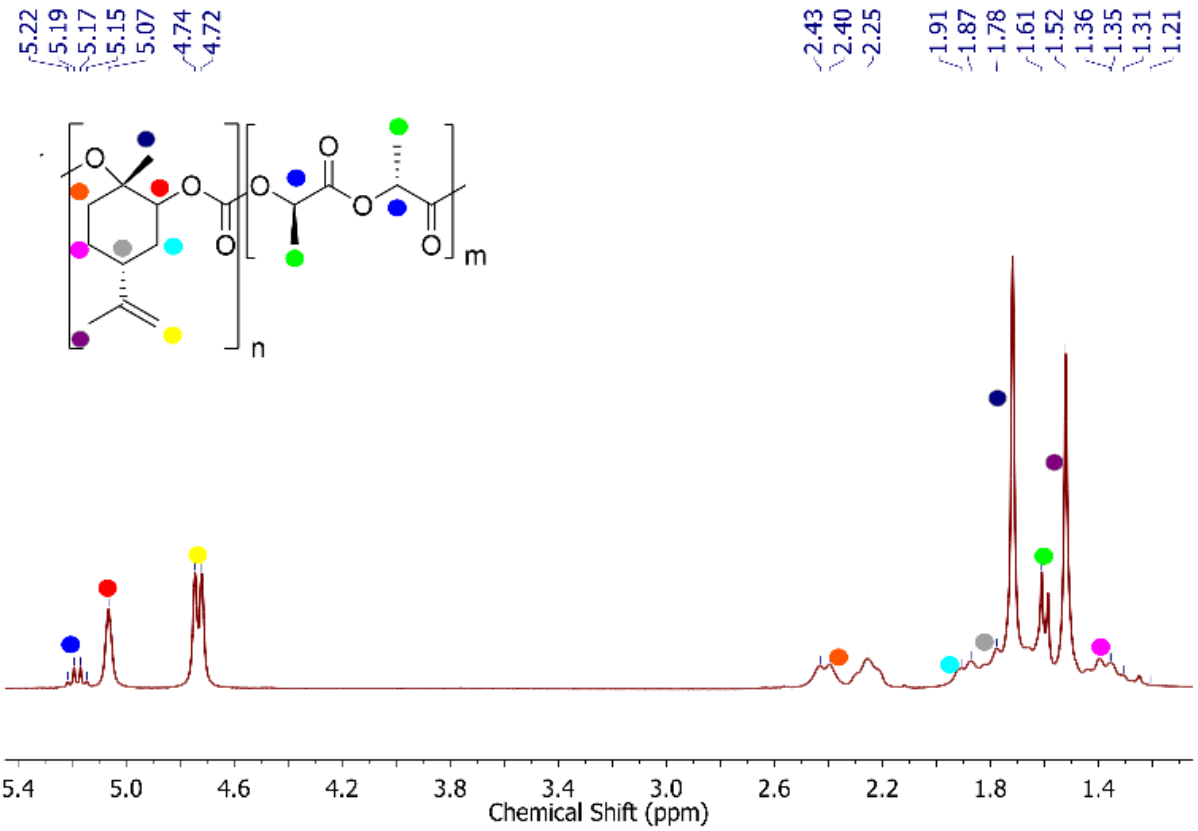


**Fig. 4** $^{1}$H-NMR (300 MHz) of PLimC-*b*-PLLA block copolymer with PLimC/PLLA = 71/29 mol% in $CDCl_3$.

## Terpolymerziation of *trans*-limonene oxide, hexyl-substituted lactide and $CO_2$ (sequential ROCP)

The studies were extended to the copolymerization of LO/$CO_2$ with other substituted bio-based cyclic esters, such as dihexylsubstituted lactide (diHLA). This served two purposes: first, the universality of the reaction of the growing PLimC chains with cyclic esters is confirmed, and second, the copolymers with different thermal transitions and physical characteristics could be generated. PLimC's mechanical properties in terms of elongation at break or the impact strength can be improved.[21] Bio-based additives (e.g.,, ethyl oleate)[21] could be used to overcome these limitations, though leaching or aging of plasticizers can occur. A way to improve the mechanical properties of PLimC without the use of additives or plasticizers would be copolymerization, which was investigated by Williams et al. by forming ABA-type block copolymers.[13] The use of diHLA is expected to provide block copolymers with an incompatible high-$T_g$ block of PLimC and low-$T_g$ block of polyester made by ROP of diHLA, improving the brittle characteristics. We synthesized dihexyl-substituted lactide (diHLA) according to a

procedure of Trimaille et al.[17–19] (**Scheme 3**). The monomer structure was confirmed by $^1$H-NMR spectroscopy (**Fig. S20†**). The copolymerization was carried out by first preparing the PLimC block followed by the polymerization of diHLA in a sequential manner. Two different copolymerizations were carried out by changing the feed ratios (**Table S2†**). $^1$H-NMR spectroscopy shows the characteristic peaks originating from both PLimC and PdiHLA (**Fig. 5**, **Fig. S21** and **S22†**). The molecular weight (~$M_n$ = 35.000 Da) and polydispersity (~$Đ$ = 1.3) are comparable to PLimC-*b*-PLLA block copolymers (**Fig. S23†**). Since the GPC curves were not unimodal, it is not appropriate to determine $M_n$ or $Đ$ from these curves, but despite the nonunimodility and low molar mass, dispersity is indicative of the control over polymerization. The copolymer with PLimC/diHLA = 62/38 mol% showed two glass transition temperatures: the soft block from polyester at −39 °C and the hard PLimC block at 106 °C (**Fig. S24†**). The decomposition of PLimC-*b*-PdiHLA copolymers occurs in the same temperature region as that of PLimC-b-PLA copolymers (~$T_{5\%}$ = 225 °C). The decomposition temperatures of PLimC and PdiHLA ($T_{max,1}$ = 254 °C and $T_{max,2}$ = 300 °C) are analogous to those of PLimC-*b*-PLA copolymers (**Fig. S25†**). The rubber-like properties and transparency were obtained from PLimC-b-PdiHLA block copolymers (**Fig. 6**). By using block copolymerization of bio-based and biodegradable PdiHLA, the mechanical properties of PLimC can be influenced. Also, the formation of PdiHLA-PLimC-PdiHLA triblocks seems possible with ROCP. This would also allow the synthesis of bio-based thermoplastic elastomers in the future with detailed characterization of the physical properties.

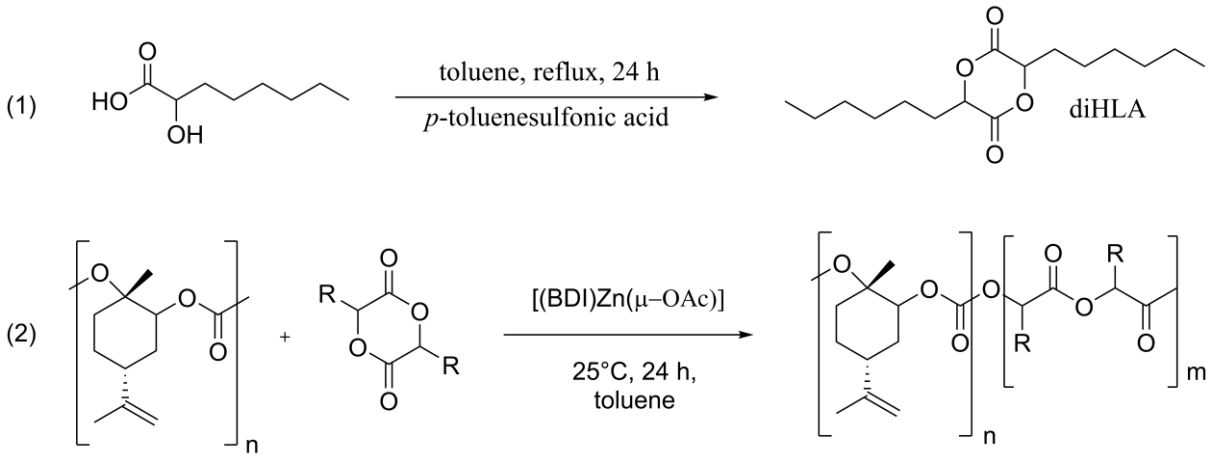


**Scheme 3** (1) Synthesis of diHLA via condensation reactions starting from 2-hydroxyoctanoic acid. (2) Synthesis of poly(limonene carbonate)-*block*-poly(diHLA).

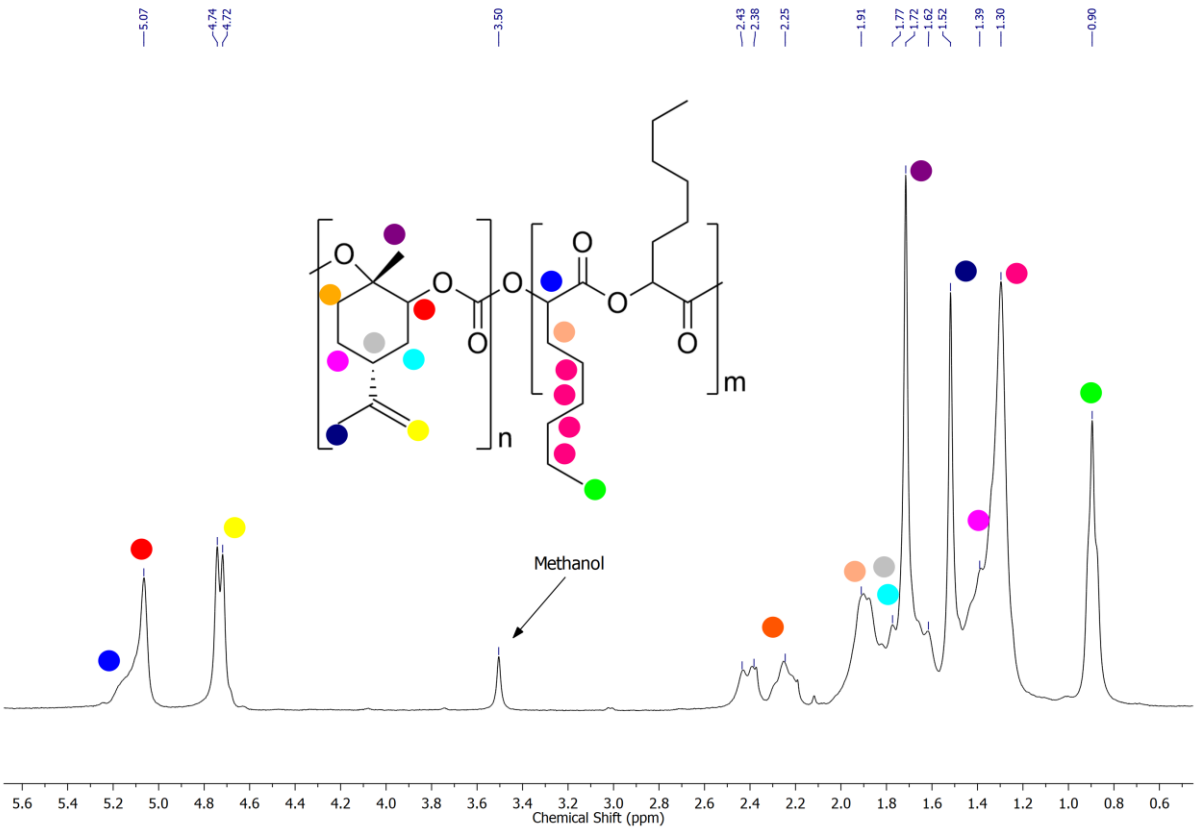


**Fig. 5** $^{1}$H-NMR (300 MHz) spectra of the PLimC-*b*-PdiHLA block copolymer (PLimC/PdiHLA = 50/50 mol%) in $CDCl_3$.

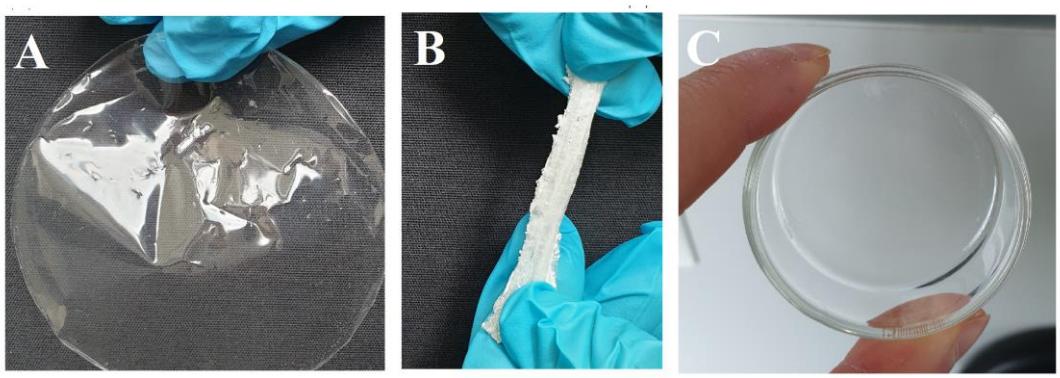


**Fig. 6** A) PLimC-*b*-PdiHLA block copolymer (PLimC/PdiHLA/ = 62/38 mol%). B) PLimC-*b*-PdiHLA block copolymer (PLimC/PdiHLA = 29/71 mol%). C) PLimC-*b*-PdiHLA block copolymer (PLimC/PdiHLA = 50/50 mol%).

## CONCLUSION

In this work, we demonstrated the living ring-opening copolymerization of lactides, trans-limonene oxide, and $CO_2$ using a catalyst [(BDI)Zn-($\mu$-OAc)] to synthesize poly(limonene carbonate)-*block*-poly(lactide) copolymers. Copolymerization studies were carried out by both simultaneous and sequential additions of monomers. We investigated the one-pot reaction of (*D/L*)-lactide and trans-limonene oxide and studied the morphology with TEM. We showed that block copolymers form in one-pot reactions of trans-limonene and cyclic diesters (e.g., lactide). The sequential living ring-opening copolymerization of trans-limonene and (*L*)-lactide was also explored and demonstrated. Additionally, we used living ring-opening copolymerization to gain access to poly(limonene carbonate)-*block*-polyesters with promising rubber-like properties by the use of dihexyl-substituted lactides. The use of bio-based and biodegradable polymers is unavoidable for a sustainable future in terms of packaging or even everyday applications. Poly(limonene carbonate) and polylactide as bio-based materials can contribute to a "greener" future, and so, their modification and improvement are essential. With living ring-opening copolymerization of trans-limonene and cyclic diesters (e.g.,, lactides), we showed an elegant way to modify and tune the properties of poly(limonene carbonate), which would help to make poly(limonene carbonate) more relevant for everyday applications. Future studies will be devoted towards mechanical and biodegradation characterization.

## EXPERIMENTAL

### Materials and methods

All reactions were carried out under an inert atmosphere ($N_2$ and Ar). The monomer trans-limonene oxide and the catalyst [(BDI)Zn-($\mu$-OAc)] were synthesized according to the literature procedure.[5] *D,L*-Lactide and *L*-lactide were purchased from Sigma-Aldrich and recrystallized from EtOAc. A procedure of Trimaille et al. was used to synthesize dihexyl-substituted lactides.[18–20] 2-Hydroxyoctanoic acid, p-toluenesulfonic acid, and 2-bromoacetyl bromide were obtained from TCI. Solvents were obtained from Carl Roth and purified with rotary evaporation. THF, triethylamine, and toluene were dried and distilled before use for synthesis or polymerization. Differential scanning calorimetry (DSC) was performed with a DSC 204 F1 Phoenix system (Netzsch) with a heating rate of 10 K $min^{-1}$ under a $N_2$ atmosphere. For thermogravimetric measurements, a TGA instrument (TG 209 F1 Libra) from Netzsch was used at a heating rate of 10 K $min^{-1}$ under a $N_2$ atmosphere. For $CHCl_3$-GPC analyses of polymers, an Agilent 1200 system equipped with an SDV precolumn (particle size 5 µm; PSS

Mainz), an SDV linear XL column (particle size 5 µm, PSS Mainz) and a refractive index detector (Agilent Technologies 1260 Infinity) was used. Toluene (HPLC grade) was used as an internal standard. $CHCl_3$ (HPLC grade) was used as a solvent at a flow rate of 0.5 mL $min^{-1}$ at room temperature. NMR spectra were recorded on a Bruker Avance 300 NMR system operating at 300 MHz/75 MHz frequency at RT using deuterated chloroform ($CDCl_3$) as a solvent. Chemical shifts δ are indicated in parts per million (ppm) with respect to residual solvent signals. TEM measurements were performed with a Zeiss CEM902 (Zeiss Microscopy, Jena/Oberkochen, Germany) energy-filtering transmission electron microscope (EFTEM) operating at an acceleration voltage of 80 kV. For cryomicrotomy of block copolymers, a Leica EM VC7 microtome was used. The ultrathin sections were stained using $OsO_4$. A steel autoclave (miniclave steel Typ 3) from Büchi was used for the polymerizations. Megafuge 16R from Heraeus was used for centrifugation.

**Synthesis of poly(limonene carbonate-*block*-poly((*D/L*)-lactide)) (one-pot ROCP)**

The following procedure should be a general procedure for the synthesis of poly(limonene carbonate-block-poly((*D/L*)-lactide) in a one-pot reaction. An oven-dried steel autoclave with a stirring bar was used for the polymerization reactions. In a glovebox, the catalyst [(BDI)Zn-(*µ*-OAc)] (24.2 mg, 51.9 µmol) was added to a steel autoclave. Additionally, *D,L*-lactide (Table S1†) was added to the autoclave. Following this, *trans*-limonene oxide (3 ml) was added. In a procedure in which the amount of LA exceeds the 1 : 1 ratio, dried THF was used to dissolve the LA completely. Consequently, the autoclave was pressurized with $CO_2$ (25 bar), and the reaction mixture was stirred for 24 h. The resulting mixture was dissolved in dichloromethane (60 ml) and precipitated in MeOH (600 ml). To purify the resulting polymer, the polymer was dissolved again in dichloromethane and precipitated again in MeOH. Afterward, the polymer was dried in a vacuum for 24 h.

**Synthesis of poly(limonene carbonate)-*block*-poly(*L*-lactide) (sequential ROCP)**

The following procedure should be a general procedure for the synthesis of poly(limonene carbonate)-*block*-poly(*L*-lactide) and poly(limonene carbonate)-*block*-poly(diHLA) in a sequential ROCP. An oven-dried steel autoclave with a stirring bar was used for the polymerization reactions. In a glovebox, the catalyst [(BDI)Zn-(*µ*-OAc)] (19.1 mg, 40.96 µmol) was added to a steel autoclave. Following this, *trans*-limonene oxide (3 ml) was added in 15 ml of toluene to the steel autoclave. Consequently, the autoclave was pressurized with $CO_2$ (25 bar), and the reaction mixture was stirred for 24 h. Subsequently, 650 mg of *L*-lactide/diHLA

in toluene (15 ml) was added to the autoclave under an inert atmosphere (Table S2†). Afterward, the reaction mixture was again pressurized with $CO_2$ (25 bar) and then stirred for 24 h. The resulting mixture was dissolved in dichloromethane (60 ml) and precipitated in MeOH (600 ml). To purify the resulting polymer, the polymer was dissolved again in dichloromethane and precipitated in MeOH again. Afterward, the polymer was dried in a vacuum for 24 h.

**Polymer fractionation**

For the fractionation of polymers, 1 g of the block copolymer mixture with a feed ratio of DLLA/LO = 34 : 66 mol% was dissolved in THF (150 mL). The obtained dispersion was stirred for 5 d at RT. Afterwards, it was centrifuged (10.000 $min^{-1}$) for 30 min at RT. The overhanging solution was decanted, and the remaining solid was dissolved again in THF. The procedure was repeated three times. The THF-soluble and the THF-insoluble fractions were dried in a vacuum for 24 h before characterization.

CONFLICTS OF INTEREST

The authors declare no conflicts of interest.

**Acknowledgements**

We would like to thank Carmen Kunert (MCII, University of Bayreuth) for sample preparation and conducting the TEM measurements. We gratefully acknowledge the use of equipment and assistance offered in the Keylab “Electron and Optical Microscopy” of the Bavarian Polymer Institute at the University of Bayreuth. The project has received funding from the European Union’s Horizon 2020 research and innovation programme under Marie Skłodowska-Curie grant agreement no. 860720.

NOTES AND REFERENCES

1 (a) D. Schneiderman and M. A. Hillmyer, Macromolecules, 2017, 50, 3733–3749; (b) X. Zhang, M. Fevre, G. O. Jones and R. M. Waymouth, Chem. Rev., 2018, 118, 839–885; (c) Y. Zhu, C. Romain and C. Williams, Nature, 2016, 540, 354–362; (d) M. Winkler, C. Romain, M. A. R. Meier and C. K. Williams, Green Chem., 2015, 17, 300–306.

2 C. M. Byrne, S. D. Allen, E. B. Lobkovsky and G. W. Coates, J. Am. Chem. Soc., 2004, 126, 11404–11405.

3 (a) C. Li, R. J. Sablong and C. Koning, Eur. Polym. J., 2015, 67, 449–458; (b) C. Li, R. J. Sablong and C. Koning, Angew. Chem., 2016, 128, 11744–11748.

4 S. J. Poland and D. J. Darensbourg, Green Chem., 2017, 19, 4990–5011.

5 O. Hauenstein, M. Reiter, S. Agarwal, B. Rieger and A. Greiner, Green Chem., 2016, 18, 760–770.

6 L. Peña Carrodeguas, J. González-Fabra, F. Castro-Gómez, C. Bo and A. W. Kleij, Chemistry, 2015, 21, 6115–6122.

7 C. Martín and A. Kleij, Macromolecules, 2016, 49, 6285– 6295.

8 O. Hauenstein, S. Agarwal and A. Greiner, Nat. Commun., 2016, 7, 11862.

9 J. Bailer, S. Feth, F. Bretschneider, S. Rosenfeldt, M. Drechsler, V. Abetz, H. Schmalz and A. Greiner, Green Chem., 2019, 21, 2266.

10 (a) O. Hauenstein, Md. M. Rahman, M. Elsayed, R. KrauseRehberg, S. Agarwal, V. Abetz and A. Greiner, Adv. Mater. Technol., 2017, 2, 1700026; (b) T. Stößer, C. Li, J. Unruangsri, P. Saini, R. Sablong, M. Meier, C. Williams and C. Koning, Polym. Chem., 2017, 8, 6099–6105.

11 (a) F. Parrino, A. Fidalgo, L. Palmisano, L. M. Ilharco, M. Pagliaro and R. Ciriminna, ACS Omega, 2018, 3, 4884– 4890; (b) M. Pagliaro, Chim. Oggi, 2018, 36(2), 57–58.

12 S. Neumann, L.-C. Leitner, H. Schmalz, S. Agarwal and A. Greiner, ACS Sustainable Chem. Eng., 2020, 8, 6442–6448.

13 L. P. Carrodeguas, T. T. D. Chen, G. L. Gregory, G. S. Sulley and C. K. Williams, Green Chem., 2020, 3, e1700782.

14 Y. Baimark, W. Rungseesantivanon and N. Prakymoramas, e-Polym., 2020, 20, 423–429.

15 R. Auras, Poly(lactic acid). Synthesis, structures, properties, processing, and applications, Wiley, Hoboken, NJ, 2010.

16 S. M. Li, H. Garreau and M. Vert, J. Mater. Sci.: Mater. Med., 1990, 1, 123–130.

17 T. Trimaille, R. Gurny and M. Möller, J. Biomed. Mater. Res., Part A, 2007, 80, 55–65.

18 T. Trimaille, M. Möller and R. Gurny, J. Polym. Sci., Part A: Polym. Chem., 2004, 42, 4379–4391.

19 T. Trimaille, K. Mondon, R. Gurny and M. Möller, Int. J. Pharm., 2006, 319, 147–154.

20 A. Chauvel and G. Lefebvre, Petrochemical processes: technical and economic characteristic: Major oxygenated, chlorinated and nitrated derivates, technical and economic characteristics, Éditions Technip, Paris, 1989.

21 S. Kernbichl, M. Reiter, F. Adams, S. Vagin and B. Rieger, J. Am. Chem. Soc., 2017, 139, 6787–6790.

22 (a) Hansen Solubility Parameters. A User's Handbook, Taylor and Francis, Hoboken, 2nd edn, 2012; (b) D. W. van Krevelen and K. T. Nijenhuis, Properties of polymers. Their correlation with chemical structure; their numerical estimation and prediction from additive group contributions, Elsevier, Amsterdam, 4th edn, 2009; (c) E. Meaurio, E. Sanchez Rexach, E. Zuza, A. Lejardi, A. d. P. Sanchez-Camargo and J.-R. Sarasua, Polymer, 2017, 113, 295–309.

23 H. Feng, X. Lu, W. Wang, N.-G. Kang and J. W. Mays, Polymers, 2017, 9(10), 494. 24 K. R. Shull and E. J. Kramer, Macromolecules, 1990, 23, 4769–4779.

Electronic Supplementary Information

# Sustainable block copolymers of biodegradable polylactides and bio-based poly(limonene carbonate)

Simon Neumann,[a] Sophia Däbritz,[a] Sophie Fritze,[a] Lisa-Cathrin Leitner,[a] Andreas Greiner[a,b] and Seema Agarwal[a,b]*

[a] University of Bayreuth, Macromolecular Chemistry II
Universitätsstraße 30, 95440 Bayreuth, Germany
E-mail: seema.agarwal@uni-bayreuth.de

[b] University of Bayreuth, Bavarian Polymer Institute (BPI), Universitätsstraße 30, 95440 Bayreuth, Germany

## Terpolymerziation of *trans*-limonene-oxide, (*D/L*)-lactide and $CO_2$ (One Pot ROCP)

**Table S5.** Experimental details of one-pot simultaneous polymerization of DLLA, LO and $CO_2$ using [(BDI)Zn-(μ-OAc)] catalyst.

| Lactide | Feed ratio | Polymer composition | Lactide | | LO | | Catalyst | THF/ Toluene | Yield | Yield |
|---|---|---|---|---|---|---|---|---|---|---|
| | DLLA/ LO | r-DLLA /r-LO | m | n | V | n | m | | | |
| | mol% | mol% | mg | mmol | mL | mmol | mg | % | % | g |
| **D/L** | 9/91 | 21/79 | 264 | 1.8 | 3.0 | 18 | 24 | - | 75 | 2.76 |
| **D/L** | 17/83 | 39/61 | 538 | 3.7 | 3.0 | 18 | 24 | - | 76 | 2.90 |
| **D/L** | 23/77 | 41/59 | 792 | 5.5 | 3.0 | 18 | 24 | - | 79 | 3.90 |
| **D/L** | 29/71 | 54/46 | 1055 | 7.3 | 3.0 | 18 | 24 | - | 82 | 3.33 |
| **D/L** | 34/66 | 60/40 | 1318 | 9.1 | 3.0 | 18 | 24 | - | 82 | 3.42 |
| **D/L** | 77/23 | 99/1 | 1318 | 9.1 | 0.44 | 2.7 | 24 | 12 | 56 | 0.66 |
| **D/L** | 91/9 | 100/0 | 1318 | 9.1 | 0.15 | 0.9 | 24 | 12 | 7 | 0.06 |
| **L** | 20/80 | 29/71 | 650 | 4.5 | 3.0 | 18 | 19 | 30 | 72 | 2.77 |

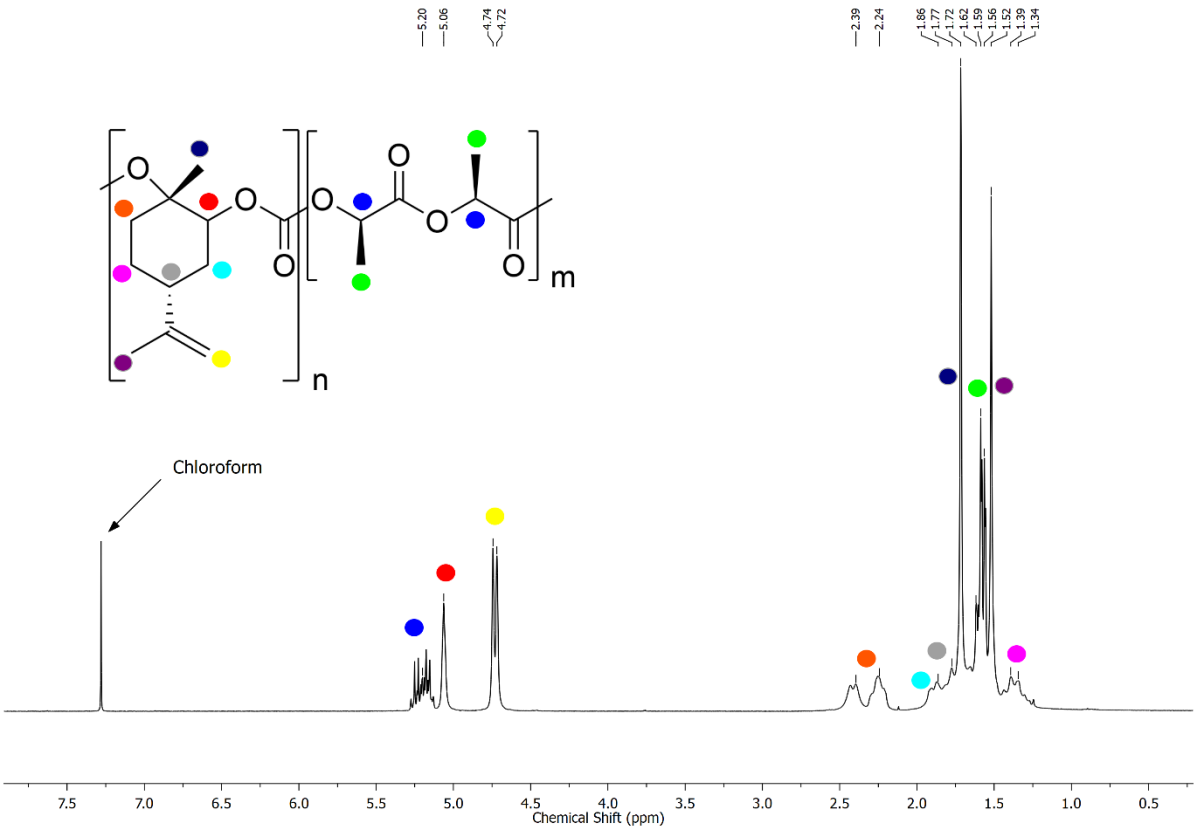


**Fig. S43** $^{1}$H-NMR (300 MHz) of copolymer prepared from DLLA:LO = 29/71 mol% (entry 4, Table 1) in the feed, measured in $CDCl_3$.

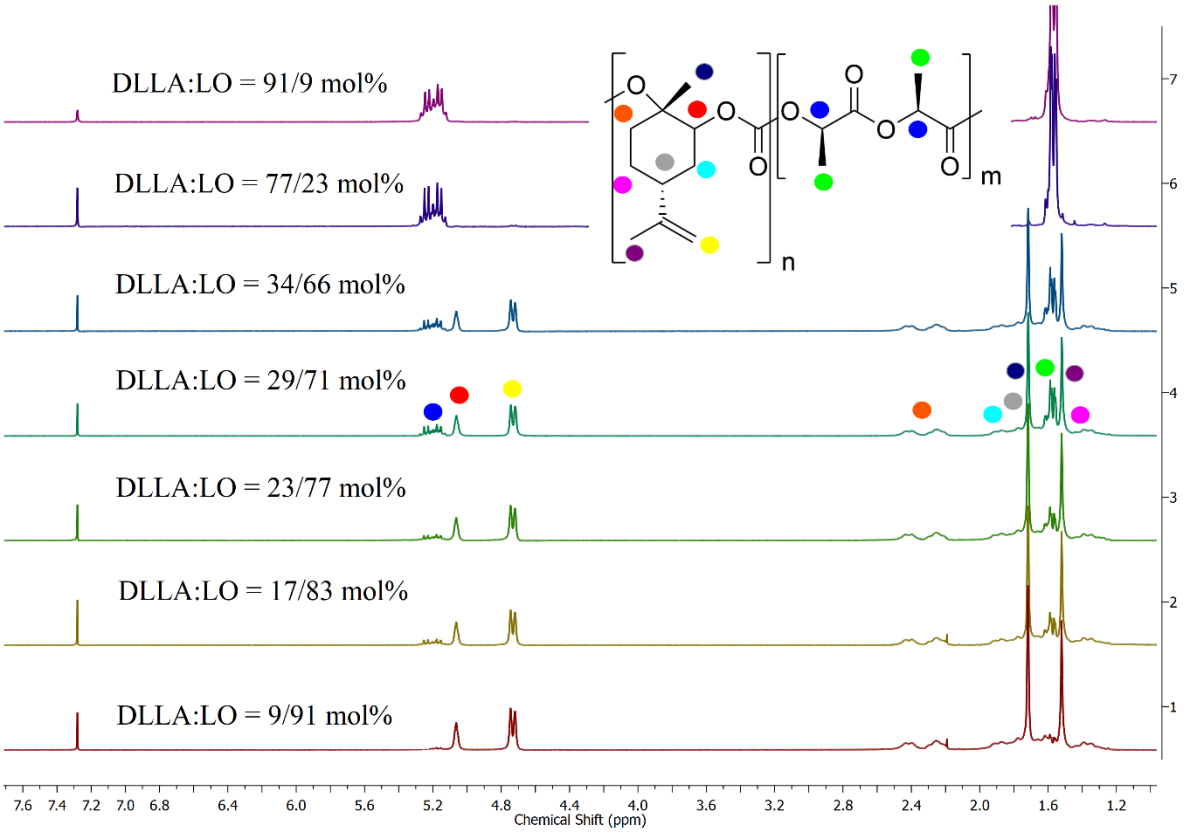


**Fig. S2** $^{1}$H-NMR (300 MHz) spectra of copolymer prepared from different molar ratio of DLLA and LO-$CO_2$ in the feed (Table 1), measured in $CDCl_3$.

$^{1}$H-NMR (300 MHz, $CDCl_3$): δ = 5.15-5.28 (m, 1H, C(13)-H), 5.06 (s, 1H, C(5)-H), 4.71-4.75 (d, *J = 9 Hz*, C(8)-$H_2$), 2.21-2.43 (m, 2H, C(1)-$H_2$), 1.86-1.91 (m, 2H, C(4)-$H_2$), 1.75-1.76 (m, 1H, C(3)-H), 1.69-1.73 (m, 3H, C(10)-$H_3$), 1.56-1.65 (m, 3H, C(14)-$H_3$), 1.50-1.52 (m, 3H, C(9)-$H_3$), 1.34-1.44 (m, 2H, C(2)-$H_2$) ppm.

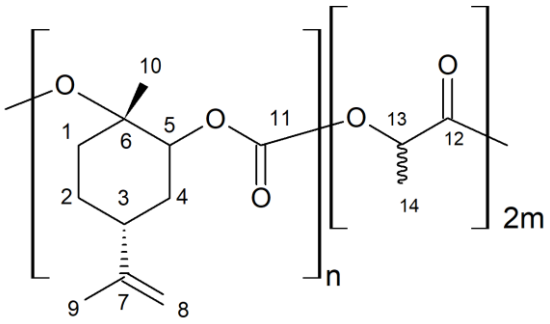

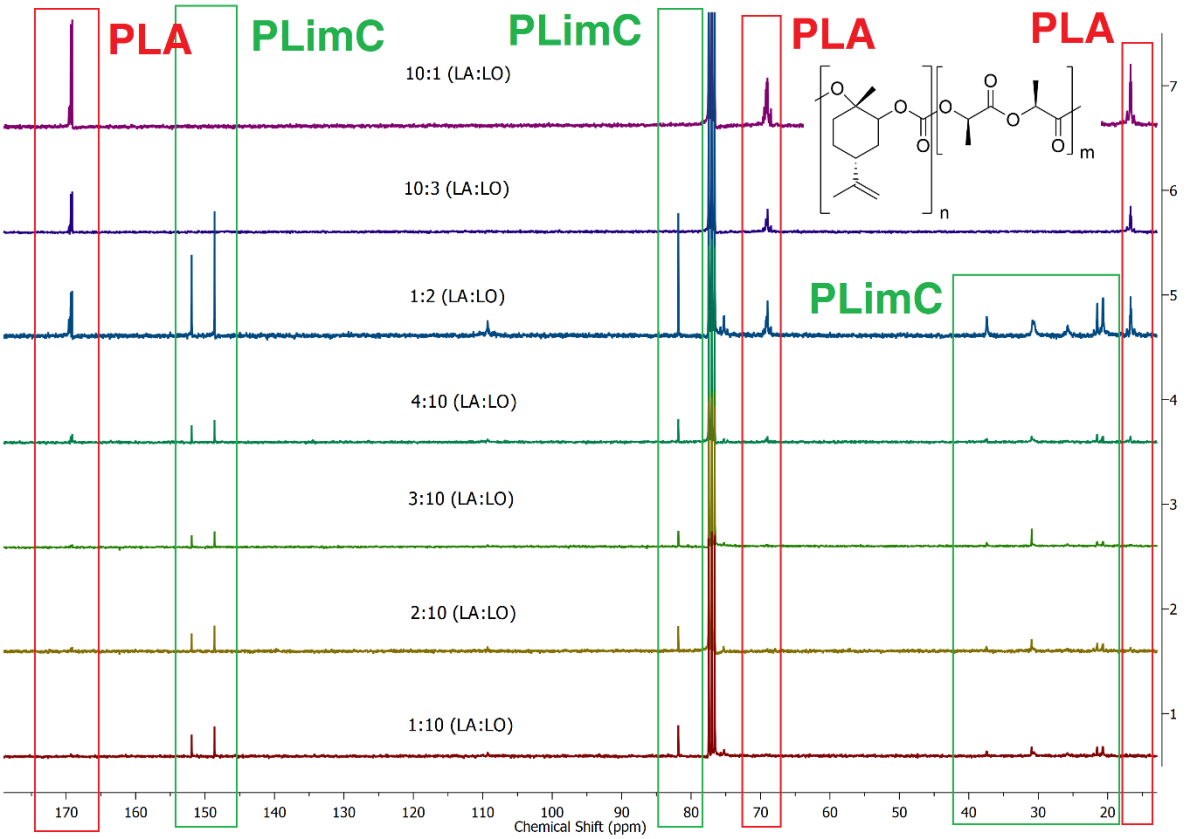


**Fig. S3** $^{13}$C-NMR spectra ($CDCl_3$, 75 MHz) of copolymers of DLLA and LO-$CO_2$ with different feed ratios.

$^{13}$C-NMR (300 MHz, $CDCl_3$): δ = 169.13 (C12), 151.92 (C11), 148.63 (C8), 109.3 (C7), 81.83 (C6), 75.32 (C5), 68.98 (C13), 37.43 (C3), 30.96 (C1), 21.54 (C4), 20.84 (C2), 20.65 (C10), 20.59 (C9), 16.07 (C14) ppm.

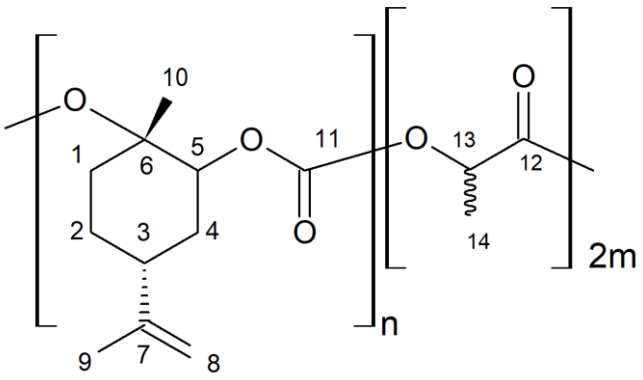

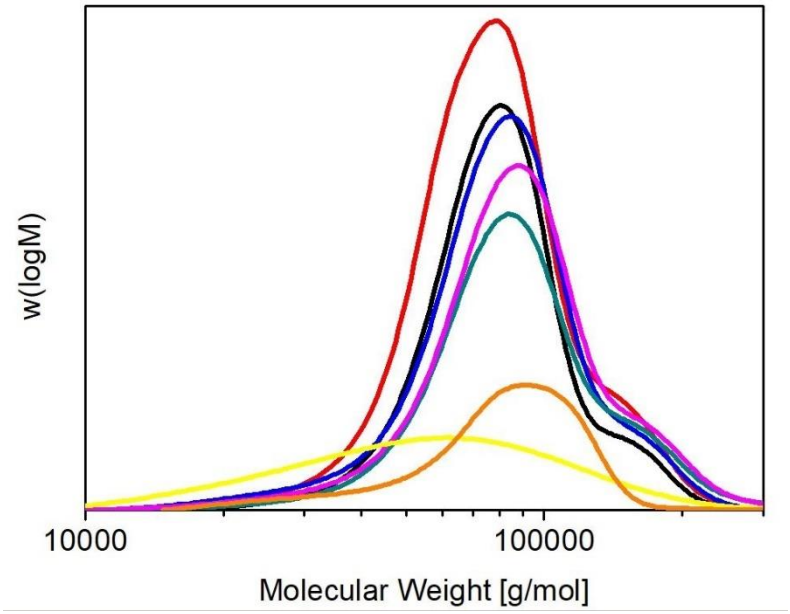


**Fig. S4** $CHCl_3$-GPC traces of copolymers of DLLA and LO-$CO_2$ with different feed ratios. Molecular weight ($M_n$) and dispersity ($Đ$) were determined from these curves cannot be taken precisely due to the non-unimodal nature of the curves. DLLA:LO = 9/91 mol% (black), DLLA:LO = 17/83 mol% (red), DLLA:LO = 23/77 mol% (blue), DLLA:LO = 29/71 mol% (green), DLLA:LO = 34/66 mol% (pink), DLLA:LO = 77/23 mol% (yellow), ), DLLA:LO = 91/9 mol% (orange).

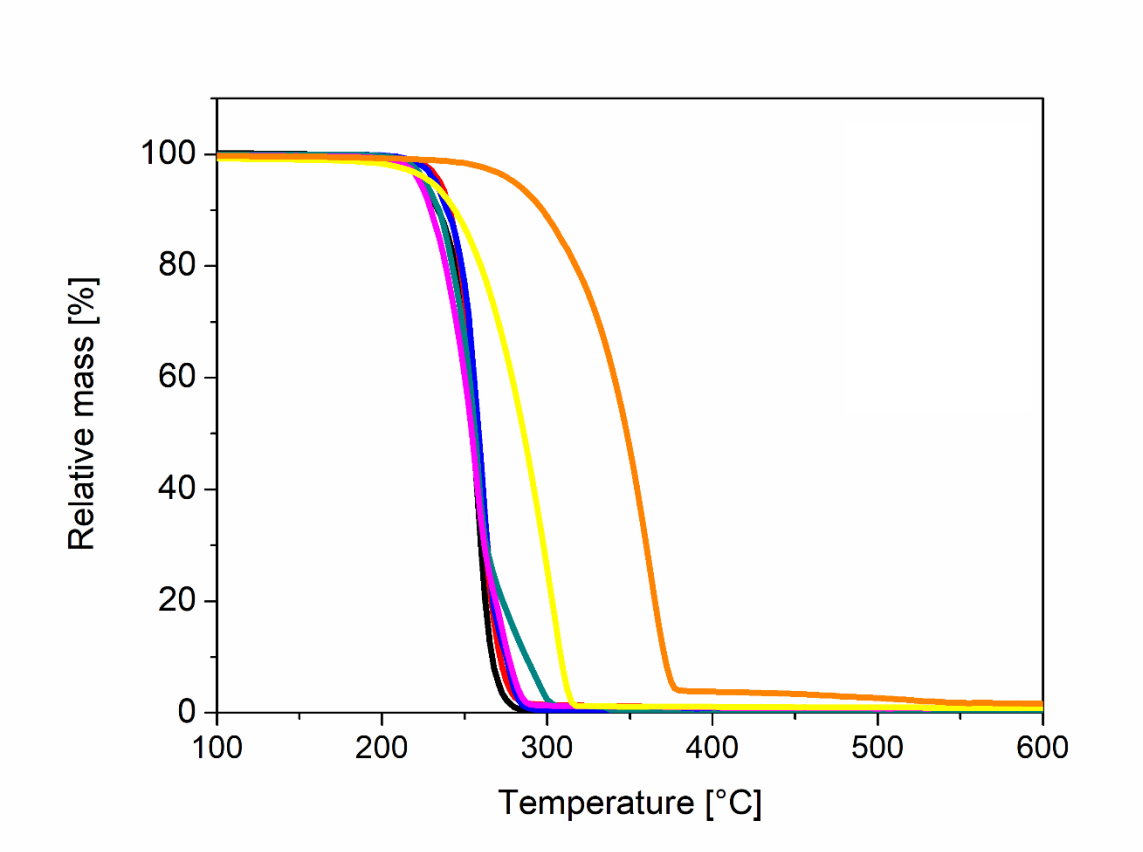


**Fig. S5** TGA thermograms of copolymers of DLLA and LO-$CO_2$ with different feed ratios, measured under nitrogen with 10K/min. DLLA:LO = 9/91 mol% (black), DLLA:LO = 17/83 mol% (red), DLLA:LO = 23/77 mol% (blue), DLLA:LO = 29/71 mol% (green), DLLA:LO = 34/66 mol% (pink), DLLA:LO = 77/23 mol% (yellow), ), DLLA:LO = 91/9 mol% (orange).

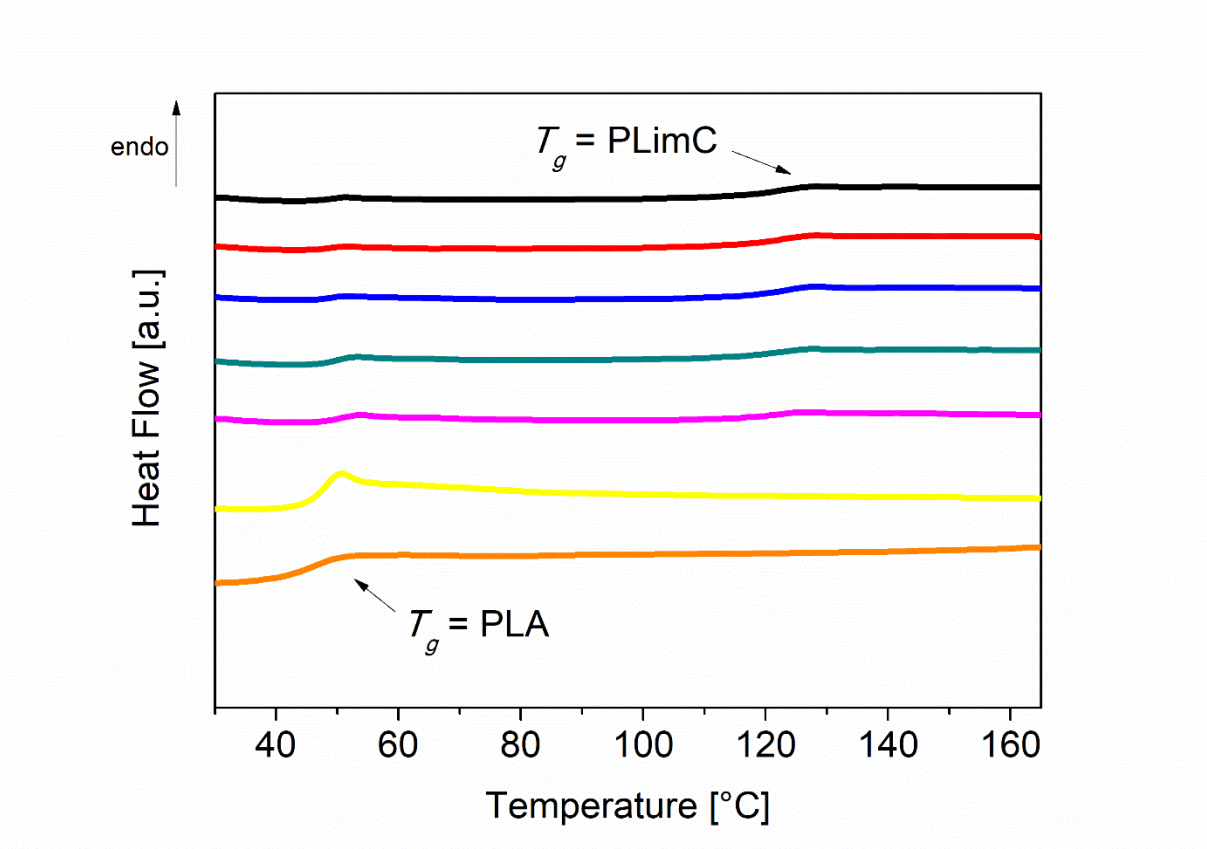


**Fig. S6** DSC thermograms of copolymers of DLLA and LO-$CO_2$ with different feed ratios The displayed traces correspond to the second heating curve measured at 10 K $min^{-1}$ under nitrogen. DLLA:LO = 9/91 mol% (black), DLLA:LO = 17/83 mol% (red), DLLA:LO = 23/77 mol% (blue), DLLA:LO = 29/71 mol% (green), DLLA:LO = 34/66 mol% (pink), DLLA:LO = 77/23 mol% (yellow), ), DLLA:LO = 91/9 mol% (orange).

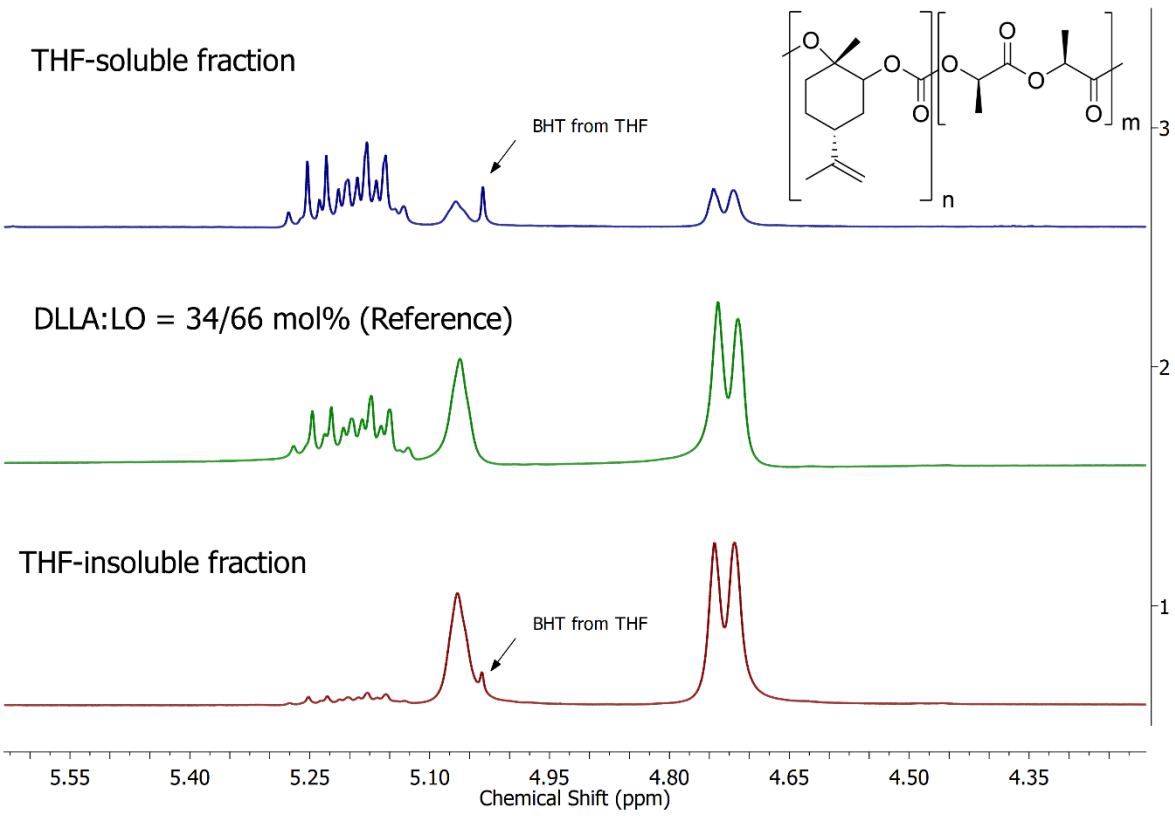


**Fig. S7** $^{1}$H-NMR spectrum ($CDCl_3$, 300 MHz) of copolymers (DLLA/ LO = 34/66 mol%) designated as reference in the figure) and the corresponding $^{1}$H-NMR spectra of THF-soluble fraction and THF-insoluble fraction. Copolymer composition: DLLA/LO mol%: Reference: 60/40; THF soluble fraction: 87/13; THF insoluble fraction: 18/82.

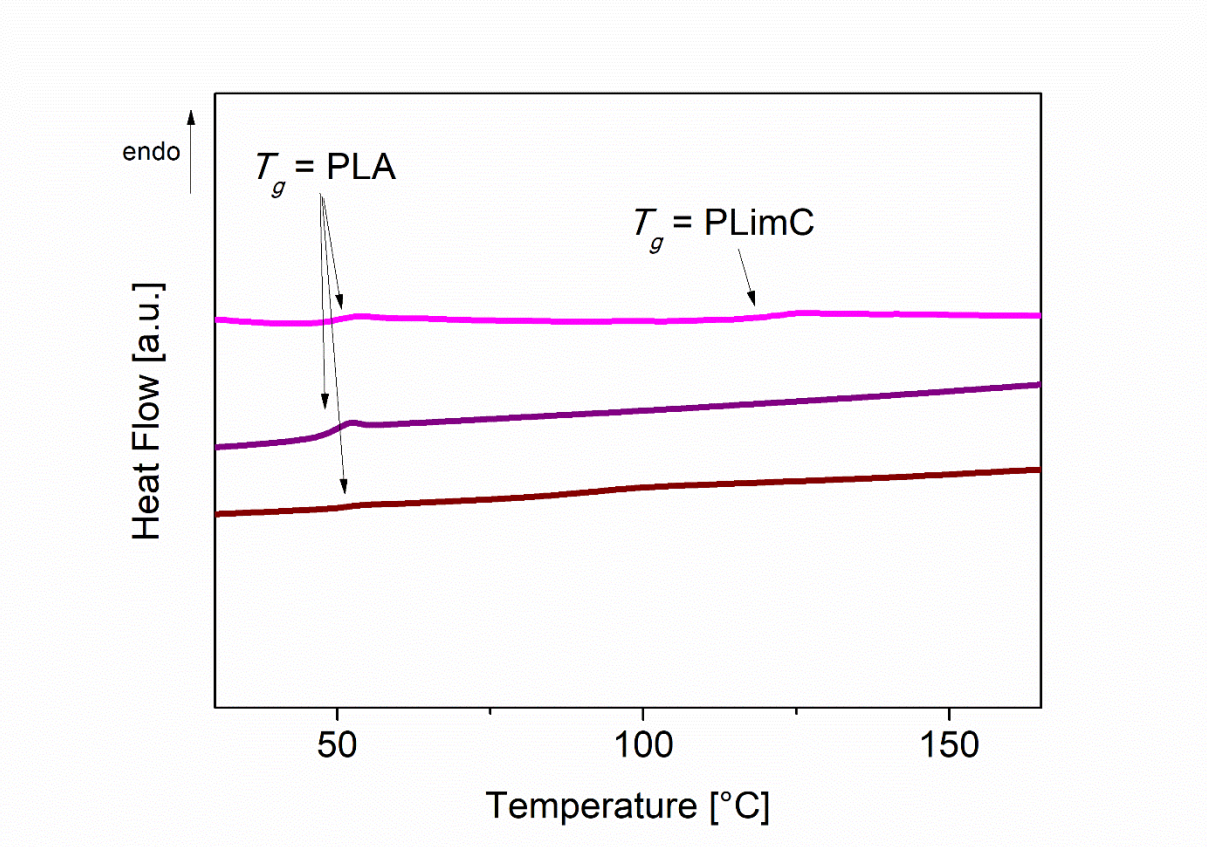


**Fig. S8** DSC thermograms of PLimC-*b*-PDLLA block copolymers (DLLA/ LO = 34/66 mol%) and the corresponding DSC thermograms of THF-soluble fraction (brown) and THF-insoluble fraction (violet). The displayed traces correspond to the second heating curve measured at 10 K $min^{-1}$.

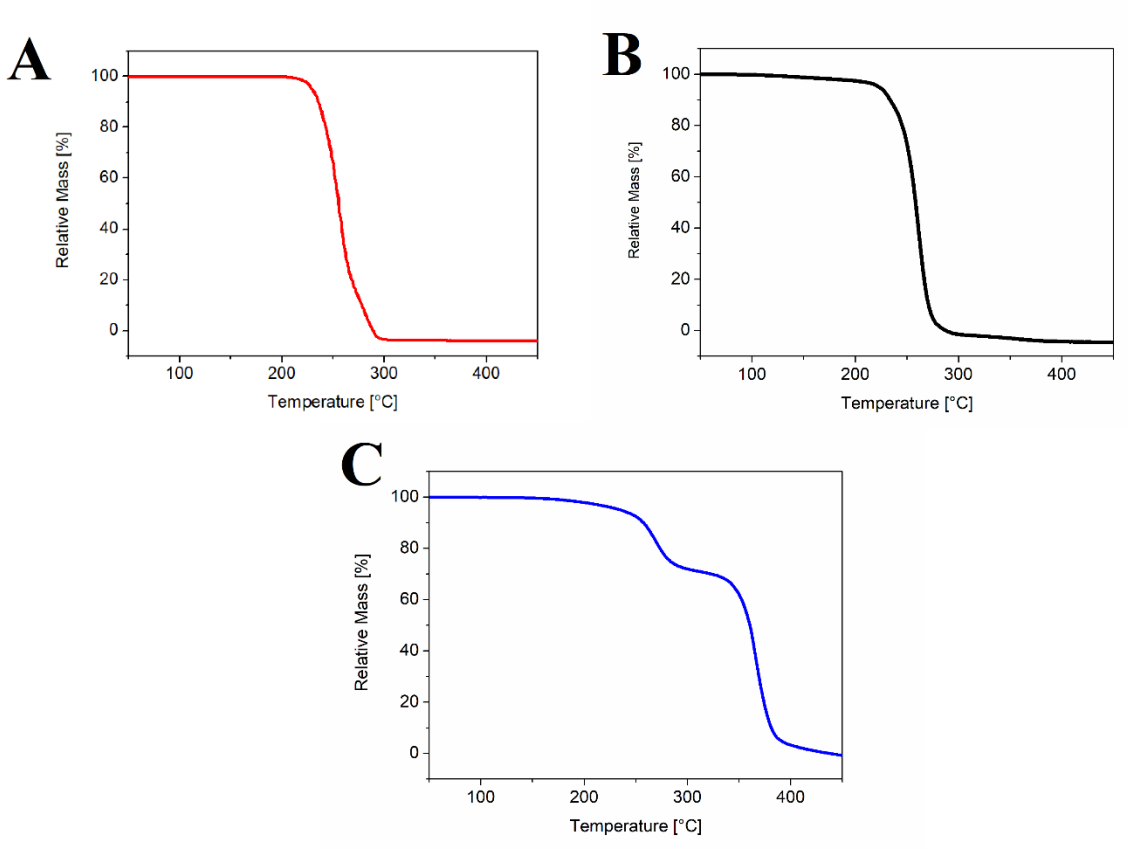


**Fig. S9** TGA thermograms of PLimC-*b*-PDLLA block copolymers (DLLA/ LO = 34/66 mol%) and the corresponding TGA thermograms of the THF-soluble fraction and THF-insoluble fraction. A) Reference with 40 mol % PLimC/ 60 mol% PDLLA. B) THF-insoluble fraction with 82 mol% PLimC/18 mol% PDLLA. C) THF-soluble fraction with 13 mol% PLimC/ 87 mol % PDLLA.

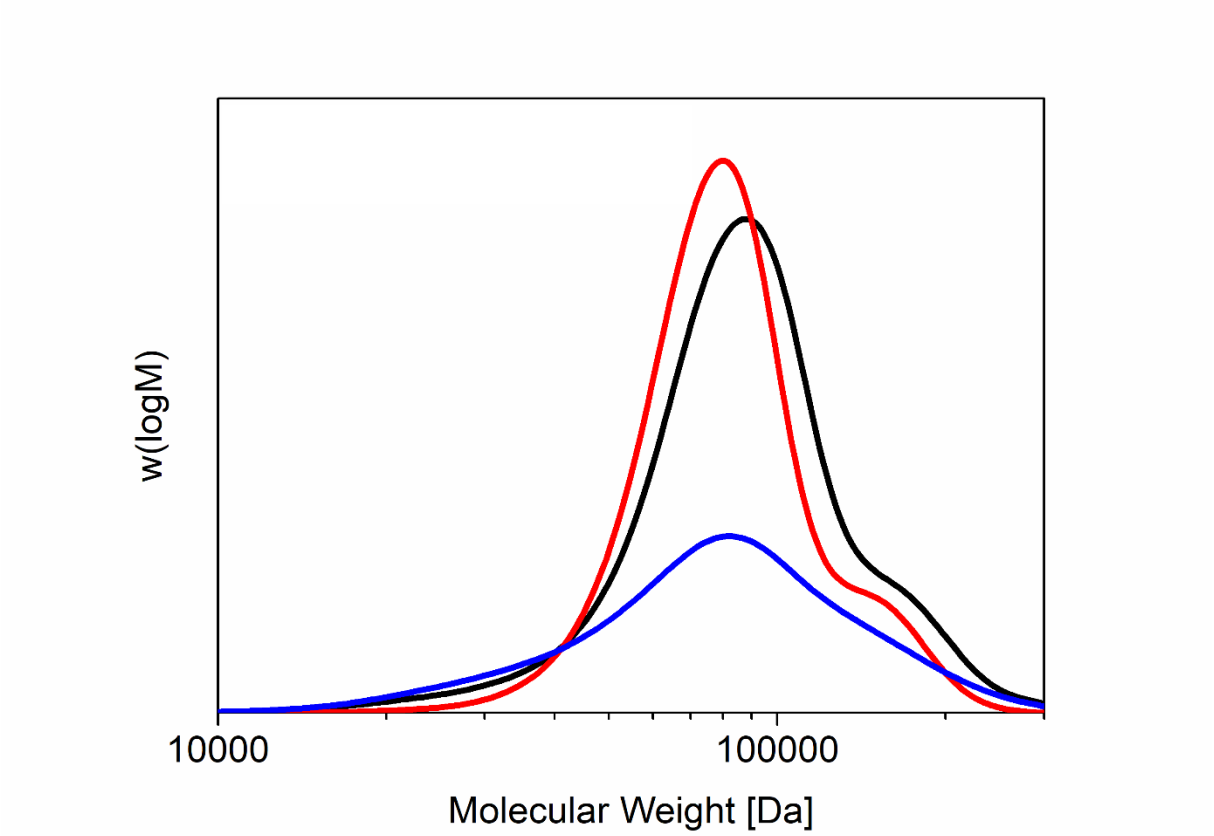


**Fig. S10** $CHCl_3$-GPC traces of PLimC-*b*-PDLLA block copolymers (DLLA/ LO = 34/66 mol%) and the corresponding $CHCl_3$-GPC traces of the THF-soluble fraction and THF-insoluble fraction. Molecular weight ($M_n$) and dispersity ($Đ$) were determined by $CHCl_3$-GPC, calibrated with narrowly distributed polystyrene standards.

*TEM micrographs of PLimC-b-PDLLA block copolymers*

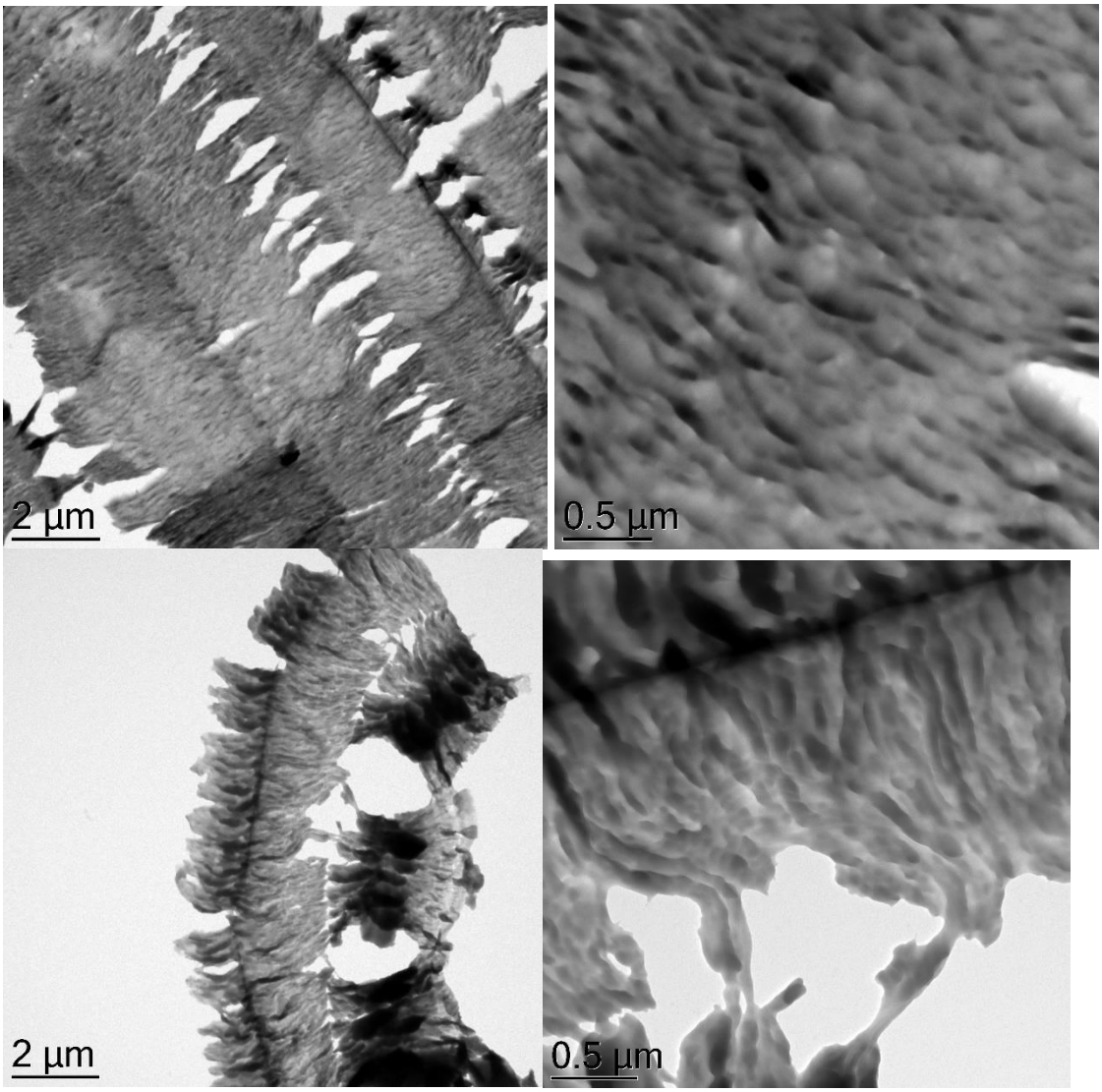


**Fig. S11** TEM micrographs of PLimC-*b*-PDLLA block copolymers (DLLA/ LO = 17/83 mol%) with PLimC/PDLLA = 39/61 mol%.

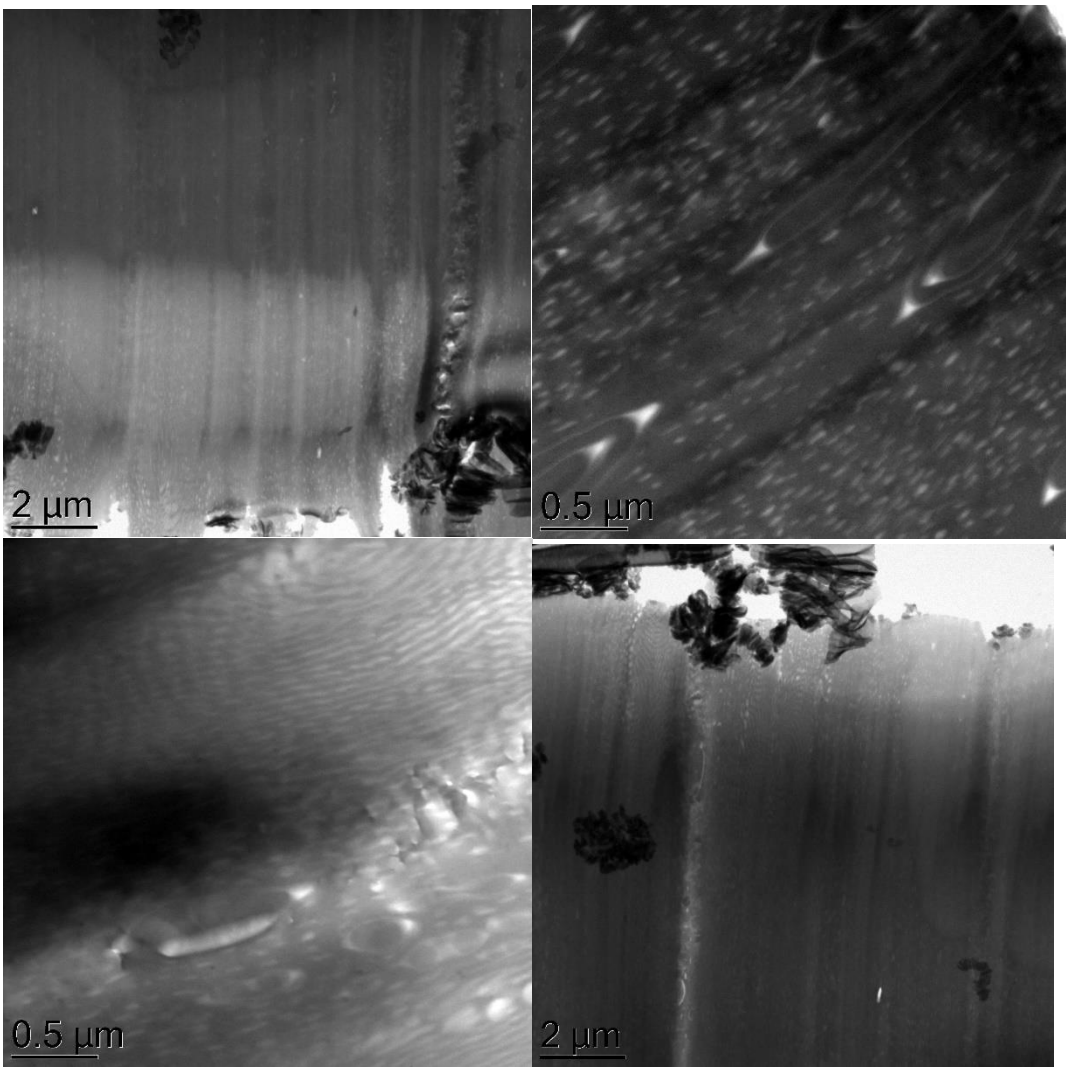


**Fig. S12** TEM micrographs of PLimC-*b*-PDLLA block copolymers (DLLA/ LO = 23/77 mol%) with PLimC/PDLLA = 59/41 mol%.

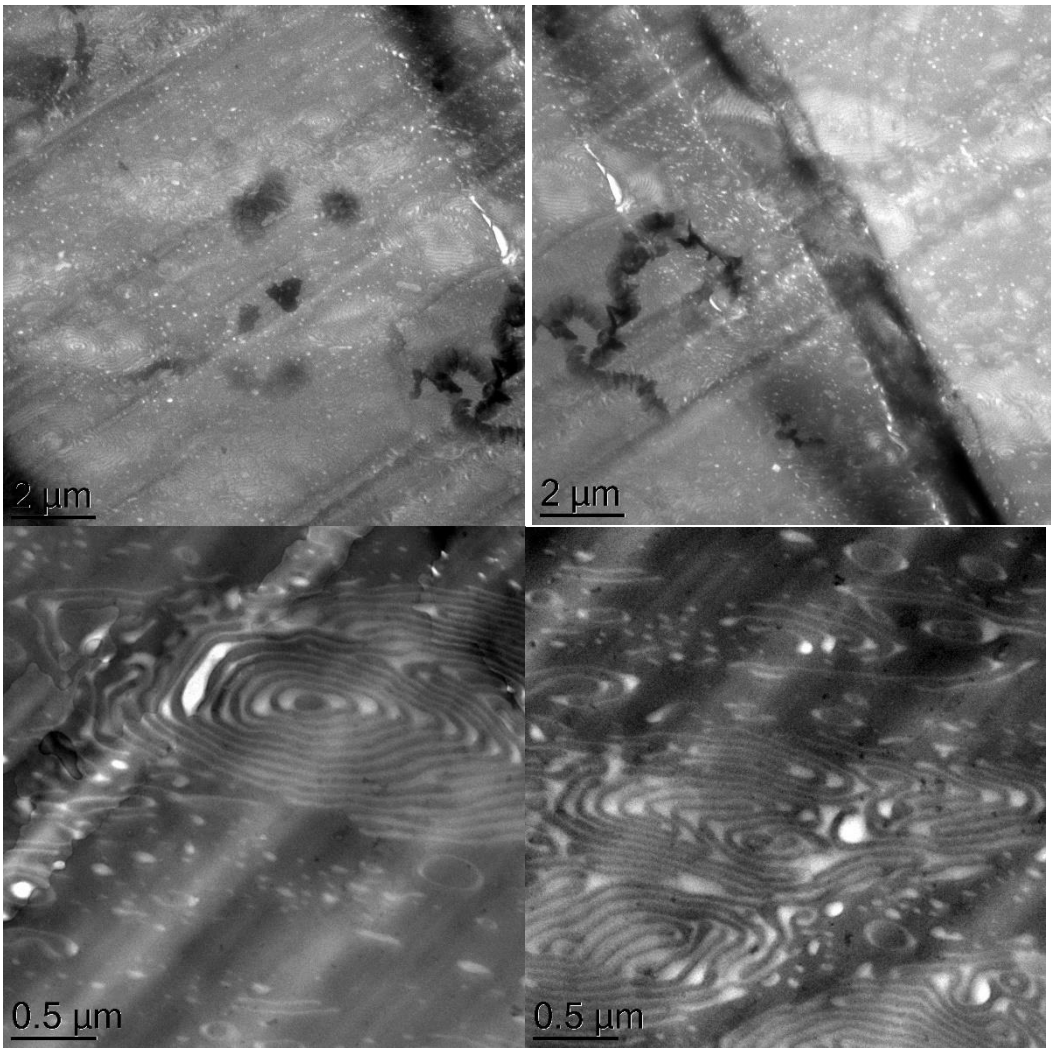


**Fig. S13** TEM micrographs of PLimC-*b*-PDLLA block copolymers (DLLA/ LO = 29/71 mol%) with PLimC/PDLLA = 46/54 mol%.

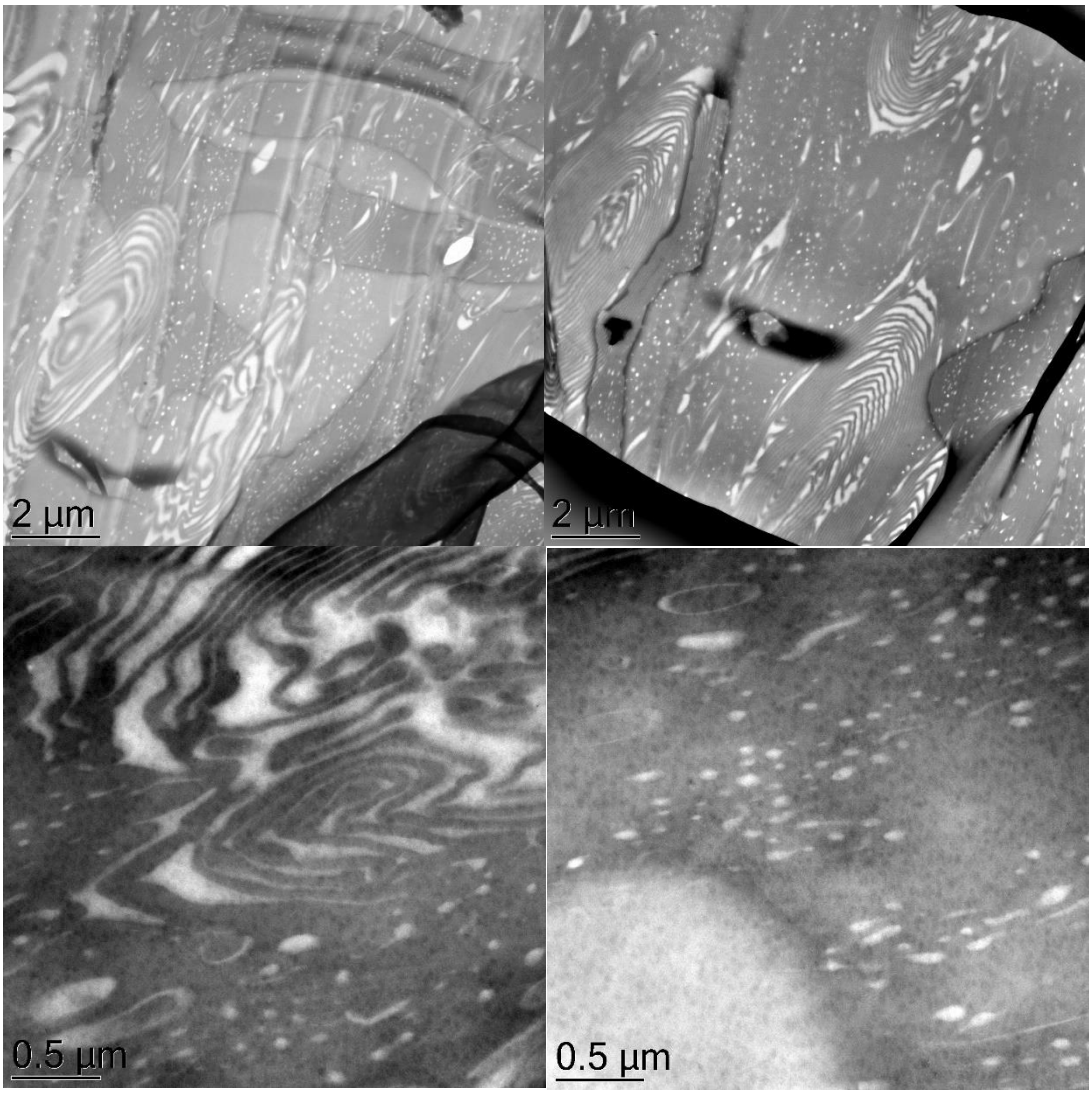


**Fig. S14** TEM micrographs of PLimC-*b*-PDLLA block copolymers (DLLA/ LO = 34/66 mol%) with PLimC/PDLLA = 40/60 mol%.

## Sequential terpolymerziation of *trans*-limonene-oxide, (*L*)-lactide and $CO_2$

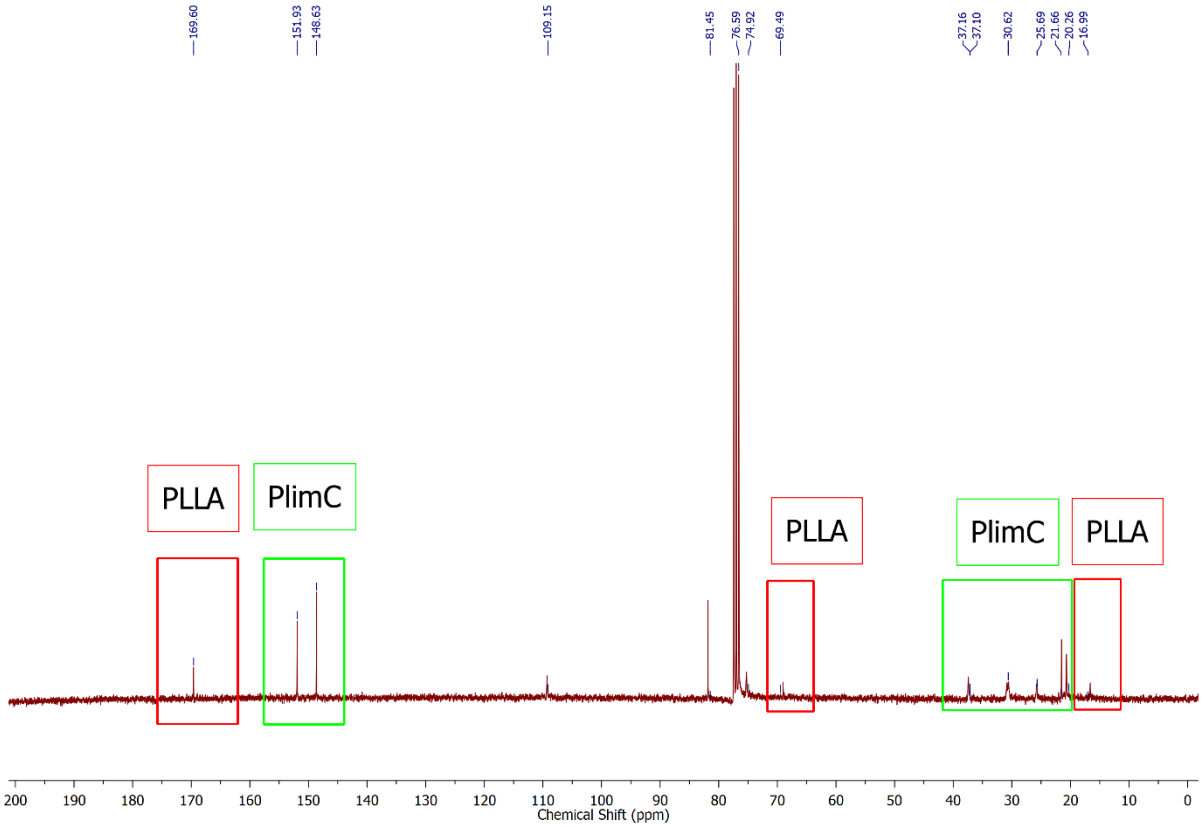


**Fig. S15** $^{13}$C-NMR ($CDCl_3$, 75 MHz) spectrum of PLimC-*b*-PLLA block copolymer (feed ratio: LA/LO = 20/80 mol%) with a composition of PLimC/PLLA = 29/71 mol%, measured in $CDCl_3$.

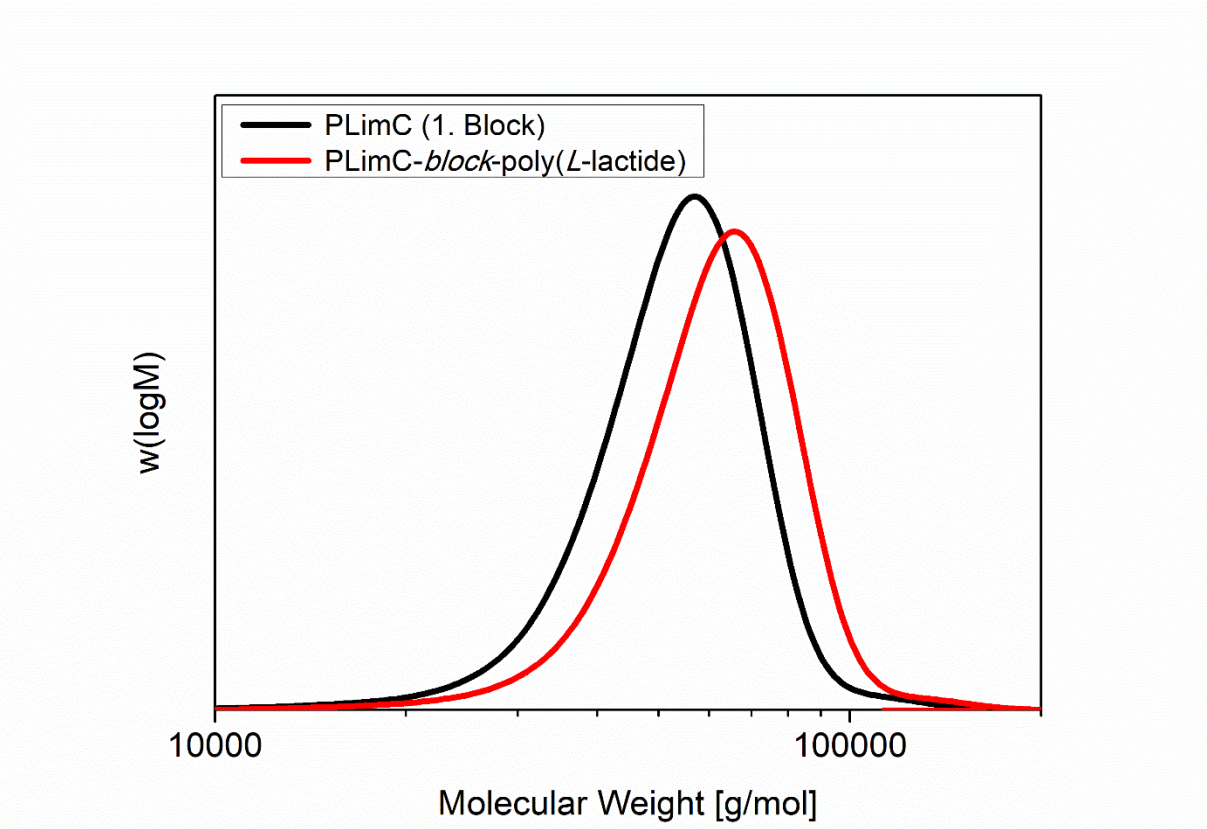


**Fig. S16** $CHCl_3$-GPC traces of PLimC-*b*-PLLA block copolymer (feed ratio: LA/LO = 20/80 mol%) with a composition of PLimC/PLLA = 29/71 mol%. Molecular weight ($M_n$) and dispersity ($Đ$) were determined by $CHCl_3$-GPC, calibrated with narrowly distributed polystyrene standards.

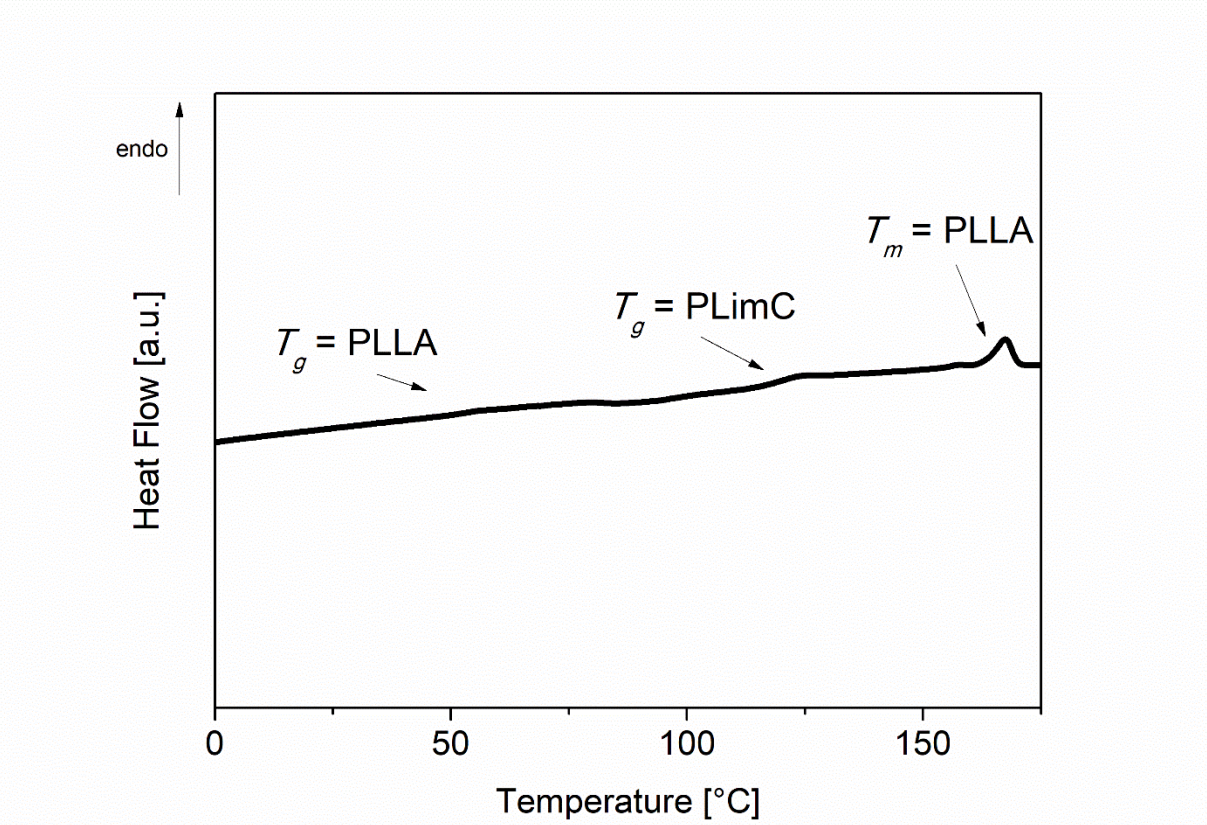


**Fig. S17** DSC thermogram of PLimC-*b*-PLLA block copolymer (feed ratio: LA/LO = 20/80 mol%) with a composition of PLimC/PLLA = 29/71 mol%. The displayed trace corresponds to the second heating curve measured at 10 K $min^{-1}$ under nitrogen.

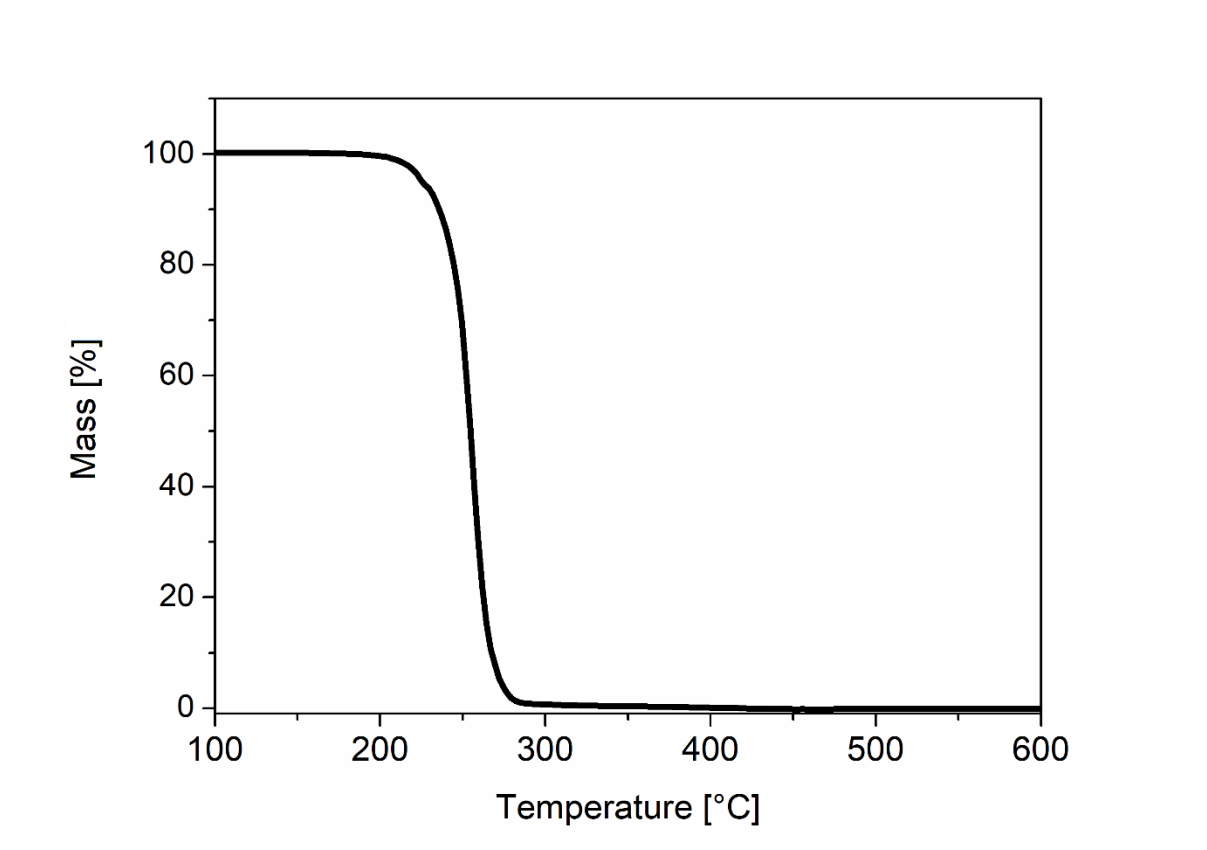


**Fig. S18** TGA thermogram for PLimC-*b*-PLLA block copolymer (feed ratio: LA/LO = 20/80 mol%) with a composition of PLimC/PLLA = 29/71 mol%, measured under nitrogen with 10K/min.

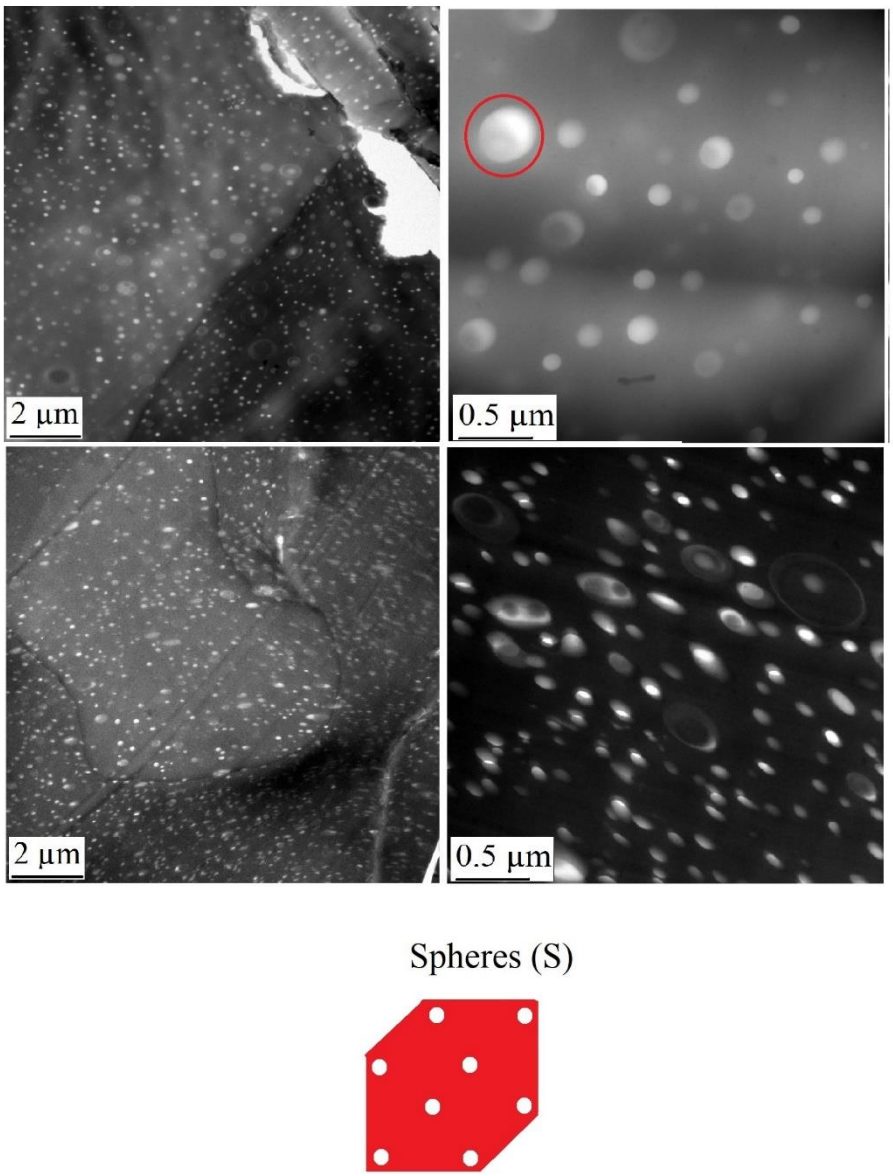


**Fig. S19** TEM micrographs of PLimC-*b*-PLLA block copolymer with PLimC/PLLA = 71/29 mol%. PLimC is selectively stained with OsO4 vapor.

## Terpolymerziation of *trans*-limonene-oxide, dihexyl-substituted lactide and $CO_2$ (Sequential ROCP)

**Table S6.** Experimental details of sequential polymerization of diHLA, LO and $CO_2$ using [(BDI)Zn-(μ-OAc)] catalyst.

| Sample | Feed Ratio | Polymer Composition | Lactide | | LO | | Catalyst | Toluene | Yield |
|---|---|---|---|---|---|---|---|---|---|
| | diHLA/ LO | r-diHLA /r-LO | m | n | V | n | m | V | |
| **Unit** | mol% | mol% | mg | mmol | mL | mmol | mg | mL | % |
| | | | | | | | | | |
| **10** | 23/77 | 29/71 | 511 | 1.80 | 1.0 | 6.1 | 33 | 6 | 89 |
| **11** | 13/87 | 50/50 | 260 | 0.91 | 1.0 | 6.1 | 33 | 11 | n.d. |
| **12** | 50/50 | 62/38 | 993 | 3.49 | 0.57 | 3.5 | 20 | 5 | 74 |

**Table S7.** Overview of the synthesized PLimC and PdiHLA block copolymers in terms of feed ratio, polymer composition, molecular weight, and thermal properties.

| Monomer Lactide | Reaction Type | Feed Ratio diHLA/ LO | r-diHLA /r-LO | $M_n$[a] | Đ[a] | $T_g$[b] PLimC | $T_g$[b] PE | $T_m$[b] PE | $T_{5\%}$[c] | $T_{max,1}$[d] PLimC | $T_{max,2}$[d] PE |
|---|---|---|---|---|---|---|---|---|---|---|---|
| | | mol% | mol% | kDa | | °C | °C | °C | °C | °C | °C |
| **diHLA** | Sequential | 23/77 | 29/71 | 35 | 1.40 | - | -36 | - | 228 | 254 | 329 |
| **diHLA** | Sequential | 13/87 | 50/50 | 14 | 1.20 | - | -39 | - | 224 | 247 | 299 |
| **diHLA** | Sequential | 50/50 | 62/38 | 49 | 1.40 | 106 | -38 | - | 229 | 254 | 289 |

[a]GPC: $M_n$ and $Đ$ were determined by $CHCl_3$-GPC, calibrated with narrowly distributed polystyrene standards.
[b]DSC: $T_g$ and $T_m$ were determined from the second heating traces (scanning rate 10 K $min^{-1}$).
[c]TGA: $T_{5\%}$ was determined with a heating rate of 10 K $min^{-1}$ under $N_2$ atmosphere.
[d]TGA: $T_{max,1}$ and $T_{max,2}$ were determined from the 1st derivative of the TGA trace.

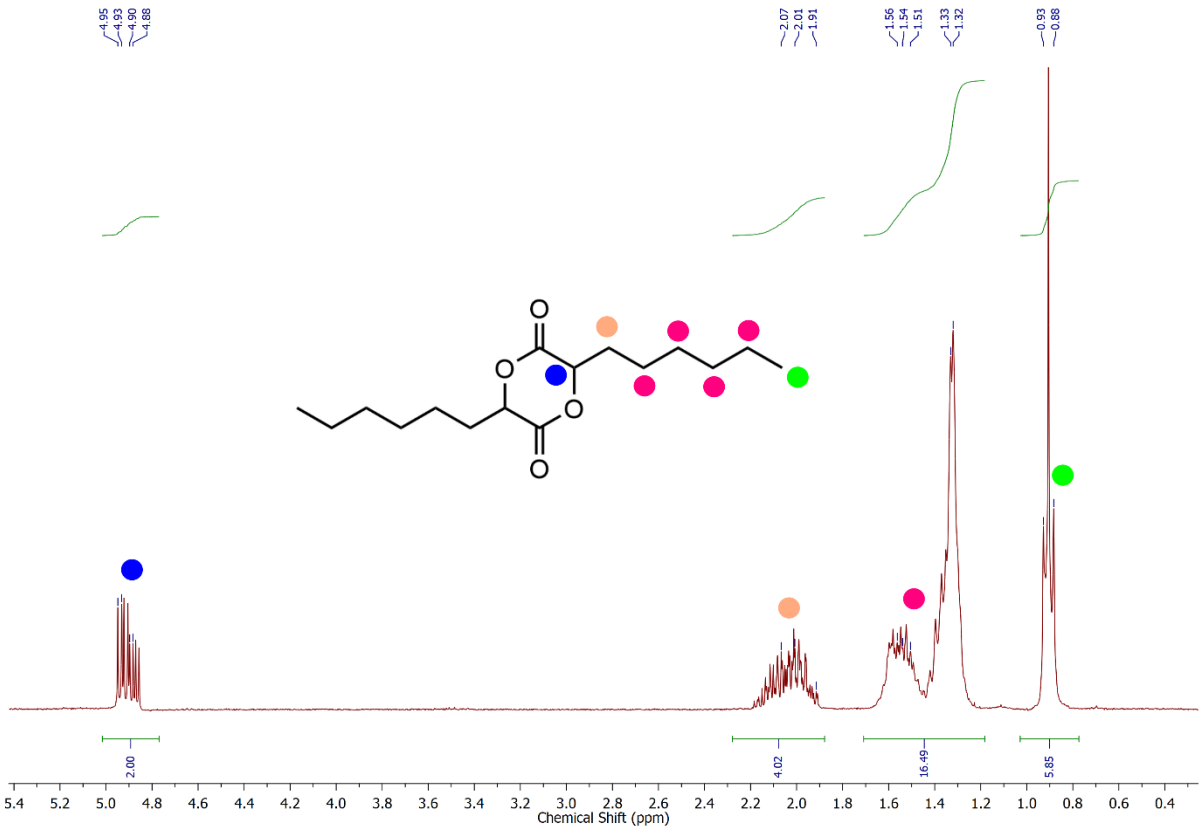


**Fig. S20** $^{1}$H-NMR spectrum ($CDCl_3$, 300 MHz) of monomer dihexyl-substituted lactide (diHLA).

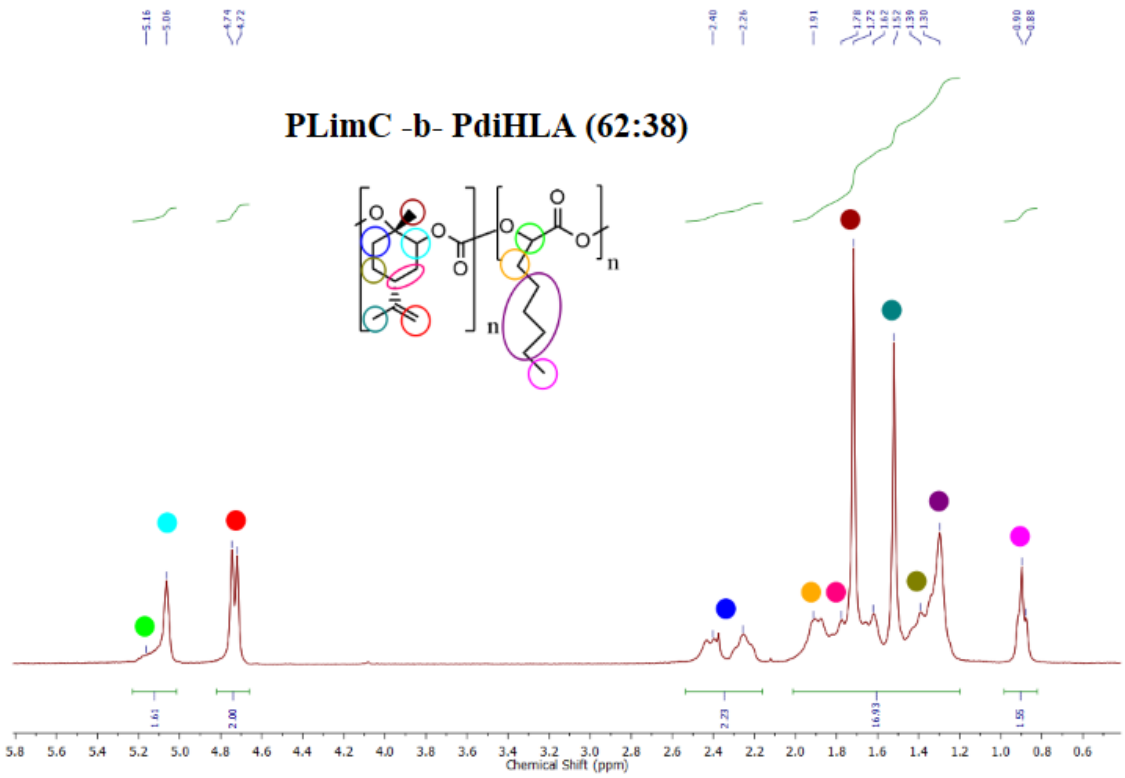


**Fig. S21** $^{1}$H-NMR spectrum ($CDCl_3$, 300 MHz) of PLimC-*b*-PdiHLA block copolymer (feed ratio: diHLA/LO = 50/50 mol%) with a composition of PLimC/PdiHLA = 62/38 mol%.

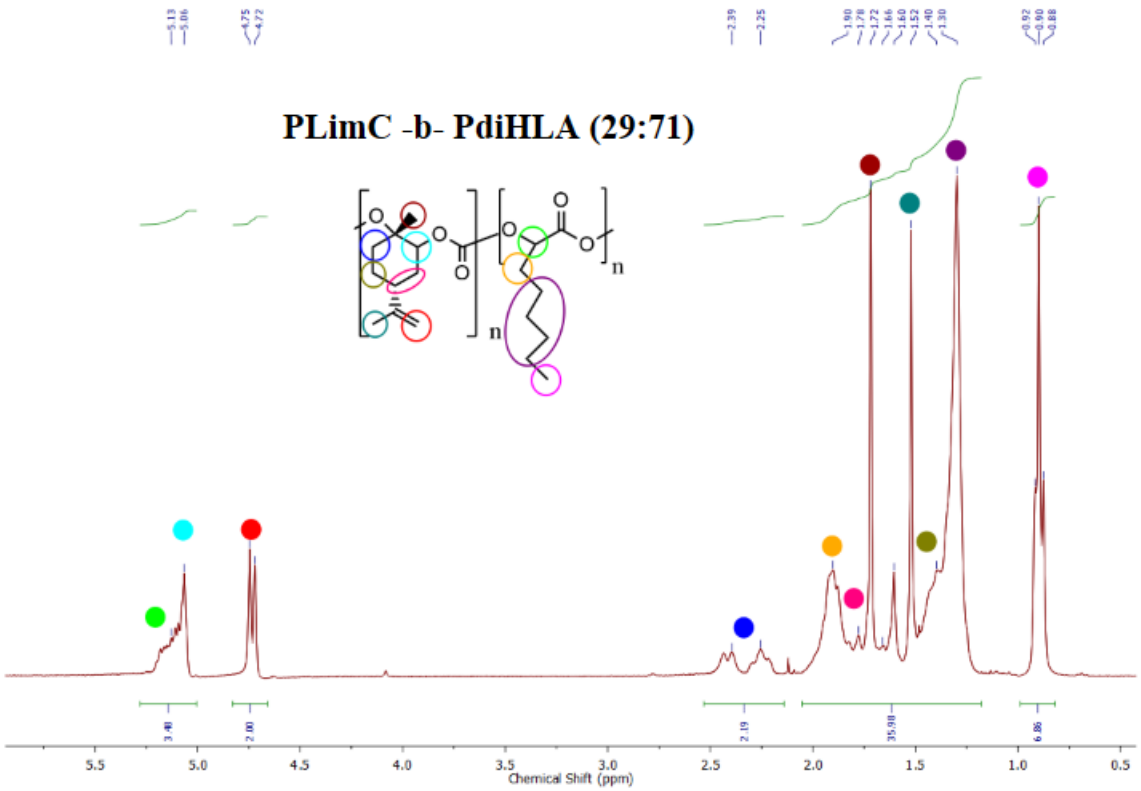


**Fig. S22** $^{1}$H-NMR spectrum ($CDCl_3$, 300 MHz) of PLimC-*b*-PdiHLA block copolymer (feed ratio: diHLA/LO = 22/78 mol%) with a composition of PLimC/PdiHLA = 29/71 mol%.

*GPC traces of PLimC-b-PdiHLA block copolymers*

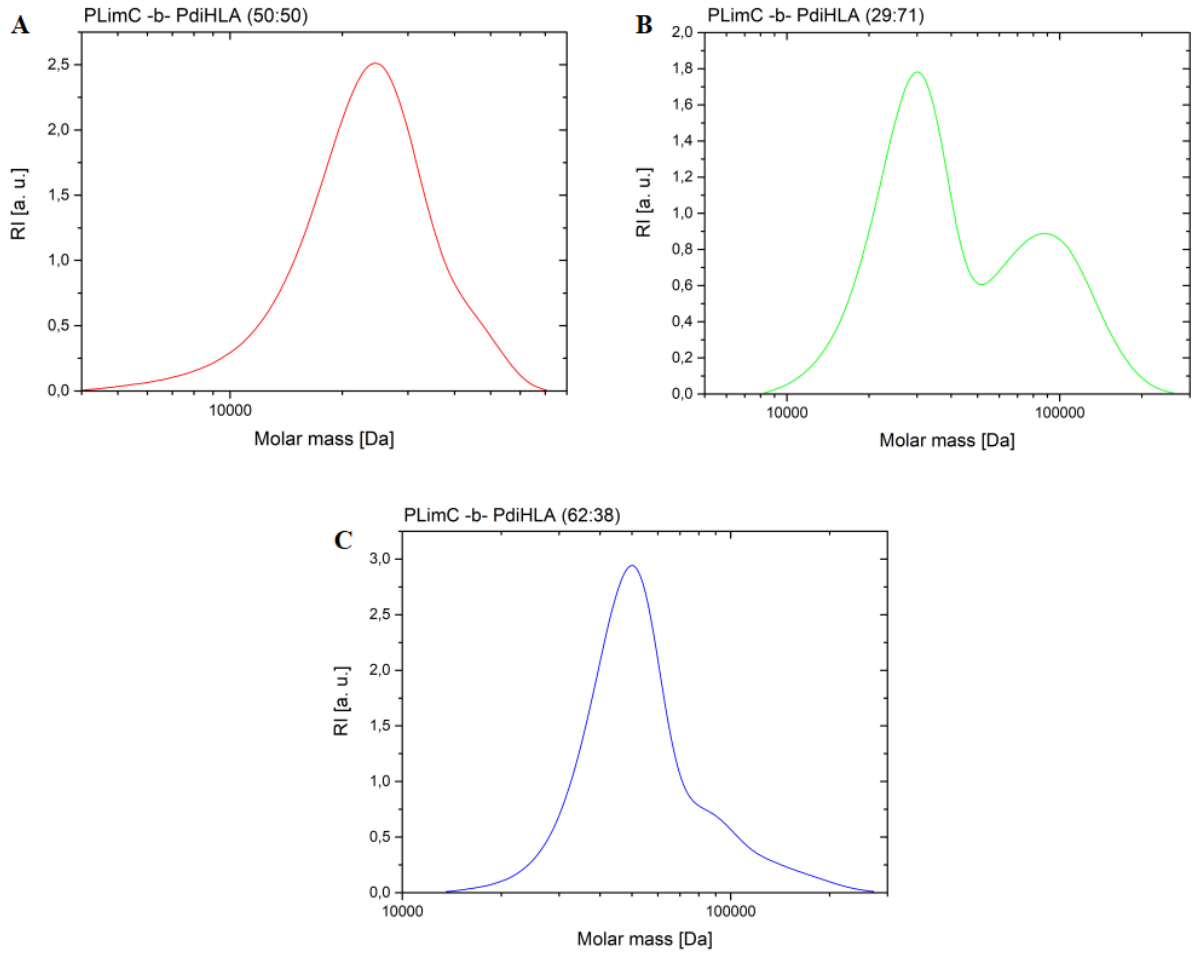


**Fig. S23** $CHCl_3$-GPC traces of PLimC-*b*-PdiHLA block copolymers. A) PLimC-*b*-PdiHLA (50:50) block copolymer, $M_n$ = 14.210 g/mol, $Đ$ = 1.4. B) PLimC-*b*-PdiHLA (29:71) block copolymer, $M_n$ = 35.070 g/mol, $Đ$ = 1.5. C) PLimC-*b*-PdiHLA. (62:38) block copolymer, $M_n$ = 48.980 g/mol, $Đ$ = 1.2. Molecular weight ($M_n$) and dispersity ($Đ$) were determined by $CHCl_3$-GPC, calibrated with narrowly distributed polystyrene standards.

*DSC thermogram of PLimC-b-PdiHLA block copolymer*

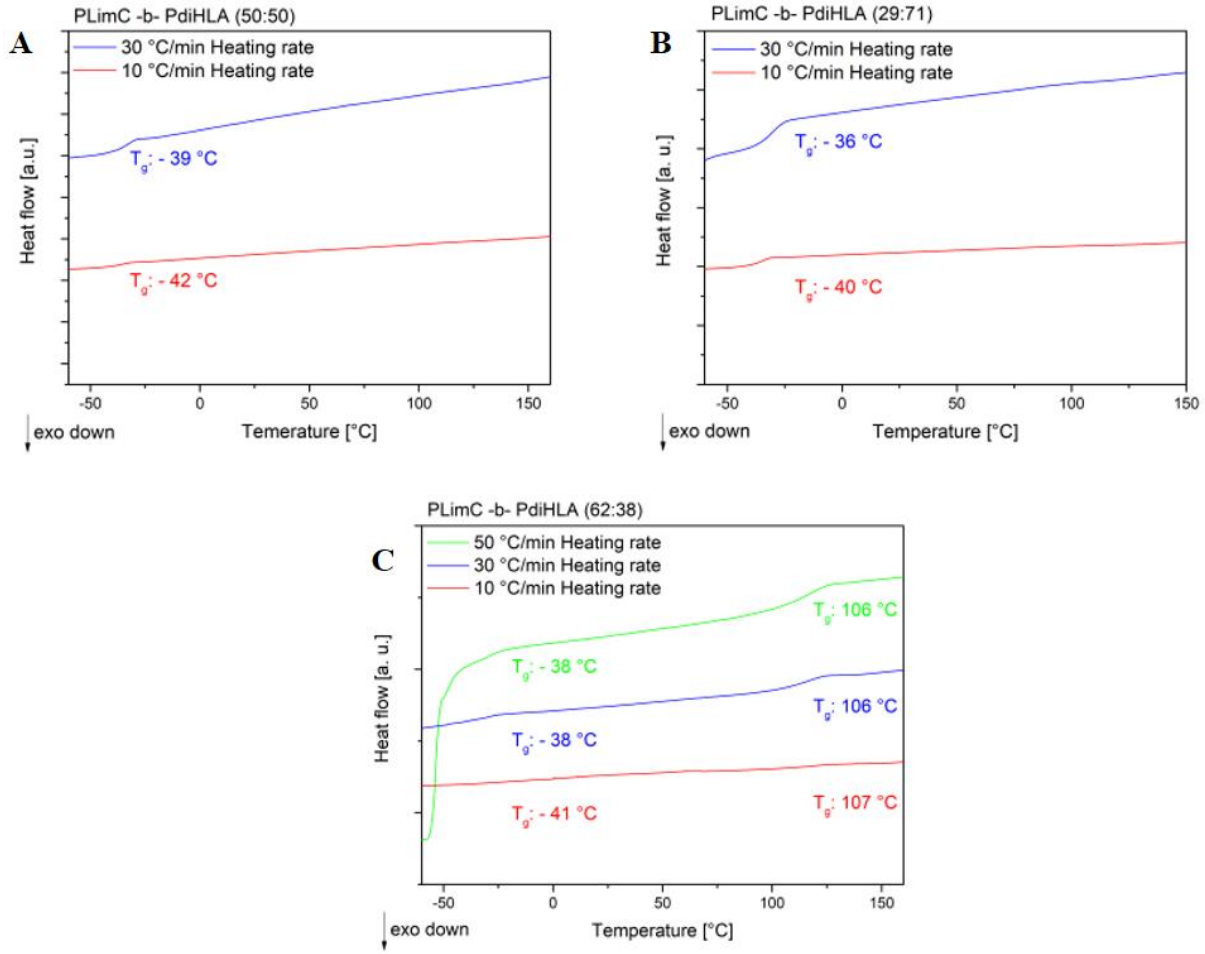


**Fig. S24** DSC thermograms of PLimC-*b*-PdiHLA block copolymers. A) PLimC-*b*-PdiHLA (50:50) block copolymer. B) PLimC-*b*-PdiHLA (29:71) block copolymer. C) PLimC-*b*-PdiHLA (62:38) block copolymer with a heating rate of 10, 30 and 50 °C/min.

*TGA thermograms of PLimC-b-PdiHLA block copolymer*

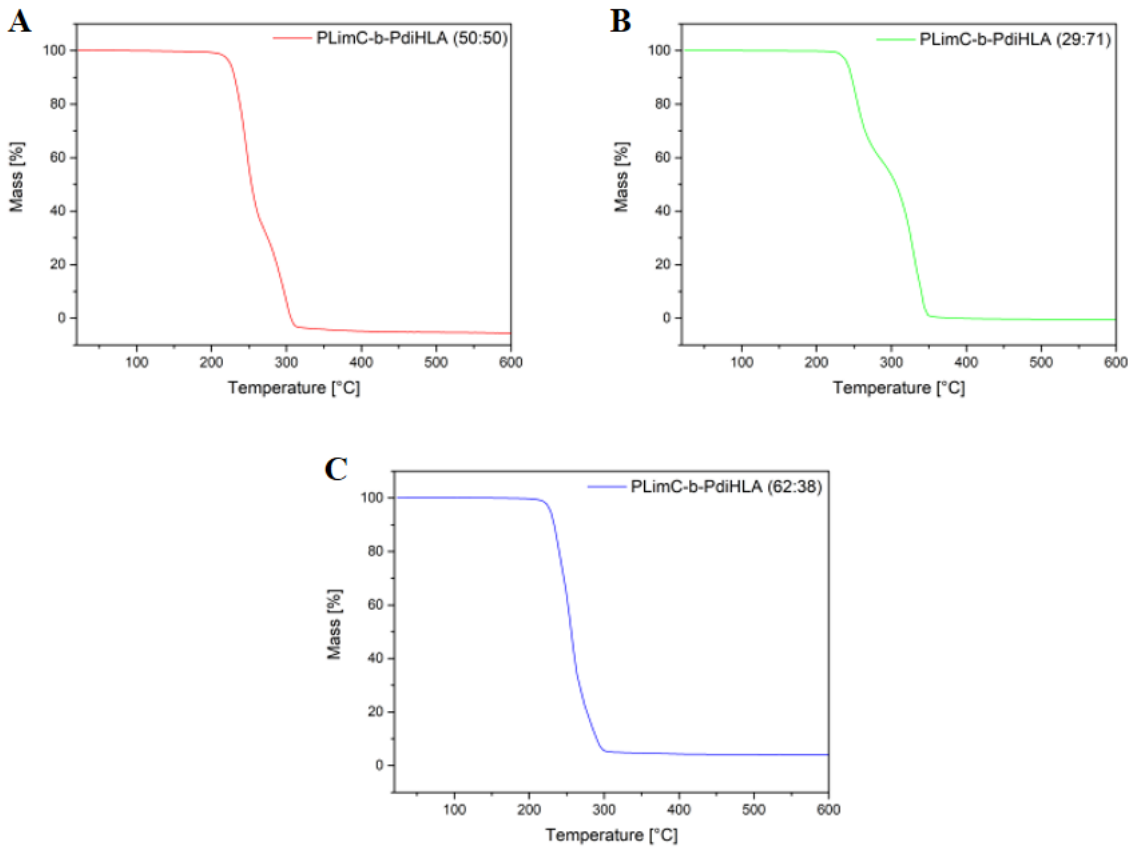


**Fig. S25** TGA thermograms of PLimC-*b*-PdiHLA block copolymer. A) PLimC-*b*-PdiHLA (50:50) block copolymer, $T_{onset}$ of PLimC degradation: 226 °C, $T_{onset}$ of PdiHLA degradation: 260 °C. B) PLimC-*b*-PdiHLA (29:71) block copolymer, $T_{onset}$ of PLimC degradation: 247 °C, $T_{onset}$ of PdiHLA degradation: 306 °C. C) PLimC-*b*-PdiHLA (62:38) block copolymer, $T_{onset}$ of PLimC degradation: 226 °C, $T_{onset}$ of PdiHLA degradation: 260 °C. The displayed traces were measured under nitrogen with 10K/min.

# 10 Summary, Conclusion and Outlook

This thesis investigated composites and copolymers of bio-based polymer poly(limonene carbonate) (PLimC). PlimC is made from *trans*-limonene oxide (LO) and the greenhouse gas $CO_2$ by ring-opening polymerization (ROP) using catalyst [(BDI)Zn-(μ-OAc)]. Both monomers can be obtained from a natural bio-based feedstock. Therefore, PLimC belongs to a group of polymers, which have possible applications in near future due to the need for replacements for petro-based polymers. PLimC traces back to COATES et al.[5], who developed the first copolymerization of LO and $CO_2$. It was further developed by Oliver Hauenstein under the supervision of GREINER. High molecular weight PLimC (<100.000 Da) with excellent optical and mechanical properties was synthesized by masking hydroxyl impurities within the monomer LO.[6] The problematic factor of neat PLimC is the processability due to its low degradation temperature and high viscosity in melt. Neat PLimC can hardly be processed without the loss of its mechanical and optical properties, so ways have to be found to overcome this issue.

This thesis solves the problem of processability by using a bio-based additive, namely ethyl oleate (EtOL), to modify viscosity in melt so that PLimC can be produced at a lower temperature without degradation. The best EtOL loading was to be found with 7.5 wt%. Here, a glass transition temperature of 90 °C and improved mechanical properties alongside good optical properties could be observed. The elongation at break and the *E*-modulus could be doubled in comparison to neat PLimC by the use of EtOL as a bio-based plasticizer. Higher loadings (>7.5 wt%) are usually leading to a lower glass transition and decreased mechanical properties. By adding EtOL, the glass transition temperature of PLimC could be altered in a broad range (25 °C - 130 °C). For future projects, different types of plasticizers could be used to explore the topic even further. Also, the possibility of self-plasticizing with low-molecular-weight PLimC should be taken into consideration.

The blending of two polymers is also an elegant way to tune the properties of a material and to achieve processability of PLimC. The thesis showed how PLimC behaves as a blending partner binary blends as a minority component. It was shown that PLimC usually forms phase-separated blends with most commodity polymers like example polyamide (PA) or polystyrene (PS). Blends of PLA/PLimC showed moderate properties, because of their phase-separate morphology. However, in some polymers blends like for example with poly(butylene adipate-*co*-terephthalate) (PBAT) or Arnitel EM400® (copolyetherester) PLimC increased the *E*-

modulus significantly. To improve the compatibility of PLimC with other blending partners block copolymers could be used as a compatibilizer to reduce the surface energy of PLimC domains. This could lead to improved mechanical properties of PLimC blends. Also, reactive processing of PLimC and a blending partner would be an option for future work.

As above-mentioned compatibilizers can be an option for improving blend properties. For PLimC/PLA blends, compatibilizers can be obtained by copolymerization of PLimC and PLA. The thesis showed that the catalytic system [(BDI)Zn-(μ-OAc)] not only polymerizes LO and $CO_2$ but also lactide (LA), which results in PLimC and PLA copolymers. PLA is an interesting polymer because it is bio-based and shows biodegradability as well. This thesis revealed also that copolymers of PLimC and PLA derivatives are possible. Long alky chain derivatives of lactide (e.g., dihexyl-substituted lactide (diHLA)) show a promising pathway for further PLimC modifications. The thesis showed that copolymers of PLimC and PdiHLA have a great elasticity and transparancy. To utilize the full potential of lactide and its derivatives, further research has to be carried out. Mechanical properties, optical properties and as well the microstructure of these copolymers should be investigated in future projects. Also, the development of thermoplastic elastomers based on lactide derivatives seems reasonable. Copolymers of PLimC and different lactide derivatives (e.g., mandelide) are also possible for future projects.

In summary, this thesis showed three different approaches to showcase the potential of PLimC as a future thermoplastic polymer. Additives, copolymerization, and blending are methods, which can be used as effective tools to achieve processability PLimC so that PLimC can pass the threshold to become a relevant industrial polymer for a “greener” future.

# 11 Acknowledgment

First of all, I want to thank Prof. Dr. Andreas Greiner and Prof. Dr. Seema Agarwal for their continuous support, their belief in me, and their kind hearts during my whole PhD journey.

I also want to express my gratitude to my third supervisor Dr. Holger Schmalz. Thank you for being a teacher and a friend to me. With your help, I could grow and develop myself.

My special thank goes to Lisa-Cathrin Leitner and Mahsa Mafi for their true friendship, their loyalty, and their positivity during my whole PhD time.

Thanks also to all my students, who I supervised during my whole PhD: Sebastian Schmitz, Lisa Schönfelder, Lisa-Cathrin Leitner, Felix Bretschneider, Linus Hager, Emma Fuchs, Yihan Zhang, Xue Lin, Sophia Däbritz, Aneesha Anand, Oliver Gallus, Sebastian Lessing, Matthias Elflinger and Sophie Fritze.

I also want to thank my direct lab mates in PNS for being good colleagues and friends: Nikola Majstorović, Thomas Schmitt, Hendrik Volz, Markus Kötzsche, Anil Kumar, Mina Heidari, Ann-Kathrin Müller, Marius Schmidt, Chen Liang and Lothar Benker.

My gratitude goes also to all other members of MCII for helping me and becoming a better version of myself.

Furthermore, I want to thank Annette Krökel, Lothar Benker, and Carmen Kunert for their help in everyday situations and all the discussions we had.

I also want to thank Gaby Oliver and Niko Plocher for their secretary work and their kindness in the right moments.

Last but not least, I want to say thank you to my family: Holger Neumann, Petra Neumann, and Tanja Neumann for their support during my study and in my whole life.

# 12 (Eidesstattliche) Versicherung und Erklärungen

(§ 9 Satz 2 Nr. 3 PromO BayNAT)
Hiermit versichere ich eidesstattlich, dass ich die Arbeit selbständig verfasst und keine anderen als die von mir angegebenen Quellen und Hilfsmittel benutzt habe (vgl. Art. 64 Abs. 1 Satz 6BayHSchG).

(§ 9 Satz 2 Nr. 3 PromO BayNAT)
Hiermit erkläre ich, dass ich die Dissertation nicht bereits zur Erlangung eines akademischen Grades eingereicht habe und dass ich nicht bereits diese oder eine gleichartige Doktorprüfung endgültig nicht bestanden habe.

(§ 9 Satz 2 Nr. 4 PromO BayNAT)
Hiermit erkläre ich, dass ich Hilfe von gewerblichen Promotionsberatern bzw. – vermittlern oder ähnlichen Dienstleistern weder bisher in Anspruch genommen habe
noch künftig in Anspruch nehmen werde.

(§ 9 Satz 2 Nr. 7 PromO BayNAT)
Hiermit erkläre ich mein Einverständnis, dass die elektronische Fassung meiner Dissertation unter Wahrung meiner Urheberrechte und des Datenschutzes einer gesonderten Überprüfung unterzogen werden kann.

(§ 9 Satz 2 Nr. 8 PromO BayNAT)
Hiermit erkläre ich mein Einverständnis, dass bei Verdacht wissenschaftlichen Fehlverhaltens Ermittlungen durch universitätsinterne Organe der wissenschaftlichen
Selbstkontrolle stattfinden können.

Bayreuth, den 28.06.2020

---

Simon Neumann